GROUND-WATER RESOURCES OF SOUTHERN COMANCHE COUNTY, SOUTHWESTERN OKLAHOMA

By

BENJAMIN BETKE GREELEY

Bachelor of Arts

University of Pennsylvania

Philadelphia, Pennsylvania

1981

Submitted to the Faculty of the Graduate College
of the Oklahoma State University
in partial fulfillment of the requirements
for the Degree of
MASTER OF SCIENCE
December, 1986

Name: Benjamin Betke Greeley Date of Degree: December, 1986

Institution: Oklahoma State University Location: Stillwater, Oklahoma

Title of Study: GROUND-WATER RESOURCES OF SOUTHERN COMANCHE COUNTY, SOUTHWESTERN OKLAHOMA

Pages in Study: 276 Candidate for Degree of Master of Science

Major Field: Geology

Scope and Method of Study: The principal aquifers of Comanche County are the alluvium within the creek valleys; the Post Oak Aquifer consisting of Permian sandstones, shales, and conglomerates; and the Arbuckle Group Aquifer comprised of Cambrian and Ordovician carbonates. The alluvial aquifer was evaluated from stream discharge data, a numerical ground-water hydraulics model was applied to the Post Oak Aquifer, and lineament analyses of aerial photographs were used to characterize the Post Oak and Arbuckle Group aquifers. Analytical methods included a grain size-permeability relationship applied to the alluvium and the Post Oak Aquifer and a relationship between transmissivity and specific capacity applied to all three aquifers.

Findings and Conclusions: The permeability of the alluvial aquifer is 990 gpd/ft^2 (4.7 x 10^{-4} m/s), the transmissivity is 15,840 gpd/ft (0.0023 m^2/s), and well yields range from 5 to 500 gpm (0.3 to 32 l/s). The average thickness of the alluvium is 33 ft (10 m) with a range from 10 to 65 ft (3 to 19.8 m). The Post Oak Aquifer has an average permeability of 800 gpd/ft^2 (3.8 x 10^{-4} m/s), an average transmissivity of 16,000 gpd/ft (0.0023 m^2/s), and an average calculated well yield of 110 gpm (6.9 l/s). The average effective thickness is 50 ft (15.2 m) and the average saturated thickness is 20 ft (6.1 m). Mean annual recharge to the aquifer is 4.1 in/yr (104 mm/yr). The Arbuckle Group Aquifer has a permeability of 3.5 gpd/ft^2 (1.7 x 10^{-6} m/s), a transmissivity of 1800 gpd/ft (2.6 x 10^{-4} m^2/s), a storativity of 1.2 x 10^{-5}, and an average calculated yield of 270 gpm (17 l/s). The Arbuckle Aquifer is recharged through the Post Oak Aquifer in the north but provides recharge to the Post Oak to the south.

ADVISER'S APPROVAL _____

GROUND-WATER RESOURCES OF

SOUTHERN COMANCHE COUNTY,

SOUTHWESTERN OKLAHOMA

Thesis Approved:

_____

Thesis Adviser

_____

_____

_____

Dean of the Graduate College

PREFACE

This study was part of a project to assess the ground-water availability in Comanche County for the Oklahoma Water Resources Board. The objective of the study herein was to evaluate the alluvial aquifer, the Post Oak Aquifer, and the Arbuckle Group Aquifer by various methods of analysis. A numerical ground-water hydraulics model was applied to the Post Oak Aquifer.

I would like to thank my committee members for their advice and guidance, and especially my thesis advisor, Dr. Douglas C. Kent, who directed this research as principal investigator of the Oklahoma Water Resources Board Project and to the Oklahoma Water Resources Board for funding my research. I am grateful, also, to Dr. Wayne A. Pettyjohn for allowing me the use of the RECHARGE program and to Dr. Gary F. Stewart for his advice on the stratigraphy. I appreciate the assistance of Dr. R. Nowell Donovan and Dr. Zuhair Al-Shaieb for lending materials concerning the geology of Comanche County.

I would like to express my sincere gratitude to the following colleagues: Lorraine LeMaster and Chang Chi-Chung for their assistance with the computer modelling; David Back for his joint effort with data collection and interpretation; Randall Ross for his assistance with the field work; Steve Bridges for providing materials on the geology of Comanche County; and Dr. Jerry Overton for his editorial assistance with the OWRB project.

I appreciate the assistance of Joe Johnson, geologist, and the drilling crew of the Layne-Western Company, Wichita, Kansas, who provided me the opportunity to participate in the drilling, completion, and testing of the Indiahoma municipal well.

Finally, I am most thankful to my parents, grandmother, and brother for their financial support, moral support, and patience during my graduate career.

TABLE OF CONTENTS

LIST OF TABLES

LIST OF FIGURES

Figure Page

Figure Page

Figure Page

Figure Page

CHAPTER I

INTRODUCTION

Purpose and Scope

The purposes of this study were to evaluate the ground-water resources of southern Comanche County from existing data and to use these data in a ground-water hydraulics computer model to characterize the Post Oak Aquifer. These data are from assessments of the ground-water availability by Kent, Greeley, and Overton (1986) and Kent and Greeley (1986), studies for the Oklahoma Water Resources Board.

The major sources of ground water in the study area are the alluvium along the creeks, the Post Oak Aquifer, and the Arbuckle Aquifer. The Rush Springs Sandstone and its associated formations in northeastern Comanche County were not considered in this study.

The computer simulation was limited to the Post Oak Aquifer because of the lack of extensive data for the Arbuckle Group Aquifer. The area of study was limited to the townships south of the Wichita Mountains (Figure 1).

Location

Comanche County is located in southwestern Oklahoma between latitudes 34°25' N and 34°51' N and between longitudes 98°5' W and 98°50' W. The study area includes townships four north to one south and part of two south and ranges nine west to 15 west (Figure 2).

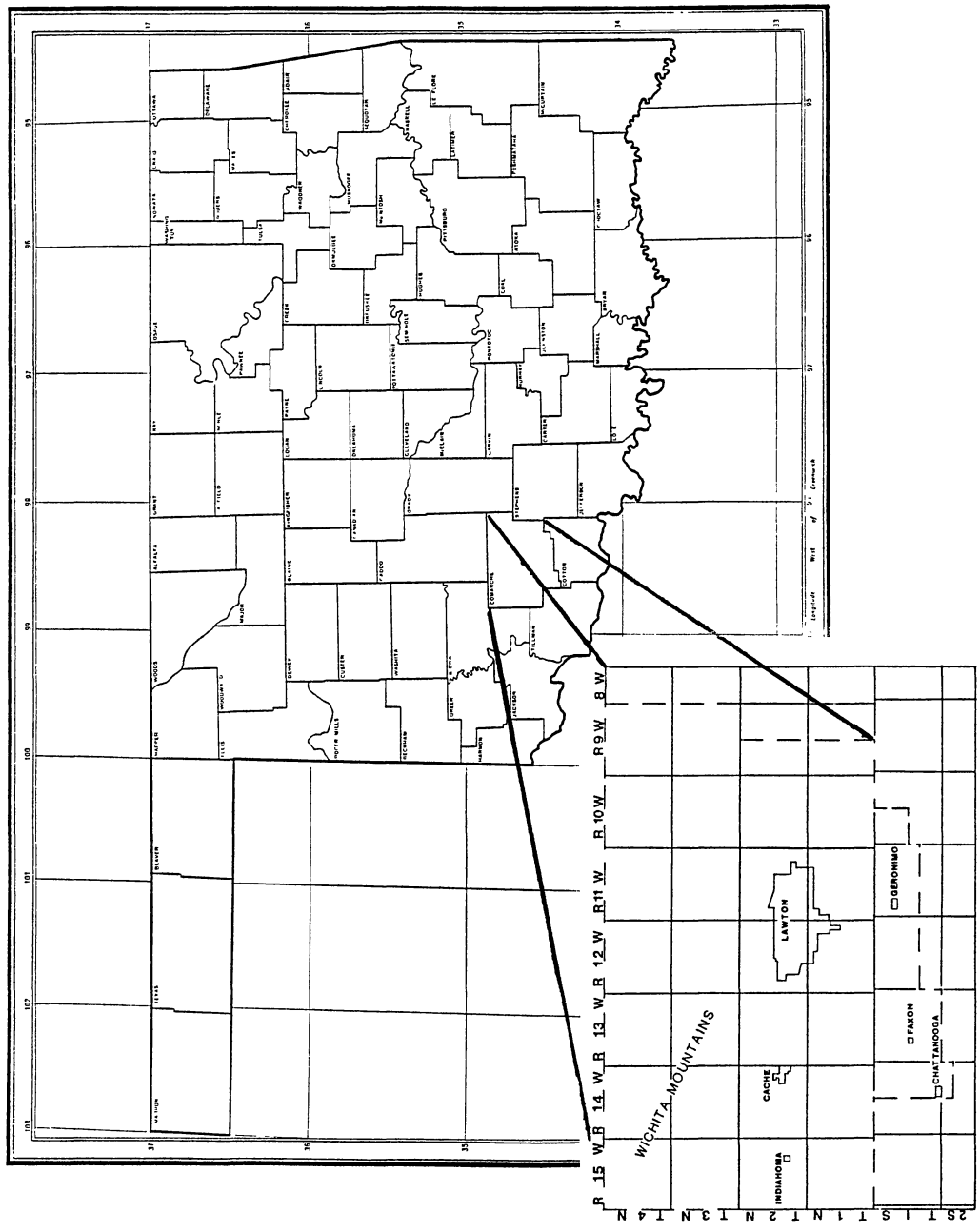

Figure 1. Location of Study Area

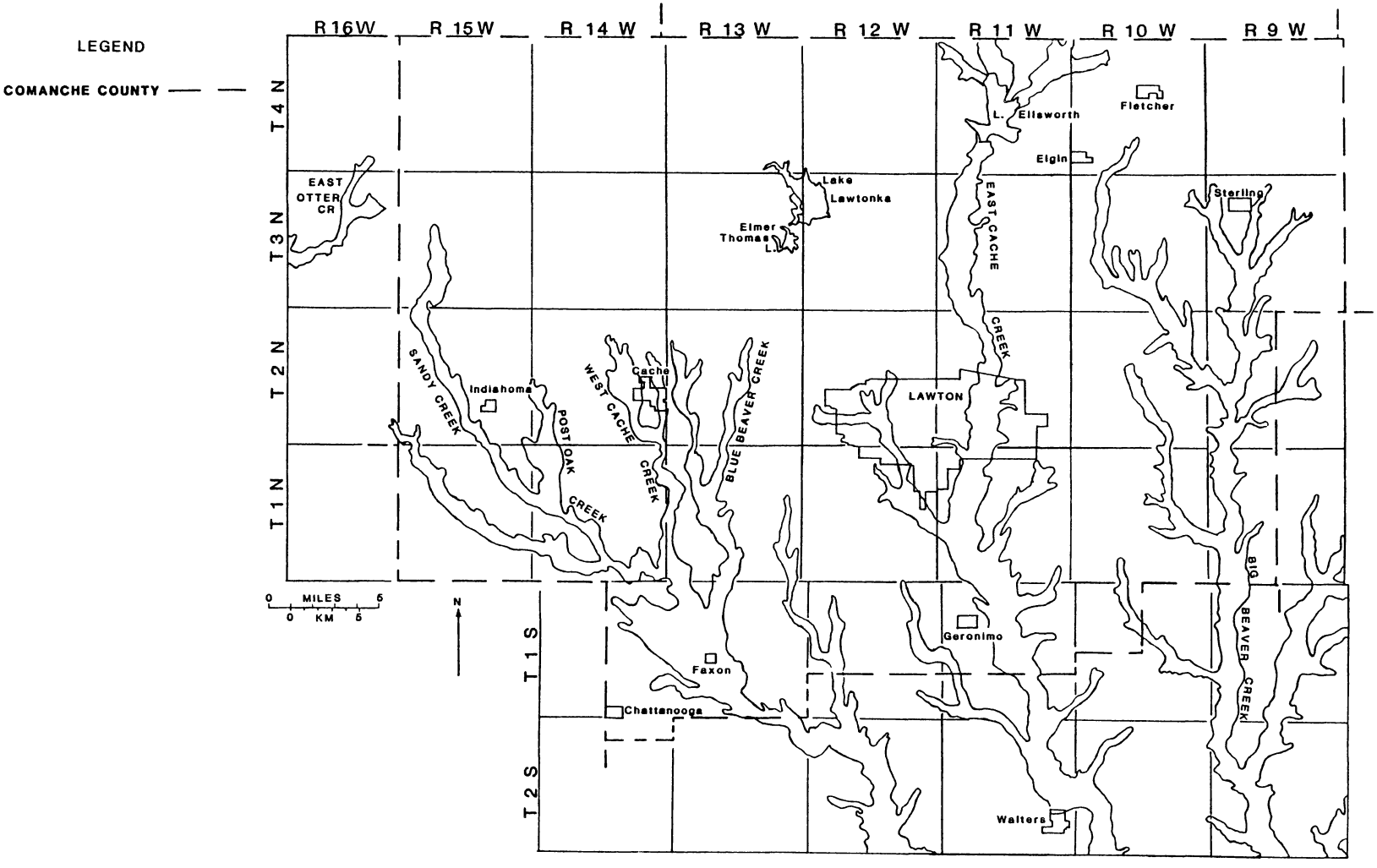

Figure 2. Map of Study Area

The area is dominated topographically by the Wichita Mountains, which trend northwestward from just north of Lawton into Kiowa and Greer Counties near Altus. Mount Scott is the most prominent of these hills with an elevation of 2464 feet (751 m), but a relief above the surrounding plains of about 1300 feet (396 m). The general relief is about 500 feet (150 m). The plains slope to the south to an elevation of about 1100 feet (340 m). On the north flank of the Wichitas are the Slick, or Limestone, Hills, a series of low ridges and hills roughly parallelling the mountains and trending northwestward from near Richards Spur and Meers into Kiowa County. These hills rise about 300 to 500 feet (91 to 150 m) above adjacent creek valleys.

Principal drainage is toward the south to the Red River by West Cache Creek, East Cache Creek, and Beaver Creek. On these creeks and their tributaries are many man-made lakes, the largest of which are Lake Lawtonka on Medicine Creek and Lake Ellsworth on East Cache Creek (Figure 2). Numerous small farm ponds and reservoirs have also been constructed in these watersheds.

Previous Investigations

Water Resources

Because of the importance of water to the development of Oklahoma, the Oklahoma Water Resources Board has surveyed the state's resources to allow planning of their use. An appraisal of these resources (Oklahoma Water Resources Board, 1968) for the basins of Cache Creek, Beaver Creek, and Mud Creek, which include Comanche County except for the far northwest and northeast corners, described the surface-water

hydrology, surface and irrigation water quality, and the surface- and ground-water resources.

The Oklahoma Comprehensive Water Plan (Oklahoma Water Resources Board, 1975) provided for the development of the state's water resources. For the Southwest Region, which includes Comanche County, there are general descriptions of the aquifers and mineral resources, summaries of streamflow data, well hydrographs, lists of water resource projects, and a table of municipal water needs and proposed solutions. The 1980 update of the Oklahoma water plan (Oklahoma Water Resources Board, 1980) was similar to the earlier publications but proposed development plans for the southwest and other planning regions.

A report by Stone (1981) for the Comanche County area is similar to the publications described above in that it assessed the quantity and quality of the current water supplies and offered possible solutions to water-supply problems. A set of maps of the ground-water quality is with that report.

The most complete and detailed investigation of the water resources in southwestern Oklahoma including Comanche County is the Hydrologic Atlas of the Lawton one-by-two degree quadrangle by Havens (1977). This study mapped the geology, located the major aquifers, indicated the surface- and ground-water quality, and discussed the surface- and ground-water hydrology. Havens' later report (1983) covers the hydrogeology around the Wichita Mountains only and discusses the availability and quality of ground water from alluvium, the Rush Springs Formation and El Reno Group, and the Arbuckle Group.

Davis (1958) presented a short discussion of the availability of ground water from the Arbuckle Group, but that report does not include

extensive hydrologic data. Tanaka and Davis (1963) reported on the geology and hydrology of the El Reno and Whitehorse Groups which include the Duncan Sandstone and the Rush Springs Sandstone. Wood and Burton (1968) discussed the geology and hydrology of the Garber Sandstone, Wellington Formation, and Hennessey Shale. Fairchild and others (1982) investigated the hydrology of the Arbuckle Mountains area, and their report includes aquifer test data for the Arbuckle and Simpson Groups. The National Uranium Resource Evaluation Program collected detailed geochemical data for the Permian aquifers in the Lawton quadrangle. Statistical analyses and maps of these data are in two reports (Union Carbide Corporation, 1978 and 1980). Green and Al-Shaieb (1981) investigated the occurrence of fluoride in ground water within Comanche County, and Back (1985) studied the geochemistry of nitrate and fluoride in the Post Oak Aquifer.

Geology

The Hydrologic Atlas by Havens (1977) is the major source of information on the geology of the Lawton one-by-two degree quadrangle, which includes Comanche County. It is a compilation by J.S. Havens and R.O. Fay of the earlier studies listed here. Chase (1954) mapped facies of the Post Oak Conglomerate around the Wichita Mountains. Chase, Frederickson, and Ham (1956) summarized the geology of the Wichita Mountains and the surrounding area and discussed the nomenclature of the formations. Stith (1968) described the mineralogy and petrography of the Permian Hennessey Shale to the northwest of Comanche County. The evaluation of the uranium resources in this area includes reports by Shelton and Al-Shaieb (1976), Al-Shaieb and others (1977 and

1982), and Al-Shaieb (1978) which summarize the Pennsylvanian and Permian stratigraphy and sedimentology. Stone (1977) mapped the areal distribution of grain sizes in the Permian Post Oak Conglomerate, and Al-Shaieb and others (1980) investigated the petrology and diagenesis of this formation. Revisions to the geology of the eastern Wichita Mountains are discussed by Gilbert and Donovan (1982). Collins (1985) described the Permian rocks in the Meers Valley north of the Wichita Mountains. Bridges (1985) mapped in detail the Lower Permian rocks in Comanche County and revised their stratigraphy.

Surficial geology of the Arbuckle and Timbered Hills Groups is discussed by several authors. Wilmott (1957) studied the stratigraphy and sedimentation of the Reagan Formation and determined the nature of its contact with the overlying Honey Creek Formation. Nelms (1958) mapped the Fort Sill Formation and established its lithologic boundaries. The lithology and stratigraphy of the Honey Creek Formation were described by Fox (1958). Barthelman (1969) and Brookby (1969) mapped Arbuckle Group outcrops north of the Wichita Mountains, and Ragland (1983) described the sedimentary geology of the Cool Creek Formation in the Slick, or Limestone, Hills.

Subsurface stratigraphy of Comanche County was compiled by Hayes (1952), McDaniel (1959), and Culp (1961). Summaries of the subsurface and regional stratigraphy of Oklahoma according to rock system were written of the Ordovician by Twenhofel (1954), of the Carboniferous by Fay and others (1979), of the Mississippian by Craig and Varnes (1979), of the Pennsylvanian by Frezon and Dixon (1975), and of the Permian by MacLachlan (1967) .

The structural history of the Wichita Mountains was discussed by Ham, Denison, and Merritt (1964). Hoffman, Dewey, and Burke (1974) and Burke and Dewey (1973, Figure 10) interpreted this structural history in terms of plate tectonics. Brewer (1982) provided the results of a deep seismic survey by COCORP (Consortium for Continental Reflection Profiling) which indicate the subsurface extent of the Meers, Mountain View, and other faults both north and south of the Wichita Mountains.

Computer Modelling

Konikow and Bredehoeft (1978) developed a numerical model that simulates solute transport in ground water by solving a solute transport equation and a ground-water flow equation. Tracy (1982) modified the Konikow model to allow for adsorption and first-order reactions of the solute. Further modifications of the ground-water flow part of the model were made by Kent and others (1986a), and an interactive (i.e., prompting) preprocessor program was added by Kent and others (1986b) to facilitate input of data into the model.

Kent and others (1982) applied both a numerical model by Trescott and others (1976) and the Konikow model to the Garber-Wellington Aquifer, and Duckwitz (1983) applied those models to both that aquifer and a contaminant plume in New York and compared the results with those from analytical models. Data were put into the Konikow model with an interactive program. The Trescott model was used to study other aquifers in Oklahoma: the alluvial aquifer along the North Fork of the Red River (Kent, 1980); the Enid terrace aquifer (Beausoleil, 1981; Kent, Beausoleil, and Witz, 1982); the Elk City sandstone aquifer (Lyons, 1981; Kent, Lyons, and Witz, 1982); and the Washita River alluvium

(Schipper, 1983; Patterson, 1984; and Kent and others, 1984). These studies were used to predict water-level changes, maximum annual yields, and maximum legal pumping allocations from the aquifer.

CHAPTER II

GEOLOGY AND SOILS OF COMANCHE COUNTY

Geology

The geology in the county (Figure 3) consists of Cambrian igneous rocks in the Wichita Mountains, Cambrian and Ordovician limestones and dolomites in the Slick Hills, and Permian red-bed conglomerates, sandstones, and shales on the plains. Within the creek valleys is Quaternary alluvium of sand, silt, and clay.

The following descriptions of the geology are summarized from Chase and others (1956), McDaniel (1959), Ham and others (1964), MacLachlan (1967), and Havens (1977).

The Wichita Mountains are composed of Precambrian and Early and Middle Cambrian gabbros, granites, and rhyolites, the oldest rocks in the area (Ham and others, 1964). The Raggedy Mountain Gabbro Group and the Wichita Granite Group were intruded as sills and plutons and, together with the Carlton Rhyolite Group, comprise a basement rock sequence about 20,000 ft (6100 m) thick. The Raggedy Mountain Gabbros total 10,000 ft (3000 m) in thickness and cover about 5000 square miles (13,000 km^2). The Wichita Granites are from 600 to 15,000 ft (180 to 4600 m) thick (Havens, 1977); the outcrop area of these groups is 300 mi^2 (800 km^2). The rhyolites comprising the Carlton Group are as much as 4500 feet (1370 m) thick. These were laid down as extensive ash flows covering 17,000 square miles (44,000 km^2).

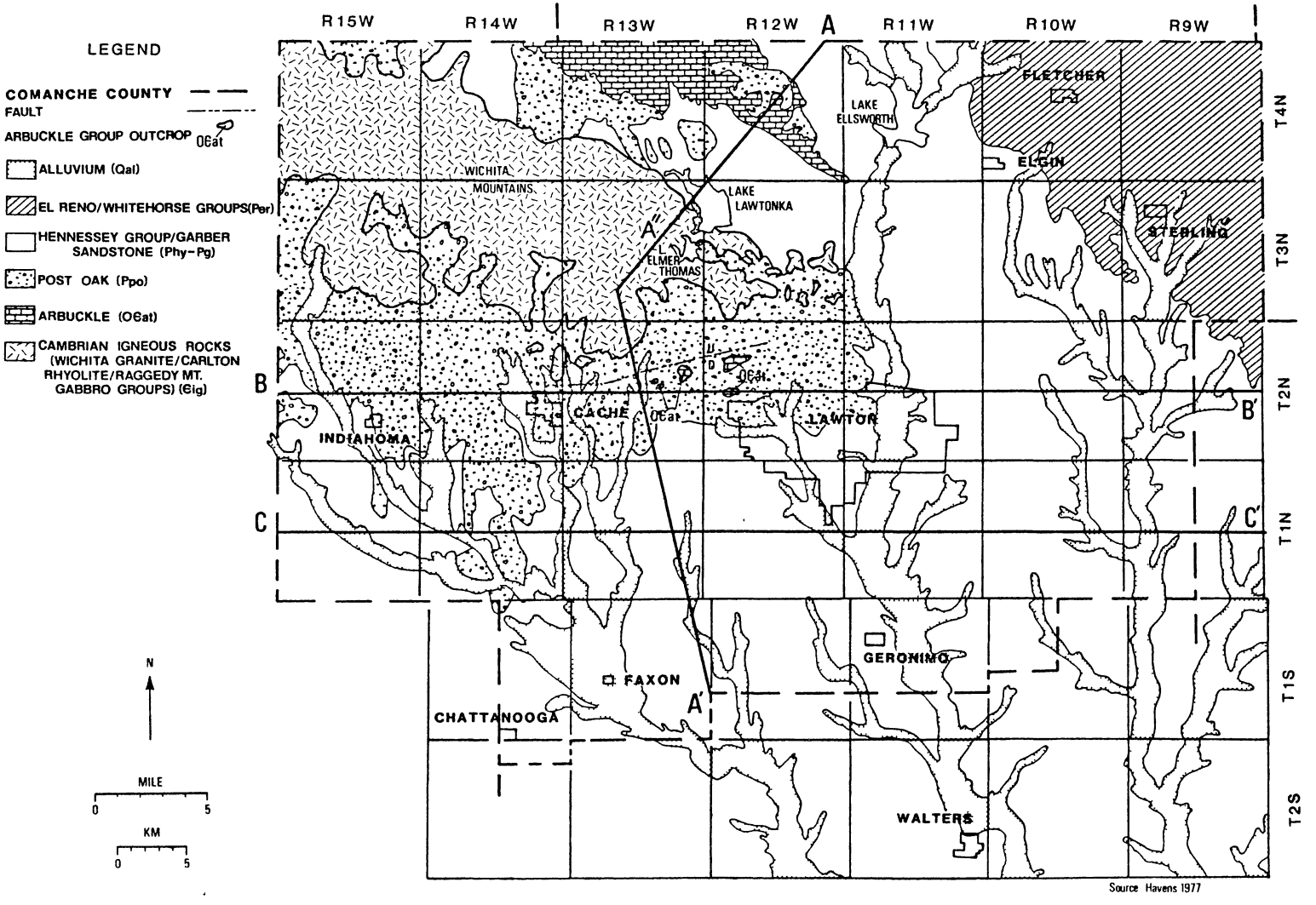

Figure 3. Geologic Map of Comanche County

Non-igneous Cambrian formations in Comanche County are the Reagan Sandstone and the Honey Creek Formation of the Timbered Hills Group and the Fort Sill Formation, Royer Dolomite, and Signal Mountain Formation of the Arbuckle Group (Figure 4). This latter group includes Ordovician rocks described below; these descriptions are summarized from Chase and others (1956).

The Upper Cambrian Reagan Sandstone records a transgression over the Carlton Rhyolite on which it lies unconformably. It ranges in thickness from 0 to 150 ft (46 m), in association with varied paleogeographic relief on the rhyolite. The lithologies include arkose and conglomerate at the base, overlain by coarse-grained quartzites and some shale, topped by glauconitic, calcareous, and ferruginous sandstones.

The Reagan grades into the glauconitic and ferruginous limestones of the Honey Creek Formation. In the Wichita Mountains, glauconitic and calcareous sandstones are at the base of this formation, which is also marked by the appearance of a trilobite fauna. The Honey Creek is from 80 to 327 ft (24 to 100 m) thick.

The Fort Sill Formation of the Arbuckle Group contains thin, sandy, shaly, oolitic, fossiliferous limestones. It is conformable to the Honey Creek. The Royer Dolomite within the Fort Sill lacks fossils and crops out in Kiowa County with thicknesses of 195 to 220 ft (59 to 67 m) but is absent in some localities.

The Signal Mountain Formation consists of coarsely crystalline, fossiliferous limestones and is 245 to 400 ft (75 to 122 m) thick. Flat-pebble conglomerates are characteristic and mark the base and top

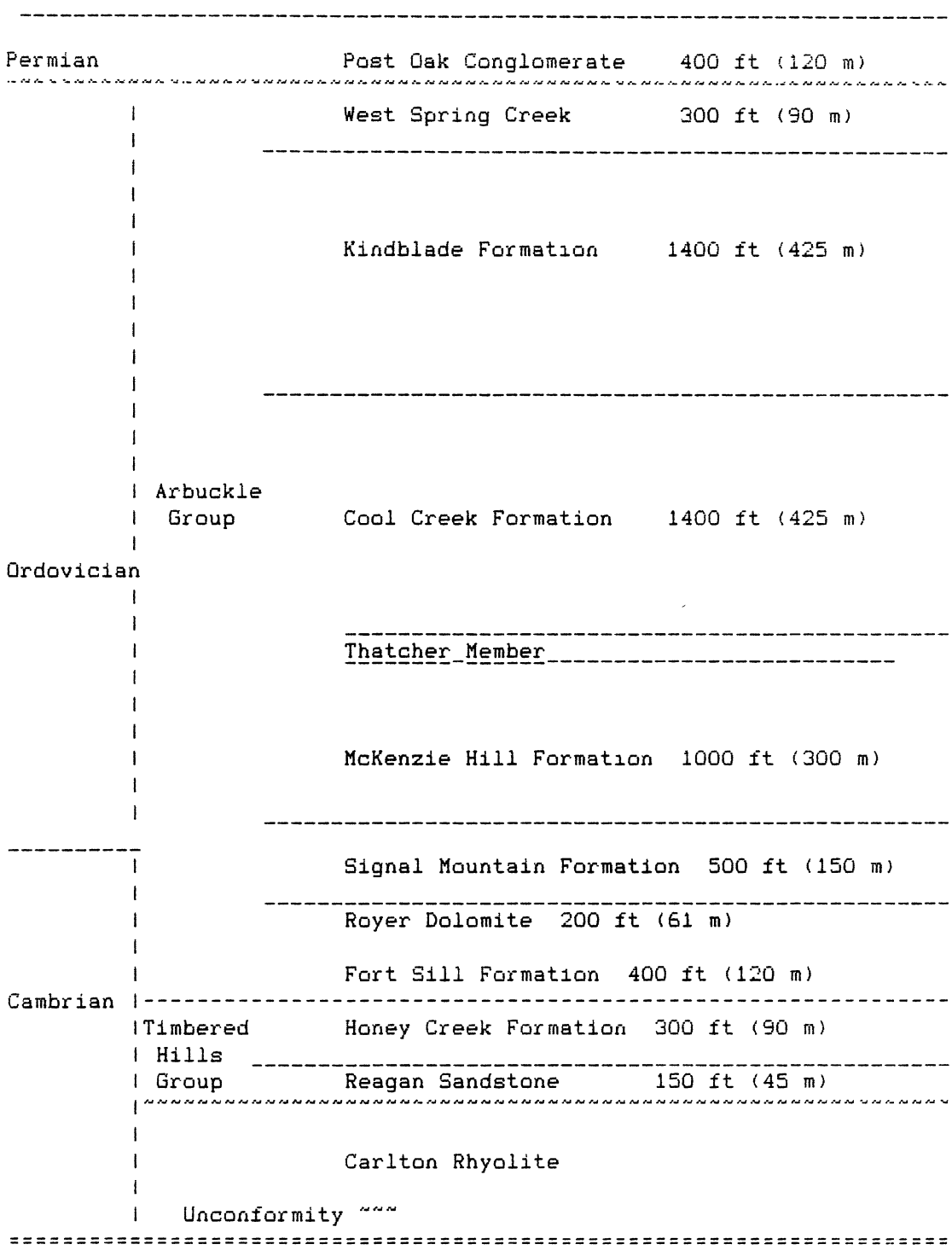

Source: Modified from Ragland, 1983, p.112.

Figure 4. General Stratigraphic Column of the Arbuckle and Timbered Hills Groups in the Slick Hills

of the formation. Beds range from less than an inch to several feet thick.

The McKenzie Hill, Cool Creek, Kindblade, and West Spring Creek Formations comprise the Lower Ordovician section of the Arbuckle Group. Their total thickness in the Wichita Mountains is 3150 ft (960 m; Chase and others, 1956).

The fossiliferous McKenzie Hill Formation contains a lower 400-foot-thick (122 m) limestone unit with fine- and medium-grained layers and a 600-foot-thick (183 m) cherty upper unit with intraformational conglomerates and algal limestones.

The 1100-foot-thick (335 m) Cool Creek Formation consists of fine- and medium-grained limestones and dolomites containing chert, oolites, quartz sand, intraformational conglomerates, and algal layers. A sandy layer marks the base, and the lower 700 feet (213 m) are unfossiliferous.

The overlying Kindblade Formation consists of about 1400 ft (427 m) of fine-grained fossiliferous limestones. Above these layers are another 1400 ft (427 m) of limestones and dolomites which comprise the West Spring Creek Formation. This formation is not well exposed in the Wichita province.

Above the Arbuckle Group are the Middle Ordovician Simpson Group and Viola Limestone. The formations comprising the Simpson -- the Joins, Oil Creek, McLish, Tulip Creek, and Bromide -- each consists of a sandstone or thin conglomerate at the base with limestones and shales above (Decker and Merritt, 1941). The lower formations have been eroded and are covered by Permian rocks in the Wichita Mountain area, but the top 86 ft (26 m) of the Bromide Formation crop out with the

Viola in Kiowa County (Chase and others, 1956) to the north of the Wichita Mountains. The Simpson Group and Viola Limestone are not present in the subsurface of southern Comanche County because of erosion from the Wichita uplift (McDaniel, 1959, Plate II).

Silurian, Devonian, Mississippian, and Pennsylvanian rocks are not exposed in Comanche County. They occur in the subsurface on the south flank of the Anadarko Basin in the northeast corner of the county and in the northwest part of the Marietta Basin in the southeast part of the county (McDaniel, 1959).

Permian rocks conformably overlie Pennsylvanian strata and comprise the surficial geology in Comanche County (MacLachlan, 1967). The Lower Permian (Wolfcampian) Wichita Formation of sandstone and mudstone occurs in the subsurface south of the Wichita Mountains. Above this formation are the Middle Permian (Leonardian) Wellington Formation and its equivalent, the Post Oak Conglomerate, the Garber Sandstone, the Hennessey Shale, and the El Reno Group. All formations above the Wichita crop out around the Wichita Mountains. Upper Permian formations cropping out in Comanche County are the Marlow Formation and the Rush Springs Formation (MacLachlan, 1967; Havens, 1977). The stratigraphic positions of these formations are discussed in Chapter V.

Except for small Quaternary terrace deposits and alluvium in the creek valleys, sediments younger than Permian are not recorded in Comanche County.

North-south cross-sections A-A' (Figure 5) and east-west cross-sections B-B' (Figure 6) and C-C' (Figure 7) show schematically the relationship of the formations in the subsurface. The Wichita Mountains are a block of igneous rocks bounded by steep faults.

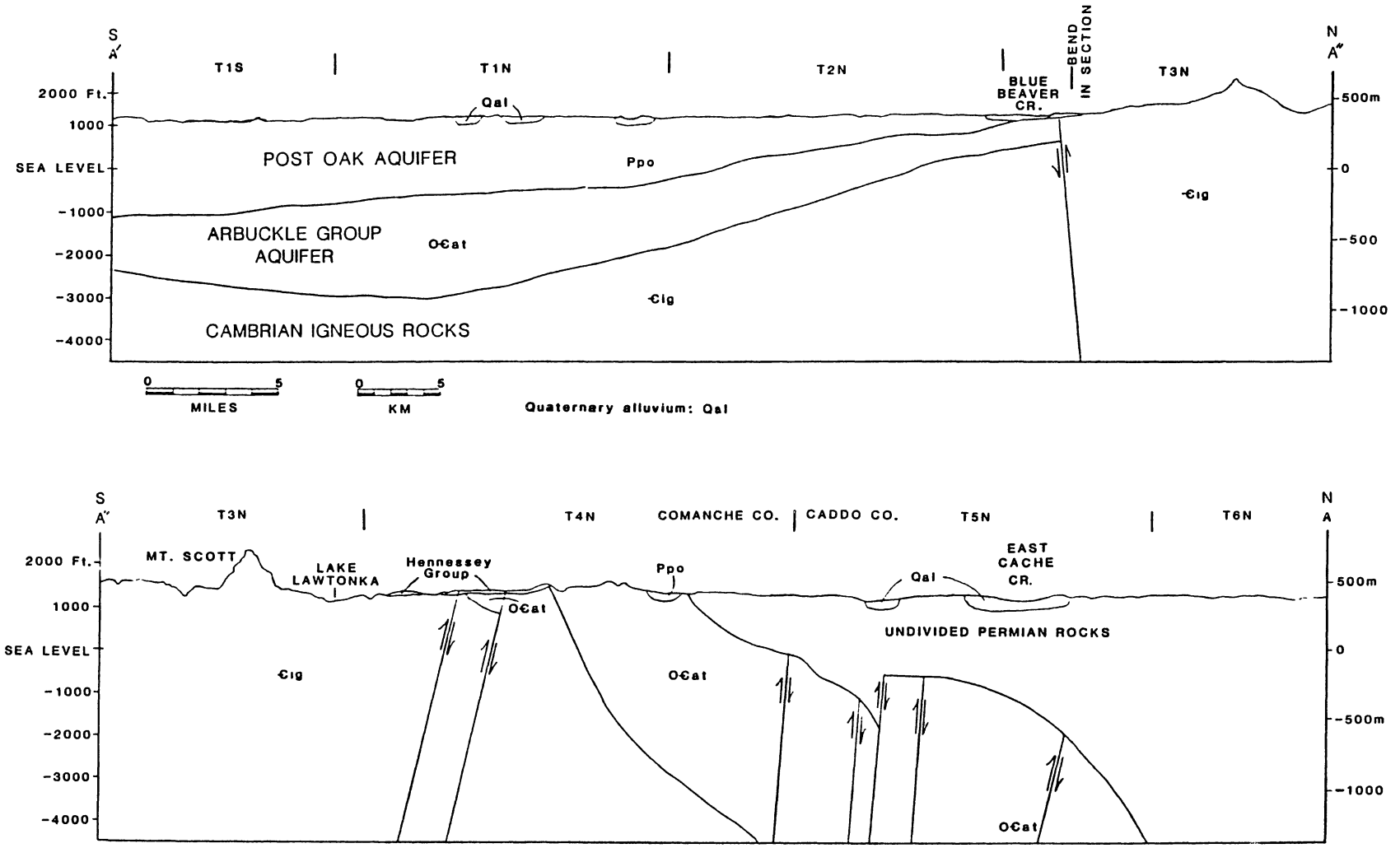

Figure 5. Geologic Cross-Section A-A'

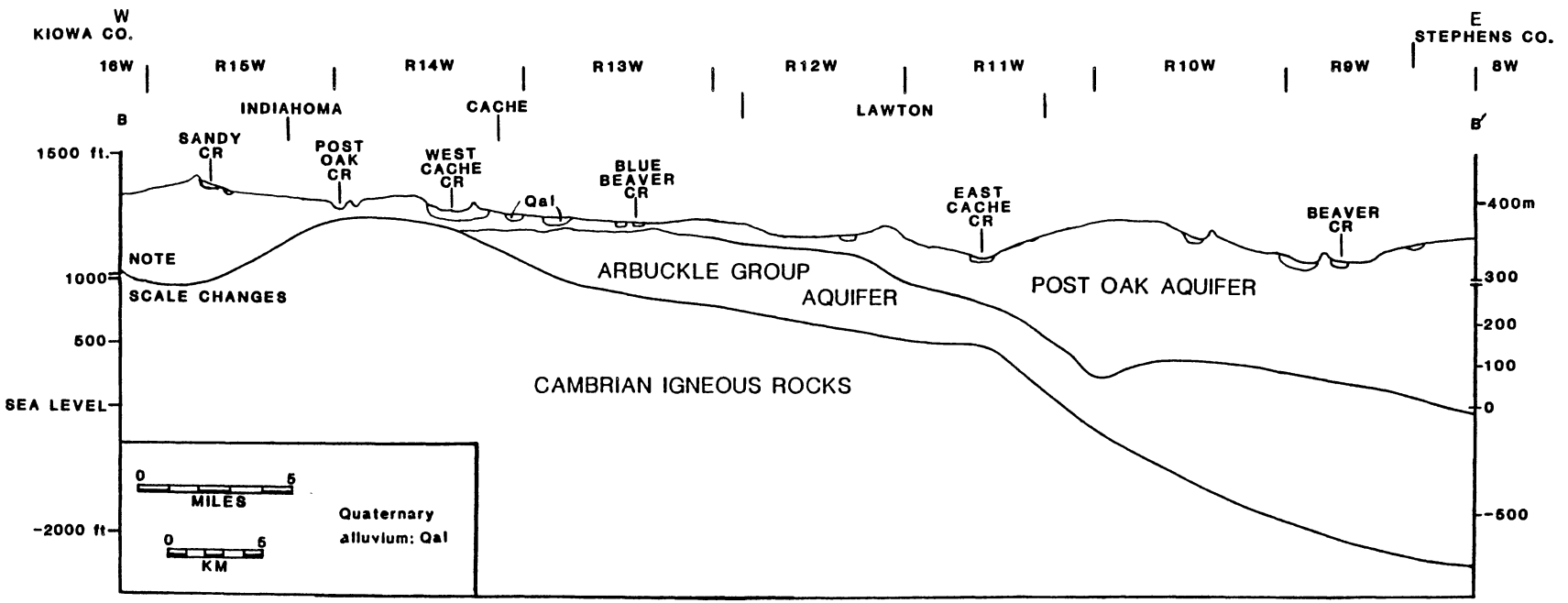

Figure 6. Geologic Cross-Section B-B'

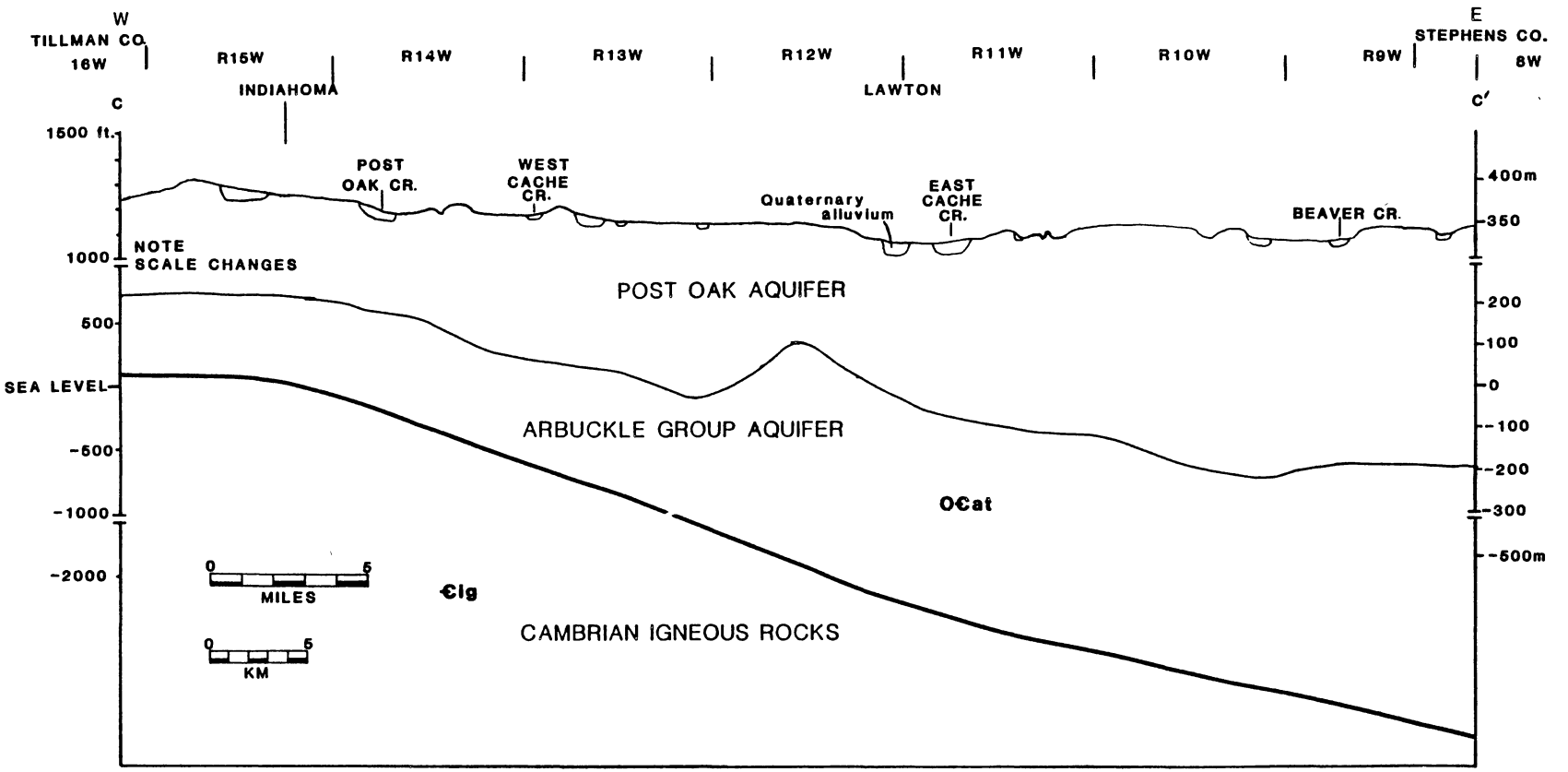

Figure 7. Geologic Cross-Section C-C'

Overlying the igneous rocks are the Arbuckle and Timbered Hills Groups of limestones and dolomites. These dip in the direction of the Anadarko Basin in the north and toward the Marietta Basin in the south. The Timbered Hills and Arbuckle Groups are considered together as the Arbuckle Group Aquifer. The steep fault separating this aquifer from the igneous rocks to the north is shown dashed on the geologic map (Figure 3) because it is covered by the Post Oak Conglomerate.

Overlying the Arbuckle Aquifer in the north are the Permian Hennessey Shale, Garber Sandstone, and El Reno and Whitehorse Groups. The Permian Post Oak Conglomerate, Hennessey Shale, and Garber Sandstone lie on the Arbuckle Aquifer to the south of the Wichita Mountains. Because these Permian formations are undifferentiable in the subsurface, they are not designated separately on the cross-sections. In the subsurface south of the Wichita Mountains, these formations are considered together as the Post Oak Aquifer.

Soils

Soils having similar profiles, or sequences of horizons, constitute a soil series, and distinctive patterns of soils in a landscape are grouped as soil associations. Within Comanche County distinctive soils have developed on the red beds, limestones, and alluvium (Figure 8).

Because the soil associations are characteristic of the underlying rocks, the soil descriptions and maps in the soil survey (Mobley and Brinlee, 1967) were used to locate wells in either the Post Oak or alluvial aquifers. For example, Port soils, which occur on flood plains, indicate alluvium, whereas Windthorst soils, which formed from

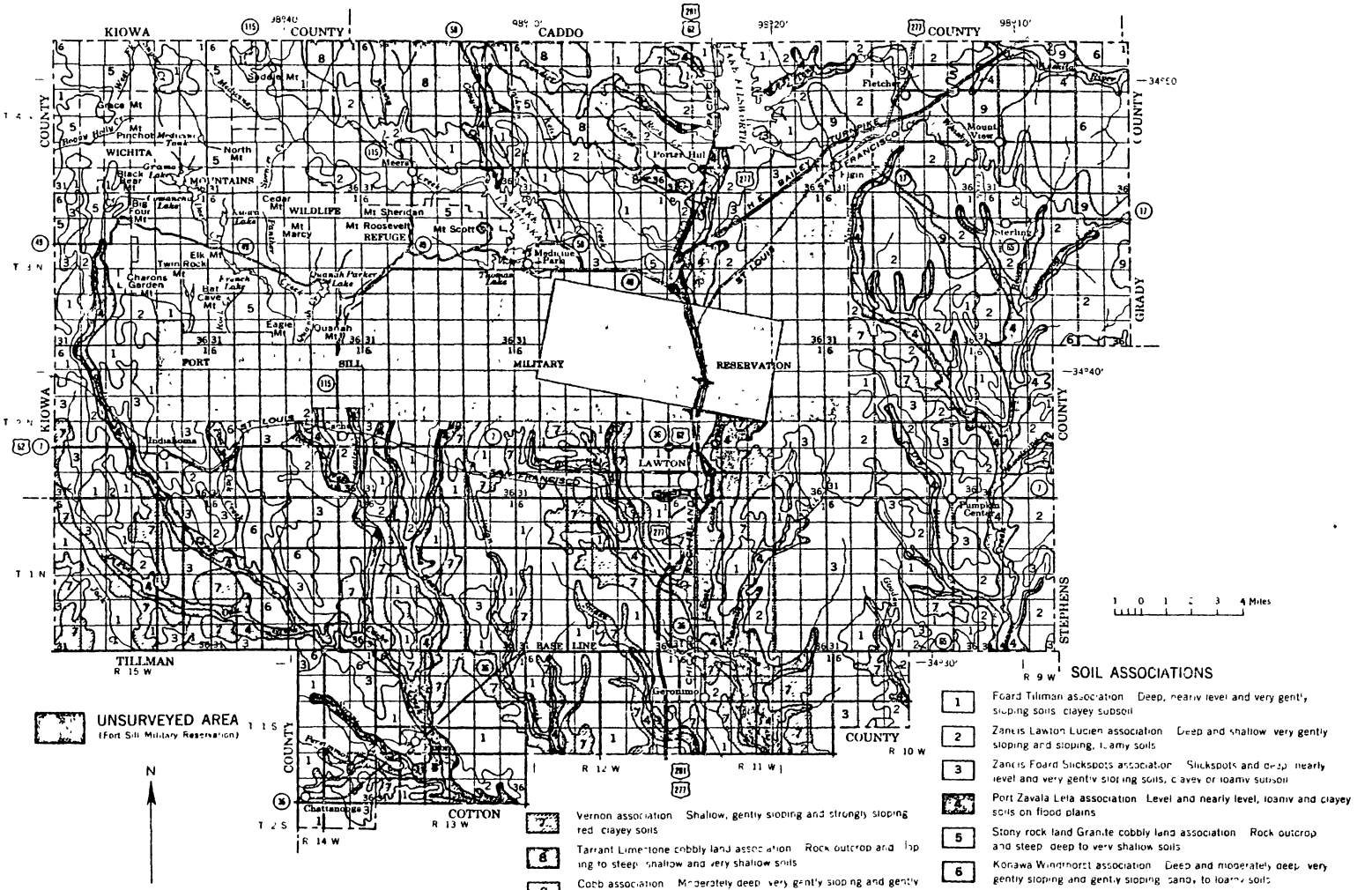

Figure 8. Soils Map of Comanche County (from Mobley and Brinlee, 1967)

granitic material eroded from the Wichita Mountains, indicate the Post Oak Aquifer. The type of soil in an area would affect the permeability and recharge rate: clayey soils would lower the permeability and allow more surface runoff. The most extensive soil association is the Foard-Tillman, which covers about 120,726 acres (48,858 hectares), or 18 percent of the county. The following descriptions are summarized from Mobley and Brinlee (1967).

Foard soils are deep, level, dark brown soils covering uplands. They formed on calcareous red-bed clays. The five- to ten-inch (13 to 25 cm) thick surface layer is calcareous.

Tillman soils are deep, gently sloping, reddish-brown clay loams. The five- to ten-inch thick surface horizon overlies a heavy, clayey subsoil which is calcareous below 15 inches (38 cm). The Waurika series also occurs in this association. These soils are level grayish-brown silt loams developed from Permian shales on uplands. The clayey subsoil lowers the permeability.

The Zaneis-Lawton-Lucien association occupies uplands and covers 132,700 a (53,700 ha), or 19 percent of the county. Zaneis soils are gently sloping, reddish-brown loams with a fine-textured subsoil. Lawton soils are deep, brown, non-calcareous, loamy, and granitic. Sand and gravel lenses are common in the profile. These soils formed from granitic "outwash" (Mobley and Brinlee, 1967, p.3) and occur along ancient drainageways. Lucien soils are shallow, reddish-brown sandy loams on fine-grained sandstone.

Foard and Zaneis soils form an association with slickspots, which are small areas having much clay in the soil profile.

On flood plains is the Port-Zavala-Lela association, which occupies 76,800 a (31,080 ha), or 11 percent of the county. Port soils are brownish loams or clay loams with a non-calcareous surface layer and a calcareous subsoil. Zavala soils are found in the northeastern part of the county; they are brown, non-calcareous fine sandy loams. Lela soils are dark, non-calcareous clays.

On the uplands in the Wichita Mountains is the Stony rock land-Granite cobbly land association. The Stony rock land is essentially granite outcrops and shallow, stony soils. The Granite cobbly land consists of deep, brown clay loams with much gravel and cobblestones; these soils occur on hills and ridges. This association covers 86,000 acres (34,800 ha), or 12 percent of the county.

The Konawa-Windthorst association covers 25,000 a (10,100 ha), four percent of the county, in the northeastern and southwestern parts of the county. These soils occur on sandy uplands. Konawa soils are deep, brown, and sandy with a reddish sandy clay loam subsoil. These soils formed on ancient alluvium. Windthorst soils are brown sandy loams with a sandy clay subsoil which formed on granitic "outwash" (Mobley and Brinlee, 1967, p.17).

The Vernon association of soils are shallow, red calcareous clays and clay loams found on slopes. These soils formed on clayey alluvium and colluvium.

The Tarrant-Limestone cobbly land association occurs on the stony ridges of the Slick, or Limestone, Hills. The Tarrant soils are thin (3 to 12 inches), dark brown silt loams between outcrops of limestone. The cobbly land is gravel and cobbles derived from the limestone outcrops.

The Cobb association is prairie soils: brown, fine sandy loams with a sandy clay loam subsoil. These soils cover 13,500 a (5460 ha) in the northeastern part of the county.

CHAPTER III

METHODOLOGY

Aquifer data were obtained from drillers' logs, field measurements, and the literature (Havens, 1977 and 1983; Union Carbide Corporation, 1978; Fairchild and others, 1983). Sources of well logs and unpublished data were the open files of the Oklahoma Water Resources Board, U.S. Geological Survey, Fox and Drechsler Engineers, Poe and Associates Engineers, the Layne-Western Company, and the town of Indiahoma.

Field Methods

Field methods included measurement of water levels in domestic wells with an electric tape measure accurate to a tenth of a foot and six electric resistivity surveys (see Figure 22) which determined the depth to the water table and the thickness of the alluvium.

A Bison model 2350 Earth Resistivity Meter was used in the resistivity surveys. Current, I, and potential, P, electrodes were arranged in the Wenner configuration in which the distances between each pair of electrodes, the A-spaces, are equal, with the P electrodes within the I electrodes (Figure 9). The current introduced into the alluvium through the outer, I, electrodes causes a potential drop, V, between the two P electrodes which is measured by the Bison meter as the apparent resistivity, ρ_a (Figure 10). The effects due to changes in

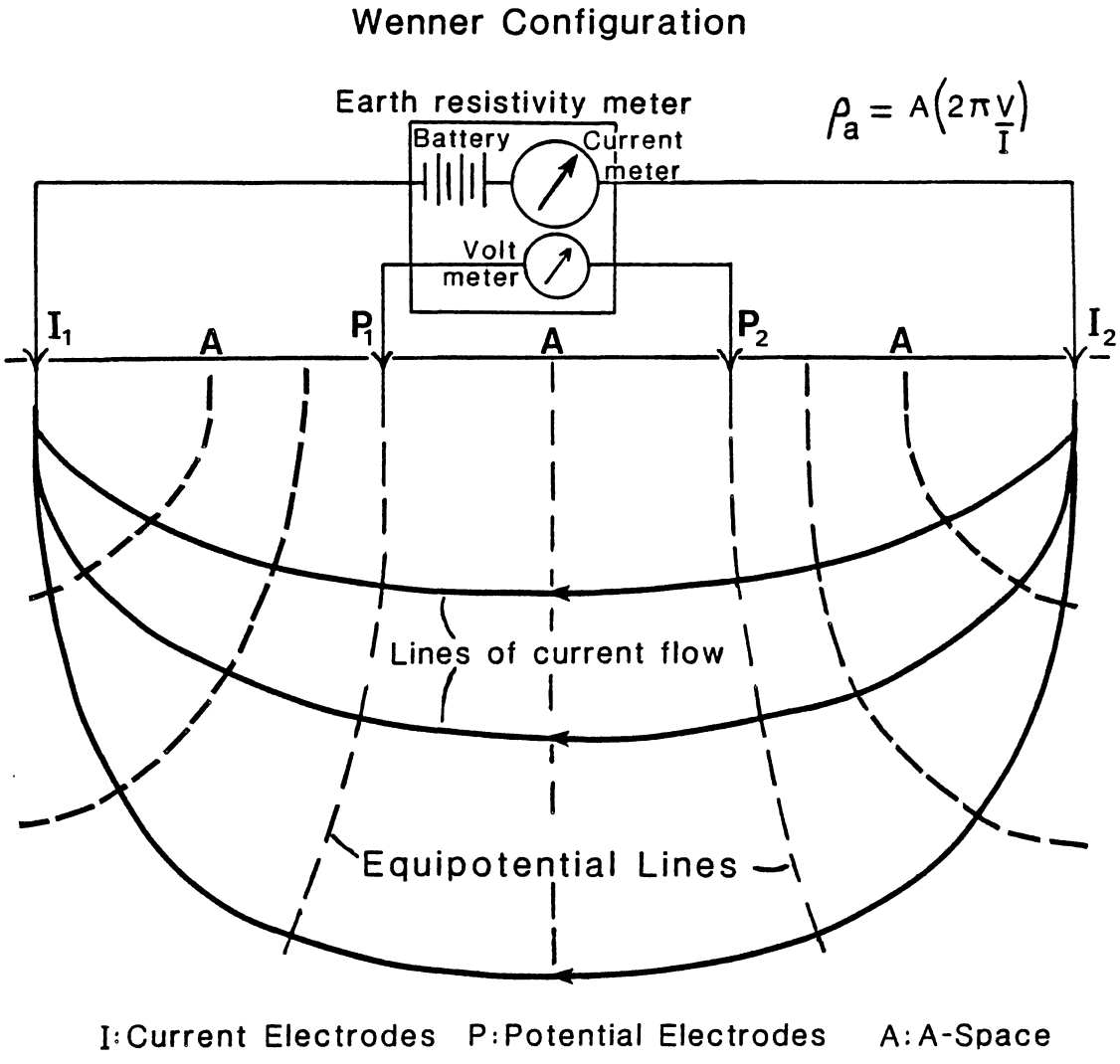

Figure 9. Wenner Configuration of Electrodes to Measure Apparent Resistivity

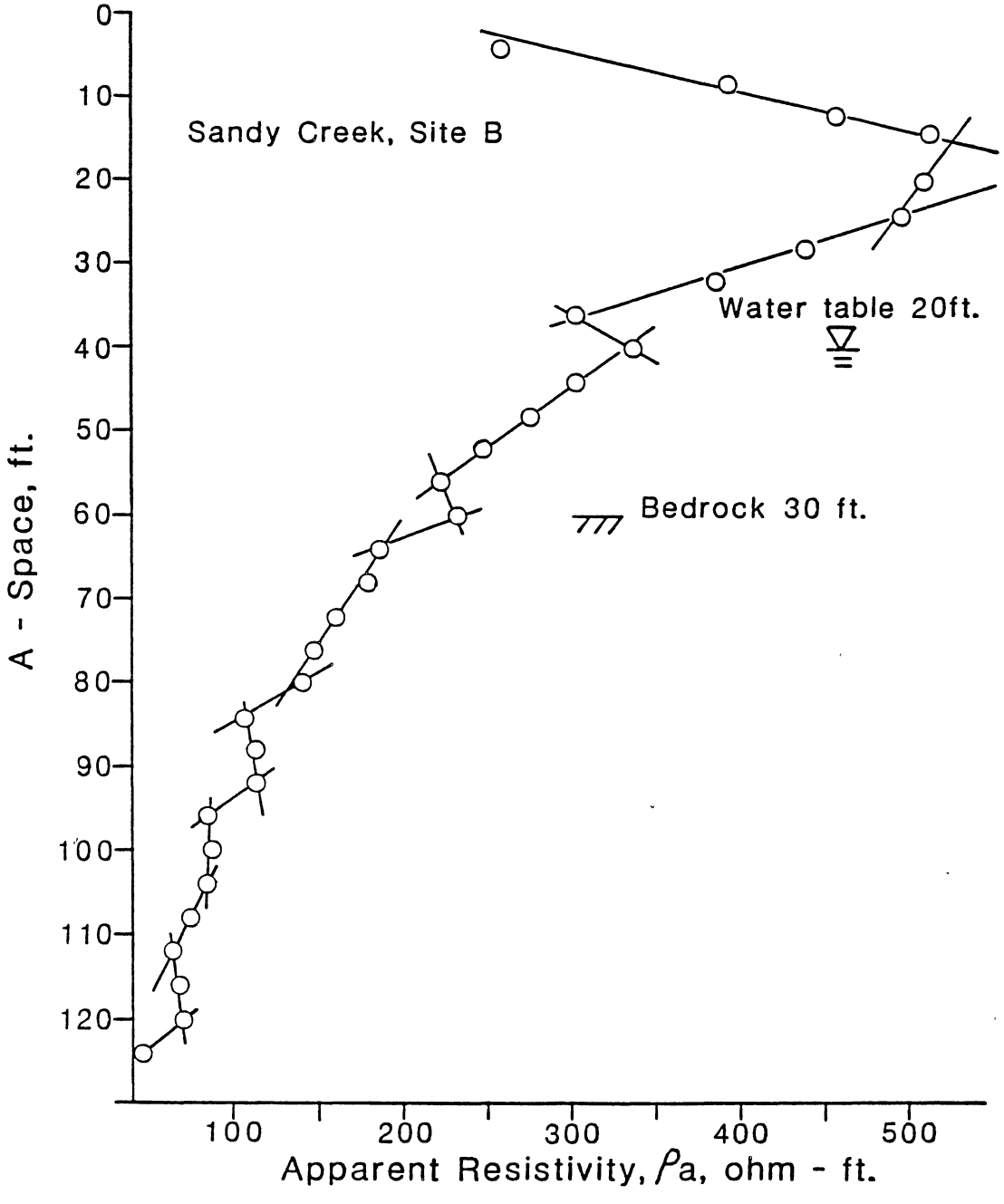

Figure 10. Apparent Resistivity Profile for Sandy Creek Site B

electrode spacing and current flow cancel out with the measurement of apparent instead of true resistivity (Bison Instruments, 1969).

The field procedure, resistivity sounding, involved expanding the electrode array parallel to the stream channel; variations in ρ_a with depth are determined by this method. Graphs of A-spacing versus apparent resistivity exhibit deflections indicating the water table and bedrock (Figure 10 and Appendix A). Comparisons with the water levels in nearby wells at the Sandy Creek and Post Oak Creek sites indicate that the A-space is approximately equal to twice the depth of current penetration. The assumption that A-spacing equals depth is not always valid (Zohdy and others, 1974, p.20; Bison Instruments, 1969, p.15).

Well Data

The extent, thickness, saturated thickness, permeability, transmissivity, and yield of the aquifers were derived from well data (Appendix B). A well was assigned to an aquifer according to its location on the geologic map or soil survey and its depth. Shallow wells on flood plains and in areas where soils were derived from alluvium were assigned to the alluvial aquifer (see Soils, Chapter II). Wells in those areas where the soils were derived from red beds, such as northwest of Faxon, were assumed to be in the Post Oak Aquifer. The depth of a well was compared with the elevation of the top of the Arbuckle Group on the structural contour map of Havens (1983, Plate 1) to determine whether the well reached the Arbuckle.

For the alluvium and Post Oak Aquifer permeabilities were obtained from lithologic well logs by using a relationship between grain size and permeability developed by Kent and others (1973; Figure 11).

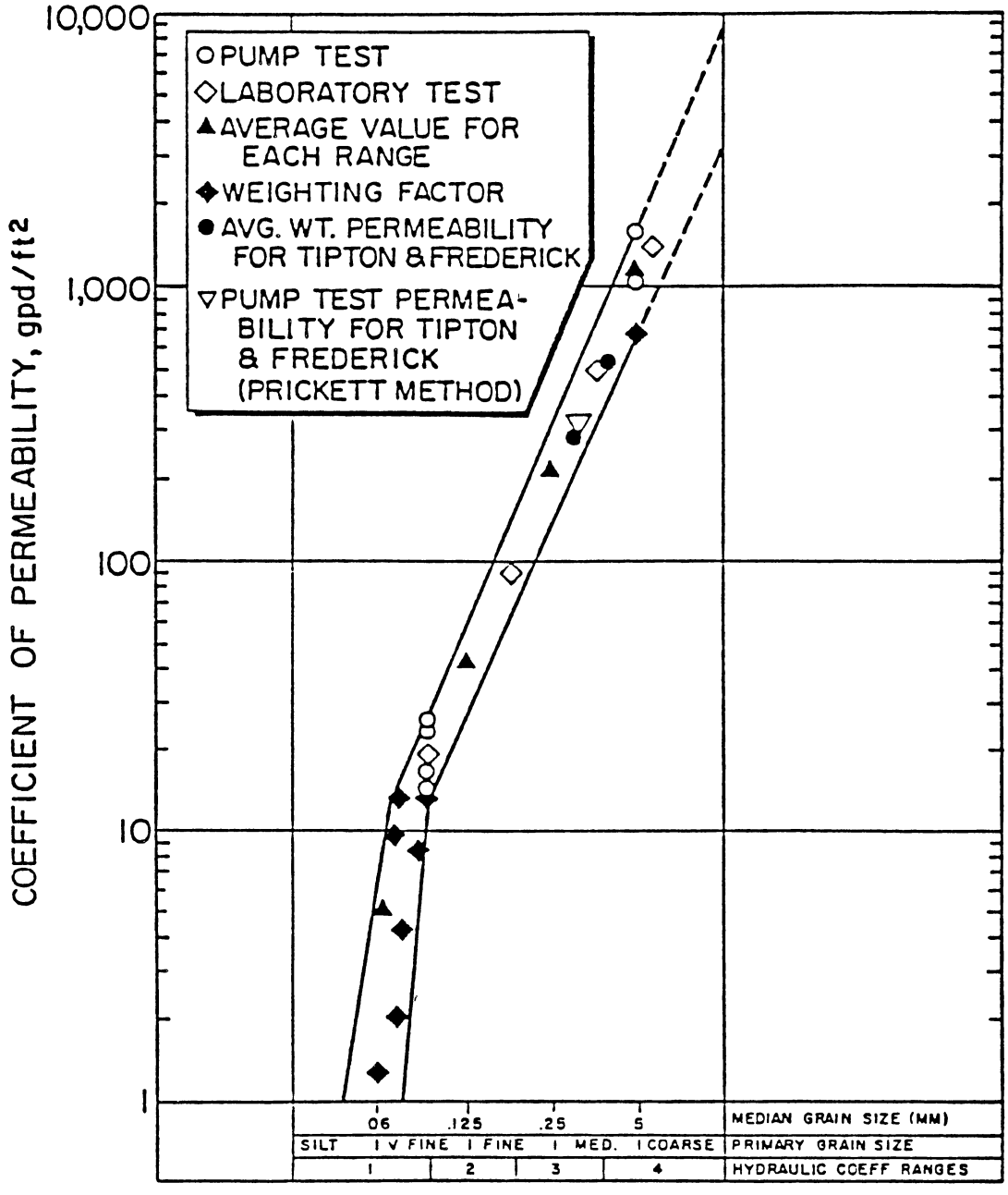

Figure 11. Relationship Between Permeability and Grain Size (from Kent, 1973, and Patterson, 1984, p.80)

Hemann (1985) confirmed the validity of this grain-size-permeability relationship. This method could not be used for the Arbuckle Aquifer because ground-water flow is through fractures and solution openings.

Each layer in the aquifer was assigned to a hydraulic coefficient (permeability) range according to its primary grain size as listed in a driller's log. From the envelope permeabilities a range of total permeabilities for the aquifer was obtained (Table VI, Appendix C). A description of this method and an example of the calculations are in Appendix C. The product of saturated thickness and the permeability is the transmissivity. Lithologic and permeability data for wells in the alluvial and Post Oak aquifers are in Tables VI and VII, Appendix C.

Production and Aquifer Test Data

For all three aquifers another method for calculating transmissivities, permeabilities, and yields used production test data from drillers' logs. Walton (1970, p.315) derived a relation between transmissivity and specific capacity, the well yield per drawdown:

$$\frac{Q}{s} = \frac{T}{264 \log \left(\frac{T\,t}{2693\, r^2\, S} \right) - 65.5} \qquad (3\text{-}1)$$

where $\frac{Q}{s}$ = specific capacity, gpm/ft,

Q = discharge or yield, gpm,

s = drawdown, ft,

T = transmissivity, gpd/ft,

S = storativity of a confined aquifer or specific yield of an unconfined aquifer, fraction,

r = nominal well radius, ft,

t = duration of pumping, minutes.

This equation provides the theoretical specific capacity of a fully penetrating well in an artesian aquifer assumed to be homogeneous, isotropic, nonleaky, and infinite in areal extent; other assumptions are that the well loss is negligible and that the effective well radius is equal to the nominal well radius. Where these assumptions are not valid, the actual transmissivity or permeability is greater than the value determined from specific-capacity data. For example, instead of 100 percent, well efficiency was assumed to be only 60 percent (Schipper, 1983, p.55) which required that the transmissivity and permeability be increased by a factor of 1.6.

A short program to calculate transmissivity from Walton's formula is listed in Appendix D. A graph of T versus Q/s for given values of S, r, and t (Figure 12) shows that uncertainties in estimating storativity do not affect greatly the values of transmissivity and specific capacity. Lower specific capacity values result from longer production tests (see Walton, 1970, Fig. 5.10b, p.319); the lengths of the tests providing the data were not uniform, however.

Using a maximum drawdown value in Walton's formula led to underestimates of transmissivity and yield. The maximum theoretical drawdown was assumed to be 70 percent of the saturated interval above a five-foot well screen (Johnson, 1966, p.108). The average saturated interval, the difference between static water level and well depth, of the unconfined alluvial aquifer is 16 feet (4.9 m); the maximum drawdown then would be eight feet (2.4 m). For the Post Oak Aquifer the average saturated thickness is 20 ft (6.1 m), and the maximum drawdown would be 11 ft (3.3 m). For the confined Arbuckle Aquifer the maximum theoretical drawdown was assumed to be 70 percent of the average well

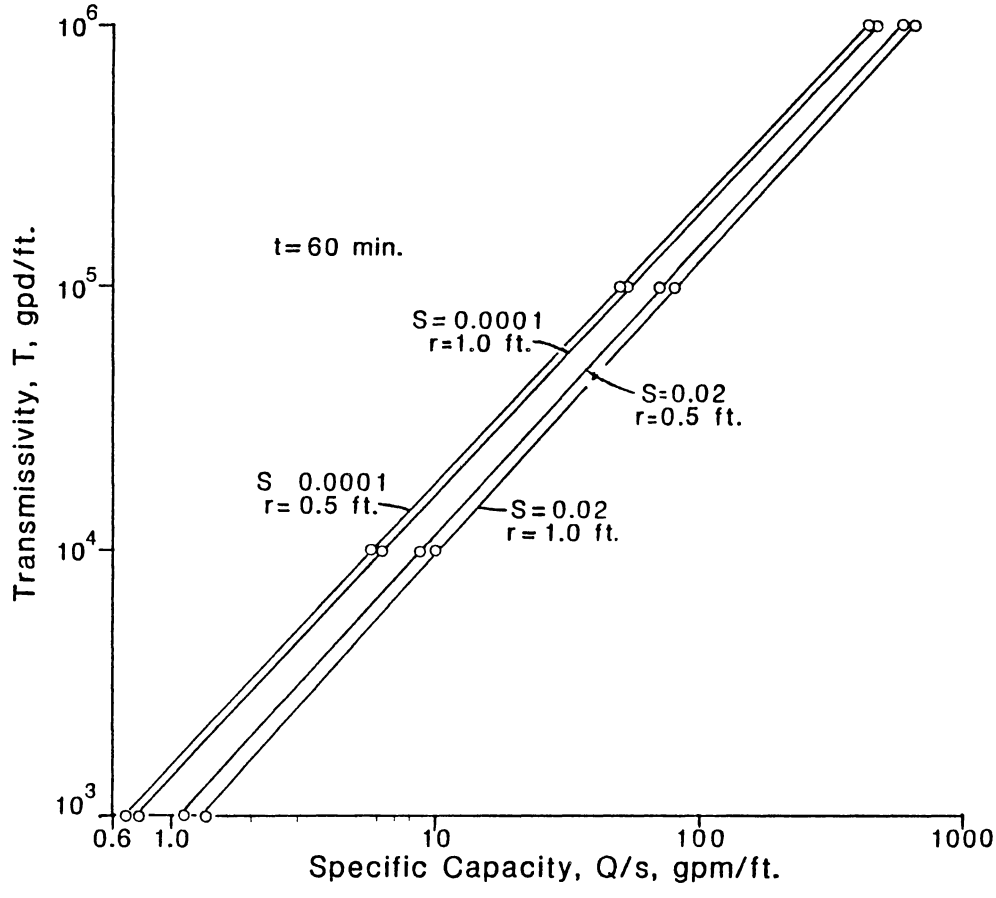

Figure 12. Relationship Between Transmissivity and Specific Capacity (Modified from Walton, 1970, p.316)

penetration, or 350 ft (107 m). Hydraulic data for the three aquifers are in Table VIII, Appendix E.

Stream Discharge Data

To determine the recharge to the alluvial aquifer and to ascertain the relationship between ground water in the alluvium and surface water, stream discharge data published by the U.S. Geological Survey (1969-1985) were used in a computer program called RECHARGE, which was developed by Pettyjohn and Henning (1979) and is described in Appendix F. This program calculates by three methods the baseflow, that portion of the stream discharge contributed by ground-water runoff (Figure 55, Appendix F). Miller (1984) described the methods, fixed interval, sliding interval, and local minima, and applied them to the Little Washita River watershed within and to the northeast of Comanche County. He found that they yield baseflow values within a 10 percent agreement, and that baseflow depends on antecedent precipitation. Similar to the Blue Beaver Creek basin, the Little Washita River watershed is characterized by rocks of relatively low permeability, clayey soils, and a subhumid climate. The RECHARGE program demonstrates the direct relationships between baseflow and recharge and between streamflow and evapotranspiration, assuming that inflow to the basin is by precipitation only, and that outflow is by stream discharge and evapotranspiration. These are valid assumptions for Blue Beaver Creek because most of the basin lies within the Fort Sill Military Reservation where there is no irrigation and no facilities upstream which discharge effluent to the stream.

Descriptions of Lineament Analyses

An approach for estimating the possible distribution of well yields in both the Post Oak and Arbuckle aquifers involved a lineament analyis of aerial photographs. Ground-water flow in the Arbuckle is through fractures and solutional openings, and fracture flow was assumed to occur in the Post Oak, also. Areas with more fracturing presumably would have more flow and greater well yield; to locate the fractures aerial photographs were examined by two methods, which are described in more detail in Appendix G.

For one method it was assumed that lineaments in the Post Oak and Permian rocks above the Arbuckle Group indicate fracture patterns in the underlying Arbuckle Aquifer. These lineaments consist of straight segments of stream valleys, segments of several stream valleys that are in alignment, or non-cultivated vegetation in linear patterns. The other method involved extending fracture patterns occurring in the Wichita Mountains into the Arbuckle Group to the south. For both methods a grid of cells was used to locate the areas of fracturing. Fractures in the Wichita Granite Group were studied by Gilbert (1982). A lineament analysis and corresponding geological interpretation of Comanche County is discussed by Donovan and others (1986).

It was assumed in the first method that the total length of fractures in an area controls the permeability. Only the lineaments in the Post Oak and Permian rocks were considered because fracture lineaments in the Wichita Mountain are outside the study area, and the lineaments in the Post Oak indicate fracture patterns in the Arbuckle Group as well as in the Post Oak.

It was assumed in the second method that a lineament might indicate only part of a fracture and that an area with many intersecting fractures would have a greater permeability; this method was applied to only the Arbuckle Group. Arbuckle well yield values derived from the two methods were compared with the average yield calculated from production well test data.

Computer Model Description

A modified Nuclear Regulatory Commission (NRC) version of the numerical ground-water model developed by Konikow and Bredehoeft (1978) was applied to the Post Oak Aquifer to determine its characteristics and to demonstrate their interaction over time. The modified version was used with a preprocessor developed under the direction of Douglas C. Kent (Kent and others, 1986a and b). A description of the variables and their application to the Post Oak Aquifer is in Appendix H. The study herein considered only the hydraulics of the Post Oak Aquifer; Back (1985) studied chemical transport in this aquifer. The modelled area covered the outcrop of the Post Oak Conglomerate as shown on the geologic map (Figure 3) and included townships 2N, 1N, 1S, part of 2S, and ranges 9W to 15W and part of 16W (Figure 13).

Calibration of the model required adjusting the aquifer characteristics until inflow to the model by recharge balanced outflow by aquifer drainage as shown by minimal values of drawdown or mounding in the drawdown matrix. These characteristics included storage coefficient, permeability, potentiometric head, and recharge. Because the modelled aquifer is unconfined, the storage coefficient actually represented specific yield, and the potentiometric head represented water-

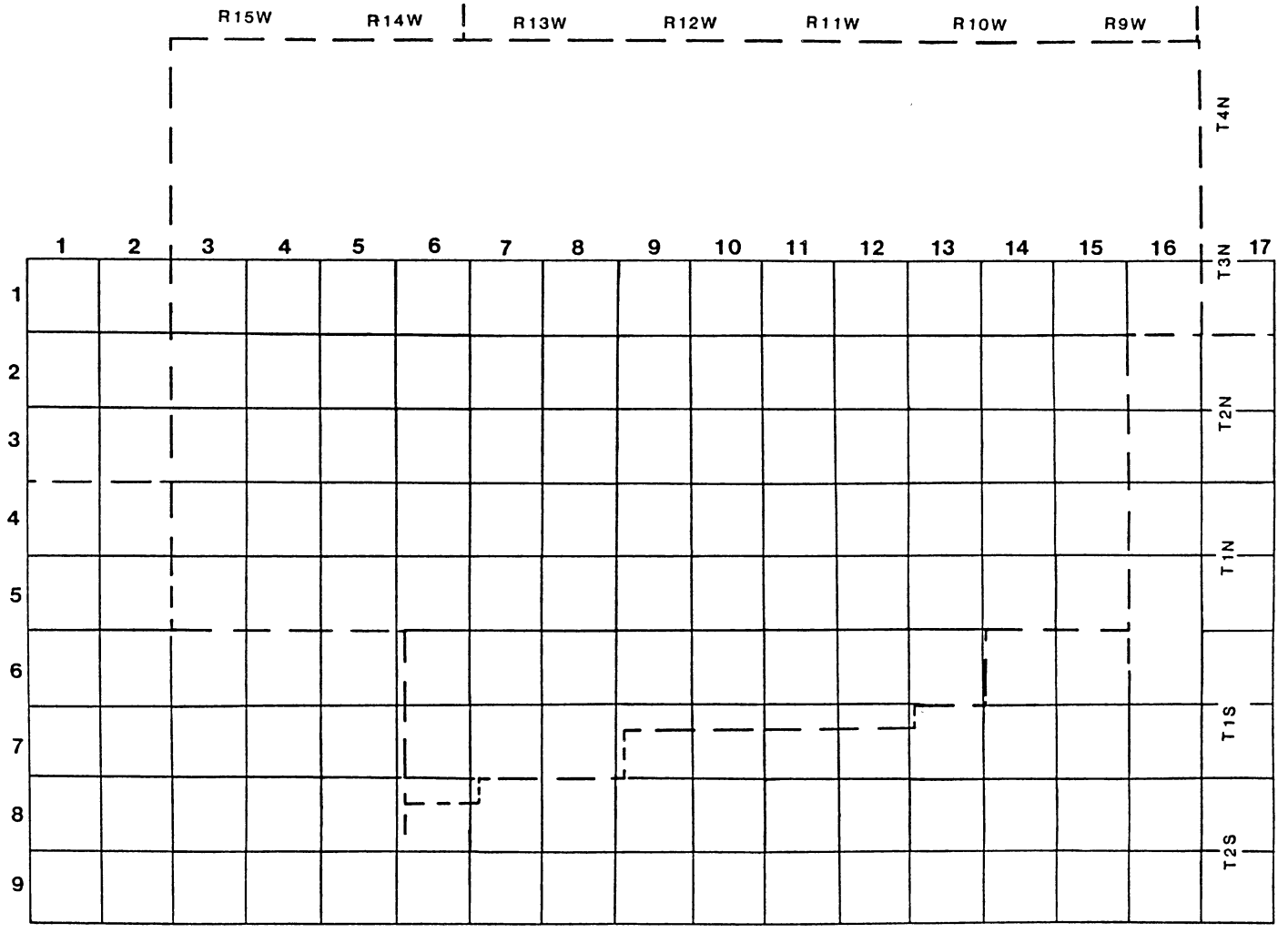

Figure 13. Computer Model Grid

table elevation. The model was not stressed by pumpage during the calibration.

Changing the specific yield opened or closed the aquifer to flow. This aquifer characteristic was set at 0.3, a high value, for the entire grid in order to increase the flow through the aquifer and to make the aquifer less sensitive to adjustments in permeability. More realistic values of specific yield were entered when pumpage was established in the model.

Permeability values for the Post Oak Aquifer were determined from lithologic well logs (Table V, Appendix C) and the grain-size-permeability relationship (Figure 11) as described previously. The areal distribution of permeability established in the model followed the mean grain size distribution pattern of the Post Oak Conglomerate determined by Stone (1977). The distribution of large mean grain size indicates the possible location of paleostream channels which would have greater permeability (Figures 26, 27, 29, and 80).

For the simulation the saturated thickness was a constant value for the entire grid. Twenty feet was the average saturated thickness as determined from well logs (Table II, Appendix B). The initial water-table elevation matrix was derived from Figure 36.

In order to account for greater flow into the aquifer at nodes with higher permeabilities, the node identification (NODEID) matrix replaced the constant recharge input.

Pumpage was established in the model following calibration according to data from the Oklahoma Water Use Data System (OWUDS) of the Oklahoma Water Resources Board (1984).

CHAPTER IV

HYDROLOGY OF THE ALLUVIAL AQUIFER

Surface-Water Hydrology

Climate

The climate of Comanche County is dry, subhumid, and continental (Mobley and Brinlee, 1967, p.46). Mean annual precipitation at Lawton (Figure 14) is 29.18 inches (741 mm), and mean annual temperature is 62.3°F (16.8°C). May is the wettest month, and January is the driest month (Figure 15). These conditions lead to an average annual lake evaporation of over 60 inches (1524 mm) and an average annual evapotranspiration of 26 inches (660 mm), according to Pettyjohn and others (1983). An isohyet map (Figure 16) shows the areal distribution of mean annual precipitation. The deflection of the isohyets to the east indicates an orographic effect by the Wichita Mountains. The average precipitation values are based on 30-year periods of record (Table XIV, Appendix F).

The average annual depth of rainfall over the Blue Beaver Creek basin is 29.17 inches (741 mm). Because this value is very close to the mean annual precipitation at Lawton, data from that weather station were used for comparisons with streamflow. A description of the method used to determine the average depth of rainfall is in Table XV, Appendix F.

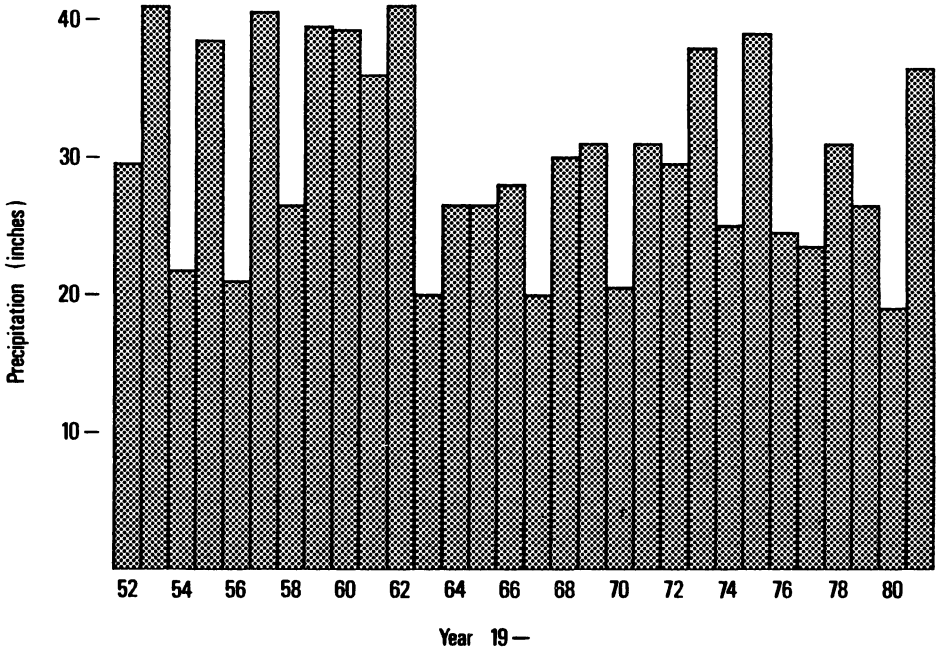

Figure 14. Mean Annual Precipitation at Lawton

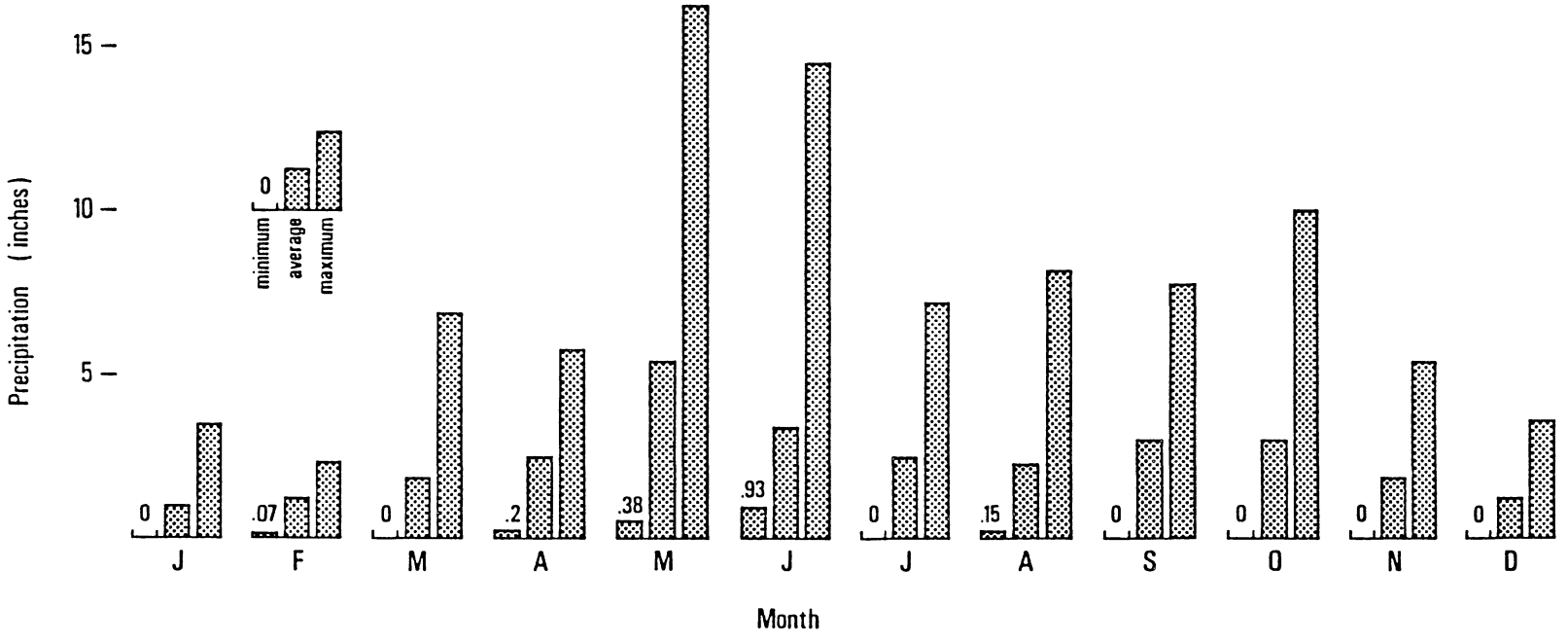

Figure 15. Average Monthly Precipitation at Lawton

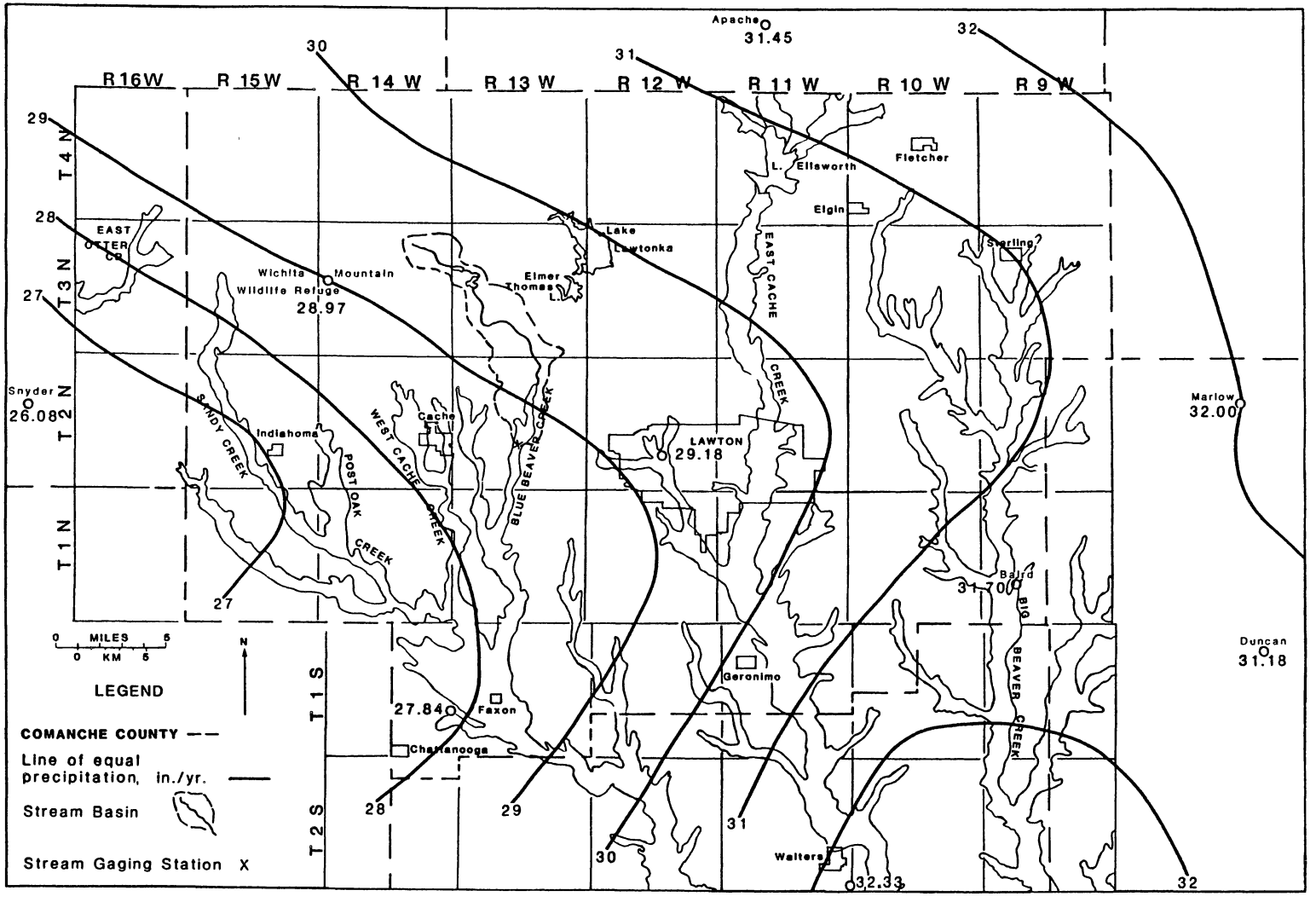

Figure 16. Isohyet Map of Comanche County

Surface Water

The major streams in Comanche County are West Cache Creek, Blue Beaver Creek, East Cache Creek, and (Big) Beaver Creek (Figure 2). West Cache Creek, Blue Beaver Creek, and their tributaries are intermittant, having no flow during short, dry periods. Beaver Creek is perennial except during droughts. The flow of East Cache Creek is regulated by discharge from Lake Lawtonka, Lake Elmer Thomas, and Lake Ellsworth; low flow is maintained by sewage plant effluent from Lawton and Walters (U.S. Geological Survey, 1983, p.435). The only U.S. Geological Survey stream gaging station in the county is on Blue Beaver Creek near Cache. There is minor regulation of this and other streams by only small reservoirs, making it suitable for gaging.

The Blue Beaver Creek basin has an area of 24.6 square miles (63.7 km^2) above the gaging station. Similar to the other streams in the area, the creek has deposited alluvium within a shallow valley cut into the Post Oak Conglomerate, Hennessey Shale, and Garber Sandstone. Port soils have developed on the alluvium: these soils are clayey with moderate to moderately slow permeability, or infiltration, and moderate runoff potential (Moblee and Brinlee, 1967, pp.37, 41).

Because the geology and soils have a relatively low permeability, the drainage is flashy: there are sudden increases in stream discharge from surface runoff during short, intense storms that characterize the climate. Within two or three days following the storm the stream returns to its previous stage because there is little or no contribution from ground-water runoff to sustain the flow.

Stream hydrographs of mean daily discharges for a wet water year, 1973 (Figure 17), and a dry water year, 1971 (Figure 58, Appendix F),

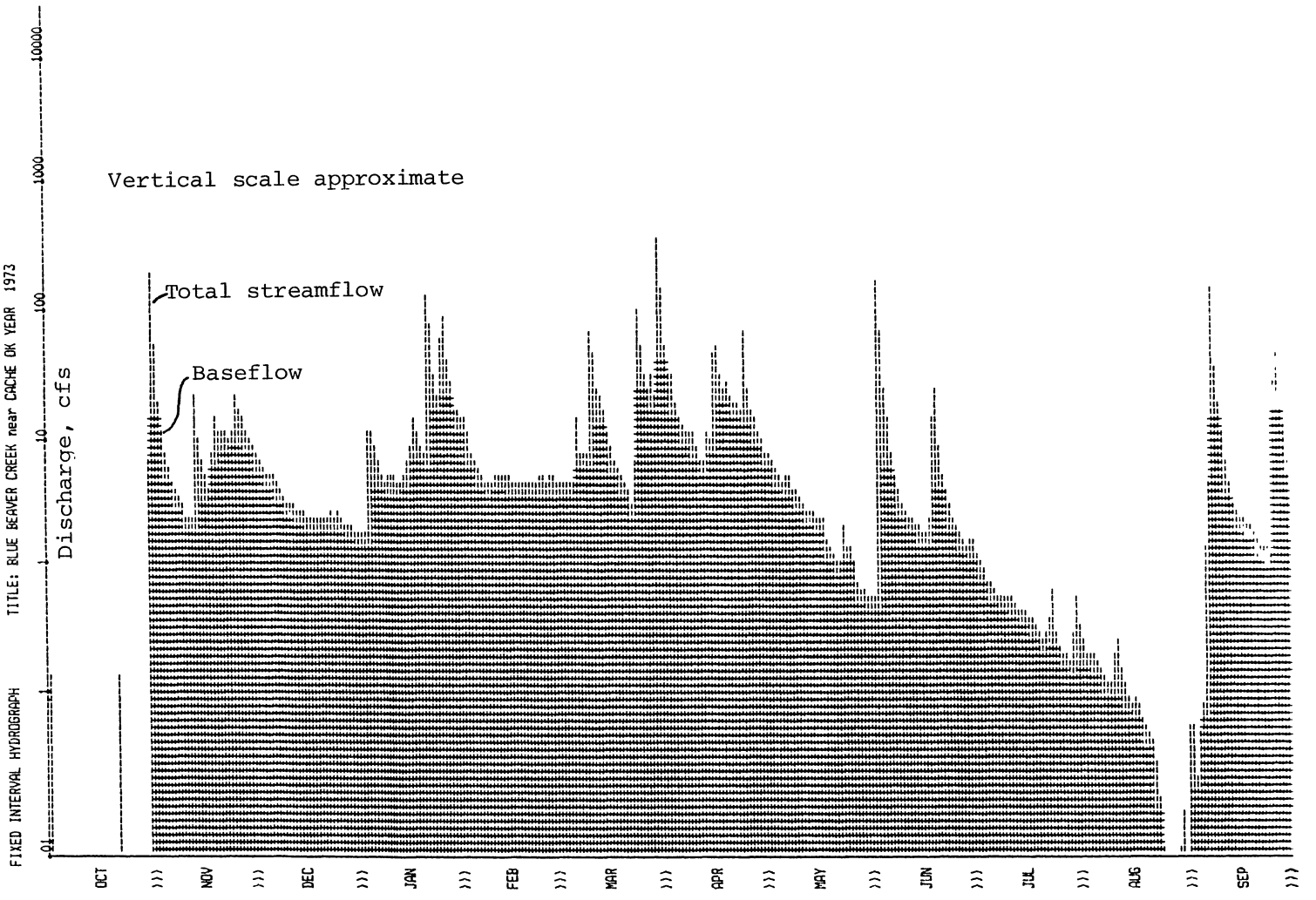

Figure 17. 1973 Stream Hydrograph of Blue Beaver Creek

show the flashy nature of Blue Beaver Creek: steep rising limbs, sharp crests, steep recession curves, and long periods of low flow. Flow duration curves for these water years (Figure 18; Figure 59, Appendix F), which show the percent of time a given discharge will be equalled or exceeded, exhibit the characteristic steepness of flashy drainage and a basin geology with a relatively low permeability. Stream discharges are characteristically of low magnitude. These hydrographs and flow-duration curves were plotted by the RECHARGE program (Appendix F), which calculates by three methods the baseflow, that portion of the stream discharge contributed by ground-water runoff (Figure 55, Appendix F). Miller (1984) described the methods, fixed interval, sliding interval, and local minima, and applied them to the Little Washita River watershed within and to the northeast of Comanche County. He found that they yield baseflow values within a 10 percent agreement, and that baseflow depends on antecedent precipitation. Similar to the Blue Beaver Creek basin, the Little Washita River watershed is characterized by rocks of relatively low permeability, clayey soils, and a subhumid climate.

The monthly and annual baseflows for Blue Beaver Creek, calculated by the fixed interval method and expressed as percentages of streamflow and precipitation, are listed in Table XIII, Appendix F. The mean baseflow for the 15-year period 1968 to 1982 was 3.18 inches (80.8 mm), or 5.76 cfs (0.16 m^3/s), and the lowest annual baseflow was 0.16 inches (4.1 mm), or 0.29 cfs (0.008 m^3/s), in 1971, a water year of below-average rainfall.

The relationship between mean monthly baseflow and precipitation for the Blue Beaver Creek basin (Figure 19) differs from that for the

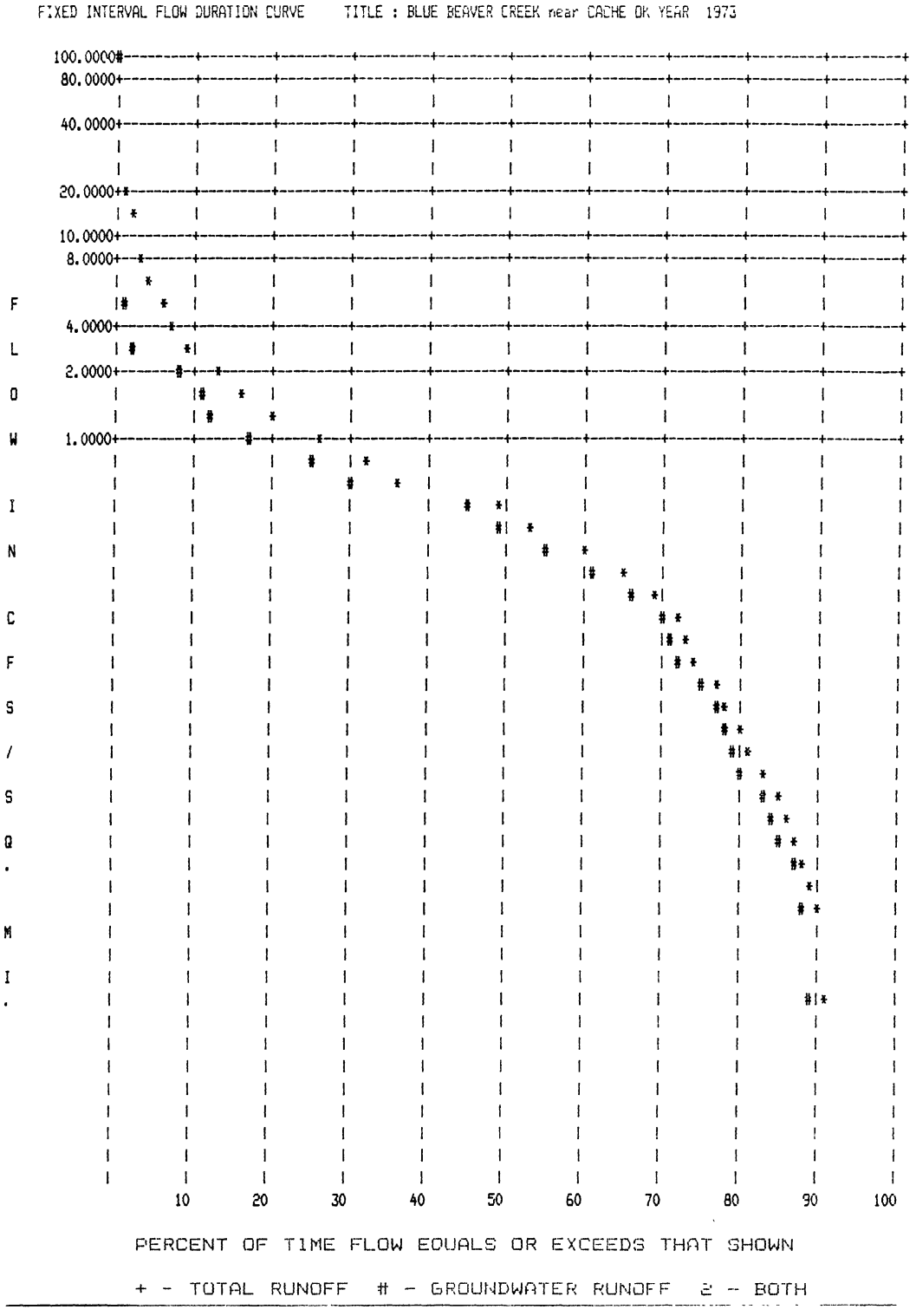

Figure 18. 1973 Flow Duration Curve of Blue Beaver Creek

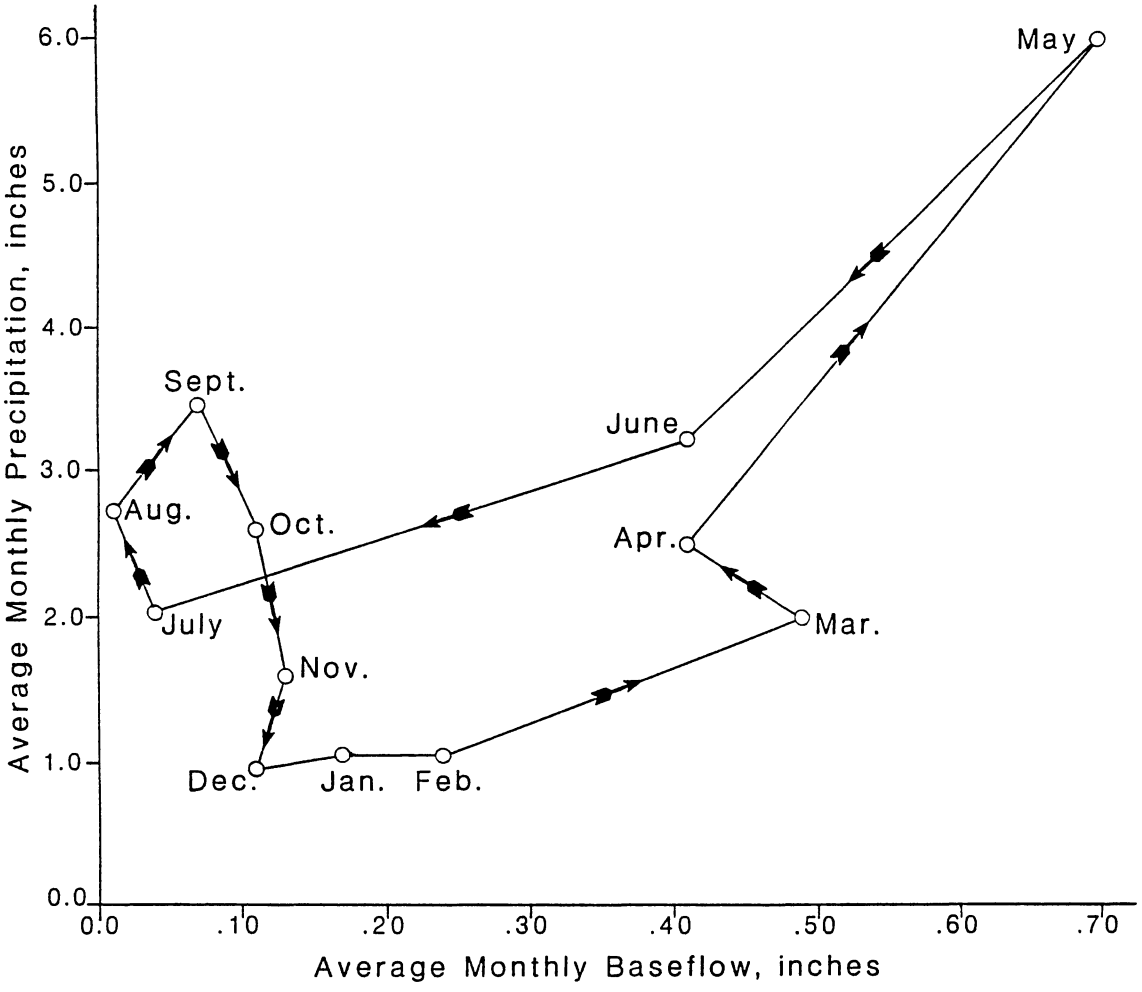

Figure 19. Relationship Between Monthly Precipitation and Monthly Baseflow

Little Washita River (Miller, 1984, p.45). During the fall baseflow increases slightly although precipitation decreases; baseflow continues to increase through the winter while precipitation remains constant. Streamflows are highest in the spring, as indicated by the dramatic increase in both baseflow and precipitation. During the summer baseflow decreases; precipitation decreases in the early summer but increases in the late summer. Streams usually have no flow in the summer when evapotranspiration is highest.

Annual baseflow and precipitation follow similar trends (Figure 20), but the two-year moving average of rainfall lags behind baseflow. These results differ from those of the Little Washita River basin (Miller, 1984, p.27) probably because the Blue Beaver Creek basin is much smaller, and precipitation would more immediately affect the baseflow.

The difference between rainfall on the basin and streamflow from the basin is evapotranspiration which is greatest during the spring when rainfall is greatest (Table IX, Appendix F). Expressed as a percentage of precipitation, however, evapotranspiration is shown to be greatest in the late summer when there is a rainfall deficit (Figure 21). For the 15-year period, 1968 to 1982, evapotranspiration ranged from 16.8 to 30.9 inches (427 to 785 mm) and averaged 81% of precipitation (Table X, Appendix F).

These surface-water data were used to characterize the hydrology of the alluvium.

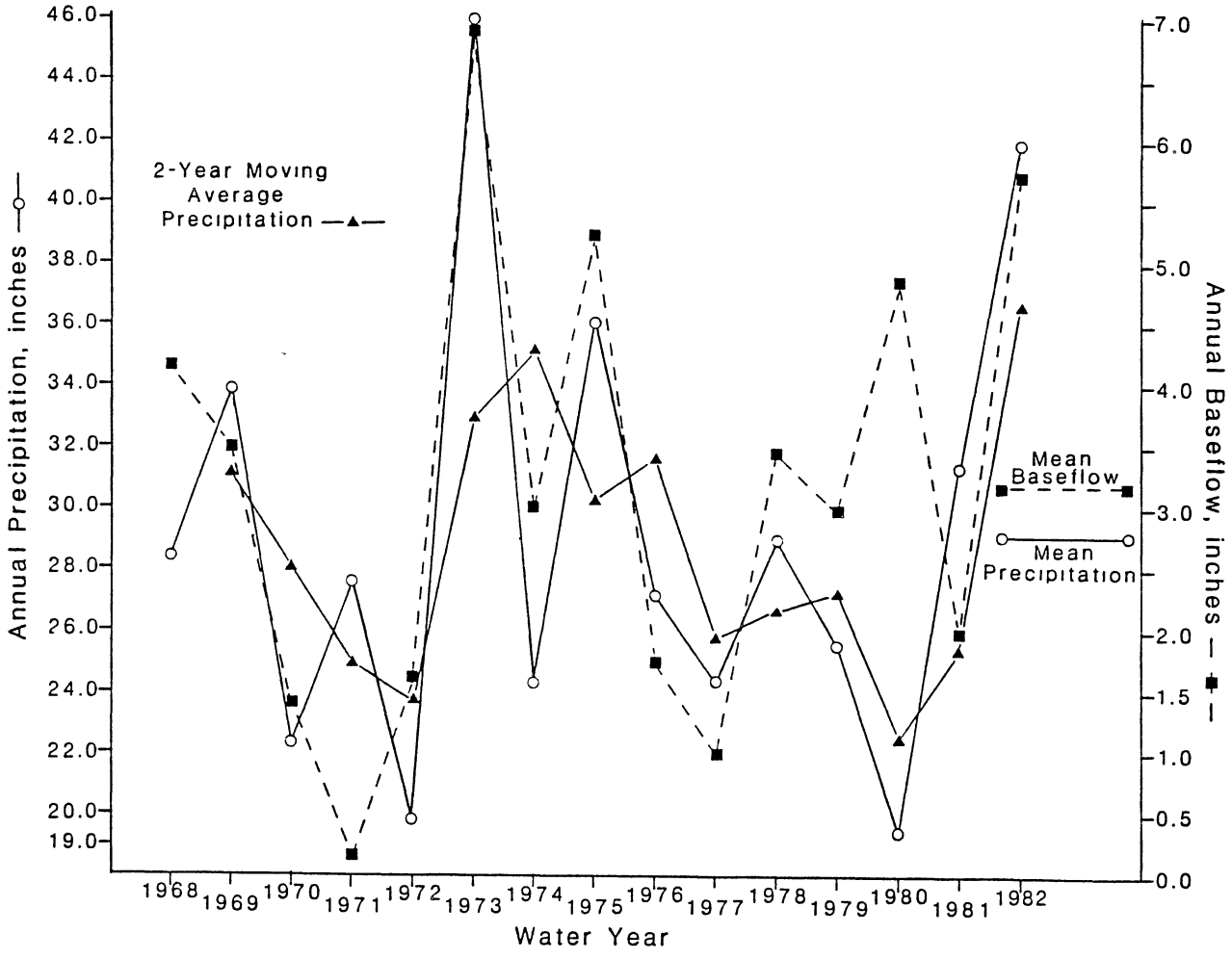

Figure 20. Correlation of Annual Baseflow, Annual Precipitation, and Two-Year Moving Average of Precipitation

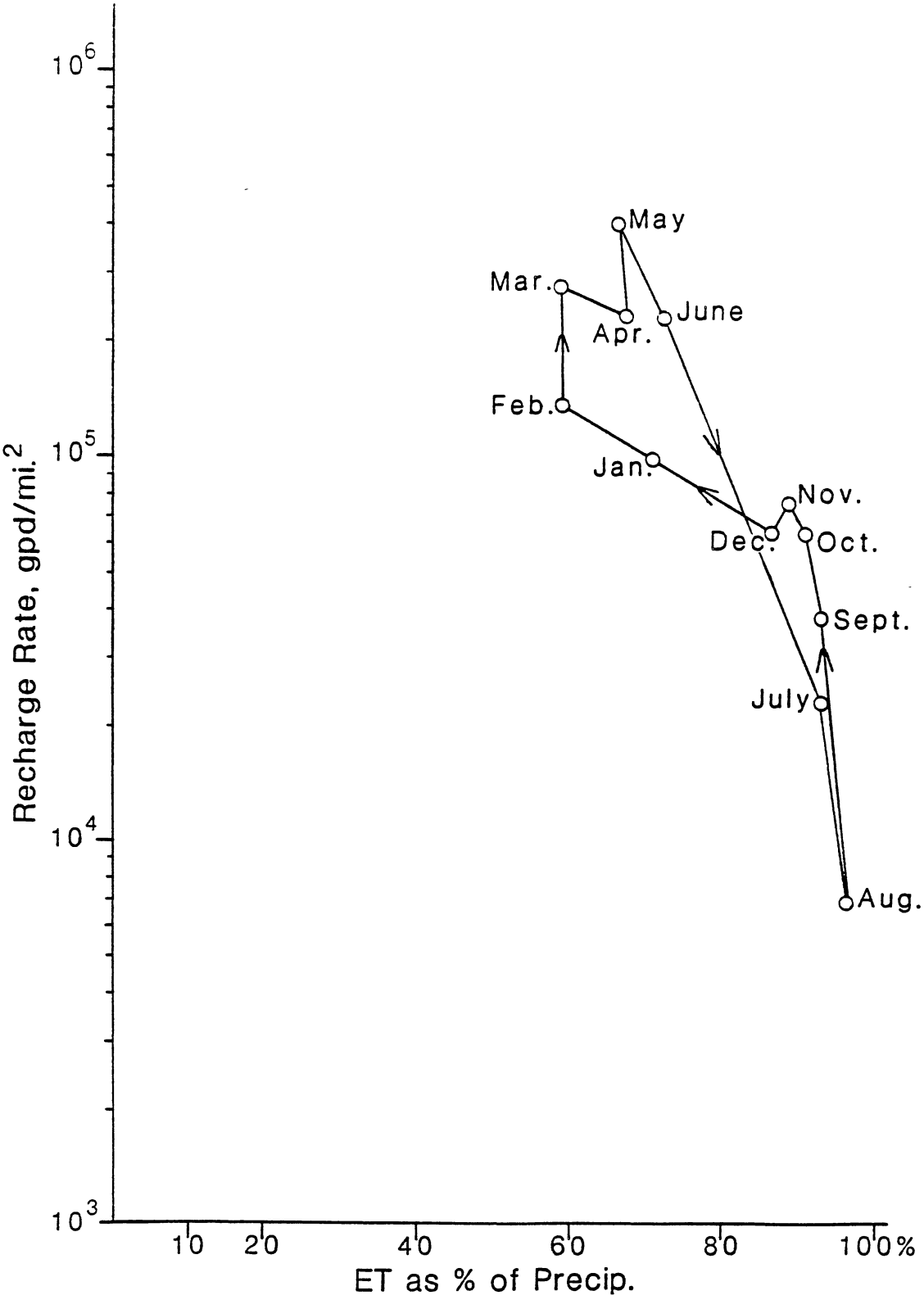

Figure 21. Relationship Between Recharge Rate and Evapotranspiration as Percentage of Precipitation

Alluvium

Description

The alluvium comprises an unconfined aquifer and consists of sands, silts, gravels, and clays within the creek valleys (Figure 22). Where field measurements and data from lithologic well logs were unavailable, the thickness of the alluvium was assumed to be equal to the well depth listed by Havens (1977). The average thickness of the alluvium is 33 feet (10 m), with a range from 10 to 65 feet (3 to 19.8 m). The alluvium generally thickens downstream and from a tributary to a main stem; therefore, the study area was separated into two areas in which the average thickness is 30 feet (9.1 m) and 40 feet (12.2 m; Figure 22). The average saturated interval is 16 feet (4.9 m) and ranges from 3.5 feet (1.1 m) to 47 feet (14.3 m).

Aquifer Characteristics

The upper range of the grain-size envelope indicated a mean permeability of 990 gpd/ft^2 (4.7×10^{-4} m/s) and a mean transmissivity of 15,840 gpd/ft (0.0023 m^2/s). Expected well yield would be 77 gpm (4.9 1/s). Havens (1983) reported yields of 5 to 500 gpm (0.3-32 1/s); pump tests have yielded up to 800 gpm (50 1/s).

Water-level gradient in the alluvium should approximate closely the topographic gradient within the creek valleys; pumping would cause local cones of depression. The gradients within Comanche County become less steep to the east. The water-table gradient along Sandy Creek is 23 ft/mi, and the gradient along Big Beaver Creek is 8 ft/mi.

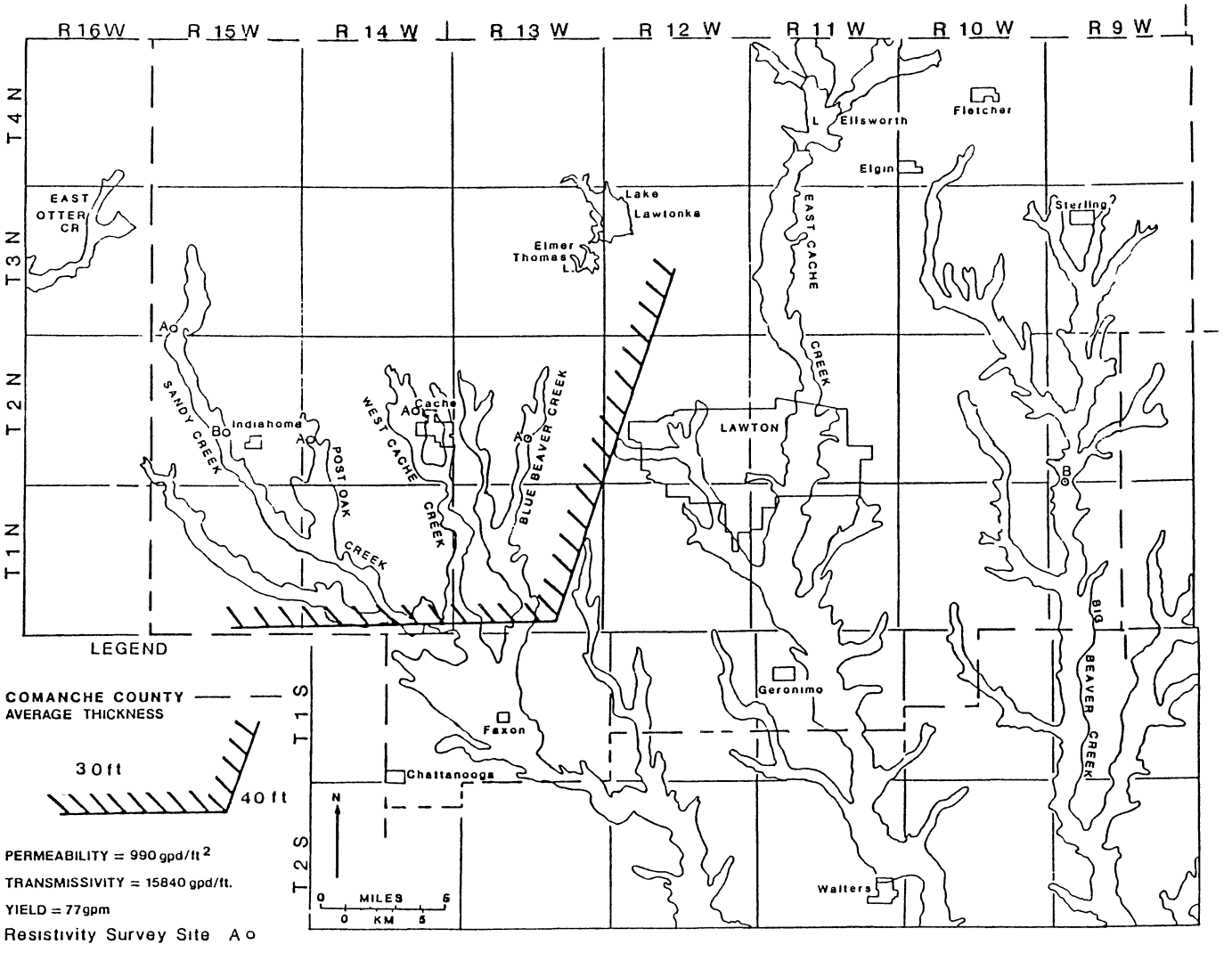

Figure 22. Distribution of Alluvium

Gradients determined from topographic maps for the other unregulated creeks are listed in Table XVI, Appendix F.

Recharge

Recharge to the alluvium has three components: infiltration from losing streams, ground-water recharge from the Post Oak Aquifer, and precipitation on the aquifer (Figure 23). Precipitation affects the aquifer the quickest, but its contribution is least because of evapotranspiration. Ground-water recharge derived as underflow from the Post Oak to the alluvial aquifer provides a relatively constant, long-term contribution. The response time of this contribution depends on the ground-water velocity and gradient in the Post Oak Aquifer.

The ground-water runoff is a measure of recharge, that part of precipitation not lost to evapotranspiration and not contributing directly to surface runoff. The net recharge rate is the ratio of baseflow to the basin area (Table XI, Appendix F), and averaged 3.45 in/yr (87.6 mm/yr) over a 15-year period. During the year recharge follows a trend opposite to that of evapotranspiration (Figure 21): it is at a maximum in spring and at a minimum in late summer.

Quality

The water quality of streams during periods of dry-weather flow indicates the quality of ground water from the alluvium in the stream valleys. Blue Beaver Creek, West Cache Creek, and Medicine Creek have dissolved solids contents up to 500 milligrams per liter (mg/l). East Cache Creek and Beaver Creek are more mineralized, exhibiting dissolved

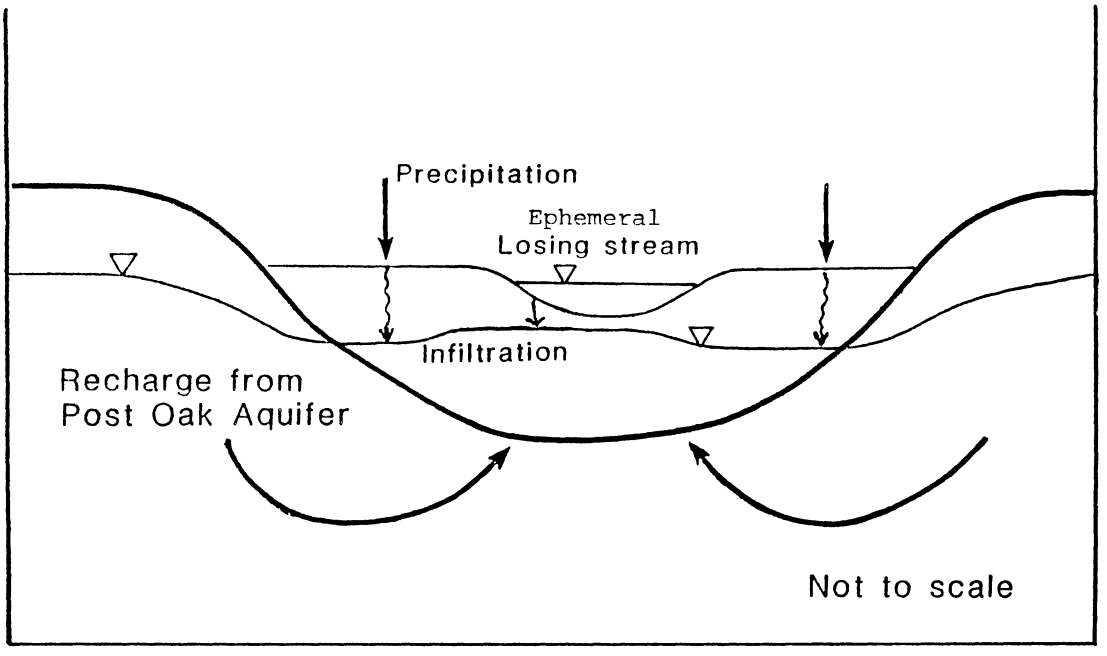

Figure 23. Components of Recharge to the Alluvial Aquifer

solids contents ranging from 500 to 1000 mg/l (Havens, 1977, Sheet 4, Fig. 12). More detailed analyses are listed in Table XVII, Appendix F.

CHAPTER V

GROUND-WATER HYDROLOGY OF THE POST OAK AQUIFER

Description

The Lower Permian Post Oak Conglomerate consists of sandstones, shales, and conglomerates. Chase (1954) first named the Permian coarse clastic sediments around the Wichita Mountains as the Post Oak Conglomerate and differentiated this unit into four facies: a granite boulder conglomerate, a rhyolite porphyry conglomerate, a limestone boulder conglomerate, and a conglomerate with zeolite-opal cement. These sediments were eroded from the Wichita Mountains and Limestone Hills. Only the granite and rhyolite boulder conglomerates occur in the study area.

Because of the significant quantities of sandstones and mudstones as well as conglomerates in the Post Oak Conglomerate, Al-Shaieb and others (1980) informally named it a formation and assigned it a Leonardian (Lower Permian) age. Collins (1985) questioned the formal status of the "Post Oak Conglomerate" and its correlation with other units that were assigned definite ages within the Lower Permian. Bridges (1985) revised the Lower Permian stratigraphy in the Wichita Mountains area (Figure 24). In the study herein "Post Oak Conglomerate" is used as an informal term of convenience (Figure 3).

On the Geologic Map of Oklahoma, Miser (1954) mapped together as the Wichita Formation the sedimentary rocks south of the Wichita

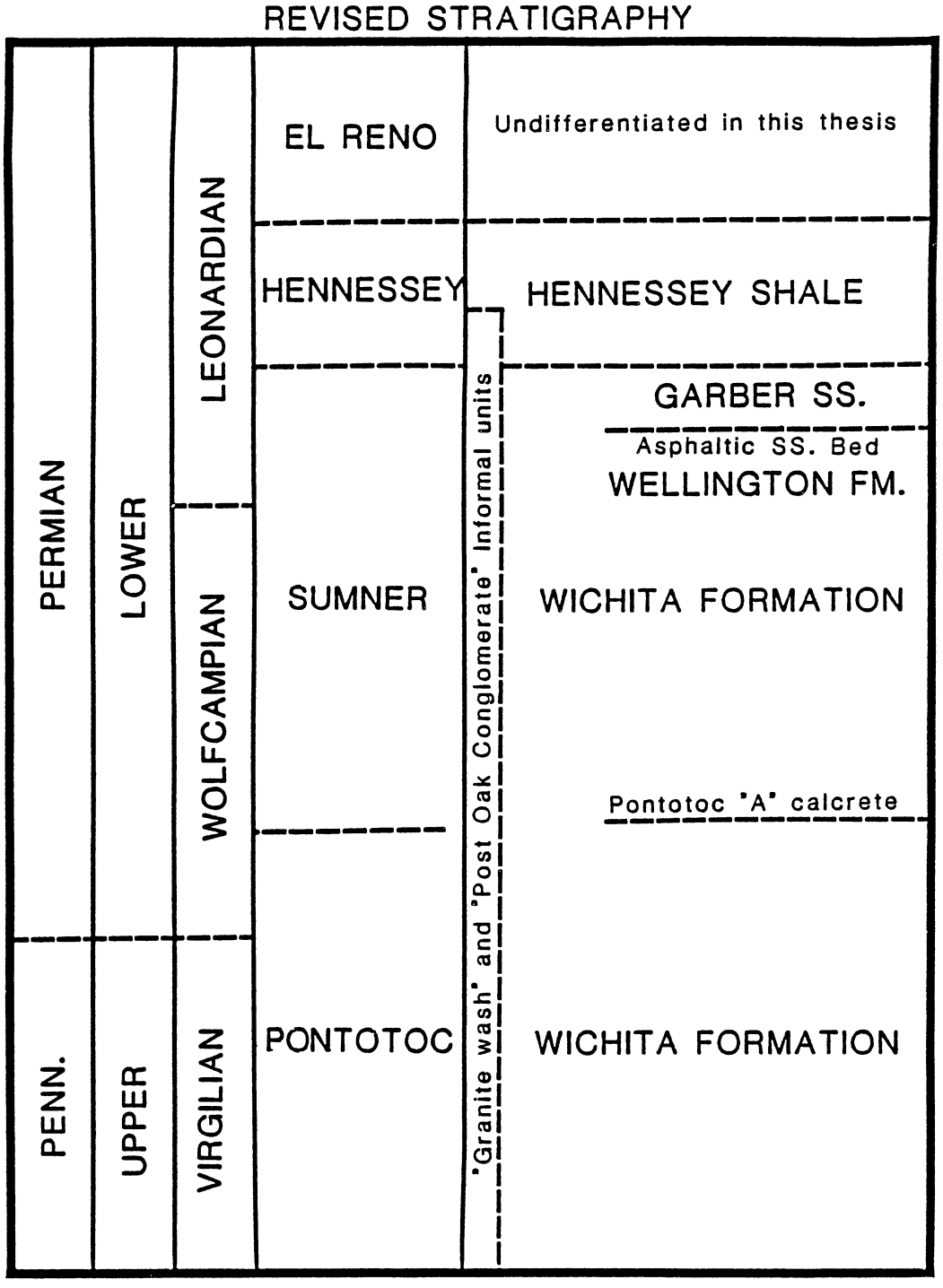

Figure 24. Revised Permian Stratigraphy According to Bridges (1985)

Mountains. Havens (1977 and 1983) showed the Post Oak Conglomerate, Hennessey Shale, and Garber Sandstone as separate, mappable units and considered them as separate aquifers. By hydrogeologic criteria they are difficult to differentiate because they are very similar texturally, and they interfinger in the subsurface. The Pennsylvanian Oscar Group is a name applied to some subsurface aquifer units, but its sandstones, shales, and arkoses are probably indistinguishable from the overlying Permian rocks. In this study the Post Oak Conglomerate, Hennessey Shale, and Garber Sandstone have been combined into the Post Oak Aquifer because they are virtually undifferentiable, and they exhibit similar hydraulic characteristics.

According to data from the National Uranium Resource Evaluation Project (Union Carbide Corporation, 1980), well depths in the Post Oak Aquifer are distributed approximately bimodally: most wells are either less than 50 feet deep (15.2 m) or greater than 200 feet (61 m) deep. The average effective aquifer thickness is the average depth of the shallower wells, which tap an unconfined aquifer; the deeper aquifers are confined or semi-confined. The total thickness of the Post Oak Aquifer (Figure 25) is the difference between the land surface elevation and the elevation of the top of the Arbuckle Aquifer shown on the structural contour map of Havens (1983, Plate 1).

In a study of the Post Oak Conglomerate, Stone (1977) determined mineralogic and grain size dispersal patterns which are indicators of alluvial fan environments of deposition. He postulated four paleostream channels along the paths of sediment dispersal (Figure 26). Stone's map was modified to show larger probable channel deposits within the Post Oak Aquifer (Figure 27). Based on that map the aquifer

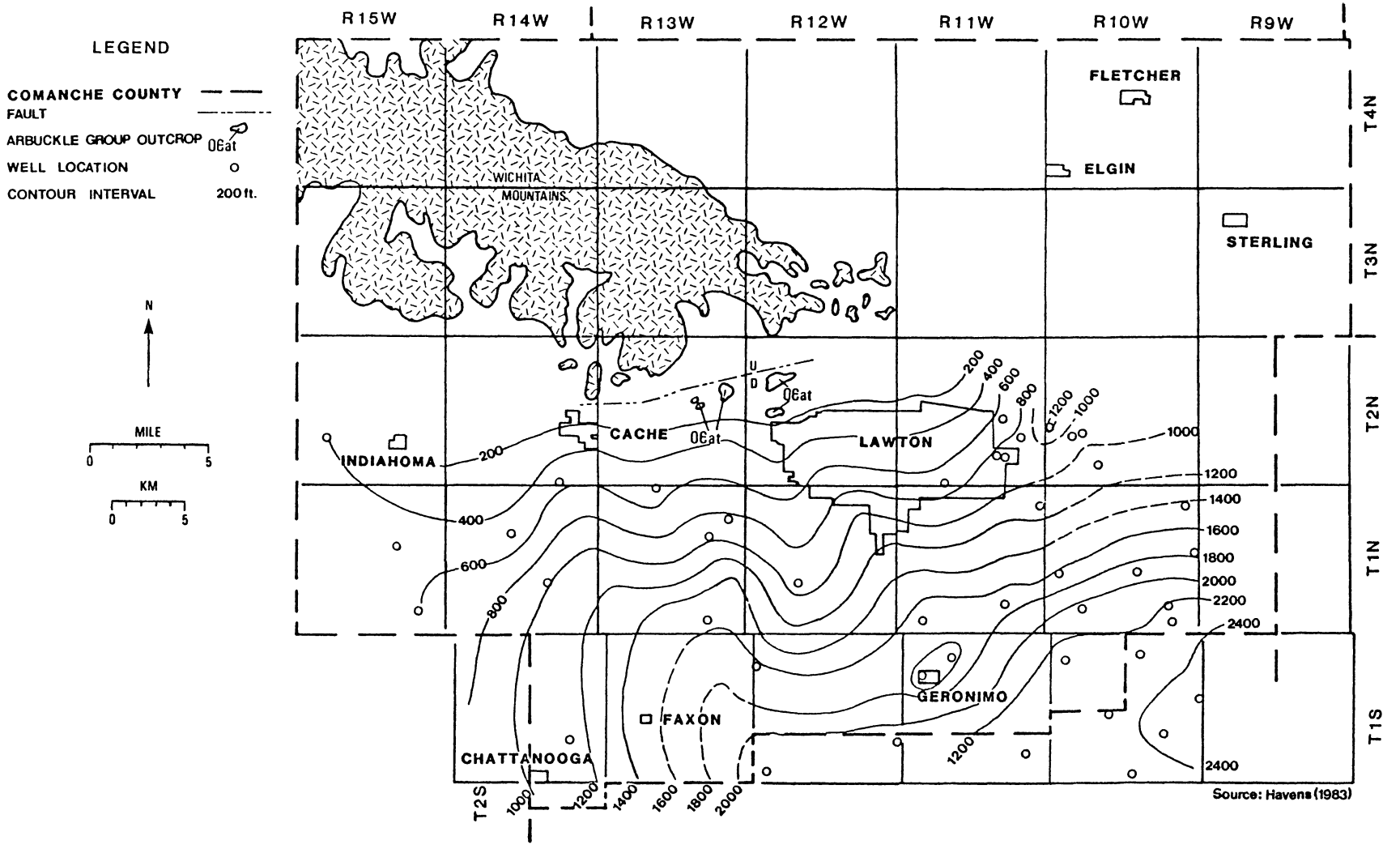

Figure 25. Total Thickness of Post Oak Aquifer

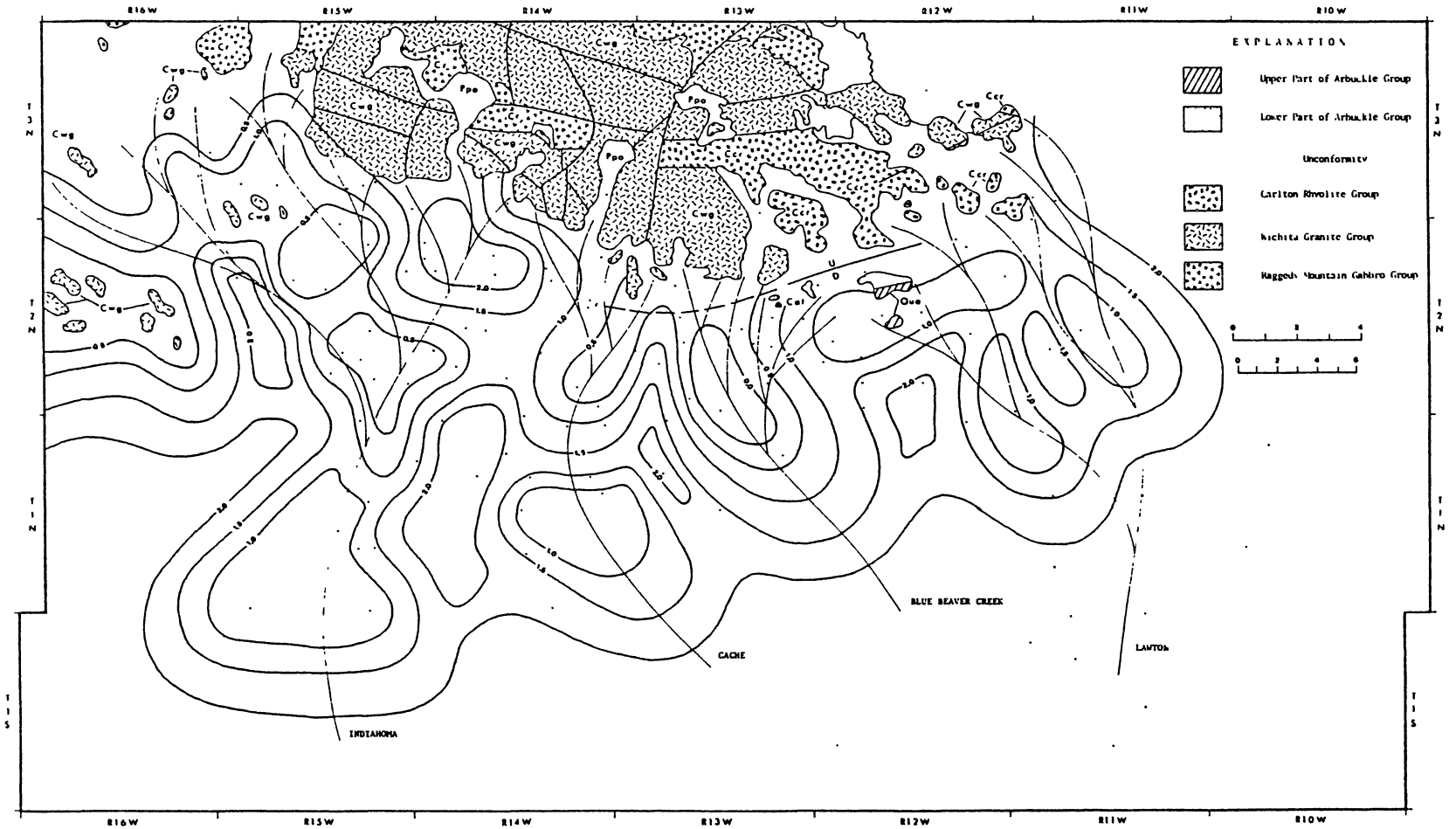

Figure 26. Distribution of Mean Grain Size, Isopleth Interval 0.5 Phi (from Stone, 1977)

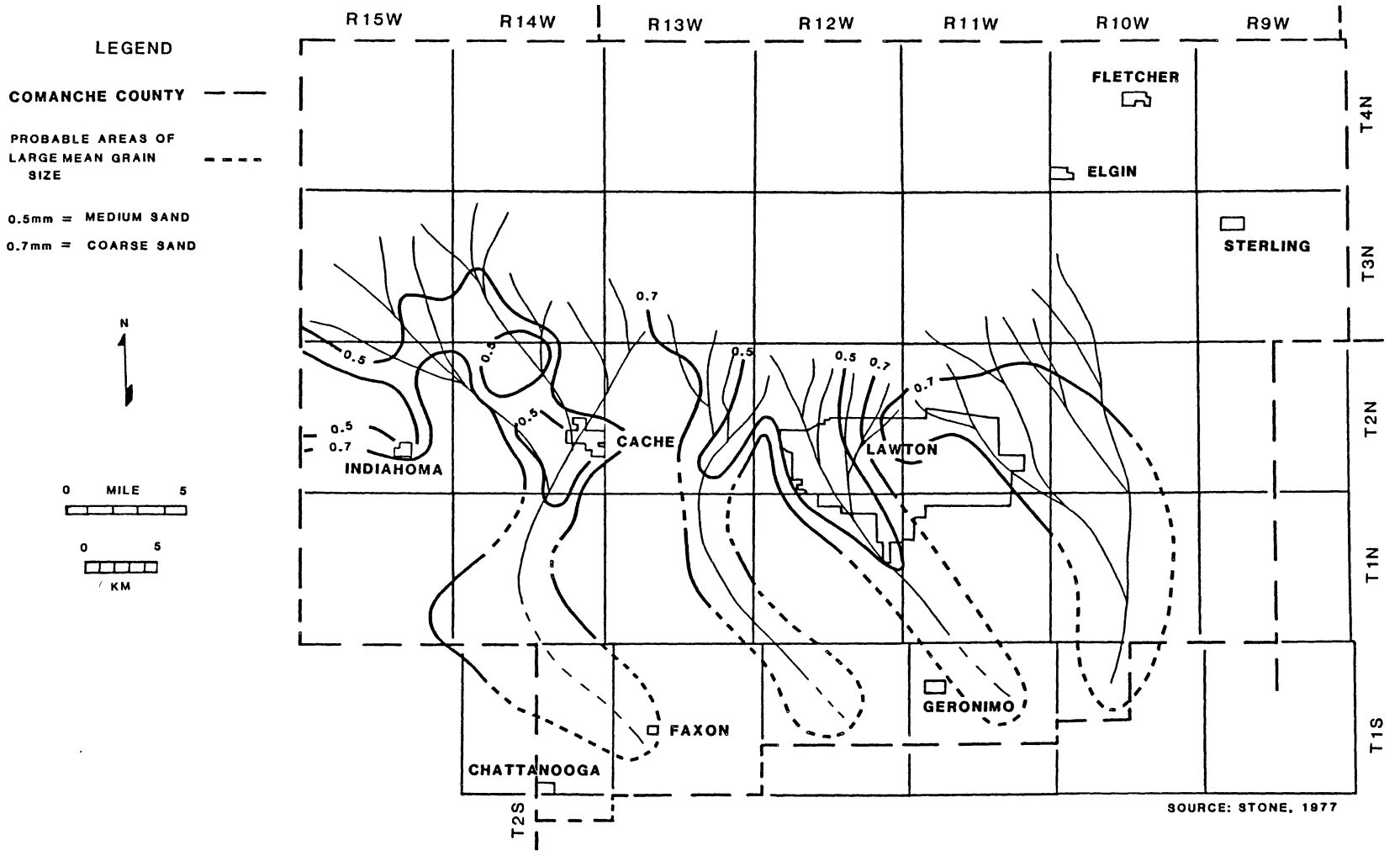

Figure 27. Modified Map of Mean Grain Size Distribution

was separated into two zones assuming that areas of coarse mean grain size in the rock have higher transmissivity (Figure 28), permeability (Figure 29), and expected well yield (Figure 30).

Channel areas indicated by large mean grain size also should have more coarse-grained layers in the vertical section. The total thickness of sand, gravel, and conglomerate layers within 50 feet (15.2 m) of the surface (Figure 31; Table III), as determined from drillers' logs, identify channels through Indiahoma, Cache, Lawton, and east of Lawton. The presence of these layers below 50 feet indicates deeper channel deposits.

Aquifer Characteristics

To determine the expected well yield in the channel areas, the grain-size-permeability relationship was applied to data from seven wells in the Post Oak Aquifer. From the upper range of the grain-size envelope the permeability is 800 gpd/ft^2 (3.8 x 10^{-4} m/s), and the transmissivity is 16,000 gpd/ft (0.0023 m^2/s). Assuming a maximum theoretical drawdown of 11 feet (3.3 m), an average pumping duration of 660 minutes (11 hours), and a specific yield of two percent, the average well yield in the channel areas would be 110 gpm (6.9 1/s) according to Walton's formula (Equation 3-1). Assuming a five percent specific yield, then the well yield would be 120 gpm (7.6 1/s). The lower specific yield value is a typical value for an unconfined aquifer listed in Walton (1970, p.315).

According to Stone's map (Figure 26), the coarser-grained channel deposit zones have mean grain sizes of 0.5 and 1.0 phi (0.7 and 0.5 mm), equivalent to the Wentworth coarse sand size class (Folk,

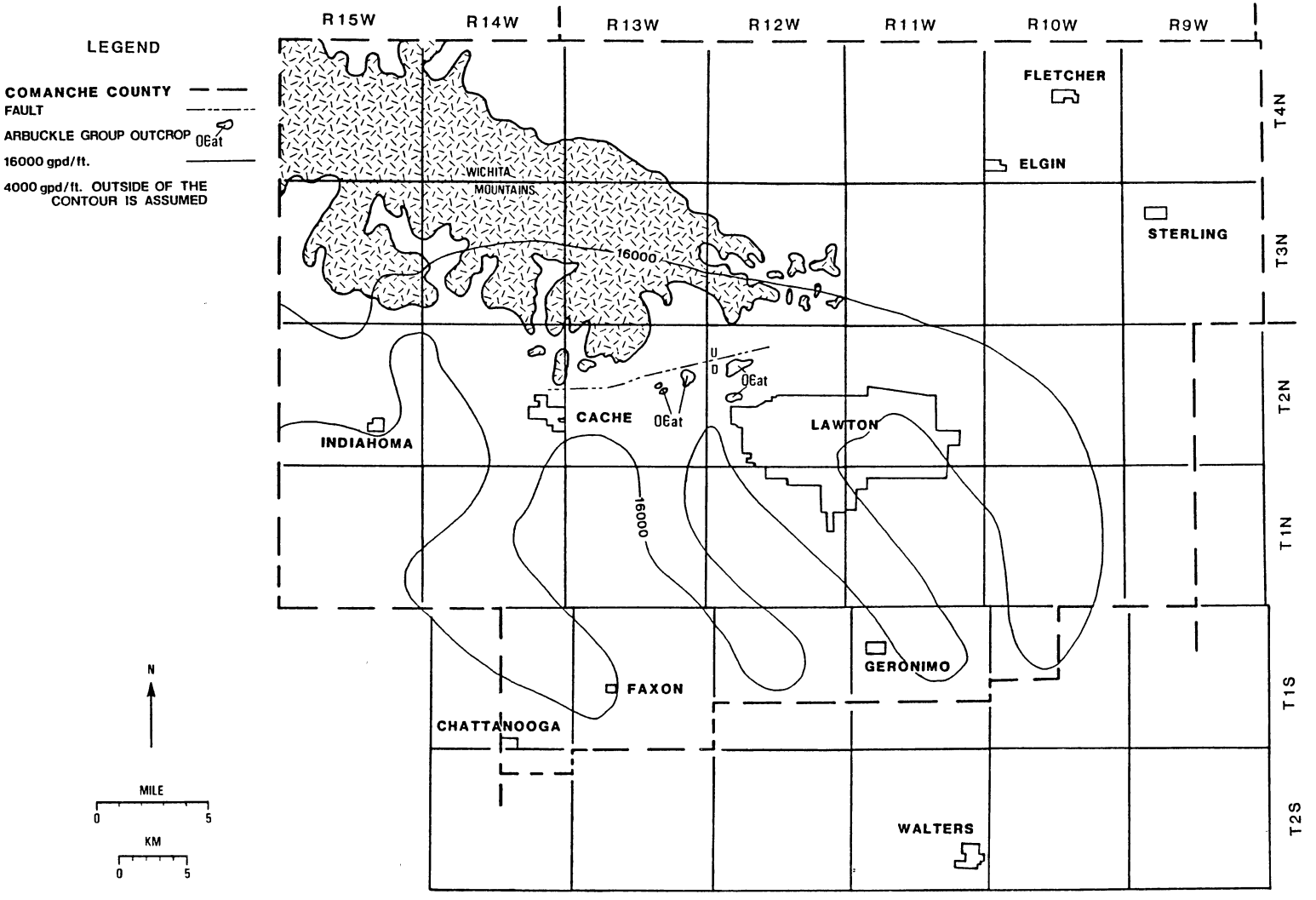

Figure 28. Transmissivity Map of the Post Oak Aquifer

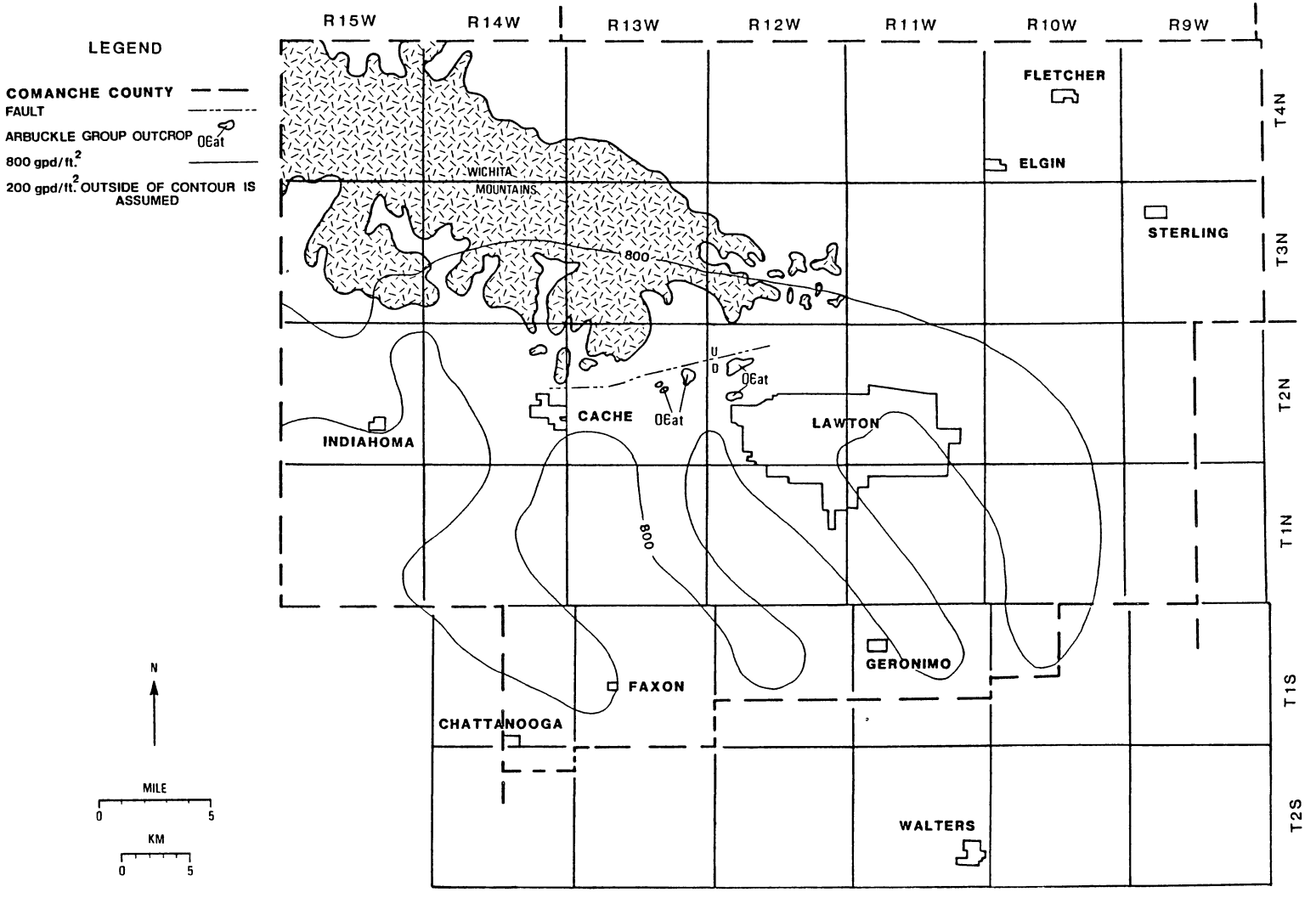

Figure 29. Permeability Map of the Post Oak Aquifer

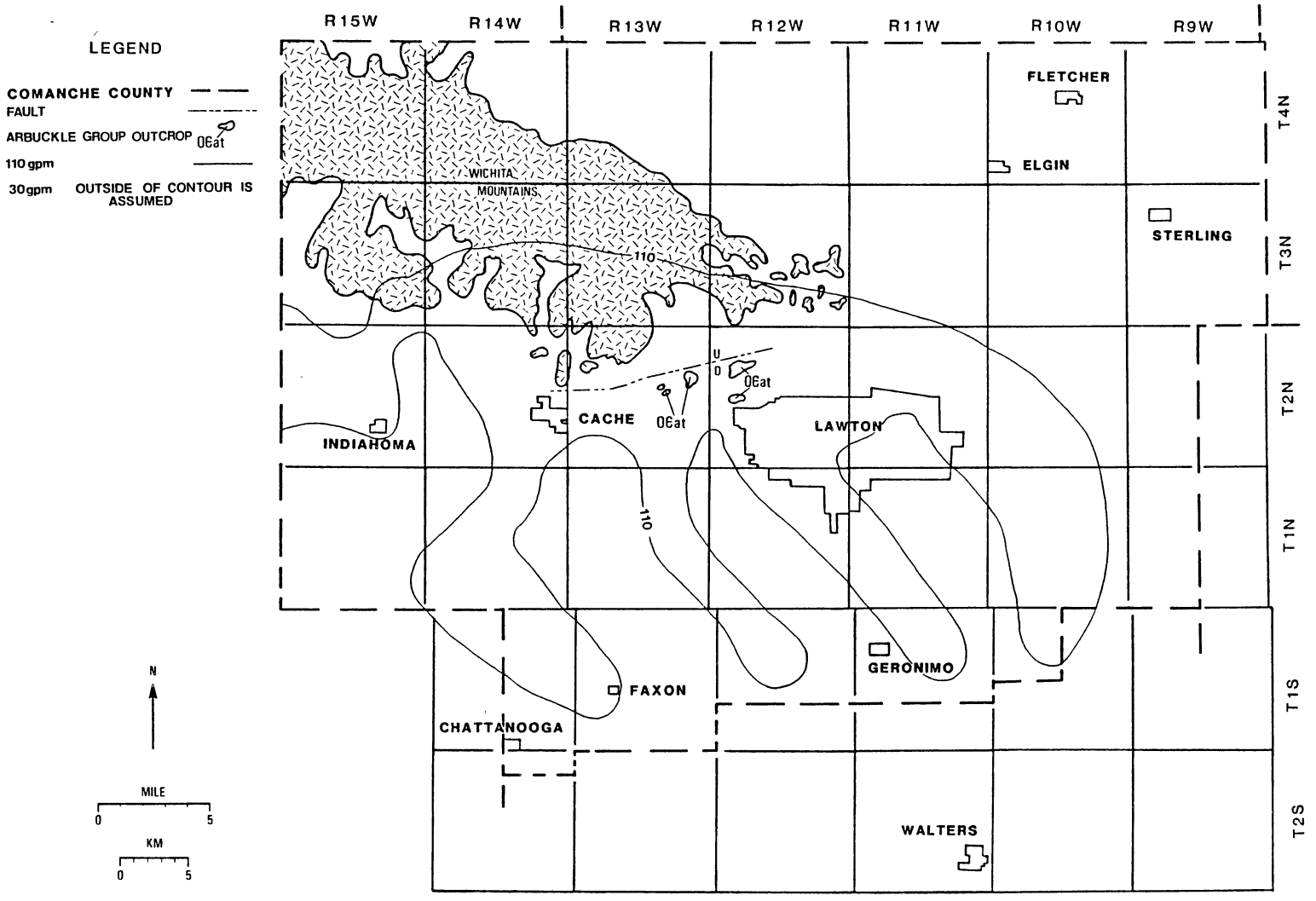

Figure 30. Expected Yield Map of the Post Oak Aquifer

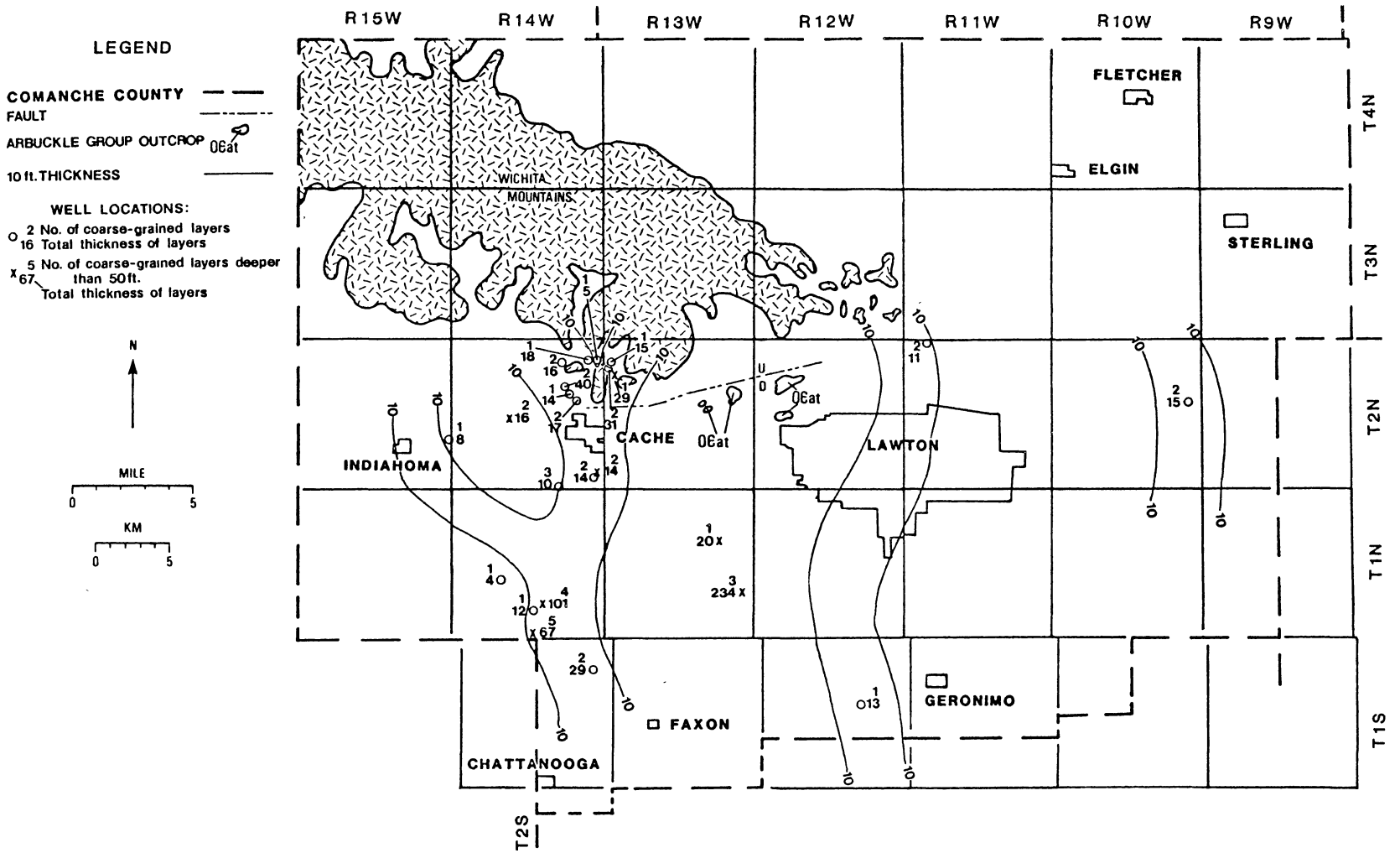

Figure 31. Total Sand Thickness of the Post Oak Aquifer

1980, p.23). A typical value of specific yield for coarse sand is 30 percent (Morris and Johnson, 1967, pp.D36-D37). From a relationship between permeability and specific yield (Figure 32) the average permeability of the coarse sand should be 900 gpd/ft^2 (4 x 10^{-4} m/s); the permeability value from the well log data, 800 gpd/ft^2, was used instead in order to underestimate the well yield in the Post Oak Aquifer. The areas outside of the channel deposits have mean grain sizes of 1.5 and 2.0 phi (0.35 and 0.25 mm), equivalent to the Wentworth medium and fine sand size classes (Folk, 1980, p.23). These grain sizes have typical vertical permeabilities of 340 and 94 gpd/ft^2 (1.6 x 10^{-4} and 4.4 x 10^{-5} m/s), the nominal average of which is 200 gpd/ft^2 (9 x 10^{-5} m/s). The transmissivity is thus 4000 gpd/ft (6 x 10^{-4} m^2/s), and by Walton's formula (Equation 3-1) and the same assumptions as above the average well yield would be 30 gpm (1.9 1/s).

Yield

Havens (1983) reported yields of less than 10 gpm (0.6 1/s) from the Post Oak Conglomerate, Hennessey Shale, and Garber Sandstone; pumping test yields from 15 wells, however, range from 0.3 to 800 gpm (0.02 to 50 1/s). The lowest yields are from the deepest wells, those greater than 200 feet (61 m). Wells less than 40 feet (12.2 m) deep generally yield less than 100 gpm (6.3 1/s), while wells deeper than 40 feet yield more than 2100 gpm (132 1/s). The shallower, lower-yield wells cluster between Cache and Indiahoma; the deeper, more productive wells are located around Faxon (Figure 33).

The lineament analysis of the Post Oak Aquifer provided another possible distribution of estimated well yield (Appendix G). Figure 34

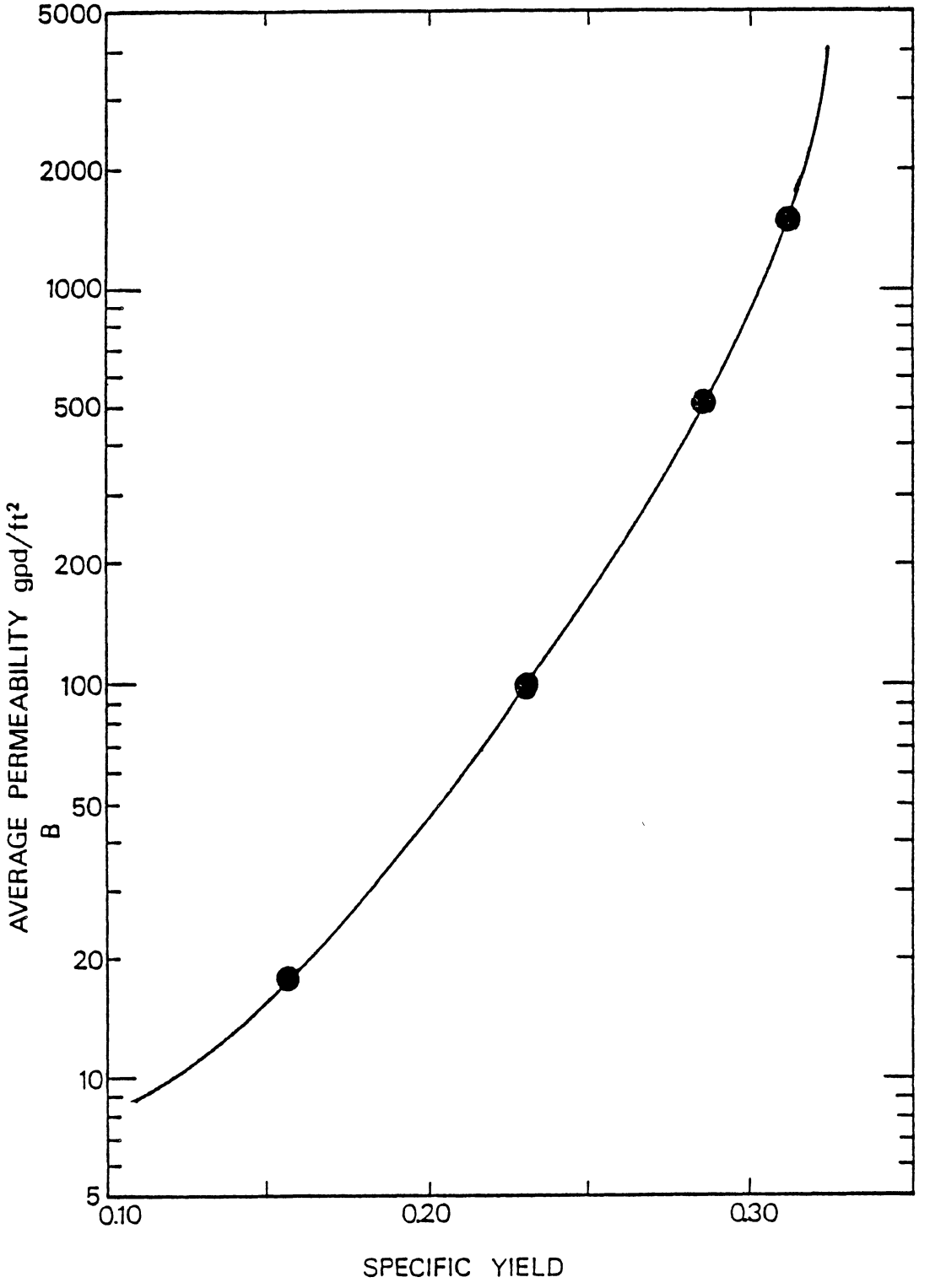

Figure 32. Relationship Between Permeability and Specific Yield (from Kent, 1980, and Patterson, 1984, p.88)

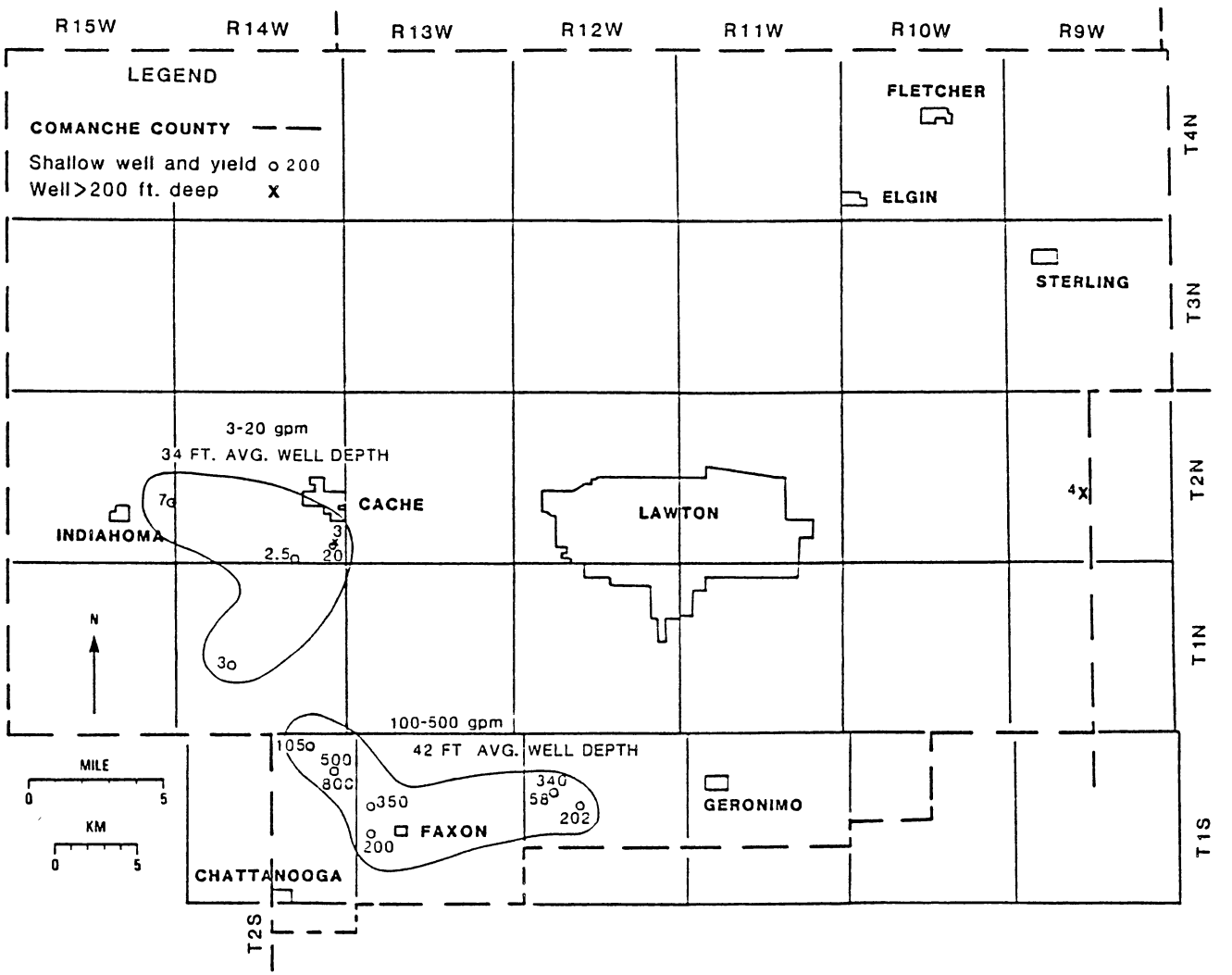

Figure 33. Depths and Yields of Wells in the Post Oak Aquifer

shows the distribution of well yields by cells in the Post Oak Aquifer according to the grain-size distribution, and Figure 35 shows those areas with greater yield because of both increased fracturing and larger grain-size. These fractures would influence flow separately from the grain-size distribution. Non-channel areas assumed to have lower permeability, transmissivity, and yield because of smaller grain size actually may be more productive because of a higher amount of fracturing. A more extensive lineament analysis was applied to the Arbuckle Group Aquifer (Chapter VI and Appendix G).

Gradient

The Post Oak water table map (Figure 36) is based on water-level measurements in November, 1984 (Table XXVI, Appendix I). The water-level contours are inferred across the channel areas because the higher permeabilities of those areas would decrease the gradient and deflect the contours. More water-level data are required to define better the water table across the channels in particular areas. For the region the gradients slope in the direction of increasing aquifer thickness, to the east and south, and decreasing topographic elevation. Cones of depression deflect the gradient in T 1 N, R 14 W, and T 3 N, R 10 W; at Lawton the gradient slopes west into a water-table valley.

Recharge

Recharge to alluvium was determined from streamflow data as described previously. To calculate recharge to the Post Oak Aquifer rainfall data were compared with well hydrograph data according to a method described by Lyons (1981, Table II, p.26). The mean annual

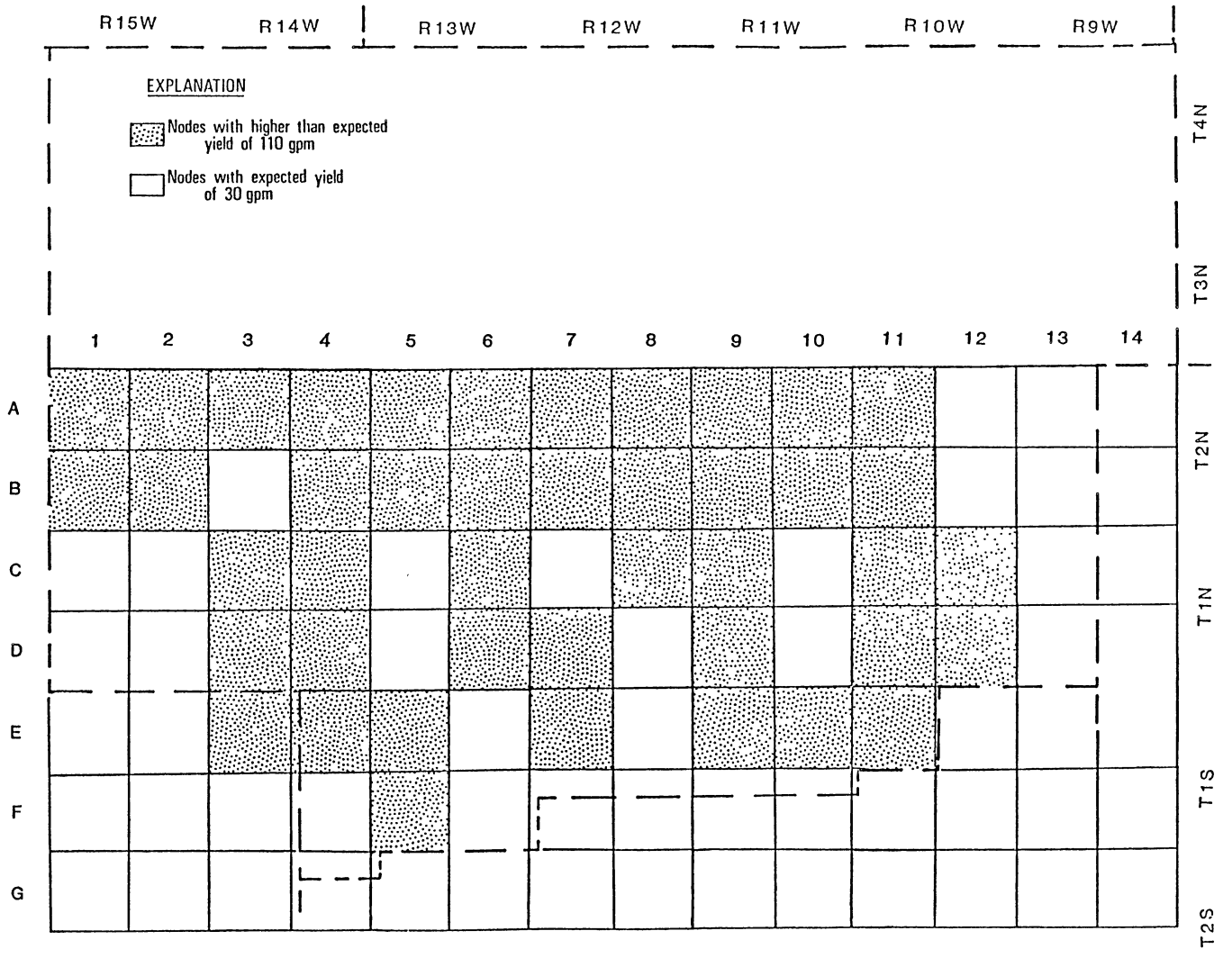

Figure 34. Expected Yield Map of the Post Oak Aquifer (Modified from Figure 30)

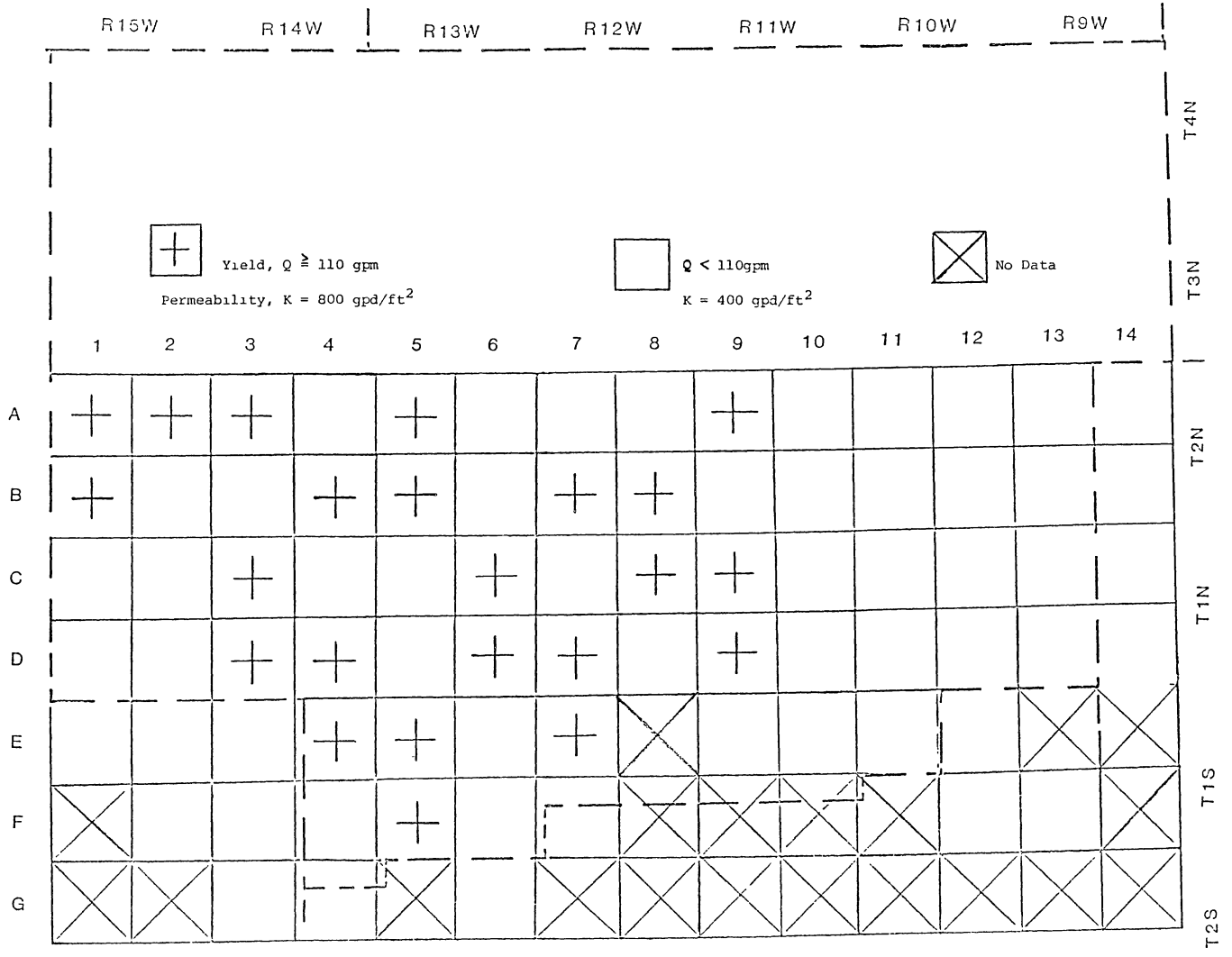

Figure 35. Expected Yield Map of the Post Oak Aquifer According to Grain-Size Distribution and Lineament Analysis

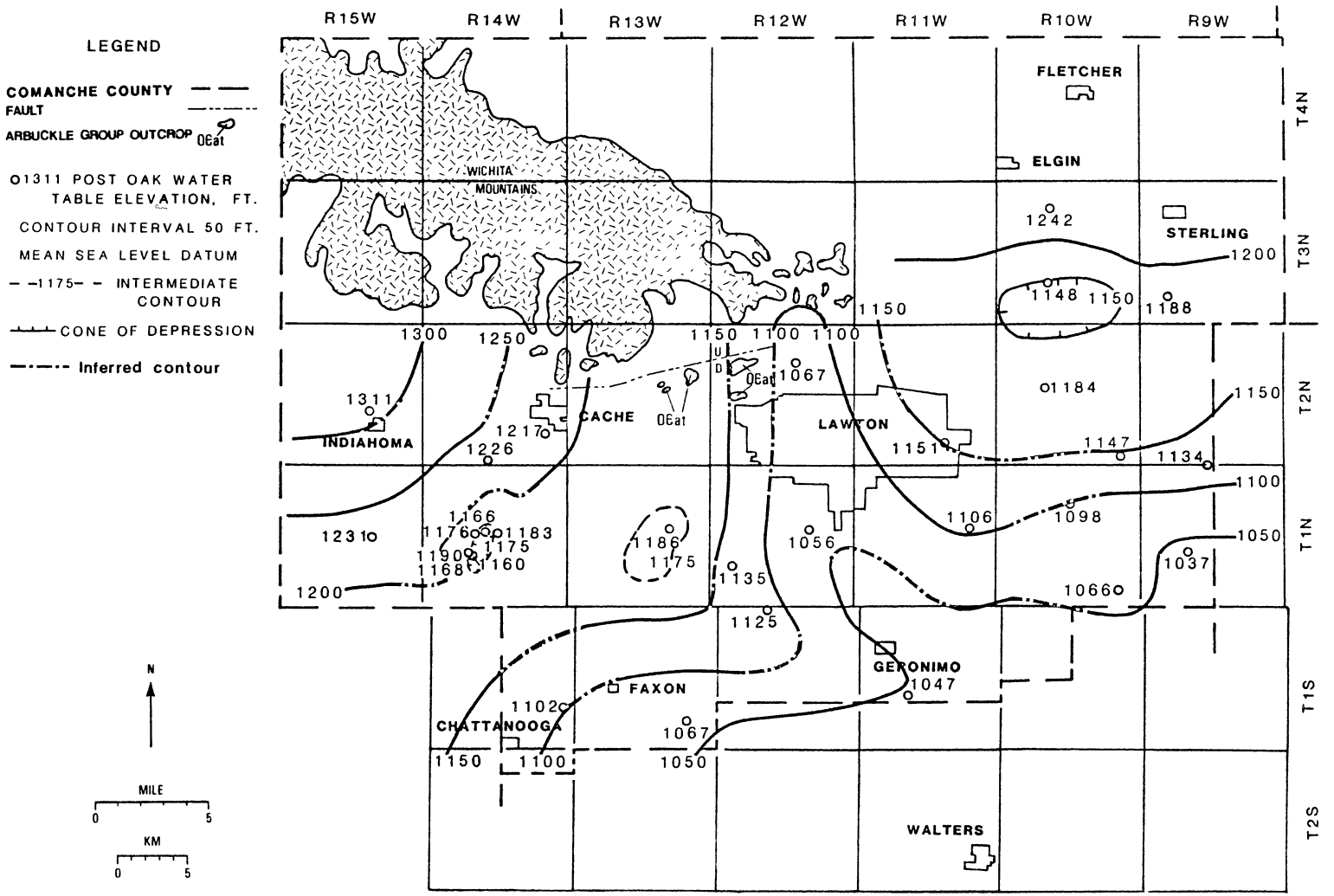

Figure 36. Water-Table Elevation Map of Post Oak Aquifer

recharge is 14 percent of rainfall, or 4.1 inches (104 mm; Table XXVIII, Appendix J).

Results of Computer Simulation

Calibration of the Konikow model as applied to the Post Oak required adjusting the storage coefficient, permeability, potentiometric head, and recharge. The original permeability values and their distribution were modified to facilitate flow through the model; the values determined previously were 800 gpd/ft^2 for the channel areas and 200 gpd/ft^2 outside the channels. The higher permeability had to be reduced to 400 gpd/ft^2 for the simulation because a low-permeability cell would act as a barrier to flow from a high-permeability cell because of the contrast between the former values.

Since water flows only across the face of a cell and not diagonally, it was difficult to duplicate exactly the geometry of the channels. Thus, it was necessary to straighten the channels in order to drain the aquifer and to prevent mounding against a low-permeability cell (Figure 80, Appendix H).

For the simulation the saturated thickness was a constant value for the entire grid. Twenty feet was the average saturated thickness as determined from well logs (Appendix B). The initial water-table elevation matrix was derived from Figure 36. During the calibration the gradient was smoothed and the matrix was modified to eliminate "holes" where water would accumulate as a mound and "hills" where water would drain and excessive drawdown would occur (Figure 81, Appendix H).

One of the purposes of the calibration was to determine the optimal recharge value, which initially was a constant for the entire grid,

4.1 inches per year (104 mm/yr). The value determined by the method of Lyons (1981), described in Appendix J (Table XXVIII), was reduced during the calibration to 0.125 and 0.4 in/yr (3.2 and 10.2 mm/yr). These compare with the mean annual recharge on the Blue Beaver Creek basin of 3.45 in/yr (87.6 mm/yr; Table XI, Appendix F) and with the recharge rate listed by Pettyjohn and others (1983, p.43) of 0.5 in/yr (13 mm/yr).

The node identification (NODEID) matrix replaced the constant recharge input in order to account for greater flow into the aquifer at nodes with higher permeabilities as described in Appendix H. The recharge and discharge in the NODEID matrix compensate for mounding and drawdown resulting from the water table and permeability matrices.

Various pumpages were established in the calibrated simulations in order to stress the aquifer. Pumpage according to the actual and assumed water use did not produce significant drawdowns (Figures 83 and 84, Appendix H). To determine the maximum allowable pumpages (Table XXIII, Appendix H), the discharges were increased to produce drawdowns of 14 ft, one foot above the five-foot well screen, at the pumping nodes. The maximum pumpages ranged from 1.6 to 1.8 ft^3/s (720 to 810 gpm; 45 to 51 l/s).

Ground-Water Quality

Nitrate and Fluoride Content

Nitrate and fluoride are regulated by the Oklahoma Department of Health according to toxic limits established by the U.S. Environmental Protection Agency. The Oklahoma water quality standards (Oklahoma

Water Resources Board, 1982) allow the maximum level of nitrate (NO_3-N) in public water supplies to be 10.0 mg/l and the level of fluoride to be 1.6 mg/l.

Ground-water quality data for the Post Oak Aquifer and alluvium were reported in Hounslow and Back (1985a and 1985b), Stone (1981), and the U.S. Geological Survey Water Data Storage and Retrieval System (WATSTORE). These data were used by the author to construct maps which indicate areas where the maximum allowable levels of nitrate (NO_3-N) and fluoride are exceeded (Figures 37 and 38). These data were not differentiated according to depth. Areas of excessive nitrate are north and west of Indiahoma, southeast of Cache, and north and east of Lawton (Figure 37). Excessive fluoride occurs between Lawton and Indiahoma, south of Cache, and north of the Wichita Mountains (Figure 38). The complex geochemistry of the occurrence of fluoride in the Post Oak Aquifer (Hounslow and Back, 1985a; Back, 1985) implies that wells within the same area would exhibit different amounts of fluoride.

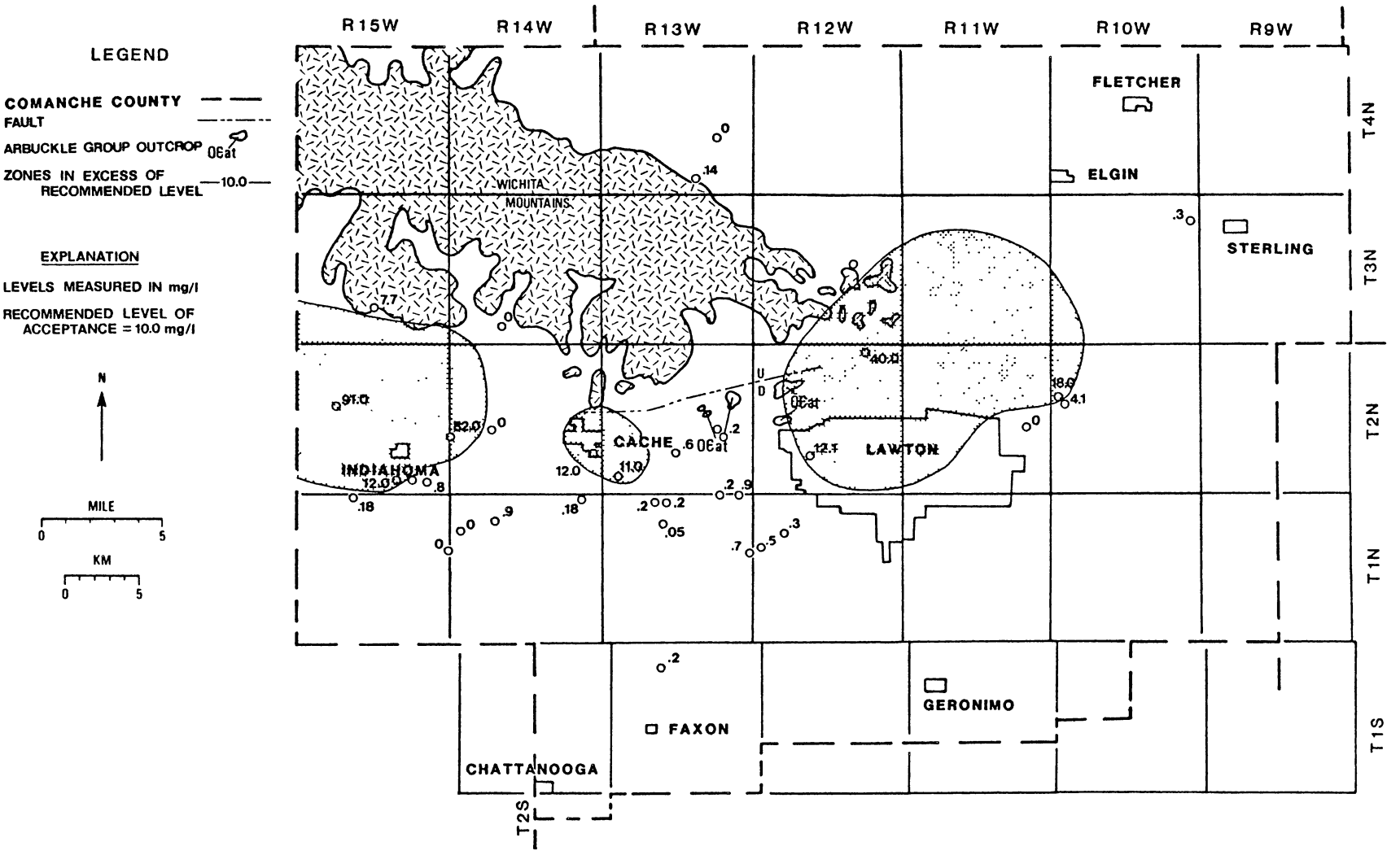

Figure 37. Areas With Nitrate (NO_3-N) in Excess of Recommended Level

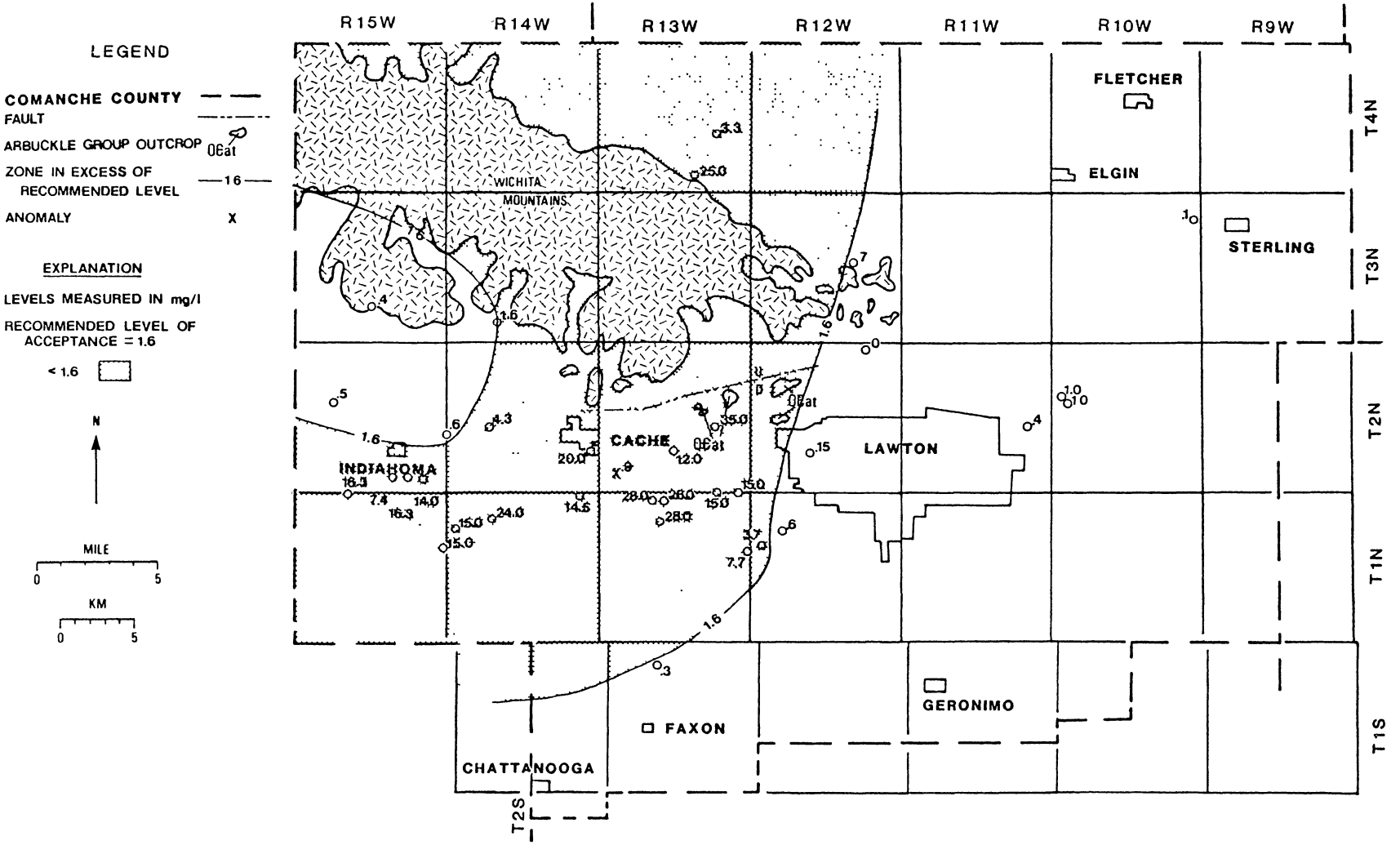

Figure 38. Areas With Fluoride in Excess of Recommended Level

CHAPTER VI

GROUND-WATER HYDROLOGY OF THE ARBUCKLE GROUP AQUIFER

Description

The Arbuckle Aquifer consists of the limestones and dolomites of the Arbuckle and Timbered Hills Groups in the subsurface south of the Wichita Mountains. These rocks crop out at three locations south of the mountains, but are separated from the aquifer by a fault not shown on the geologic maps by Havens (1977 and 1983). The absence of a fault would indicate significant erosion of the upper part of the Arbuckle Group. The Arbuckle rocks have probably been faulted into several blocks south of the mountains as they have been to the north (Harlton, 1972), and the structural contour map by Havens (1983) shows a sharp change in structural style southwest of Lawton which is probably evidence of a fault. Unfortunately, the deep seismic survey by the Consortium for Continental Reflection Profiling (Brewer, 1982) does not indicate the shallow structures in the Arbuckle rocks.

The Arbuckle is absent in the subsurface adjacent to the Wichita igneous block, south of Faxon, and west of Indiahoma (Figure 39). In those locations the Permian sediments lie unconformably on the basement igneous rocks. The thickness map of the Arbuckle Aquifer (Figure 39) was modified from an Arbuckle isopach map (McDaniel, 1959, Plate I) according to the elevation of the top of the Arbuckle shown in

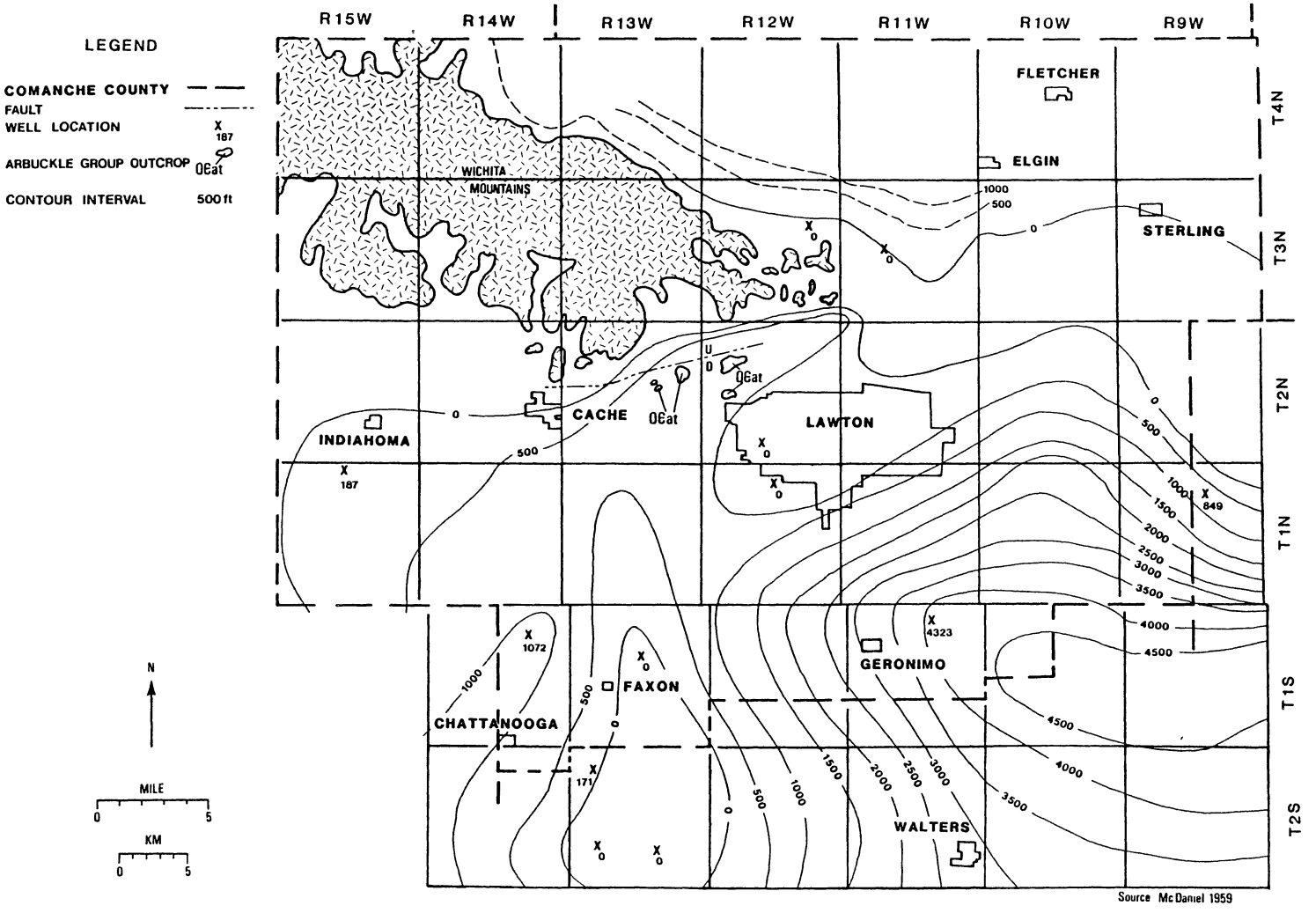

Figure 39. Thickness Map of Arbuckle Group Aquifer

Havens (1983, Plate 1) and the depth to basement shown in Ham and others (1964, Plate II). The aquifer thickens to the southeast in the Marietta Basin (Figure 39).

Aquifer Characteristics

For the Arbuckle-Simpson Aquifer in the Arbuckle Mountains region, Fairchild and others (1983) reported specific capacities of 0.26 to 77 gpm/ft (0.05 to 16 1/s/m), transmissivities of 40 to 67,600 ft^2/d (300 to 506,000 gpd/ft.) and storage coefficients of 0.006 to 0.011, with an average of 0.008. These values were determined from aquifer recovery tests, ground-water hydrographs, and stream hydrographs (Fairchild and others, 1983, p.114). Fairchild and others (1983) cautioned that the aquifer tests only roughly estimated the transmissivity because the Arbuckle Aquifer did not satisfy the assumptions of homogeneity, isotropy, infinite areal extent, and complete well penetration.

Aquifer test data for the Arbuckle Aquifer south of the Wichita Mountains is scarce. Havens (1983) reported specific capacities of 0.25 and 0.88 gpm/ft (0.05 and 0.2 1/s/m) from two U.S. Geological Survey wells. Applying the Theis equations to aquifer test and recovery data from those wells (Table XXIX, Appendix K) provided mean transmissivities of 1300 (1.9×10^{-4} m^2/s) and 3800 gpd/ft (5.5×10^{-4} m^2/s). Walton's formula (Equation 3-1) applied to specific capacity data from the U.S.G.S. and other wells gave a representative transmissivity of 1720 gpd/ft (2.47×10^{-4} m^2/s; Figure 40); assuming an effective aquifer thickness equal to the average well penetration of 500 feet (152 m) provided a permeability of 3.5 gpd/ft^2 (1.7×10^{-6} m/s; Figure 41) for the Arbuckle Aquifer.

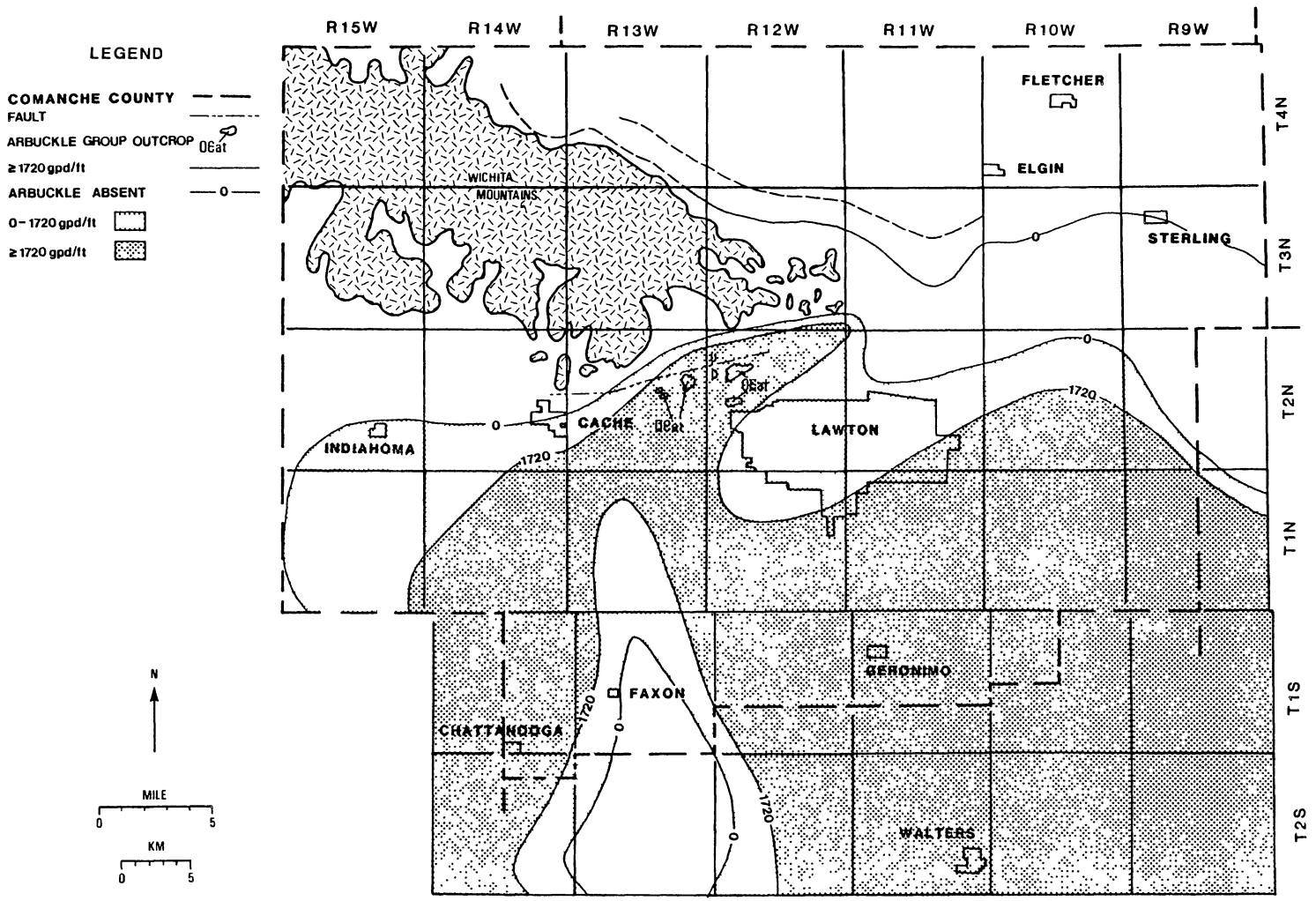

Figure 40. Transmissivity Map of Arbuckle Group Aquifer

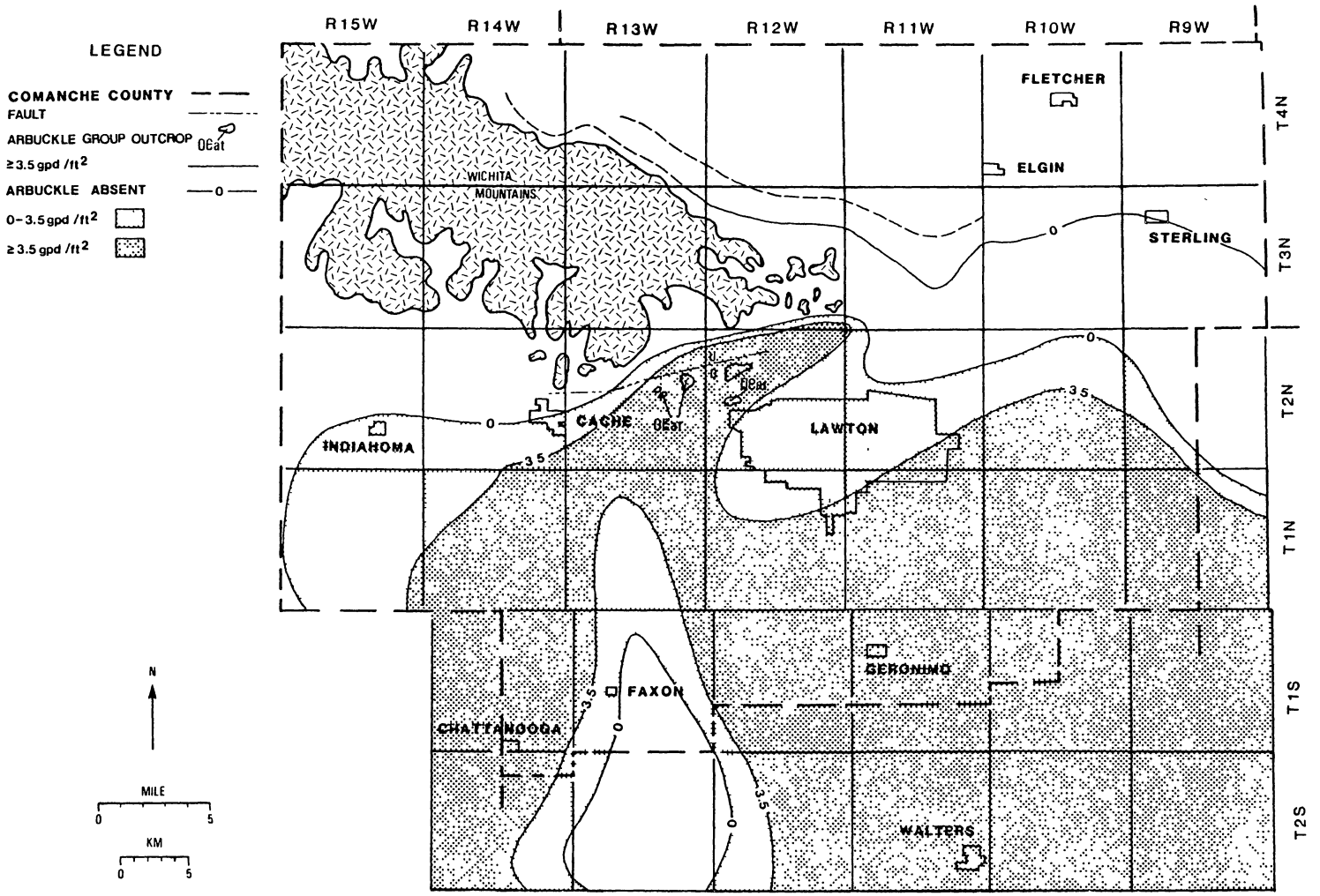

Figure 41. Permeability Map of Arbuckle Group Aquifer

A 24-hour aquifer test in May, 1986, performed by the Layne-Western Company on Indiahoma municipal supply well #4 provided more data on the Arbuckle Aquifer. Drillers' logs for this well and other wells, aquifer test data, and analyses of these data are in Appendix L.

A preliminary estimate of the transmissivity was calculated from the specific capacity by a formula for confined aquifers from Logan (1964):

$$T = \frac{1750\ Q}{s} \qquad (6\text{-}1)$$

where T = transmissivity, gpd/ft.,

Q = well yield, gpm, and

s = drawdown, ft.

Given an average well yield from the test of 53.3 gpm (3.36 1/s) and a total drawdown of 296 ft (90.2 m), then the specific capacity is 0.18 gpm/ft (3.7×10^{-2} 1/s/m), and the transmissivity is 315 gpd/ft (4.5×10^{-5} m^2/s). Assuming a storativity of 0.008 (Fairchild and others, 1983, p.146) and a well efficiency of 60%, then Walton's formula (Equation 3-1) yields a transmissivity for the Arbuckle Aquifer of 410 gpd/ft (5.9×10^{-5} m^2/s).

For further analysis the aquifer was assumed to be homogeneous, isotropic, non-leaky, and infinite in areal extent compared to the well radius, with water released instantaneously from storage. A logarithmic graph of drawdown measured in the pumped well versus time exhibits a significant deviation from the Theis nonequilibrium type curve (Figure 42) because of leakage to the Arbuckle Aquifer. The type curve could be fitted to only the early part of the time-drawdown graph, and later deviations were caused by a varying pumping rate. For the Theis equations the distance between the pumped well and the observation

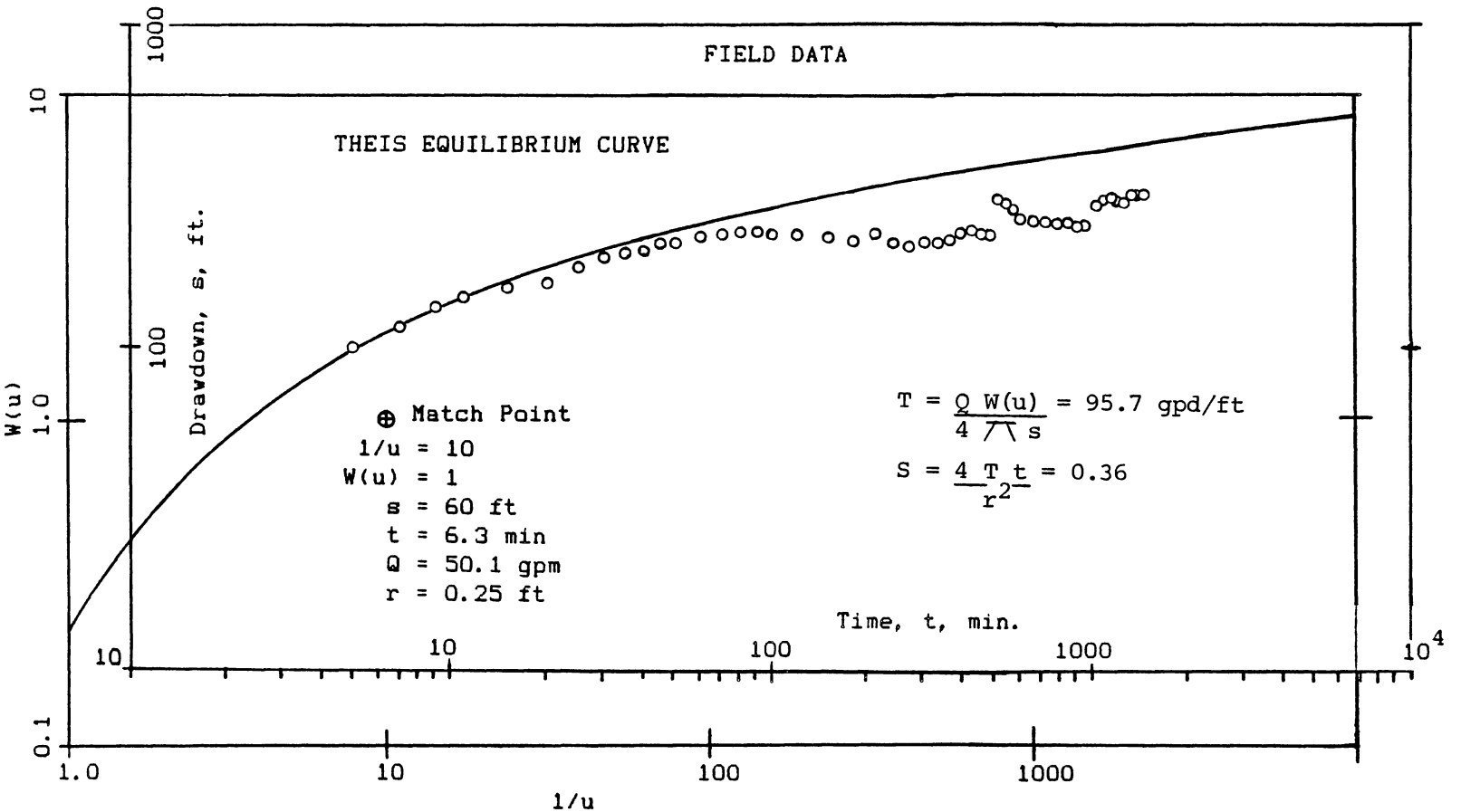

Figure 42. Theis Nonequilibrium Time-Drawdown Analysis for Indiahoma Well #4

well, r, was assumed to be equal to the radius of the pumped well. The calculated transmissivity is 96 gpd/ft (1.4 x 10^{-5} m^2/s), a low value, and the storativity is 0.36, an extreme value not characteristic of a confined aquifer (Appendix L).

A semi-logarithmic graph of drawdown (linear) versus time (logarithmic) is linear when u = 0.01 (Walton, 1970, p.212), usually after a sufficient amount of time has elapsed during an aquifer test. The following equation provides the length of this time period for the drawdown data to become linear and for the straight-line (Cooper-Jacob) method to be valid (Walton, 1970, p.212):

$$t_s = \frac{1.35\ (10^5)\ r^2\ S}{T} \qquad (6\text{-}2)$$

where t_s = elapsed time required for a semi-logarithmic time- or distance-drawdown graph to describe a straight line, minutes,

r = distance from pumped well to observation well, ft,

S = storativity, fraction, and

T = transmissivity, gpd/ft.

Applying this equation to the Arbuckle Aquifer with transmissivity derived from specific capacity data (Table XXIX, Appendix K), storativity from Fairchild and others (1983, p.146), and distance to the observation well equal to the radius of the pumped well, gives a required time of 0.2 minutes (Appendix L). Thus, this straight-line method is valid for the data from the pumped well. The assumptions associated with this method are the same as those for the Theis analysis. The graph of drawdown versus time deviates from a straight line because of leakage (Figure 43); the transmissivity calculated from the graph is 58 gpd/ft (8.3 x 10^{-6} m^2/s), a low value (Appendix L).

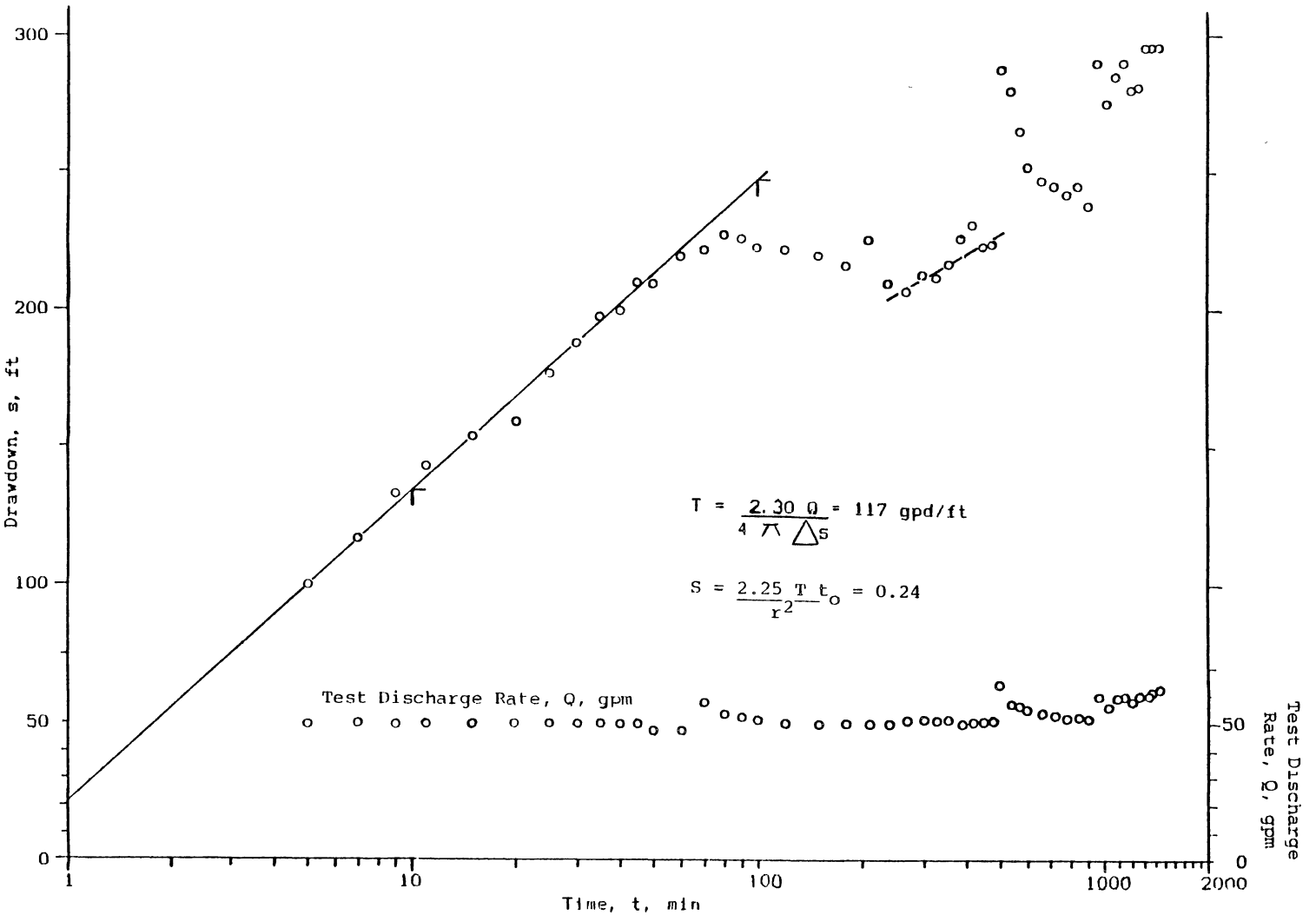

Figure 43. Cooper-Jacob Time-Drawdown Analysis for Indiahoma Well #4

Drawdowns in nearby monitoring wells (wells #1 and #2) were measured too early for the data to become linear.

Drawdown measurements from wells #1 and #2 allowed the calculation of aquifer characteristics according to a distance-drawdown method of Walton (1970, p.217) which uses the Hantush-Jacob formulas for field units (Fetter, 1980, p.275):

$$s = \frac{2.3\ Q\ W(u,r/B)}{4\ \pi\ T} \qquad (6\text{-}3)$$

$$u = \frac{r^2\ S}{4\ \pi\ T} \qquad (6\text{-}4)$$

$$\frac{r}{B} = \frac{r}{(T\ b'/\ K')^{\frac{1}{2}}} \qquad (6\text{-}5)$$

where s = drawdown, ft,

Q = discharge, gpm,

r = radial distance from pumped well, ft,

T = transmissivity, gpd/ft,

S = storativity, dimensionless,

t = time, min,

b' = thickness of aquitard, ft,

K' = vertical permeability of aquitard, gpd/ft^2, and

$W(u,r/B)$ = well function for leaky artesian aquifers.

This method assumes a leaky artesian aquifer with no storage in a thin, relatively permeable aquitard. A graph of drawdown versus distance to the pumped well was matched with a graph of $W(u,r/B)$ against r/B for various values of u (Figure 44). Because drawdown measurements were not simultaneous but were taken six minutes apart, there are only two data points on the distance-drawdown graph. The transmissivity determined by this method was 1800 gpd/ft (2.6×10^{-4} m^2/s), and the

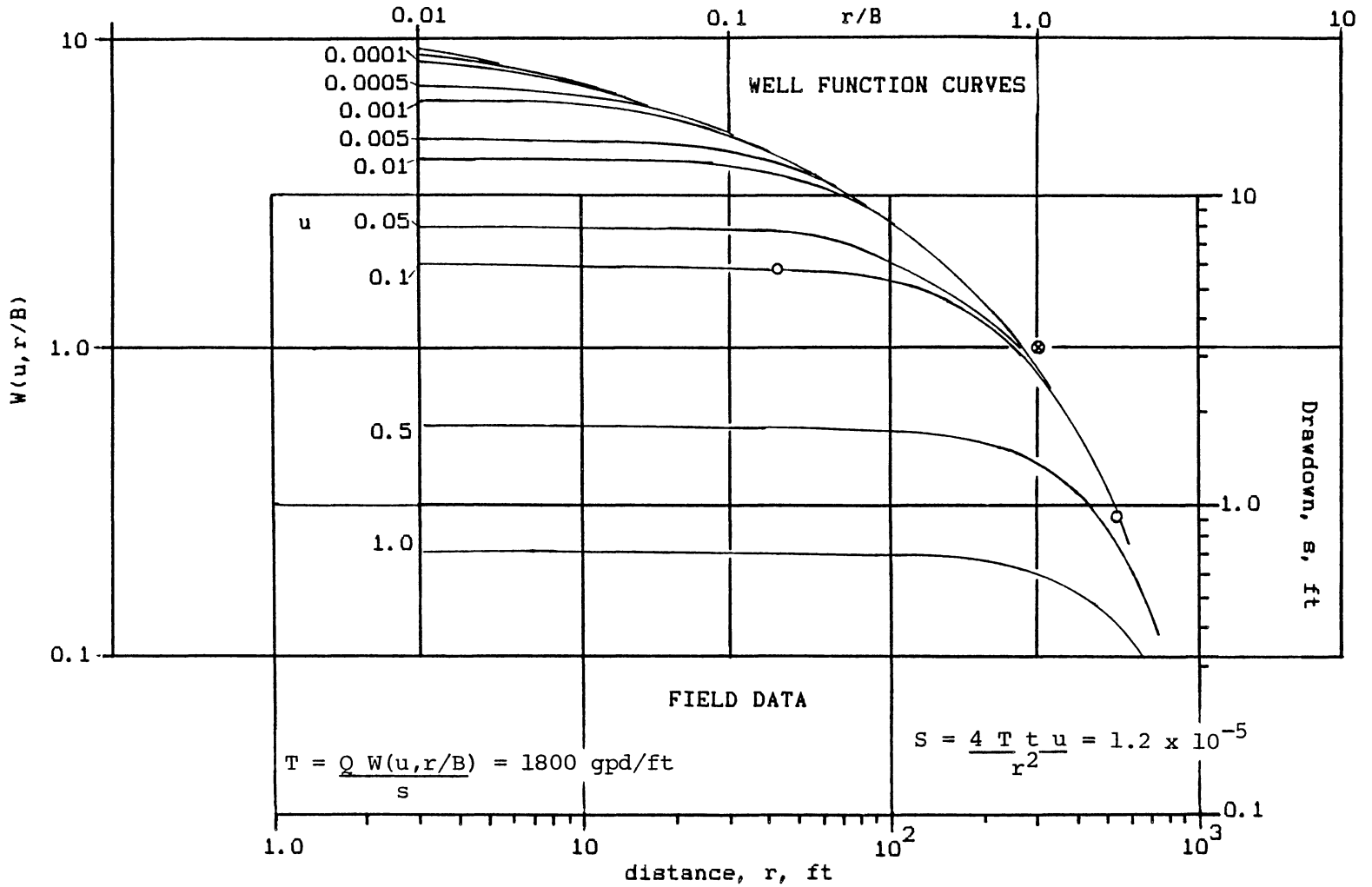

Figure 44. Leaky Artesian Aquifer Time-Drawdown Analysis for Indiahoma Well #4

storativity was 1.2 x 10^{-5} (Appendix L), very low values compared to those from Fairchild and others (1983, p.146) of 112,000 gpd/ft (0.016 m^2/s) and 0.008.

A source of the leakage during pumping could be the Permian strata above the Arbuckle Aquifer as predicted by the recharge regime in the area (see Recharge below and Figure 51). Solution openings filled with red-bed material in the Arbuckle rocks provide a pathway for leakage. Because of the varied lithology of the Permian red beds, it is difficult to differentiate an actual aquitard. Assuming that the complete Permian section below the Post Oak Aquifer acts as an aquitard, then its thickness, b' or m', is about 400 ft (122 m). Its maximum vertical permeability, K' or P', would be about 390 gpd/ft^2 (1.8 x 10^{-4} m/s; Appendix L).

Residual drawdowns in the pumped well were measured during a recovery test (Figure 45) which provided a transmissivity of 350 gpd/ft (5.0 x 10^{-5} m^2/s; Appendix L), a value comparable to that derived from the specific capacity data. Neither the distance from the pumped well nor well efficiency are factors in this calculation.

The methods previously applied to the aquifer test data assume radial porous-media flow to the pumped well. As noted above, however, ground-water flow in the Arbuckle Aquifer is through fractures. The time-drawdown data (Figure 43) exhibit an influence by fracture flow in the decreased rate of drawdown after 100 minutes indicating contribution from a fracture then the increased rate of drawdown after 200 minutes indicating drainage of the fracture. Jenkins and Prentice (1982) developed a method for aquifer test analysis in fractured rocks assuming linear, or non-radial, flow towards a fracture or "extended

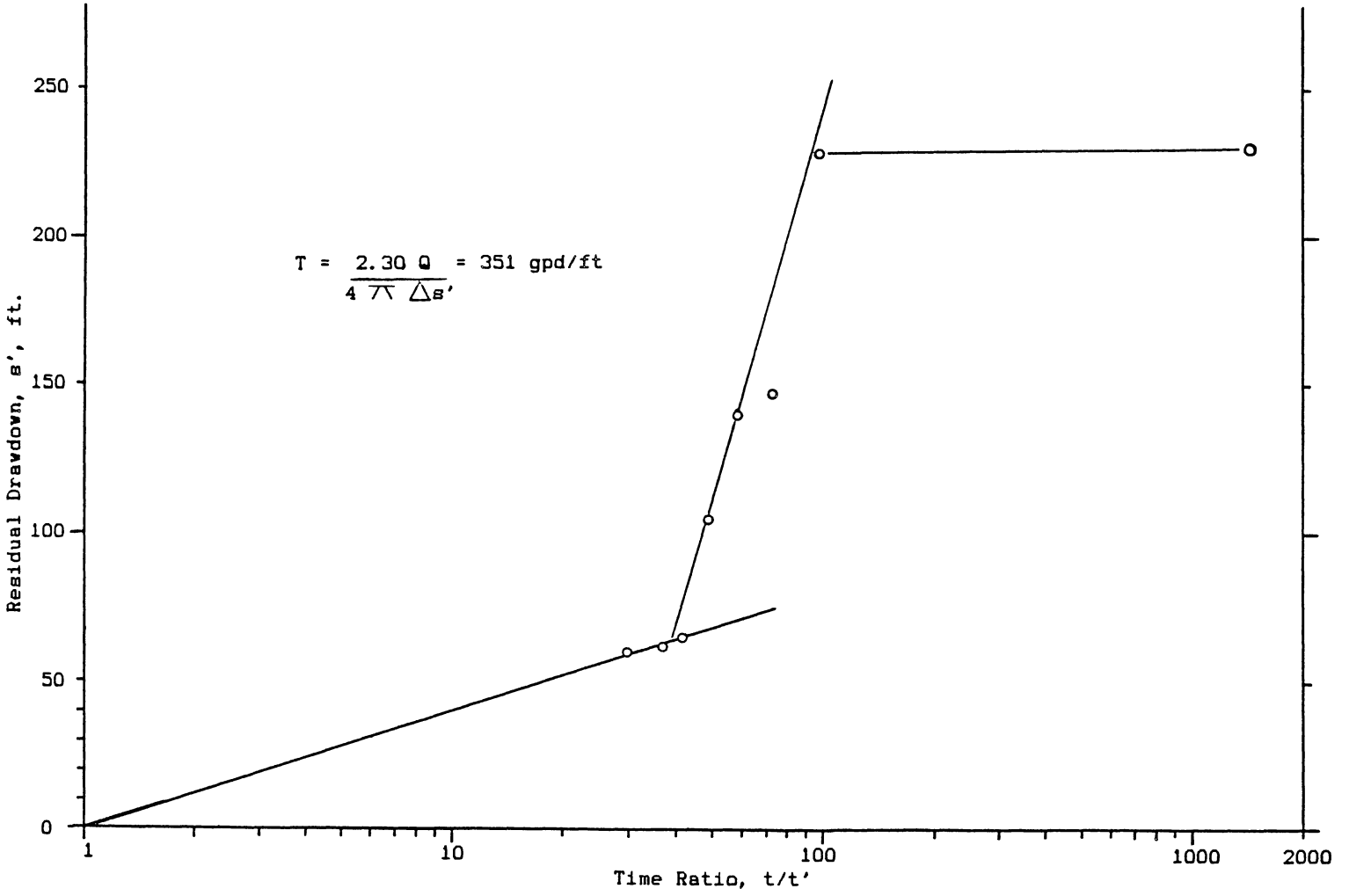

Figure 45. Recovery Graph for Indiahoma Well #4, Residual Drawdown vs. Time Ratio

well". An arithmetic plot of drawdown, s, in the pumping or observation well versus the square root of time, $t^{\frac{1}{2}}$ (Figure 46), should be a straight line if flow is linear towards the fracture. It is not necessary that the well intersect the fracture for this analysis.

Early drawdown data from the Indiahoma wells plot on straight lines indicating possible linear flow, but more accurate data from a longer aquifer test ($t^{\frac{1}{2}} > 40$) would be required to confirm this result.

The analysis allows calculation of the length and orientation of the fracture contributing to the well, but geologic evidence should be used to confirm these parameters. Although the calculated orientation, 40° W of N (Appendix L), coincides with a number of surface lineaments (Figure 62, Appendix G), the method assumes that the observation wells are on the same side of the fracture, an assumption considered beyond the precision of the drawdown data and the geologic evidence.

These aquifer test analyses provided transmissivity values over a two-order-of-magnitude range (Table I) and storativity values that were not characteristic of a confined aquifer (Appendix L). Previous studies (Havens, 1983; Fairchild and others, 1983) have relied on recovery tests to determine aquifer characteristics. For this study Walton's distance-drawdown analysis assuming a leaky aquifer (Figure 44) was believed to provide the best value of transmissivity, although the distance-drawdown graphs were based on only two data points and the assumptions may have been invalid (Walton, 1970, p.217). This method accounts for leakage and for flow between an observation well and the pumped well, and well loss is not a factor.

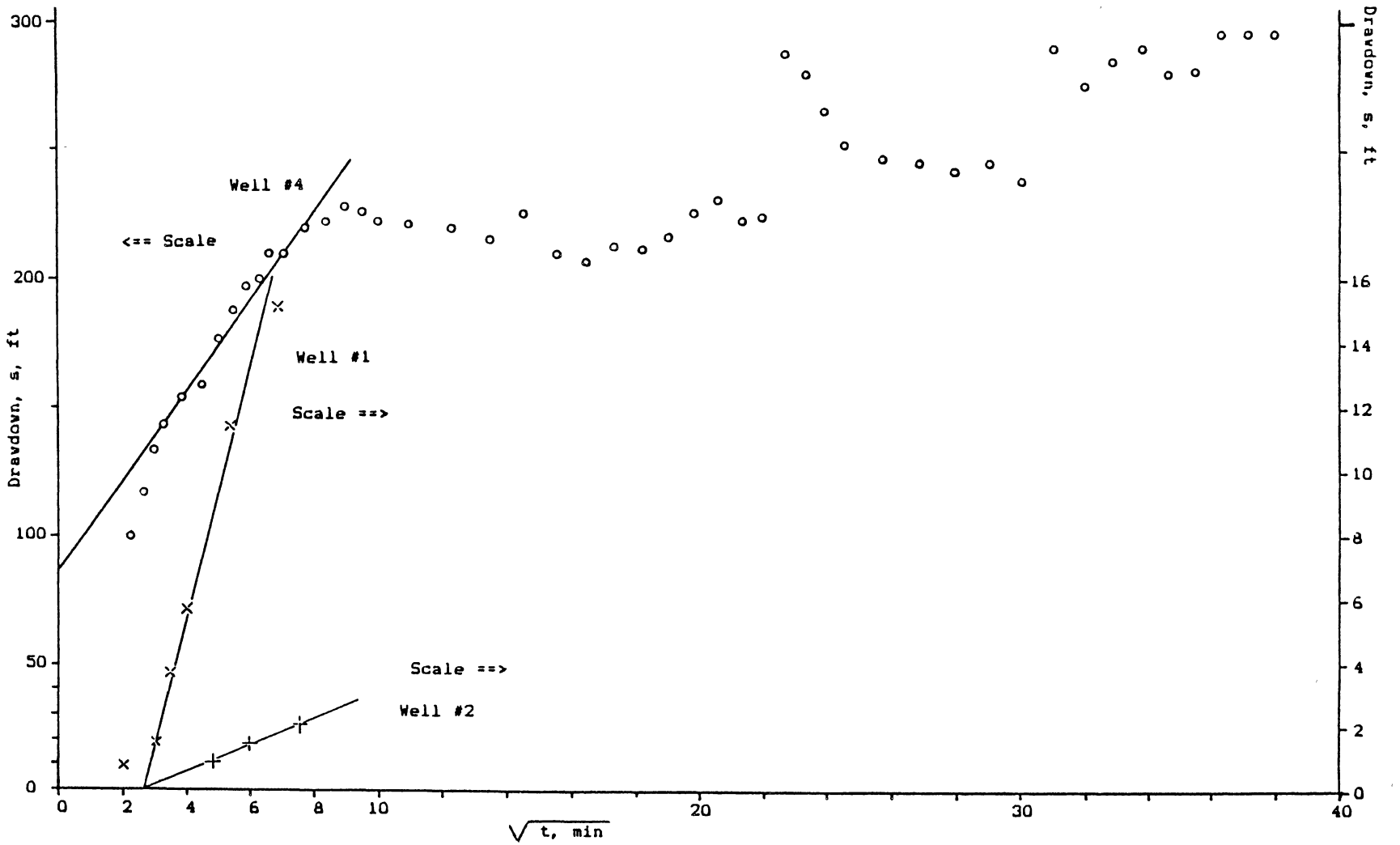

Figure 46. Linear (Nonradial) Flow Analysis for Indiahoma Well #4, Drawdown vs. Square Root of Time

TABLE I

TRANSMISSIVITY AND STORATIVITY VALUES
FROM AQUIFER TEST OF INDIAHOMA
MUNICIPAL WELL #4

Method	Transmissivity gpd/ft	Storativity
Theis	96	*
Cooper-Jacob	117	*
Recovery	350	--
Specific Capacity, 100 %	246	--
60%	410	--
Logan (1964)	320	--
Walton: distance-drawdown	1800	1.2×10^{-5}
Fracture flow	1400	0.001 assumed

* Value is uncharacteristic of confined aquifer (Appendix L).

Yield

Arbuckle wells yield 300 to 2500 gpm (19 to 158 1/s) in the Lawton area; further west the yields range from 25 to 150 gpm (1.6 to 9.5 1/s; Havens, 1977). The wells typically are cased to the top of the limestone aquifer and either produce from an open hole or are screened opposite producing intervals (Figure 52).

The calculated yield of the Arbuckle Aquifer is 270 gpm (17 1/s; Figure 47), based on an average well radius of 0.28 feet (3 3/8 in; 8.6 cm), an average pumping duration of 5000 minutes (30 hours), and a

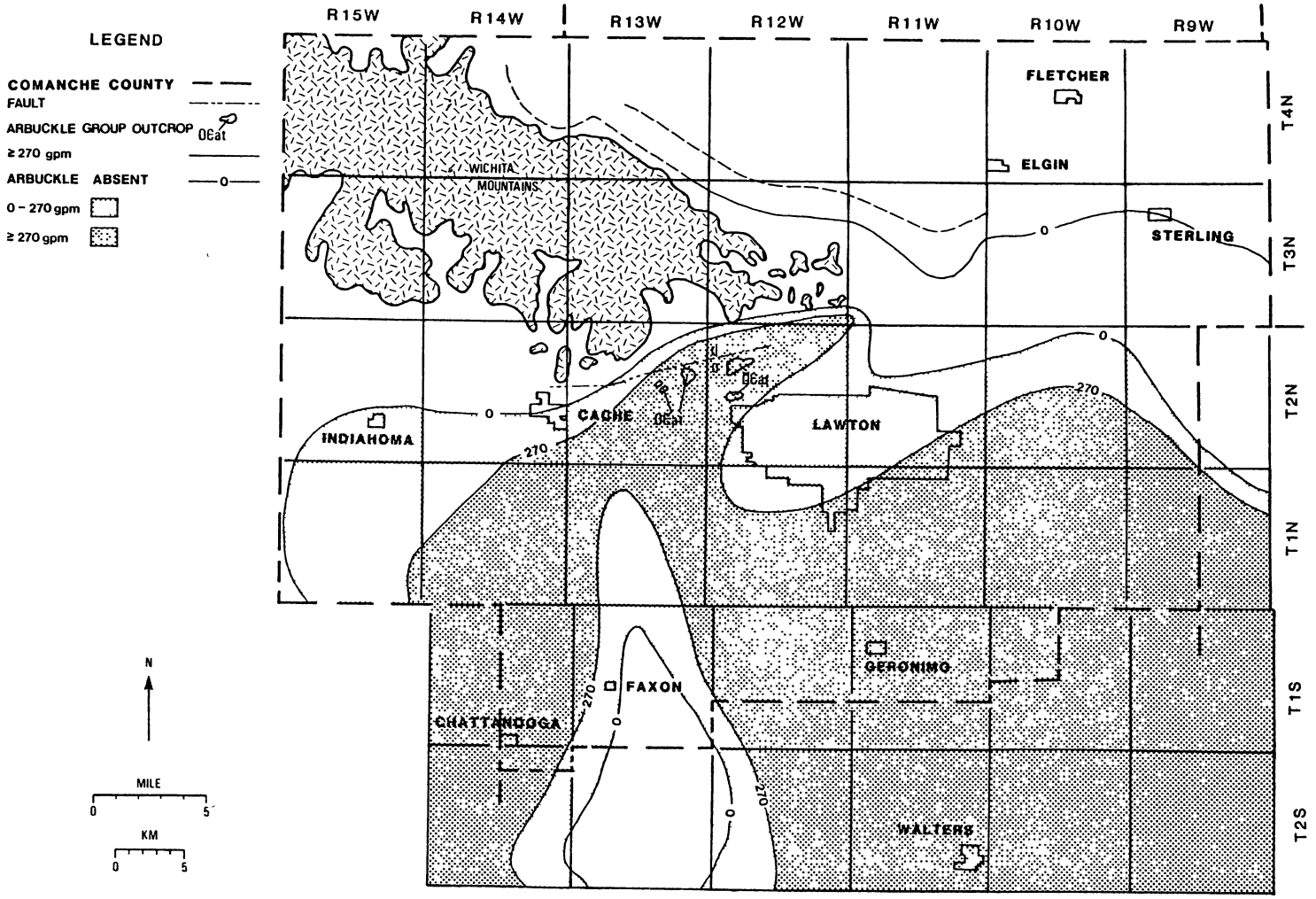

Figure 47. Yield Map of Arbuckle Group Aquifer

maximum drawdown of 350 ft (107 m). Storativity was assumed to be 0.0001, a typical value listed in Walton (1970, p.315) for a confined aquifer. With a storativity of 0.008, calculated yield should be 350 gpm (22 1/s).

The lineament analysis of the Arbuckle Aquifer provided the possible distribution of estimated well yield. The two methods of analysis (Appendix G) located areas which would yield more than 270 gpm (Figure 48), the average yield calculated from production well test data.

Gradient

The Arbuckle Aquifer is confined, with considerable artesian pressure: deep wells in Lawton have flowed, and in a 997-foot (304 m) U.S.G.S. observation well southeast of Cache (Figure 49) the water rises 452 feet (138 m) above the top of the aquifer. Water-table elevations were measured at three locations in Lawton and Indiahoma in March, 1985 (Table XXVII). Land-surface elevations were determined from topographic maps. The Oklahoma Water Resources Board reported a 2800-foot (853 m) flowing well east of Lawton, and the U.S.G.S. observation well provided a fifth control point. A well at Cache was reported to have a water-level elevation of 1116 feet in May, 1972. Assuming a subsequent rise equal to that at the observation well, 10.5 feet (3.2 m), then the water level at Cache in March, 1985, should have been 1126 feet. The same procedure applied to Indiahoma well #2 provided an expected water-level elevation of 1134 feet, which compares with an elevation measured in May, 1986, of 1140 feet. This figure should approximate the elevation for the previous year because the

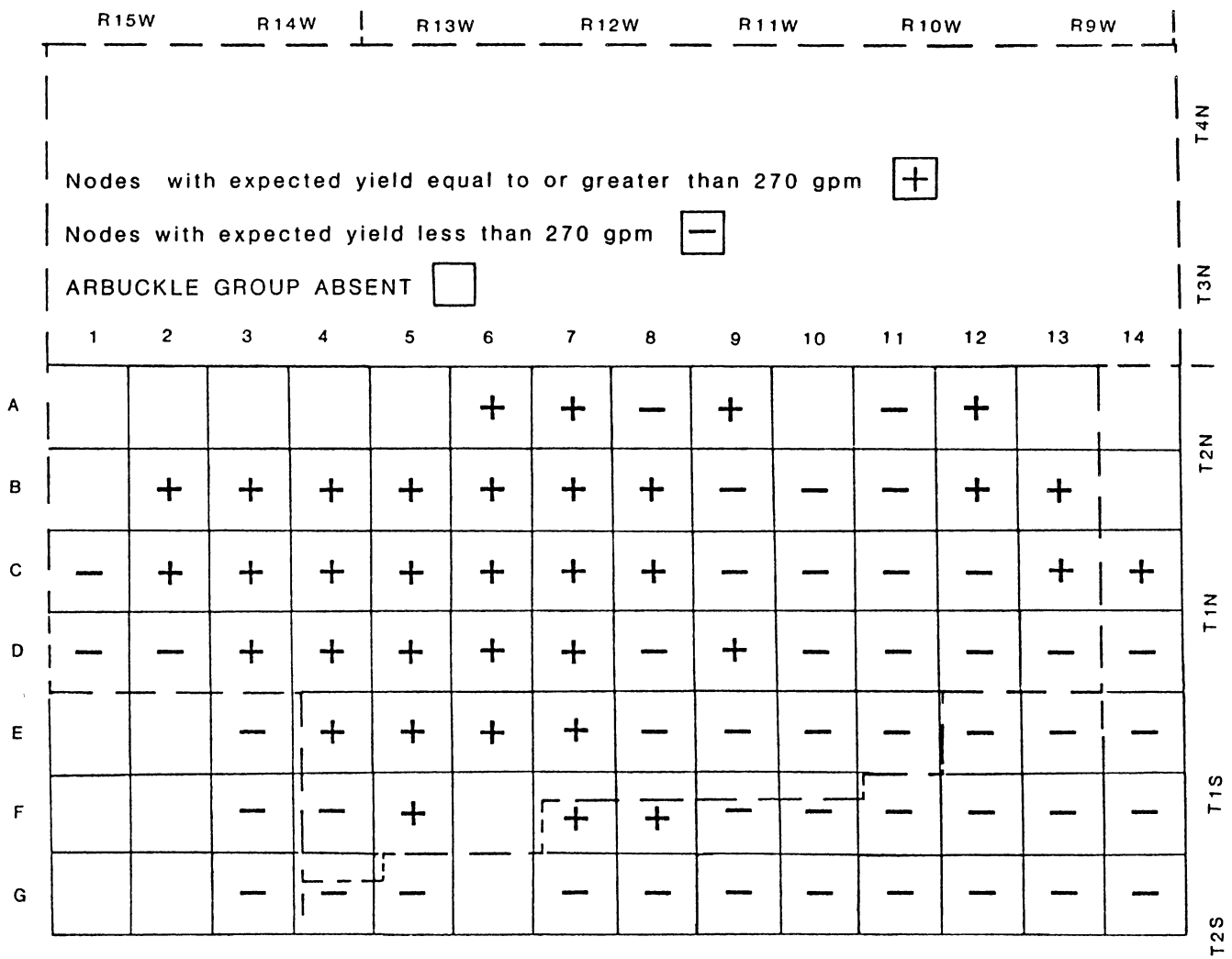

Figure 48. Expected Yield Map of the Arbuckle Group Aquifer According to Lineament Analysis

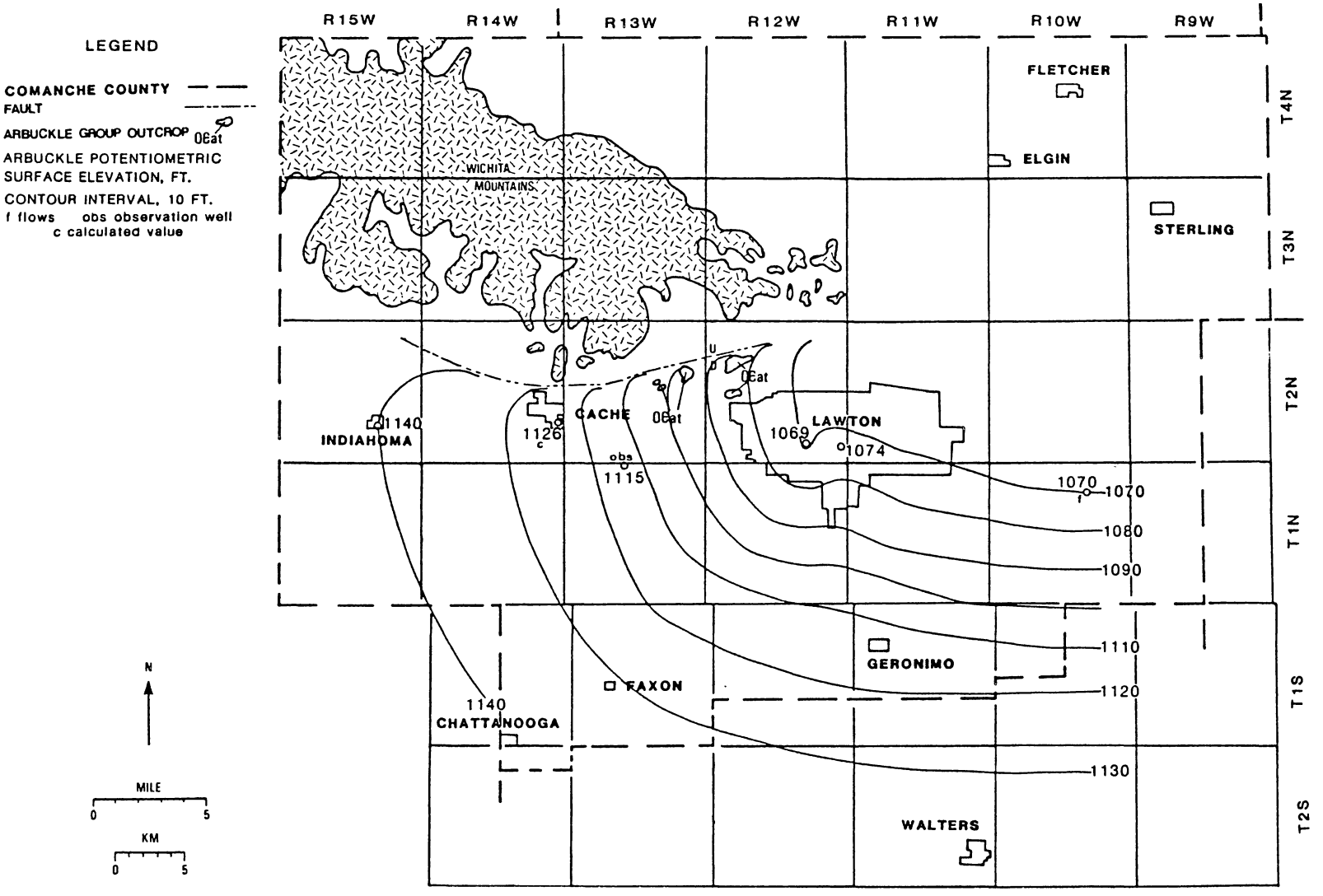

Figure 49. Potentiometric Surface Map of Arbuckle Group Aquifer

water table has not fluctuated more than two feet since 1980 (Figure 50).

These six control points indicate a gradient dipping to the east and north (Figure 49). The fault between the Wichita Mountains and the Arbuckle Group and outcrops of Arbuckle rocks to the south are minor recharge areas; the potentiometric surface is higher adjacent to these features. The Arbuckle rocks dip to the south and east, and the gradient should follow this geologic control. However, deeper burial and higher pressure to the south raises the potentiometric surface as shown by deep flowing wells in this area.

A hydrograph of the U.S.G.S. observation well (Figure 50) shows a major rise in water level of 16 feet (4.9 m) in 1972 and 1973 followed by lesser fluctuations and a decline in water level from 1974 to 1984. The recovery of water level was probably the result of the decreased pumpage from the Arbuckle Aquifer because Lawton no longer used ground water for municipal supply; subsequent fluctuations were caused probably by minor pumpage for non-municipal supply. Because the observation well is within the area of recharge for the Arbuckle Aquifer (Figure 51), the hydrograph would record the effects of recharge; these are the yearly changes in water level in response to longer precipitation trends. However, because detailed pumpage data for the Arbuckle Aquifer were not available, it was not possible to determine whether a particular water-level fluctuation was due to either pumpage or recharge. Recharge fluctuations are long-term, whereas pumpage fluctuations are both long- and short-term. Because the Arbuckle lies below a thick aquitard, particular fluctuations should not be corre-

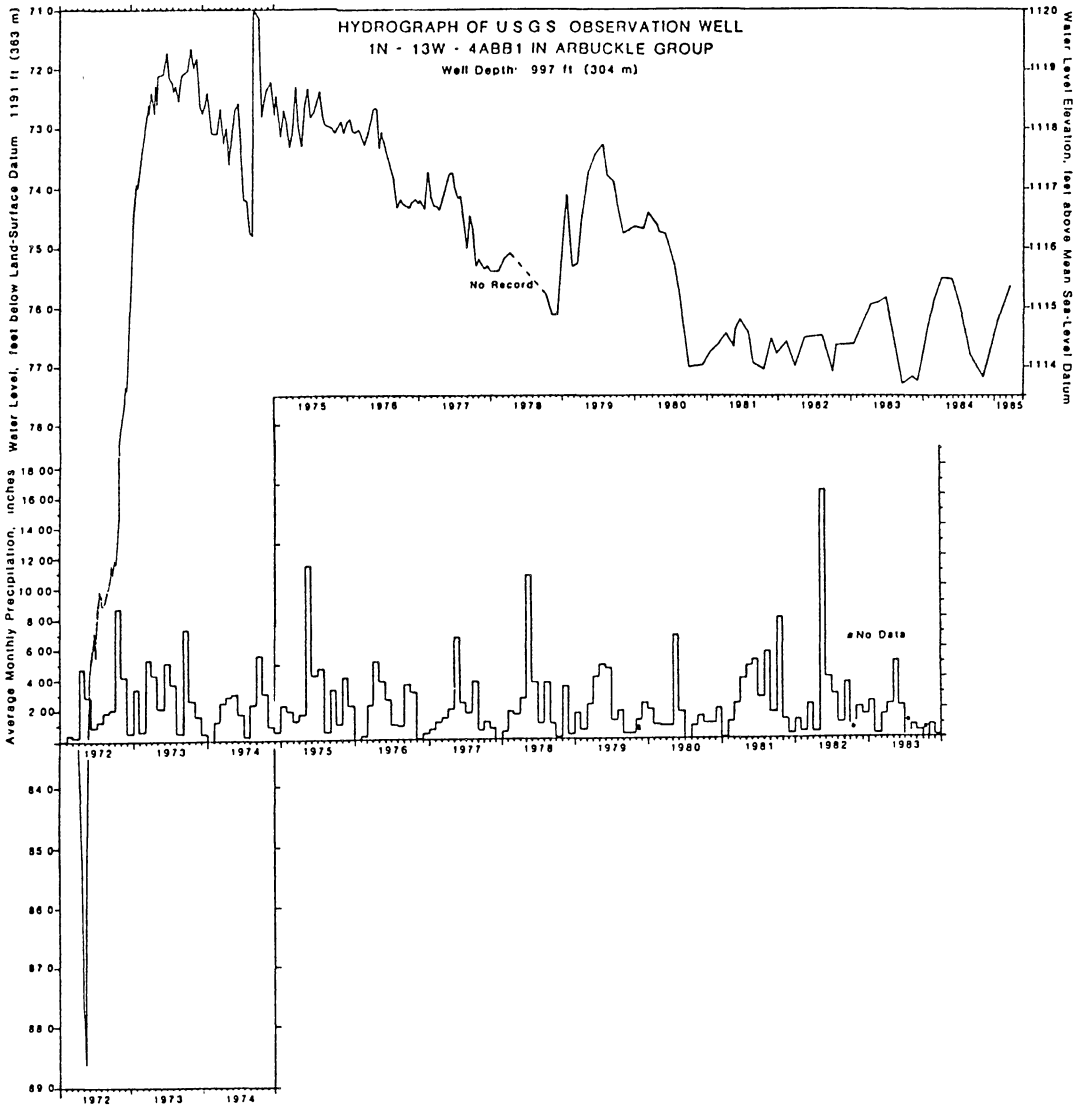

Figure 50. Well Hydrograph From Arbuckle Group Aquifer and Precipitation Data

lated with specific precipitation events because of the unknown recharge lag time. The hydrographic data lacks the precision required to determine the barometric efficiency of the aquifer, or its response to changes in atmospheric pressure (Walton, 1970, p.208).

Recharge

The potentiometric surface of the Arbuckle Aquifer and the water table of the Post Oak Aquifer define a recharge regime between the two aquifers. Arbuckle potentiometric surface elevations were interpolated for the locations of wells in the Post Oak Aquifer (Figure 94, Appendix I). The difference between the potentiometric surface elevations of the Post Oak and Arbuckle aquifers indicates the direction of recharge between them (Figure 51). To the north the Post Oak potentiometric head is higher, and recharge is to the Arbuckle. To the south the Arbuckle potentiometric head is higher, and recharge is to the Post Oak, although pumping can disrupt this recharge regime as seen in T 2 N, R 12 W. This relationship shows that all areas of the Arbuckle are not recharged through the Post Oak, as stated by Davis (1958) and Havens (1983).

Flow through the Arbuckle Aquifer is along joints and fractures which have developed with the tectonic movements of the Wichita uplift and subsequently have been enlarged by solution. These solutional openings are evident on the caliper log, which measures drill-hole diameter, in Havens (1983, Figure 4). Intragranular porosity is assumed to be low in most of the Arbuckle rocks (Fairchild and others, 1983). The occurrence of red-bed material below limestone layers in a well into the Arbuckle Aquifer (Figure 100, Appendix L) along with other

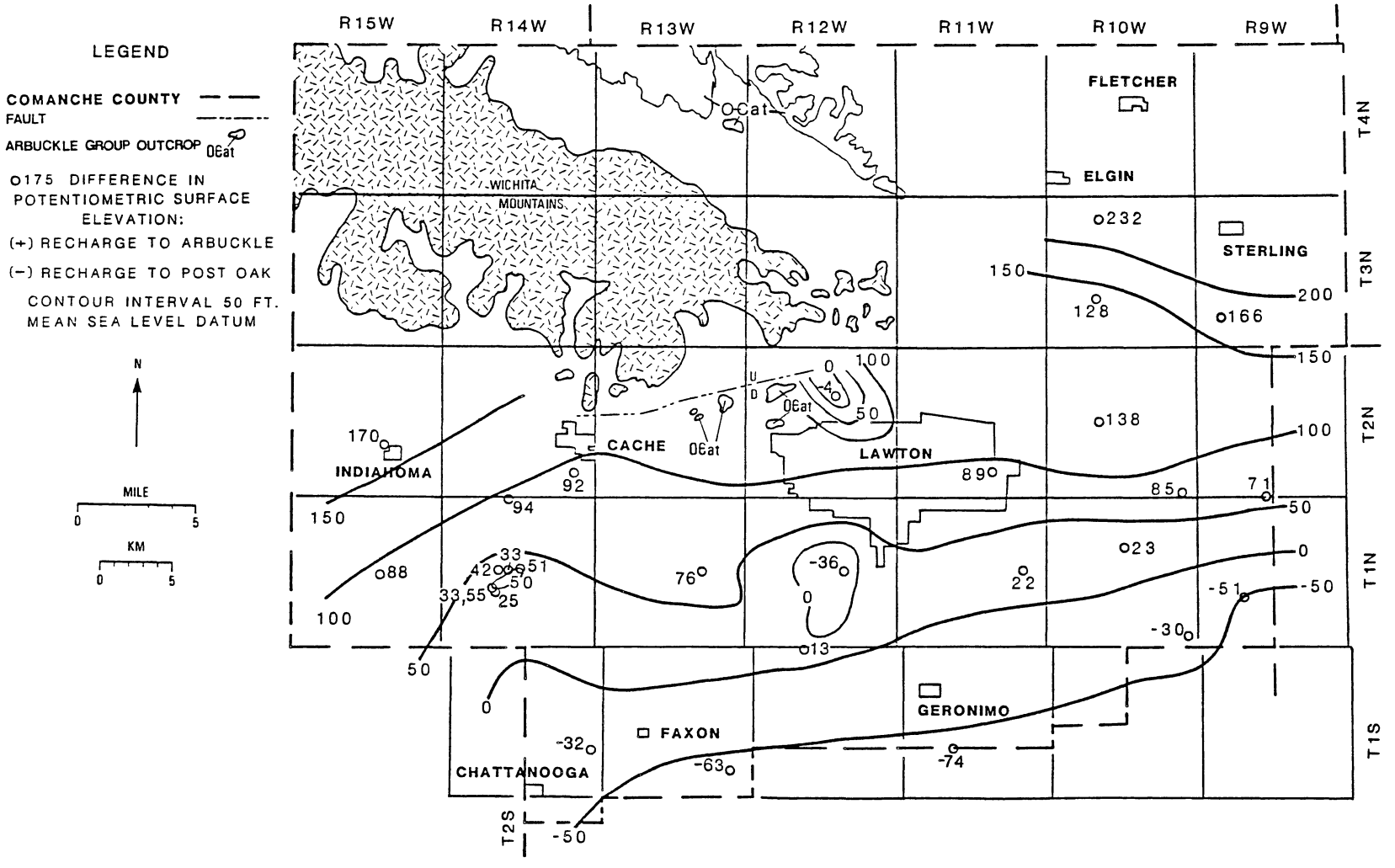

Figure 51. Recharge Regime Between Post Oak and Arbuckle Group Aquifers

evidence (Donovan, personal communication) indicates that the Arbuckle rocks were eroded, karst features developed, and these filled with Permian sediments (Figure 52).

Ground-Water Quality

Nitrate and Fluoride Content

The nitrate (NO_3-N) content in the Arbuckle Aquifer within the study area ranges from 0 to 1.2 mg/l. Havens (1983, Table I) listed an analysis from a 550-foot (168 m) well that showed 85 mg/l nitrate, but this sample probably was contaminated. The fluoride level ranges from 1.6 to 17 mg/l (Havens, 1983, Table 1). Water samples from a test well into the Arbuckle at Indiahoma exhibited fluoride contents ranging from 4.2 to 16.0 mg/l, generally increasing with depth from 420 to 655 ft (128 to 200 m). Nitrate contents of these samples ranged from 0 to 2.8 mg/l. The location of this well is within the area of excessive fluoride discussed previously (Figure 38). A discussion of the water analyses is in Appendix M.

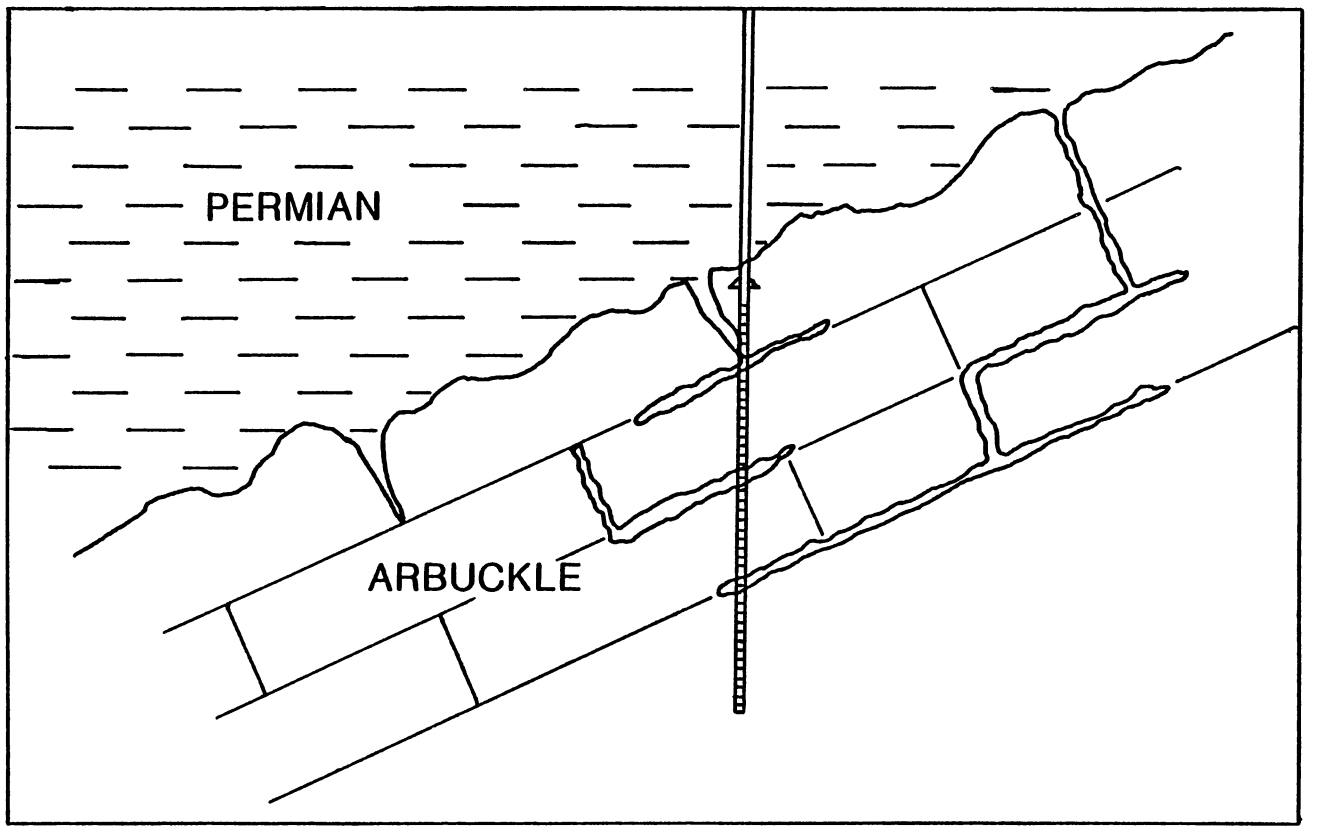

Figure 52. Schematic Diagram of Paleokarst and Well in Arbuckle Group

CHAPTER VII

RESULTS AND CONCLUSIONS

Summary of Methods

The principal aquifers in Comanche County are the alluvial aquifer, the Post Oak Aquifer, and the Arbuckle Group Aquifer. The alluvial aquifer consists of silts, sands, gravels, and clays within the creek valleys; the Post Oak Aquifer consists of Permian sandstones, shales, and conglomerates. Cambrian and Ordovician carbonates comprise the Arbuckle Group Aquifer, which lies below the Post Oak. These aquifers were evaluated by various methods.

Field methods included the measurement of water levels in the three aquifers, electric resistivity surveys to determine the thickness of the alluvium, and an aquifer test of the Arbuckle Group Aquifer. A grain size-permeability relationship was applied to data from lithologic well logs in order to estimate the permeability and transmissivity of the alluvium and the Post Oak Aquifer. Transmissivity, permeability, and yield of all the aquifers were calculated from production and aquifer test data according to a relationship between transmissivity and specific capacity.

A computer program which calculates baseflow, RECHARGE, also calculated the recharge to the alluvial aquifer and was used to determine the relationship between ground water in the alluvium and surface water. A numerical ground-water hydraulics model applied to the Post

Oak Aquifer determined its aquifer characteristics and demonstrated their interaction over time.

It was assumed that ground-water flow in both the Post Oak and Arbuckle aquifers is through fractures which should be evident as lineaments. A lineament analysis of aerial photographs showed the possible distribution of well yields in the aquifers.

Aquifer Characteristics

The grain size-permeability relationship indicated a mean permeability for the alluvium of 990 gpd/ft^2 (4.7 x 10^{-4} m/s) and a mean transmissivity of 15,840 gpd/ft (0.0023 m^2/s). Well yields range from 5 to 500 gpm (0.3 to 32 1/s), but an average expected well yield calculated from well log data is 77 gpm (4.9 1/s). The average thickness of the alluvium is 33 ft (10 m), with a range from 10 to 65 ft (3 to 19.8 m).

The Post Oak Aquifer has an average effective thickness of 50 ft (15.2 m) and an average saturated thickness of 20 ft (6.1 m). Well log data and the grain size-permeability relationship provided an average permeability of 800 gpd/ft^2 (3.8 x 10^{-4} m/s) and an average transmissivity of 16,000 gpd/ft (0.0023 m^2/s). Average well yield would be 110 gpm (6.9 1/s) according to a relationship between well yield and specific capacity. Areas of greater well yield according to the lineament analysis are shown in Figure 35. Recharge to the aquifer, determined from rainfall and hydrographic data, is 4.1 in/yr (104 mm/yr).

The aquifer parameters in the ground-water hydraulics model of the Post Oak Aquifer were modified to facilitate flow through the model. The higher permeability value, 800 gpd/ft^2, was reduced to 400 gpd/ft^2,

the geometry of channel areas of higher permeability was modified to drain the aquifer, and the water table was smoothed to prevent excessive drawdown or mounding. Calibration of the model determined the recharge rates to be 0.125 in/yr (3.2 mm/yr) in the channel areas and 0.4 in/yr (10.2 mm/yr) in the less permeable areas.

According to a specific yield-permeability relationship the specific yield for the more permeable areas is 0.279 and that for the less permeable areas is 0.255. Actual pumpages from both areas did not stress the aquifer with excessive drawdowns. To stress the aquifer, pumpages were approximately doubled in order to create drawdowns to the top of the assumed well screen length. Pumpages an order of magnitude greater than the actual values did not stress the more permeable nodes, but they caused excessive mounding in the less permeable nodes.

The simulations were considered accurate because the mass balance residuals and errors were minimal. In response to actual pumpage the modelled aquifer gained water, which was added to storage. With increased pumpage, water was released from storage to compensate for the loss of water from the modelled aquifer. Although two simulations were designed without pumpage, the model labelled as pumpage water that was not removed by either leakage or addition to storage.

The Arbuckle Aquifer is recharged through the Post Oak Aquifer in the north but provides recharge to the Post Oak to the south. Specific capacity data provided a transmissivity for the Arbuckle of 1720 gpd/ft (2.47×10^{-4} m^2/s) and a permeability of 3.5 gpd/ft^2 (1.7×10^{-6} m/s). The aquifer test data and various methods of analysis gave a two-order-of-magnitude range of transmissivity and storativity values. Analysis of the aquifer test data assuming a leaky artesian aquifer with no

storage in the aquitard was considered to provide the best values of transmissivity, 1800 gpd/ft (2.6 x 10^{-4} m^2/s), and storativity, 1.2 x 10^{-5}. The calculated yield of the Arbuckle Aquifer was 270 gpm (17 l/s); areas of higher well yields according to lineament analysis are in T 2 N/R 12 W, T 2 N/R 10 W, T 1 N/R 11 W to 14 W, T 1 N/R 9 W, T 1 S/R 14 W, and T 1 S/R 12 W (Figure 48).

REFERENCES CITED

Al-Shaieb, Z., 1978, Guidebook to Uranium Mineralization in Sedimentary and Igneous Rocks of Wichita Mountains Region, Southwestern Oklahoma: Okla. City Geol. Society, American Association of Petroleum Geologists Convention, Energy Minerals Division, 1978, 73p.

Al-Shaieb, Z., Shelton, J.W., Donovan, R.N., Hanson, R.E., and May,R.T., 1977, Evaluation of Uranium Potential in Selected Pennsylvanian and Permian Units and Igneous Rocks in Southwestern and Southern Oklahoma: U.S. Department of Energy Open-File Report GJBX-35(78), Grand Junction, Colo., 248p.

Al-Shaieb, Z., Hanson, R.E., Donovan, R.N., and Shelton, J.W., 1980, Petrology and Diagenesis of Sandstones in the Post Oak Formation (Permian), Southwestern Oklahoma: Jour. Sed. Pet., V. 50, no. 1, March, 1980, pp.43-50.

Al-Shaieb, Z., Thomas, R.G., and Stewart, G.F., 1982, National Uranium Resource Evaluation, Lawton Quadrangle, Oklahoma and Texas: U.S. Department of Energy, GJQ-017(82), 82p.

American Public Health Association, 1981, Standard Methods for the Examination of Water and Wastewater, 1980, 15th ed.: Am. Public Health Assoc., Am. Water Works Assoc., and Water Pollution Control Federation, 1134p.

Back, D.B., 1985, Hydrogeology, Digital Solute-Transport Simulation of Nitrate and Geochemistry of Flouride in Ground Waters of Comanche County, Oklahoma: Oklahoma State University unpubl. MS thesis., 134p

Barthelman, W.B., 1969, Upper Arbuckle (Ordovician) Outcrops in the Unap Mountain-Saddle Mountain Area, Northeastern Wichita Mountains, Oklahoma: University of Oklahoma unpubl. MS thesis, 67p.

Bison Instruments, 1969, Instruction Manual, Bison Instruments Earth Resistivity Meters: Bison Instruments, Inc., Minneapolis, MN, 21p.

Brewer, J.A.,1982, Study of Southern Oklahoma Aulacogen, Using COCORP Deep Seismic-Reflection Profiles, pp.31-39 in M.C. Gilbert, and R.N. Donovan, Geology of the Eastern Wichita Mountains, Southwestern Oklahoma: Okla. Geol. Surv., Guidebook 21, 160p.

Bridges, S.D., 1985, Mapping, Stratigraphy, and Tectonic Implications of Lower Permian Strata, Eastern Wichita Mountains, Oklahoma: Oklahoma State University unpubl. MS thesis, 125p.

Brookby, H.E., 1968, Upper Arbuckle (Ordovician) Outcrops in the Richards Spur-Kindblade Ranch Area, Northeastern Wichita Mountains, Oklahoma: University of Oklahoma unpubl. MS thesis, 73 p.

Burke, K., and Dewey, J.F., 1973, Plume-Generated Triple Junctions: Key Indicators in Applying Plate Tectonics to Old Rocks: Jour. Geol., V. 81, No. 4, pp. 406-433.

Chase, G.W., 1954, Permian Conglomerate Around Wichita Mountains, Oklahoma: A.A.P.G. Bull., V. 31, no. 9, pp.2028-2035.

Chase, G.W., Frederickson, E.A., and Ham, W.E., 1956, Resume of the Geology of the Wichita Mountains, Oklahoma, pp.36-55 in Petroleum Geology of Southern Oklahoma, V. 1: American Association of Petroleum Geologists, 402p.

Collins, K.H., 1985, Depositional and Diagenetic History of the Permian Rocks in the Meers Valley, Southwestern Oklahoma: Oklahoma State University unpubl. MS thesis, 110p.

Craig, L.C., and Varnes, K.L., 1979, History of the Mississippian System -- An Interpretive Summary, Chap. R, pp.371-406 in L.C. Craig, C.W. Connor, and others, Paleotectonic Investigations of the Mississippian System in the United States, Part II -- Interpretive Summary and Special Features of the Mississippian System, pp.371-559: U.S. Geol. Surv. Prof. Paper 1010, 559p.

Culp, C.K., Jr., 1961, Stratigraphic Relations of the Sycamore Limestone (Mississippian) in Southern Oklahoma: Shale Shaker Digest III, papers from Shale Shaker, Vols. IX-XI, 1958-1961, Okla. City Geol. Surv, pp.446-457.

Davis, L.V., 1958, Oklahoma's Underground Water: Okla. Geol. Surv., Okla. Geology Notes, V. 18, no. 12, pp.189-202.

Decker, C.E., and Merritt, C.A., 1931, The Stratigraphy and Physical Characteristics of the Simpson Group: Okla. Geol. Surv. Bull. 55, 112p.

Donovan, R. N., Bridges, S.D., Pettyjohn, W.A., and Stone, J.E., 1986, Lineaments and Their Possible Relationship to Well Yields and Ground-Water Quality in Comanche County, Southwestern Oklahoma: Final Report to the Okla. Water Resources Board.

Dreiss, S.J., 1984, Effects of Lithology on Solution Development in Carbonate Aquifers: Jour. Hydrology, V. 70, pp.295-308.

Fairchild, R.V., Hanson R.L., and Davis, R.E., 1983, Hydrology of the Arbuckle Mountain Area: U. S. Geol. Surv. Open-File Report 82-775, 153p.

Fay, R.O., Friedman, S.A., Johnson, K.S., and others, 1979, Oklahoma, pp.R1-R35 in The Mississippian and Pennsylvanian (Carboniferous) Systems in the United States: U.S. Geol. Surv. Prof. Paper 1110 M-DD, 487p.

Fetter, C.W., Jr., 1980, Applied Hydrogeology: Charles E. Merrill Publishing Company, Columbus, 488 p.

Folk, R.L., 1980, Petrology of the Sedimentary Rocks: Hemphill Publishing Company, Austin, Texas, 182p.

Fox, C.S., 1958, The Honey Creek Formation of the Wichita Mountains, Oklahoma: University of Oklahoma unpubl. MS thesis, 61p.

Frezon, S.E., and Dixon, G.H., 1975, Texas Panhandle and Oklahoma, Chap. J, pp.177-195 in E.D. McKee and E.J. Crosby, coordinators, Paleotectonic Investigations of the Pennsylvanian System in the United States, Part I, Introduction and Regional Analyses of the Pennsylvanian System: U.S. Geol. Surv. Prof. Paper 853, 349p.

Gilbert, M.C., 1982, Geologic Setting of the Eastern Wichita Mountains with a Brief Discussion of Unresolved Problems, pp. 1-30 in M.C. Gilbert and R.N. Donovan, eds., Geology of the Eastern Wichita Mountains, Southwestern Oklahoma: Okla. Geol. Surv. Guidebook 21, 160p.

Gilbert, M.C., and Donovan, R.N., 1982, Geology of the Eastern Wichita Mountains, Southwestern Oklahoma: Okla. Geol. Surv. Guidebook 21, 160p.

Green, N.L., and Al-Shaieb, Z., 1981, Source of High-Fluoride Ground Water, West-Central Comanche County, Oklahoma: Water Research Institute, Oklahoma State University, Stillwater, Oklahoma, 20 p.

Hach Chemical Company, 1972, Hach Direct Reading-Engineer's Laboratory, Model DR-EL/2, Methods Manual, 1st printing: Hach Chemical Company, Ames, Iowa, 105p.

Hart, D.L., Jr., 1966, Base of Fresh Ground Water in Southern Oklahoma: U.S. Geol. Surv. Hydrologic Investigations Atlas HA-223, 1:250,000, 2 sheets.

Hauth, L.D., Kurklin, J.K., Walters, D.M., and Ferree, D.M., 1984, Water Resources Data for Oklahoma, Water Year 1982: U.S. Geol. Surv. Water-Data Report OK-82-1, 336p.

Hauth, L.D., 1985, Water Resources Data for Oklahoma, Water Year 1983: U.S. Geol. Surv. Water-Data Report OK-83-1, 1985, 286p.

Havens, J.S., 1977, Reconnaissance of the Water Resources of the Lawton Quadrangle, Southwestern Oklahoma: Okla. Geol. Surv. Hydrologic Atlas 6, 1:250,000, 4 sheets.

Havens, J.S., 1983, Reconnaissance of Ground Water in Vicinity of Wichita Mountains, Southwestern Oklahoma: Okla. Geol. Surv. Circular 85, 13p.

Hayes, L.N., 1952, A Study of the Subsurface Geology of the Northeastern Part of Comanche County, Oklahoma: University of Oklahoma unpubl. MS thesis. Also: Shale Shaker, Okla. City Geol. Soc., V. 3, no. 2, October, 1952, pp.5-10, 12-21.

Hem, J.D., 1970, Study and Interpretation of the Chemical Characteristics of Natural Water, 2nd ed.: U.S. Geol. Surv. Water-Supply Paper 1473, 363p.

Hemann, M., 1985, Field Evaluation of the Relationships Between Transmissivity, Permeability and Particle Size Distribution in the Washita River Alluvial Aquifer, near Anadarko, Oklahoma: Oklahoma State University unpubl. MS thesis, 180p.

Hoffman, P., Dewey, J.F., and Burke, K., 1974, Aulacogens and Their Genetic Relation to Geosynclines, with a Proterozoic Example from Great Slave Lake, Canada, pp.38-55 in R.H. Dott, Jr., and R.H. Shaver, eds., Modern and Ancient Geosynclinal Sedimentation: Soc. of Econ. Paleontologists and Mineralogists Spec. Publ. 19, Proc. of symp., Madison, Wisc., Nov. 10-11, 1972, 380p.

Hounslow, A.W., and Back, D.B., 1985a, Evaluation of Chemical Data from Water Supplies in Southwestern Oklahoma: Final Report to the Okla. Water Resources Board.

Hounslow, A.W., and Back, D.B., 1985b, Investigation of the Source and Occurance of Nitrate in Well Water in Southwestern Oklahoma: Final Report to Okla. Water Resources Board.

Jenkins, D.N., and Prentice, J.K., 1982, Theory for Aquifer Test Analysis in Fractured Rocks Under Linear (Nonradial) Flow Conditions: Ground Water, V. 20, no. 1, pp.12-21, and no.2, pp.231-232.

Johnson, A.I., 1967, Specific Yield -- Compilation of specific yields for Various Materials: U.S. Geol. Surv. Water-Supply Paper 1662-D, pp. D1-D74.

Johnson, E.E., 1966, Ground-Water and Wells -- A Reference Book for the Water-Well Industry, 1st ed.: Edward E. Johnson, Inc., Saint Paul, Minn., 440p.

Kent, D.C., 1980, Evaluation of Aquifer Performance and Supply Capabilities of Alluvial and Terrace Deposits of the North Fork of the Red River in Beckham, Greer, Kiowa, and Jackson Counties, Oklahoma: Okla. Water Resources Board, 132 p.

Kent, D.C., Beausoleil, Y.J., and Witz, F.E., 1982, Evaluation of Aquifer Performance and Water Supply Capabilities of the Enid Isolated Terrace Aquifer in Garfield County, Oklahoma: Final Report to Okla. Water Resources Board, May, 1982, 58 p.

Kent, D.C., and Greeley, B.B., 1986, Distribution of Well Yields in the Arbuckle Group Aquifer Based on Lineament Analysis, pp.61-79, Addendum to D.C. Kent, B.B. Greeley, and J.V. Overton, Analytical Assessment of Ground-Water Availability for Communities and Rural Water Districts in Comanche County, Southwestern Oklahoma: Final report to the Okla. Water Resources Board, 79p.

Kent, D.C., Greeley, B.B., and Overton, J.V., 1986, Analytical Assessment of Ground-Water Availability for Communities and Rural Water Districts in Comanche County, Southwestern Oklahoma: Final report to the Okla. Water Resources Board, 79p.

Kent, D.C., LeMaster, L., and Wagner, J., 1986a, Modified N.R.C. Version of the U.S.G.S. Solute Transport Model, Volume 1: Modifications: Final Report, U.S. Environmental Protection Agency Cooperative Agreement No. CR811142-01-1, 248 p.

Kent, D.C., LeMaster, L., and Wagner, J., 1986b, Modified N.R.C. Version of the U.S.G.S. Solute Transport Model, Volume 2: Interactive Preprocessor Program: Final Report, U.S. Environmental Protection Agency Cooperative Agreement No. CR811142-01-1, 294p.

Kent, D.C., Lyons, T., and Witz, F.E., 1982, Evaluation of the Aquifer Performance and Water Supply Capabilities of the Elk City Aquifer in Washita, Beckham, Custer, and Roger Mills Counties, Oklahoma: Final Report to the Okla. Water Resources Board, May, 1982, 96p.

Kent, D.C., Naney, J.W., and Barnes, B.B., 1973, An Approach to Hydrogeologic Investigations of River Alluvium: Ground Water, V. 11, no. 4, pp. 30-42.

Kent, D.C., Neafus, R.J., Patterson, J.W., and Schipper, M.R., 1984, Evaluation of Aquifer Performance and Water Supply Capabilities of the Washita River Alluvium in Oklahoma: Final Report, Okla. Water Resources Board, 108 p.

Kent, D.C., Wagner, J., Witz, F., Duckwitz, G., Majeed, A., and Yu, W., 1982, Ground Water and Contaminant Transport Modeling: Garber-Wellington Aquifer in Oklahoma: National Center for Ground Water Research, Oklahoma State University.

Konikow, L.F., and Bredehoeft, J.D., 1978, Computer Model of Two-Dimensional Solute Transport and Dispersion in Ground Water, Chap.2 in Book 7, Automated Data Processing and Computations, Techniques of Water-Resources Investigations of the U.S. Geological Survey: U.S. Geol. Surv., 90p.

Kurklin, J.K., 1979, Statistical Summaries of Surface-Water-Quality Data for Selected Sites in Oklahoma, Through the 1975 Water Year: U.S. Geol. Surv. Open-File Report 79-219, 171p.

Layne-Western Company, 1983, Water, Geological and Mineral Exploration Utilizing Dual-Wall Reverse Circulation: Layne-Western Company, Inc., Mission, Kansas, brochure, 6p.

Linsley, R.K., Jr., Kohler, M.A., and Paulhus, J.L.H., 1982, Hydrology for Engineers, 3rd ed.: McGraw-Hill Book Company, New York, 508p.

Logan, J., 1964, Estimating Transmissibility from Routine Production Tests of Water Wells: Ground Water, V. 2, no. 1, pp.36-37.

McDaniel, G.A., 1959, Isopachous and Paleogeologic Studies of Southwest Oklahoma: Shale Shaker, V. 10, no. 3, Nov. 1959, pp. 4-27.

MacLachlan, M.E., 1967, Oklahoma, Chap. E, pp.85-92 in E.D. McKee, S.S. Oriel, and others, Paleotectonic Investigations of the Permian System in the United States: U.S. Geol. Surv. Prof. Paper 515, 271p.

Miser, H.D., 1954, Geologic map of Oklahoma: Okla. Geol. Survey and U.S. Geol. Survey, 1:500,000, 3 sheets.

Mobley, H.L., and Brinlee, R.C., 1967, Soil survey, Comanche County, Oklahoma: U.S. Department of Agriculture, Soil Conservation Service, 58 p.

Morris, D.A., and Johnson, A.I., 1967, Summary of Hydrologic and Physical Properties of Rock and Soil Materials, As Analyzed by the Hydrologic Laboratory of the U.S. Geological Survey 1948-60: U.S. Geol. Surv. Water-Supply Paper 1839-D, 42p.

National Oceanic and Atmospheric Administration, 1952-1981, Climatological Data, Annual Summaries, Oklahoma, Vols. 61-90, no. 13.

Nelms, J.L., 1958, The Fort Sill Formation of the Wichita Mountains, Oklahoma: University of Oklahoma unpubl. MS thesis, 91p.

Oklahoma Water Resources Board, 1968, Appraisal of the Water and Related Land Resources of Oklahoma, Region II: Okla. Water Resources Board Publ. 19, 130p.

Oklahoma Water Resources Board, 1975, Oklahoma Comprehensive Water Plan, Phase 1: Okla. Water Resources Board Publ. 60, 131p.

Oklahoma Water Resources Board, 1980, Oklahoma Comprehensive Water Plan: Okla. Water Resources Board Publ. 94, 248p.

Oklahoma Water Resources Board, 1982, Oklahoma's Water Quality Standards: Okla. Water Resources Board Publ. 111, 117p.

Oklahoma Water Resources Board, 1984, Oklahoma Water Rights Manual: Accessing the Oklahoma Water Use Data System (OWUDS): Okla. Water Resources Board Publ., 46p.

Oklahoma Water Resources Board, 1985, Rules, Regulations, and Modes of Procedure, 1985: Okla. Water Resources Board Publ. 126, 118p.

Patterson, J.W., Jr., 1984, A Ground-Water Management Model of the Washita River Alluvial Aquifer in Grady, McClain, Garvin, Murray, Carter, and Johnston Counties in South-Central Oklahoma: Oklahoma State University unpubl. MS thesis, 285p.

Pettyjohn, W.A., and Henning, R.J., 1979, Preliminary Estimate of Ground-Water Recharge Rates, Related Streamflow and Water Quality in Ohio: Water Resources Center, The Ohio State University, Columbus, Ohio, Project Completion Report No. 552, U.S. Department of the Interior Contract No. A-051-Ohio, 323p.

Pettyjohn, W.A., White, H., and Dunn, S., 1983, Water Atlas of Oklahoma: University Center for Water Research, Oklahoma State University, Stillwater, Oklahoma, 72p.

Ragland, D.A., 1983, Sedimentary Geology of the Ordovician Cool Creek Formation As It Is Exposed in the Wichita Mountains of Southwestern Oklahoma: Oklahoma State University unpubl. MS thesis, 170p.

Rauch, H.W., and White, W.B., 1970, Lithologic Controls on the Development of Solution Porosity in Carbonate Aquifers: Water Resources Research, V. 6, No. 4, pp.1175-1191.

Reed, J.E., 1980, Type Curves for Selected Problems of Flow to Wells in Confined Aquifers, Chap. B3 in Book 3, Applications of Hydraulics, Techniques of Water-Resources Investigations of the United States Geological Survey: U.S. Geol. Surv., 106p.

Schipper, M.R., 1983, A Ground-Water Management Model for the Washita River Alluvial Aquifer in Roger Mills and Custer Counties, Oklahoma: Oklahoma State University unpubl. MS thesis, 147p.

Shelton, J.W., and Al-Shaieb, Z., 1976, Summary of the Stratigraphy, Sedimentology, and Mineralogy of Pennsylvanian and Permian rocks of Oklahoma in Relation to Uranium-Resource Potential: U.S. Energy Research and Development Administration, ERDA contract AT(05-1)-1641, 156p.

Stith, D.A., 1968, Petrology of the Hennessey Shale (Permian), Wichita Mountain Area: University of Oklahoma unpubl. MS thesis, 113p.

Stone, J.E., 1981, Sources of Municipal and Rural Water Supplies in the Comanche County Area, Southwestern Oklahoma: Okla. Water Resources Board, 38p.

Stone, W.B., Jr., 1977, Mineralogic and Textural Dispersal Patterns Within the Permian Post Oak Formation of Southwestern Oklahoma: University of Oklahoma unpubl. MS thesis, 117p.

Tanaka, H.H., and Davis, L.V., 1963, Ground-Water Resources of the Rush Springs Sandstone in the Caddo County Area, Oklahoma: Okla. Geol. Surv. Circular 61, 63p.

Todd, D.K., 1980, Groundwater Hydrology, 2nd ed.: John Wiley and Sons, New York, 535p.

Tracy, J.V., 1982, Users Guide and Documentation for Adsorption and Decay Modifications to the U.S.G.S. Solute Transport Model: U.S. Nuclear Regulatory Commission, Office of Nuclear Material Safety and Standards, Division of Waste Management, NUREG/CR-2502, 136p.

Trescott, P.C., Pinder, G.F., and Larson, S.P., 1976, Finite-Difference Model for Aquifer Simulation in Two Dimensions with Results of Numerical Experiments, Chap. C1, in Book 7, Automated Data Processing and Computations, U.S. Geological Survey Techniques of Water-Resources Investigations: U.S. Geol. Surv., 116p.

Twenhofel, W.H., and others, 1954, Correlation of the Ordovician Formations of North America: Bull. of Geol. Soc. Am., V. 65, No. 3, March, 1954, pp.247-298.

U.S. Department of Agriculture, 1981, Agricultural Stabilization and Conservation Service, Invitation No. ASCS 19-81 SLC Item 7, flown by WAC Corp., Eugene, Oregon, Aerial Negative Scale 1:40,000, Code 40031, 6" camera, 6 sheets, Comanche County, Oklahoma.

U.S. Environmental Protection Agency, 1976a, National Interim Primary Drinking Water Regulations: U.S. Environmental Protection Agency, Office of Water Supply, EPA-570/9-76-003, 159p.

U.S. Environmental Protection Agency, 1976b, Quality Criteria for Water: U.S. Environmental Protection Agency, U.S. Government Printing Office, Washington, D.C., 256p.

U.S. Geological Survey, 1969-1985, Water Resources Data for Oklahoma, 1968-1983 Water Years.

U.S. Geological Survey, 1974a, Water Resources Data for Oklahoma, 1971, Part 2, Water Quality Records: U.S. Geol. Surv., 271p.

U.S. Geological Survey, 1974b, Water Resources Data for Oklahoma, 1973, Part 2, Water Quality Records: U.S. Geol. Surv., 249p.

U.S. Geological Survey, 1975, Surface Water Supply of the United States, 1966-70, Part 7, Lower Mississippi River Basin, V. 1, Lower Mississippi River Basin Except Arkansas River Basin: U.S. Geol. Surv. Water-Supply Paper 2120, 1278p.

U.S. Geological Survey, 1983, Water Resources Data, Oklahoma, Water Year 1981: U.S. Geol. Surv. Water-Data Report OK-81-1, 546p.

Union Carbide Corporation, Oak Ridge Gaseous Diffusion Plant, 1978, Hydrogeochemical and Stream Sediment Reconnaissance Basic Data for Lawton NTMS Quadrangle, Oklahoma, Texas: Union Carbide Corp., Nuclear Division, Oak Ridge Gaseous Diffusion Plant, Oak Ridge, Tenn., Report K/UR-116, 98p.

Union Carbide Corporation, Oak Ridge Gaseous Diffusion Plant, 1980, Hydrogeochemical and Stream Sediment Detailed Geochemical Survey for Wichita Uplift Region, Oklahoma: National Uranium Resource Evaluation Program, U.S. Department of Energy, Grand Junction, Colo., Report No. GJBX-66(80), 36p.

Waldbott, G.L., 1973, Health Effects of Environmental Pollutants: C.V. Mosby Company, St. Louis, 316p.

Walton, W.C., 1970, Groundwater Resource Evaluation: McGraw-Hill Book Company, New York, 664p.

Wang, H.F., and Anderson, M.P., 1982, Introduction to Groundwater Modeling: Finite Difference and Finite Element Methods: W.H. Freeman and Company, San Francisco, 237p.

Wilmott, C.L., Jr., 1957, The Reagan Formation of the Wichita Mountains, Oklahoma: University of Oklahoma unpubl. MS thesis, 60p.

Wood, P.R., and Burton, L.C., 1968, Ground-Water Resources, Cleveland and Oklahoma Counties: Okla. Geol. Surv. Circular 71, 75p.

Zohdy, A.A.R., Eaton, G.P., and Mabey, D.R., 1974, Applications of Surface Geophysics to Ground-Water Investigations, Chap. D1 in Book 2, Collection of Environmental Data, Techniques of Water-Resources Investigations of the United States Geological Survey: U.S. Geol. Surv., 116p.

APPENDIXES

APPENDIX A

APPARENT RESISTIVITY GRAPHS

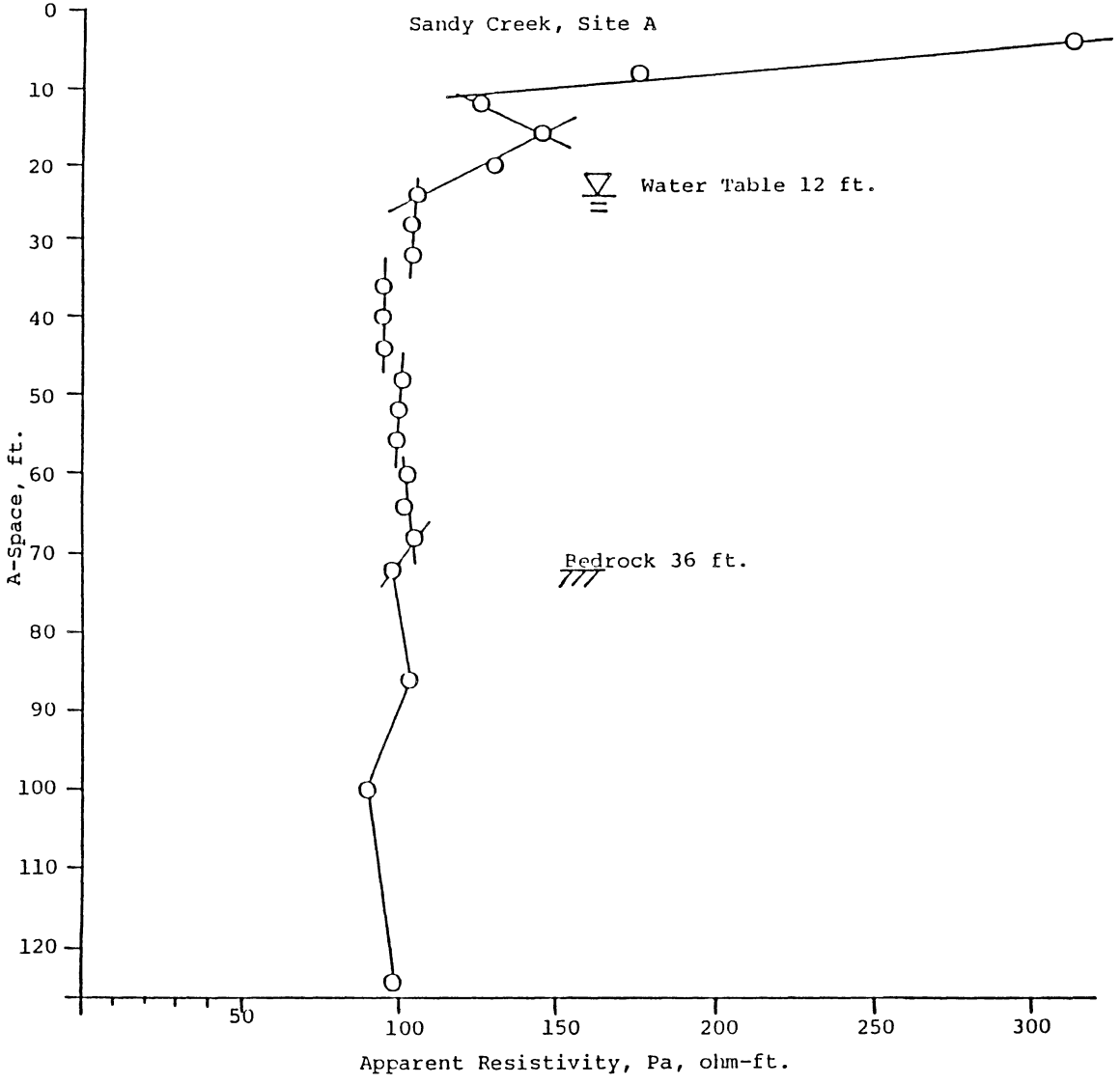
Sandy Creek, Site A
Water Table 12 ft.
Bedrock 36 ft.
A-Space, ft.
0
10
20
30
40
50
60
70
80
90
100
110
120
50
100
150
200
250
300
Apparent Resistivity, Pa, ohm-ft.

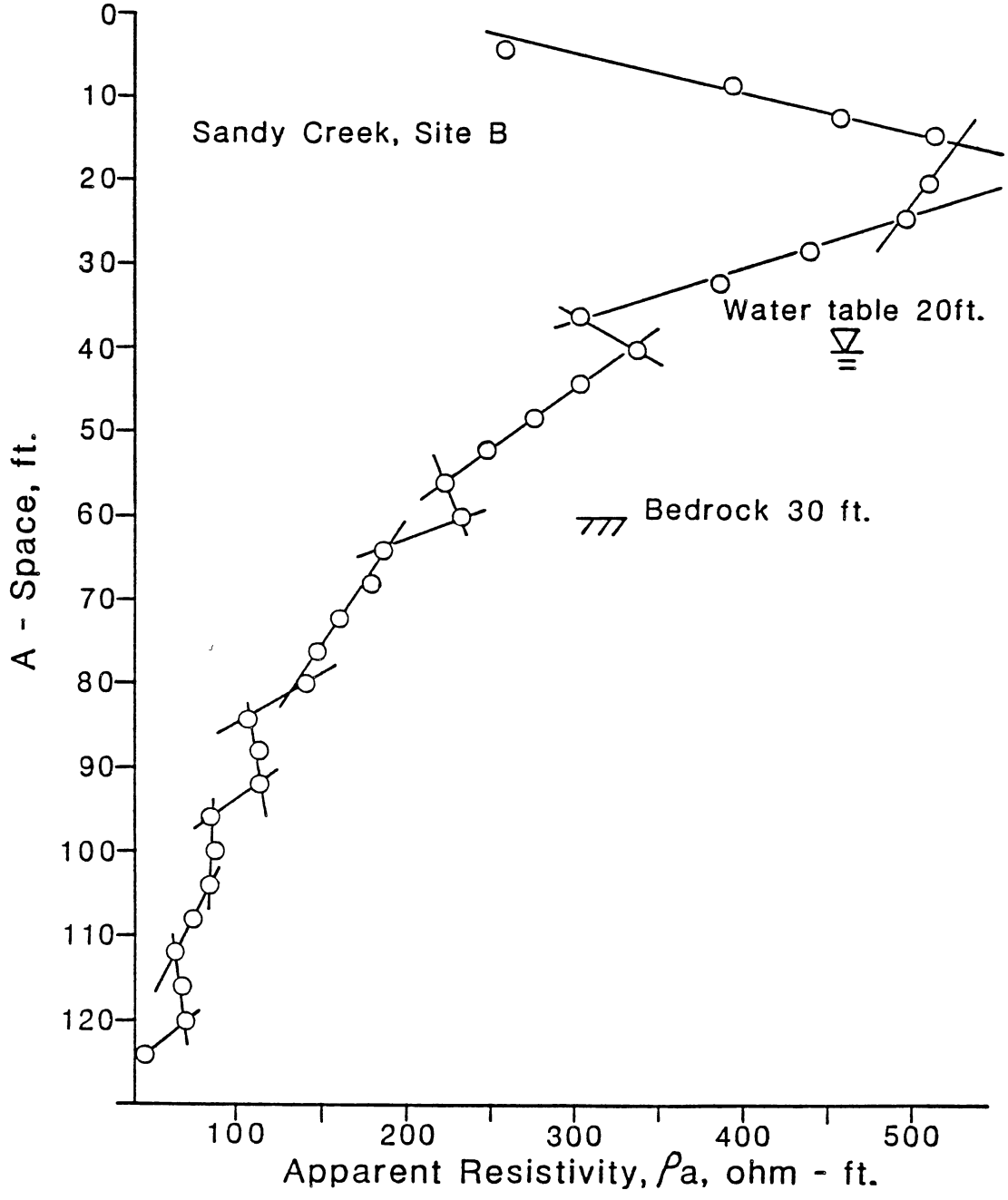
Sandy Creek, Site B
Water table 20ft.
Bedrock 30 ft.
A - Space, ft.
0
10
20
30
40
50
60
70
80
90
100
110
120
100
200
300
400
500
Apparent Resistivity, ρa, ohm - ft.

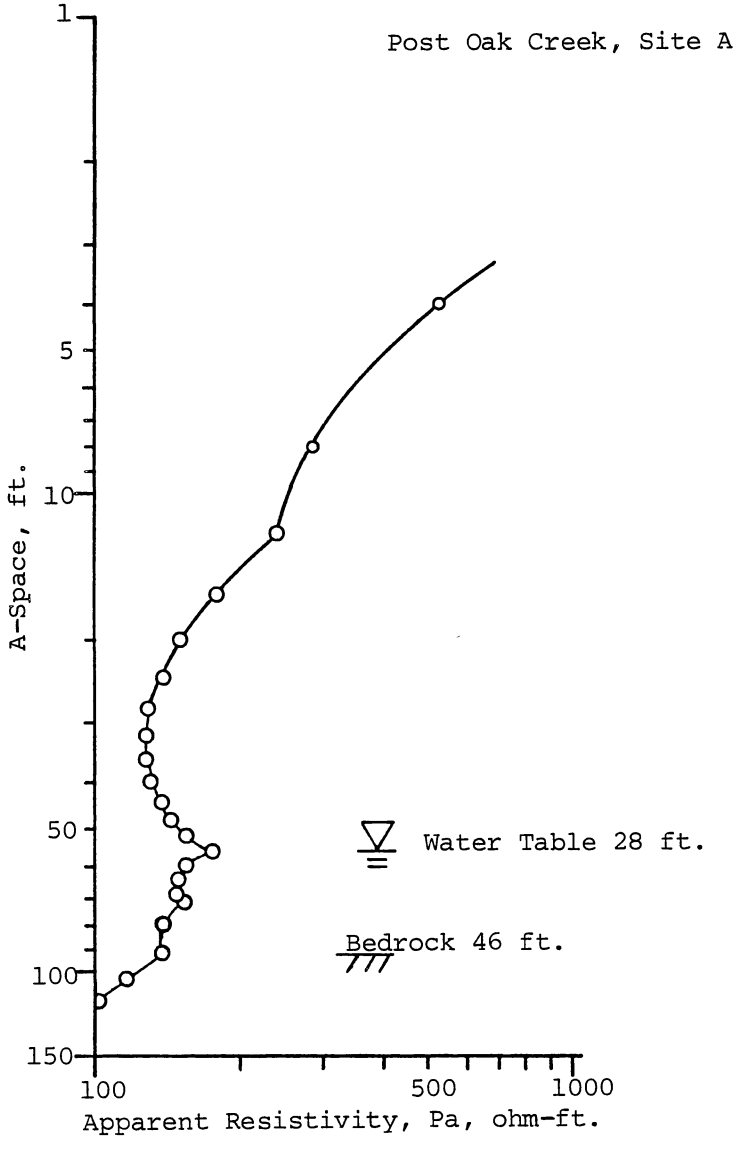
Post Oak Creek, Site A
A-Space, ft.
1
5
10
50
100
150
100
500
1000
Apparent Resistivity, Pa, ohm-ft.
Water Table 28 ft.
Bedrock 46 ft.

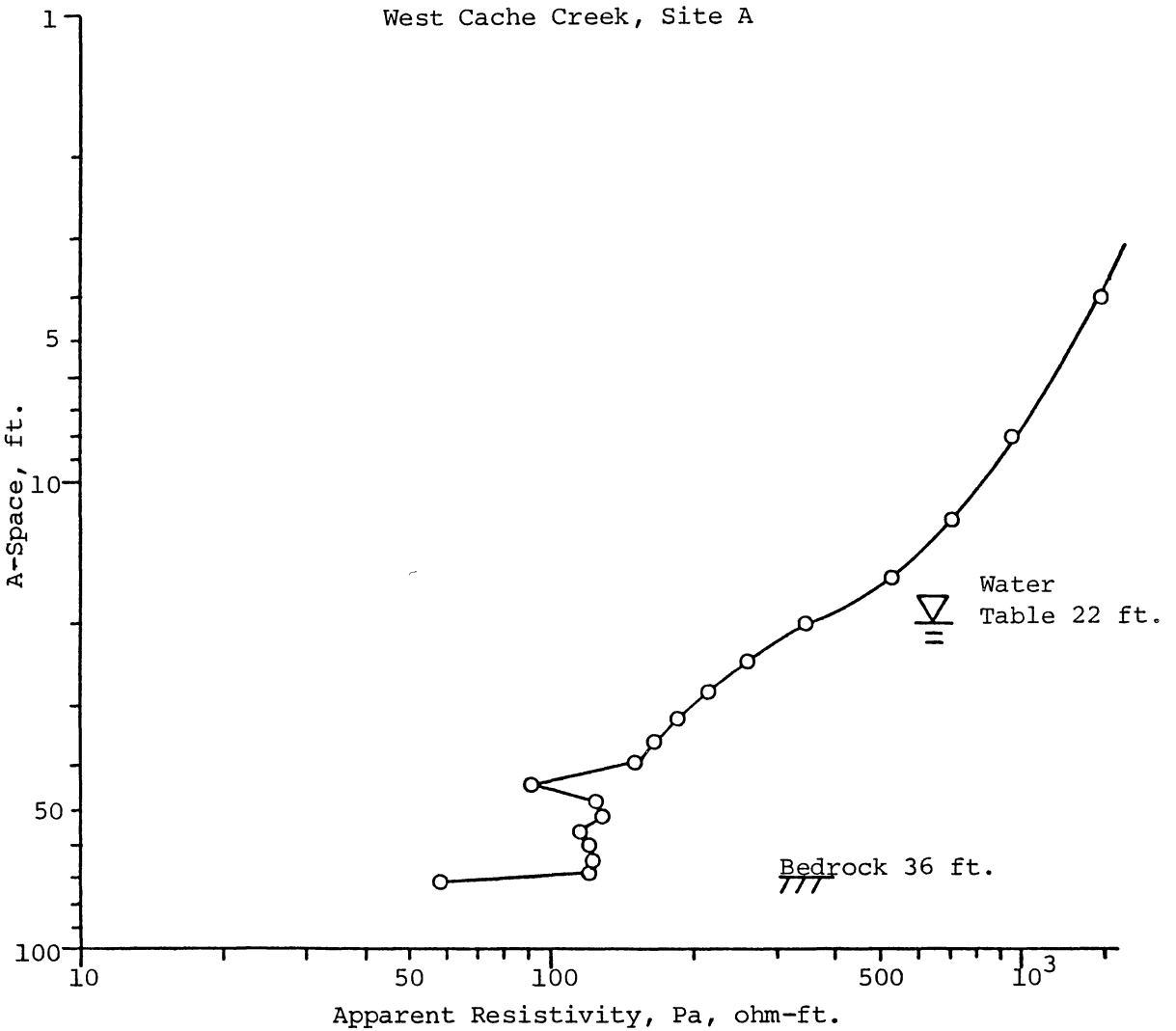
West Cache Creek, Site A
1
5
10
50
100
A-Space, ft.
10
50
100
500
10^3
Apparent Resistivity, Pa, ohm-ft.
Water
Table 22 ft.
Bedrock 36 ft.

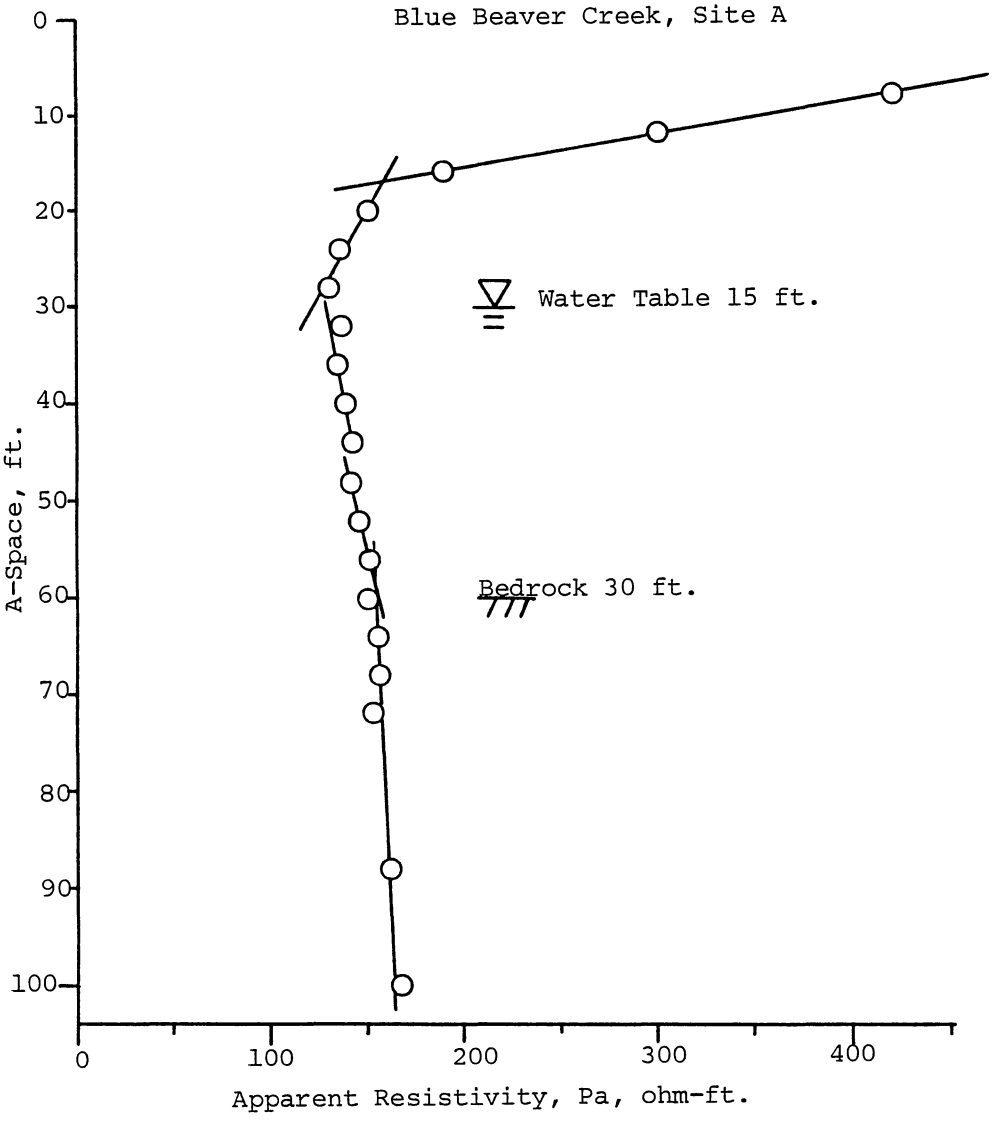
Blue Beaver Creek, Site A
Water Table 15 ft.
Bedrock 30 ft.
A-Space, ft.
0
10
20
30
40
50
60
70
80
90
100
0
100
200
300
400
Apparent Resistivity, Pa, ohm-ft.

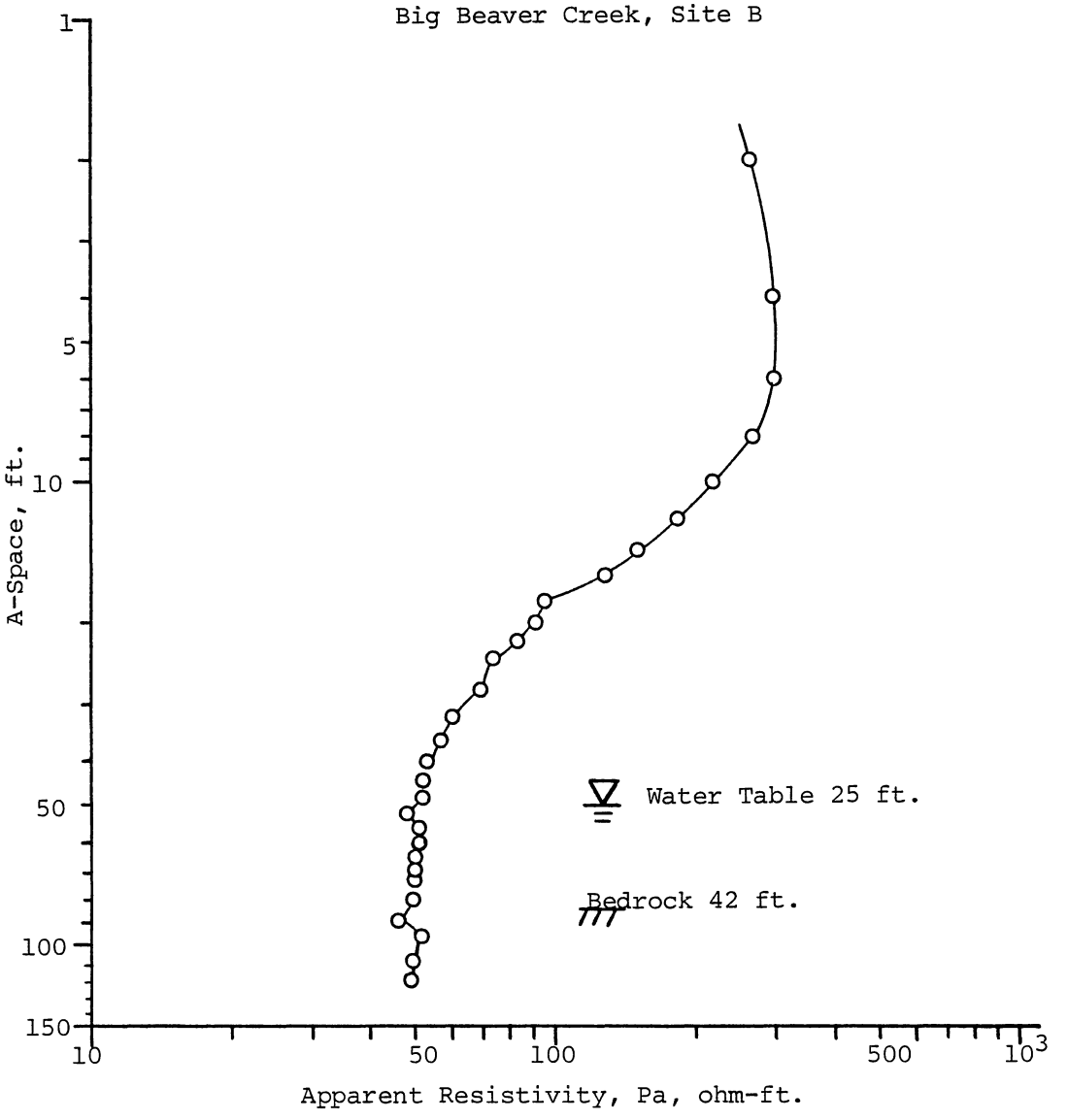
Big Beaver Creek, Site B
A-Space, ft.
1
5
10
50
100
150
10
50
100
500
10³
Apparent Resistivity, Pa, ohm-ft.
Water Table 25 ft.
Bedrock 42 ft.

APPENDIX B

WATER WELL DATA

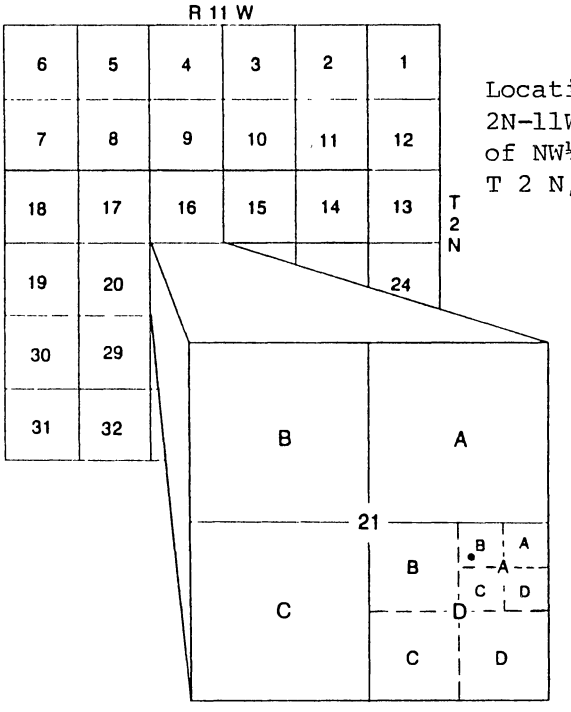

Location of well at 2N-11W-21dab (instead of NW¼NE¼SE¼ sec.21, T 2 N, R 11 W).

Figure 53. Well Location System (from Havens, 1983, p.3)

TABLE II

REPORTED WATER WELL DATA

Aquifer Well Number	Location	Owner	Depth ft.	Static Water Level	Well Radius ft.	Test Yield gpm	Drawdown ft.	Pumping Duration hrs.
Alluvium								
Q1	3N-16W-29ba	Soukup	35	20	0.5	100	10	100
Q2	3N-11W-5b east well	Comanche Co. RWD 2	46	7.5	---	150	23	--
Q3	3N-11W-5b west well	Comanche Co. RWD 2	22	3.5	---	90	11	--
Q4	3N-11W-5bac	Glover	45	8	1.0	800	18	30
Q5	2N-15W-34daa	Williams	33.5	15.2	0.21	12.5	--	1
Q6	2N-14W-23ccb	Dreith	29	12	0.21	6	--	1
Q7	2N-14W-23ccd	Kissick	28.5	15.5	0.21	20	--	1
Q8	1N-11W-32adaa	Doye	18	--	0.5	30	--	24
Q9	1S-11W-9dbad	Geronimo 1	60	28.7	0.08	60	8.15	24
Q10	1S-11W-9dabb	Geronimo 2	50	21	0.08	55	12.7	5
Q11	2S-12W-8dddd	Johnson	65	26	0.33	105.3	6	23
Q12	2S-12W-18aaa	Cotton Co. RWD 2	52	32.6	0.45	240	41.4	24
Q13	2S-12W-28aaa	Comanche Co. RWD 3	21	4	0.5	273	14.3	0.17
Q14	2N-14W-24 Cache	Fry	22.5	12.5	0.21	14.5	--	1
Q15	2N-14W-24 Cache	Turner	26	9.8	0.21	15	--	1
Post Oak Aquifer								
P1	2N-15W-24ddd	Browning	36	22	0.21	7	--	1
P2	2N-14W-21bbd	Caudle	230	90	0.19	0.33	230	48
P5	2N-14W-35ccd	Hennesse	35.5	2	0.21	2.5	--	1
P6	2N-14W-36aca	Ware	200	70	0.19	3	150	1
P7	2N-14W-36acc	Seigler	25.5	9.8	0.21	20	--	1
P8	2N-9W-21dab	Butler	250	80	0.19	4	180	0.5
P9	1N-14W-20daa	Young	39	35.5	0.21	3	--	1
P10	1S-14W-2bd	CKT RWD Bohl	43	--	0.75	105	20	14

TABLE II (Continued)

Aquifer Well Number	Location	Owner	Depth ft.	Static Water Level	Well Radius ft.	Test Yield gpm	Drawdown ft.	Pumping Duration hrs.
Post Oak Aquifer								
P11	1S-14W-12b	McCollum	44	20	0.58	800	17	10
P12	1S-14W-12b	Stall	42	14	0.5	500	15	10
P13	1S-13W-18	Peters	32	15	0.5	350	8	12
P14	1S-13W-19	Peters	30	9	0.25	200	15	72
P15	2S-12W-17bbb	Witt	50	25	0.53	340	22	3
P16	2S-12W-17bbb	Cotton Co. RWD 2, Witt	46	23	0.45	58	26	1
P17	2S-12W-21bbbb	Cotton Co. RWD 2, Petty	48	21.5	0.33	202	11	24
Arbuckle Aquifer								
A1	2N-15W-26bcc	Indiahoma 3	660	275	0.28	120	400	96
A2	2N-14W-24cccc	Cache 1	715	125	0.42	40	60	10
A3	2N-14W-24cccc	Cache 2	913	120	--	145	140	--
A4	2N-14W-24cccc	Cache 3	962	97	--	93	160	--
A5	2N-14W-25adb	USGS 2 Moore	1002	--	0.28	28	32	8
A6	1N-13W-4baa	USGS 1 Green	997	--	0.28	35	140	5.5
A7	1S-11W-7daaa	Geronimo	2243	1750	0.29	100	--	--

TABLE III

DEPTH AND THICKNESS OF COARSE-GRAINED LAYERS
IN POST OAK AQUIFER

Well Number	Location	Owner	Well Depth ft	Sand Depth: Thickness ft	Total Thickness ft	Number of Sands*
P1	2N-15W-24ddd	Browning	36	23: 8	8	1
#7	2N-14W-1ddc e½	Camp Eagle	50	4: 5	5	1
#9	2N-14W-1cda w½	Camp Eagle	40	3:18	18	1
#12	2N-14W-2cdc s½	Camp Eagle	40	18: 8 29: 8	16	2
#13	2N-14W-11cdd	Camp Eagle	134	6:10 20:30 62:18 84: 2 93:12	40 (72)§	2 (5)§
#14	2N-14W-14abca	Camp Eagle	40	16:14	14	1
#15	2N-14W-14add w½	Camp Eagle	258	3:14 120: 3	17	2
P2	2N-14W-21bbd	Caudle	230	118: 5 182:11	16	2
P5	2N-14W-35ccd	Hennesse	35.5	0: 5 29: 1 30: 4	10	3
P6	2N-14W-36aca	Ware	200	153: 3 180:11	14	2
P7	2N-14W-36acc	Seigler	25.5	8:10 18: 4	14	2
#2	2N-13W-6cdcc	Camp Eagle	74	4:15	15	1
#3	2N-13W-7bdc	Camp Eagle	105	15:29	29	1
#8	2N-13W-7bbbd	Camp Eagle	54	3: 2 18:29	31	2

* Includes sand, gravel, and conglomerate. § Includes layers below 50 ft.

TABLE III (Continued)

Well Number	Location	Owner	Well Depth ft	Sand Depth: Thickness ft	Total Thickness ft	Number of Sands*
#10	2N-11W-6aaa	Fort Sill	42	30: 6 36: 5	11	2
	2N-10W-13	U.S.G.S. ?	32	7: 3 20:12	15	2
#1	1N-14W-27	C.K.T. Fisher	382	130:14 180: 8 240:31 288:48	101	4
#2	1N-14W-27c	C.K.T. Fisher	300	48:12 146:11 200: 7 216: 8 238:11 264: 8	12 (57)§	1 (6)§
#4	1N-14W-34c w½	C.K.T. Fisher	360	52: 7 161:10 214:10 242: 8 260:32	67	5
	1N-13W-14abb	Gibson	1663	390:20	(20)§	(1)§
	1N-13W-25abb	Powers	2015	120: 34 232:195 439: 5	(234)§	(3)§
P12	1S-14W-12b	Stall	42	10:13 23:16	29	2
#1	1S-12W-15daa	Carmichael Rogers	2095	37:13	13	1

* Includes sand, gravel, and conglomerate. § Includes layers below 50 ft.

APPENDIX C

PERMEABILITY DATA FOR AQUIFERS

DETERMINING PERMEABILITY FROM WELL LOGS

For the alluvium and the Post Oak Aquifer, permeabilities were obtained from lithologic well logs by using a relationship between grain size and permeability developed by Kent and others (1973; Patterson, 1984, p.80; Figure 54). This method could not be used for the Arbuckle Aquifer because ground-water flow is through fractures and solution openings.

Each layer in the aquifer was assigned to a hydraulic coefficient (permeability) range according to its primary grain size as listed in a driller's log. A shale, clay, silt, or very fine sand would be in range 1, while a coarse sand or gravel would be in range 4. Sandy layers of unspecified texture were assigned to range 5. The median grain size of each range is associated with upper, middle, and lower permeability values from the grain size envelope (Table IV). The product of the permeability from the envelope and the ratio of the saturated thickness of each layer to the total saturated thickness is the weighted average permeability of the layer. The sum of the weighted permeabilities is the total permeability:

$$Kw = \sum_{i=1}^{n} Ki \frac{ts_1}{ts}$$

where Kw = weighted average permeability, gpd/ft^2,

Ki = permeability from grain-size envelope for each layer, gpd/ft^2,

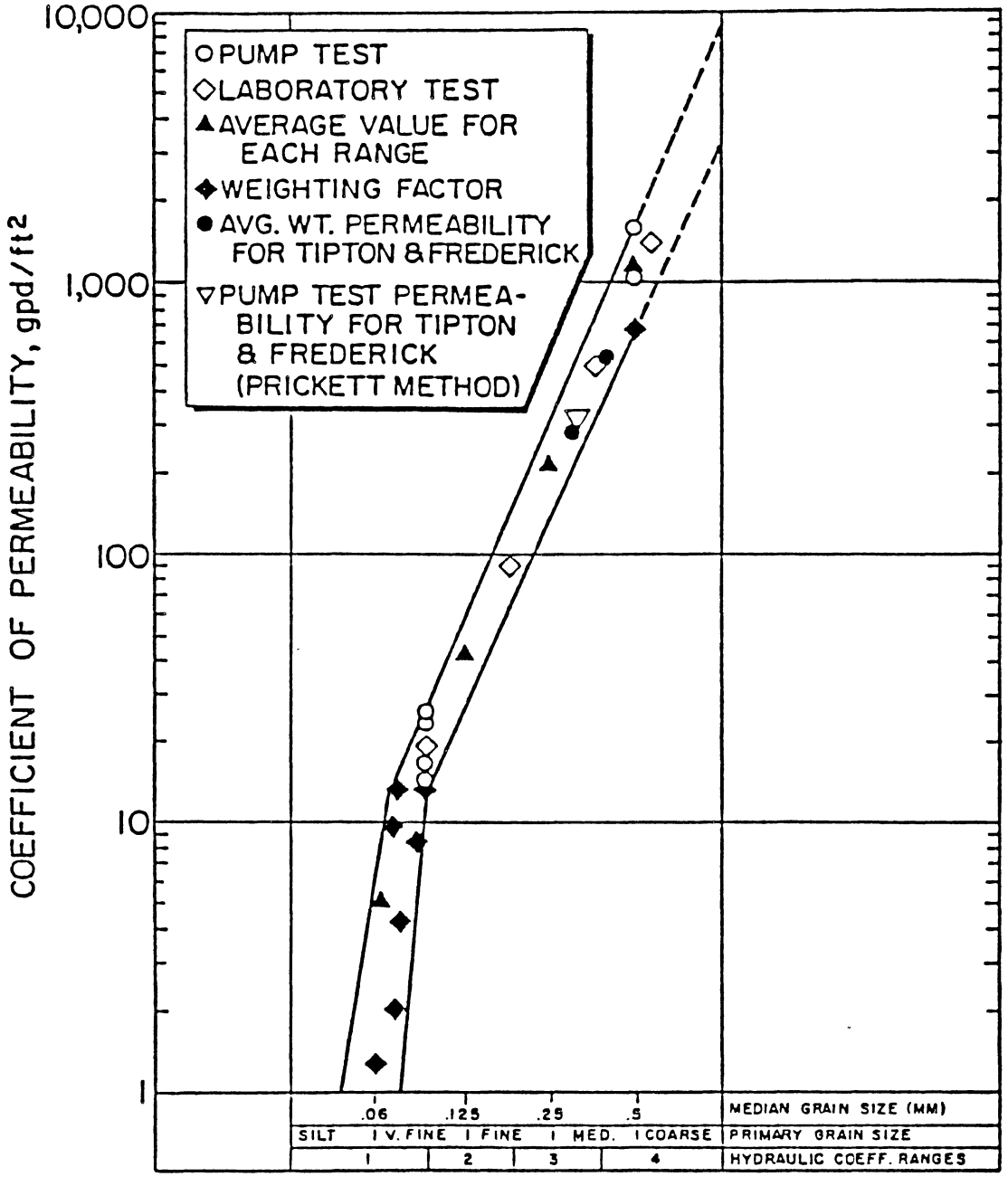

Figure 54. Relationship Between Permeability and Grain Size (From Kent, 1973, and Patterson, 1984, p.80)

ts = total saturated thickness, ft,

ts_1 = saturated thickness of each layer, ft,

n = number of layers in aquifer zone.

From the envelope permeabilities a range of total permeabilities for the aquifer was obtained (Table V).

TABLE IV

PERMEABILITY VALUES FOR MEDIAN GRAIN SIZES

Permeability Range	Median Grain Size mm	Upper K Value gpd/ft^2	Middle K Value gpd/ft^2	Lower K Value gpd/ft^2
1	0.06	5.2	2.3	41
2	0.125	64	42	28
3	0.25	328	217	144
4	0.5	1931	1028	788
5	0.19	202	124	76

TABLE V

CALCULATION OF PERMEABILITY FROM LITHOLOGIC LOG
FOR POST OAK AQUIFER

Well No. Owner	Depth ft.	SWL ft.	ts ft.	Lith-ology	t_1 ft.	Range	ts_1 ft.	$\frac{ts_1}{ts}$ %	Weighted Permeability Range Upper	Middle gpd/ft^2	Lower
P1	36	22	14	cl	23	1	1	7.1	0.37	0.16	0.07
Browning				sd,cl	8	5	8	57.1	115	70.8	43.4
				cl	5	1	5	35.7	1.86	0.82	0.36
								Sum	117	71.8	43.8

SWL: static water level ts: total saturated thickness t_1: thickness of each layer
ts_1: saturated thickness of each layer
cl: clay sd: sand

TABLE VI

PERMEABILITY DATA FOR ALLUVIAL AQUIFER

Well No. Owner	Depth ft.	SWL ft.	ts ft.	Lith-ology	t_1 ft.	Range	ts_1 ft.	$\frac{ts_1}{ts}$ %	Weighted Permeability Range Upper gpd/ft^2	Middle gpd/ft^2	Lower gpd/ft^2
Q5	33.5	15.2	18.3	f sd	5	2	4.8	26.2	16.8	11.0	7.34
Williams				mud	5	2	5	27.3	17.5	11.5	7.64
				cs gr	8	4	8	43.7	844	449	344
				rd bd cl	0.5	1	0.5	2.7	0.14	0.06	0.03
								Sum	878	472	359
Q6	29	12	17	cl	8	1	6	35.3	1.84	0.81	0.35
Dreith				mud	8	2	8	47.1	30.1	19.8	13.2
				bould, mud	2.5	2	2.5	14.7	9.41	6.17	4.12
				rd bd cl	0.5	1	0.5	2.9	0.15	0.07	0.03
								Sum	41.5	26.8	17.7
Q7	28.5	15.5	13	gr	13	4	12.5	96.2	1857	988	758
Kissick				rd bd cl	0.5	1	0.5	3.8	0.2	0.09	0.04
								Sum	1857	988	758
Q9	60	28.8	31.2	sd, gr	14	4	5.2	16.7	322	172	132
Geronimo 1				cl, gr	10	2	10	32.0	20.5	13.4	8.96
				rd sh	16	1	16	51.3	2.67	1.18	0.05
								Sum	345	187	141
Q10	50	21	29	f slt sd	5	2	4	13.8	8.83	5.80	3.86
Geronimo 2				cl	10	1	10	34.5	1.79	0.79	0.34
				sh	15	1	15	51.7	2.69	1.19	0.52
								Sum	13.3	7.78	4.72
Q11	65	26	39	sd, gr	34	4	14	35.9	693	369	283
Johnson				rd sh	25	1	25	64.1	3.33	1.47	0.64
								Sum	696	370	284
Q12	52	32.6	19.4	cs sd	25	4	9.4	48.4	936	498	382
Cotton Co. RWD 2				cs gr	10	4	10	51.5	995	530	406
								Sum	1931	1028	788
Q14	22.5	12.5	10	cl	16	1	3.5	35	1.82	0.80	0.35
Fry				gr	6.5	4	6.5	65	1255	668	512
								Sum	1257	669	512
Q15	26	9.8	16.2	cl	10	1	0.2	1.2	0.06	0.03	0.01
Turner				sd	3	5	3	18.5	37.4	22.9	14.1
				cl	6	1	6	37.0	1.92	0.85	0.37
				sd	7	5	7	43.2	87.3	53.6	32.8
								Sum	127	77.4	47.3
								Mean	794	425	324
								Range	13.3-1931	7.78-1028	4.72-788

SWL: static water level
ts_1: saturated thickness of each lithology
bould: boulders
cl: clay
cs: coarse
f: fine
ts: saturated thickness
gr: gravel
rd bd: red bed
sd: sand
sdy: sandy
t_1: thickness of each lithology in aquifer zone
sh: shale
slt: silty
ss: sandstone

TABLE VII

PERMEABILITY DATA FOR POST OAK AQUIFER

Well No. Owner	Depth ft.	SWL ft.	ts ft.	Lithology	t_1 ft.	Range	ts_1 ft.	$\frac{ts_1}{ts}$ %	Weighted Permeability Range Upper	Middle gpd/ft^2	Lower
P1	36	22	14	cl	23	1	1	7.1	0.37	0.16	0.07
Browning				sd,cl	8	5	8	57.1	115	70.8	43.4
				cl	5	1	5	35.7	1.86	0.82	0.36
								Sum	117	71.8	43.8
P5	35.5	2	33.5	slt sd	5	2	3	9.0	5.76	3.78	2.52
Hennesse				cl	24	1	24	71.6	3.72	1.65	0.72
				gr,cl	1	4	1	3.0	57.9	30.8	23.6
				ss	4	5	4	11.9	24.0	14.8	9.04
				cl	1.5	1	1.5	4.5	0.23	0.10	0.04
								Sum	91.6	51.1	35.9
P7	25.5	9.8	15.7	gr	10	4	8.2	52.2	1008	537	411
Seigler				ss	4	5	4	25.5	51.5	31.6	19.4
				cl	3.5	1	3.5	22.3	1.16	0.51	0.22
								Sum	1061	569	431
P9	39	35.5	3.5	sdy cl	4	2	3.5	100	64	42	28
Young											
P11	44	20	24	cs sd	11	4	5	20.8	402	214	164
McCollum				cs sd,gr	18	4	18	75.0	1448	771	591
				sh	1	1	1	4.2	0.22	0.10	0.04
								Sum	1850	985	755
P12	42	14	28	f sd	13	2	9	32.1	20.5	13.5	8.99
Stall				cs sd	2	4	2	7.1	138	73.4	56.3
				cs sd,gr	14	4	14	50.0	966	514	394
				ss	0.5	5	0.5	1.8	3.61	2.21	1.36
				sh	2.5	1	2.5	8.9	0.46	0.20	0.09
								Sum	1129	603	461
P17	48	21.5	26.5	gr	18	4	16.5	62.3	1202	640	491
Cotton Co.				cl	4	1	4	15.1	0.78	0.35	0.15
RWD 2,				gr	4	4	4	15.1	291	155	119
Petty				sh	2	1	2	7.5	0.39	0.17	0.08
								Sum	1494	795	610
								Mean	830	445	338
								Range	64-1850	42-985	28-755

SWL: static water level
ts_1: saturated thickness of each lithology
bould: boulders
cl: clay
cs: coarse
f: fine
ts: saturated thickness
gr: gravel
rd bd: red bed
sd: sand
sdy: sandy
t_1: thickness of each lithology in aquifer zone
sh: shale
slt: silty
ss: sandstone

APPENDIX D

PROGRAM TO CALCULATE TRANSMISSIVITY FROM SPECIFIC CAPACITY

CALCULATOR PROGRAM FOR HEWLETT-PACKARD HP-11C

A calculator program written by Patterson (1984, p.142) for the Texas Instruments TI-59 and modified for the Hewlett-Packard HP-11C calculates transmissivity, T, from specific capacity, Q/s, according to a formula by Walton (1970, p.315):

$$T = \frac{Q}{s}\left[264 \log\left(\frac{T\,t}{2693\,r^2\,S}\right) - 65.5\right]$$

where T = transmissivity, gpd/ft.,

$\frac{Q}{s}$ = specific capacity, gpm/ft.,

Q = discharge, gpm,

s = drawdown, ft.,

S = storativity of a confined aquifer or specific yield of an unconfined aquifer, fraction,

r = nominal well radius, ft.,

t = duration of pumping, minutes.

Enter the program into calculator memory with the following:

Step	Keystrokes	
1	g P/R	Program mode
2	f LBL A	Labels and defines beginning of program; A = any alphabetic or numeric key.
3	RCL 2	pumping duration, t
4	X	multiplication
5	RCL 1	well radius, r
6	g x^2	
7	RCL 0	storativity, S, or specific capacity, Sy

Step	Keystrokes	
8	X	
9	2693	
10	X	
11	÷	division
12	g LOG	
13	264	
14	X	
15	65.5	
16	-	subtraction
17	RCL 3	specific capacity, Q/s
18	X	
19	g RTN	End of program

To run the program store the following parameters in the registers, Rn:

R_0: S or Sy

R_1: r

R_2: t

R_3: $\frac{Q}{s}$.

Enter (key in) any initial transmissivity value and begin the program with the keystrokes f A. The "running" display flashes until a calculated T value is shown. Enter this transmissivity and subsequent values with the keystrokes f A until the final transmissivity equals the initial transmissivity. The permeability is the ratio of the transmissivity to the saturated thickness:

$$K = T/b$$

where K = permeability, gpd/ft^2,

T = transmissivity, gpd/ft.,

b = saturated thickness, ft.

APPENDIX E

HYDRAULIC DATA

TABLE VIII

AQUIFER HYDRAULIC DATA

Aquifer Well	Specific Capacity gpm/ft.	Transmissivity from Specific Capacity, 100% Efficiency gpd/ft.	Transmissivity from Specific Capacity, 60% Efficiency gpd/ft.	Transmissivity from Aquifer Test gpd/ft.	Permeability from Specific Capacity, 100% Efficiency gpd/ft^2	Permeability from Specific Capacity, 60% Efficiency gpd/ft^2	Permeability from Lithologic Log Upper gpd/ft^2	Middle gpd/ft^2	Lower gpd/ft^2	Permeability from Aquifer Test gpd/ft^2
Alluvium										
Q9	7.36	14648	25030	15840	468	800	344	187	141	506
Q10	4.33	7507	12912	7433	259	445	---	---	---	303
Q11	17.5	30530	52388	16593	783	1343	696	370	284	425
Q12	5.8	8916	15407	---	460	794	1931	1028	788	---
Mean	8.7	15400	26434	13289	492	846	990	528	404	411
Post Oak Aquifer										
P11	47.1	76544	131944	-----	3189	5498	1850	985	755	---
P12	33.3	53912	92986	-----	1925	3321	1129	603	461	---
P17	18.4	32309	55445	24970	1219	2092	1494	795	610	942
Mean	32.9	54255	93458		2111	3637				
Arbuckle Aquifer							Well Penetration into Arbuckle			
A1	0.3	633	1085	---	15.8†	27.1††	40ft.	---	---	---
A2	0.67	1228	2103	---	3.4†	5.8††	365	---	---	---
A5	0.88	1705	2919	3800*	2.7†	4.6††	639	---	---	0.47
A6	0.25	434	757	1300**	0.93†	1.6††	469	---	---	0.20
Mean	0.52	1000	1716	2550	5.7	9.8	491 Mean of highest 3 values			

* Mean of 3 values

** Mean of 4 values

† $K = \frac{\text{transmissivity (100\% efficiency)}}{\text{well penetration}}$ K (from aquifer test) = $\frac{T \text{ (from test)}}{\text{well penetration}}$

†† $K = \frac{\text{transmissivity (60\% efficiency)}}{\text{well penetration}}$

APPENDIX F

SURFACE-WATER HYDROLOGIC AND CHEMICAL DATA

DESCRIPTION OF RECHARGE PROGRAM

RECHARGE, a computer program developed by Pettyjohn and Henning (1979), calculates by three methods the baseflow, that portion of the stream discharge contributed by ground-water runoff (Figure 55). Miller (1984) described the methods, fixed interval, sliding interval, and local minima. The RECHARGE program demonstrates the direct relationships between baseflow and recharge and between streamflow and evapotranspiration, assuming that inflow to the basin is by precipitation only, and that outflow is by stream discharge and evapotranspiration. These are valid assumptions for Blue Beaver Creek because most of the basin lies within the Fort Sill Military Reservation where there is no irrigation and no facilities upstream which discharge effluent to the stream. The relationships are expressed as the following:

$$I = O \qquad \text{(F-1)}$$

$$P = Qt + ET \qquad \text{(F-2)}$$

$$P = Qs + Qg + ET \qquad \text{(F-3)}$$

$$P - ET = Qs + Qg \qquad \text{(F-4)}$$

where I = inflow

O = outflow

P = precipitation on the basin

Qt = total discharge from the basin

ET = evapotranspiration

Qs = surface runoff

Qg = ground-water runoff, or baseflow.

By equation (F-2), the difference between rainfall on the basin and streamflow from the basin is evapotranspiration (Tables IX and X). For the Blue Beaver Creek basin, annual evapotranspiration ranged from 16.8 to 30.9 inches (427 to 785 mm) for the 15-year period 1968 to 1982. According to this equation, evapotranspiration is greatest during the spring when rainfall is greatest, but the percentage of precipitation lost to evapotranspiration is greater during the summer. Part of what is called evapotranspiration in equation (F-2) is actually precipitation held in temporary storage as soil moisture in the unsaturated zone during the spring. This soil moisture is later removed by evapotranspiration in the summer. Expressed as a percentage of precipitation, evapotranspiration is shown to be greatest in the late summer (Figure 56); over the 15-year period evapotranspiration averaged 81% of precipitation.

By equation (F-4), the ground-water runoff is a measure of recharge, that part of precipitation not lost to evapotranspiration and not contributing directly to surface runoff. The net recharge rate is the ratio of baseflow to the basin area (Table XI). The annual recharge rate ranged from 7500 to 327,000 gpd/mi^2 (0.13 to 5.53 l/s/km^2), or 0.97 to 8.4 in/yr (24.6 to 213 mm/yr), and averaged 3.45 in/yr over a 15-year period. During the year recharge follows a trend opposite to that of evapotranspiration (Figure 56): it is at a maximum in spring and at a minimum in late summer.

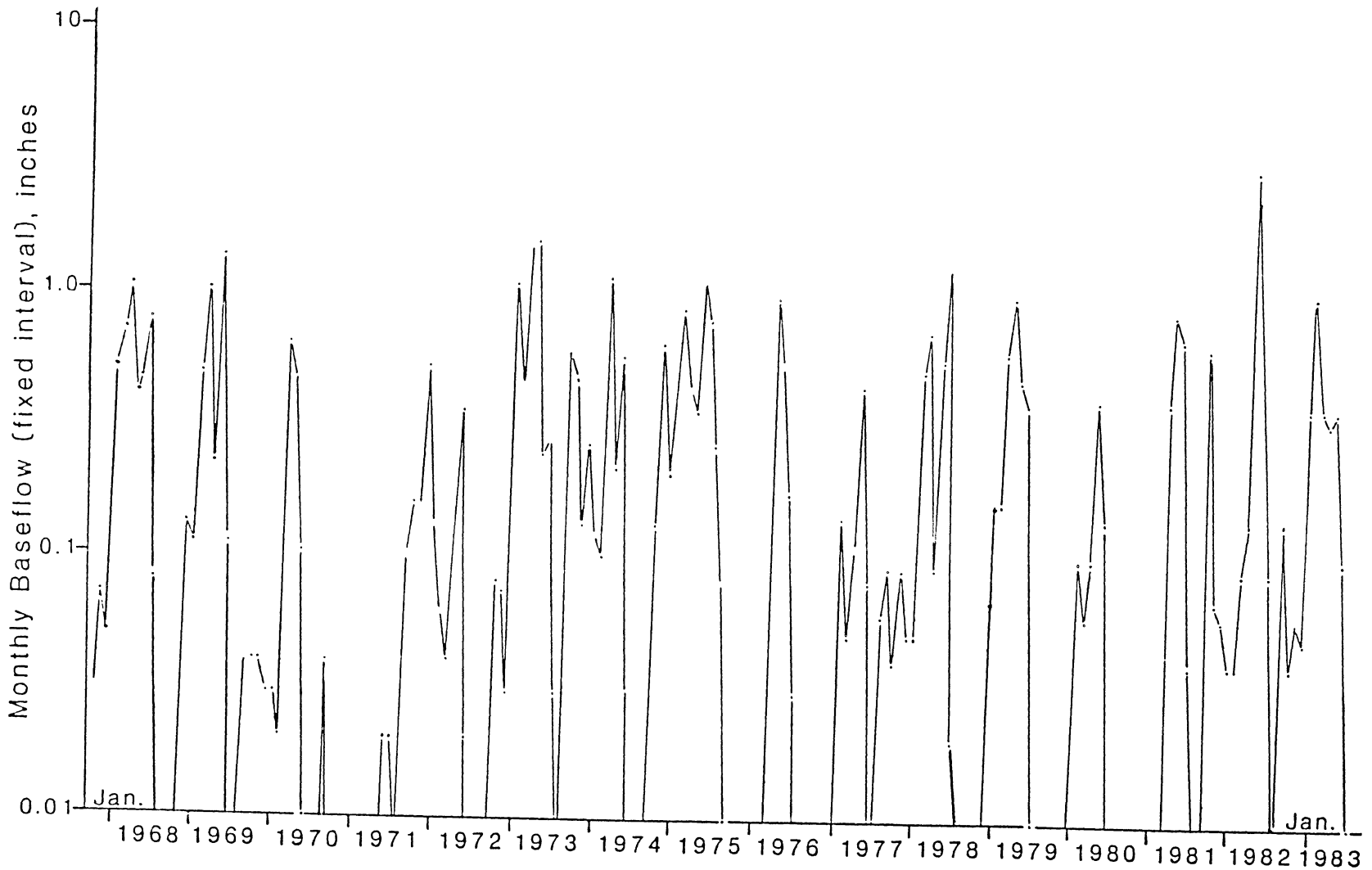

Figure 55. Average Monthly Baseflow of Blue Beaver Creek, 1968 - 1983, Fixed Interval Method

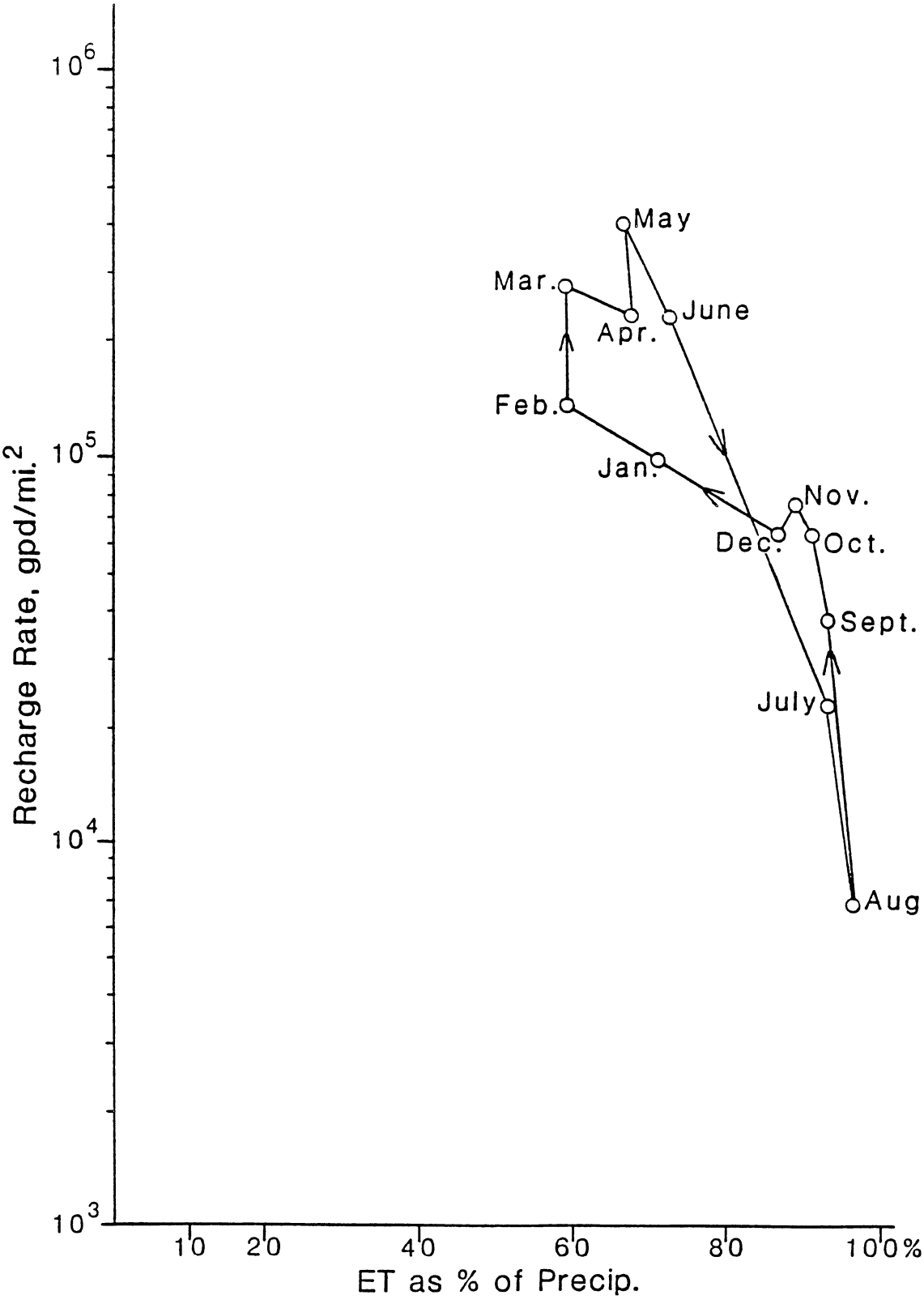

Figure 56. Relationship Between Recharge Rate and Evapotranspiration as Percentage of Precipitation

TABLE IX

MONTHLY EVAPOTRANSPIRATION, BLUE BEAVER CREEK BASIN, 1968-1982 WATER YEARS

(1) Month	(2) Mean Monthly Precip., inches	(3) Total Discharge, inches	(4) Evapo-trans-piration, inches (2)-(3)	ET as % of Precip. (4)/(2)x100
Jan.	1.06	0.31	0.75	70.6
Feb.	1.05	0.43	0.62	59.0
Mar.	1.99	0.82	1.17	58.8
Apr.	2.49	0.81	1.68	67.5
May	5.97	2.00	3.97	66.5
June	3.21	0.89	2.32	72.3
July	2.03	0.14	1.89	93.1
Aug.	2.73	0.10	2.63	96.3
Sept.	3.46	0.24	3.22	93.1
Oct.	2.60	0.24	2.36	90.8
Nov.	1.59	0.18	1.41	88.7
Dec.	0.96	0.13	0.83	86.5

TABLE X

ANNUAL EVAPOTRANSPIRATION, BLUE BEAVER CREEK BASIN,
1968-1982 WATER YEARS

(1) Water Year	(2) Total Precip., inches	(3) Total Discharge, inches	(4) Evapo-trans-piration, inches (2)-(3)	(5) ET as % of Precip. (4)/(2)x100	2 yr. Moving Avg. Total Precip.
1968	28.35	7.89	20.46	72.2	---
1969	33.83	6.14	27.69	81.8	31.09
1970	22.30	1.92	20.38	91.4	28.06
1971	27.61	0.67	26.94	97.6	24.96
1972	19.80	2.98	16.82	85.0	23.70
1973	45.99	15.08	30.91	67.2	32.90
1974	24.25	5.53	18.72	77.2	35.12
1975	36.05	9.78	26.27	72.9	30.15
1976	27.15	3.18	23.97	88.3	31.60
1977	24.36	3.65	20.71	85.0	25.76
1978	28.95	9.78	19.17	66.2	26.66
1979	25.50	5.77	19.73	77.4	27.2
1980	19.42	2.04	17.38	89.5	22.46
1981	31.32	3.96	27.36	87.4	25.37
1982	41.94	12.62	29.32	69.9	36.63
Avg.	29.12	6.07	23.06	80.6	---

TABLE XI

RECHARGE RATES, BLUE BEAVER CREEK BASIN, 1968-1982 WATER YEARS

Units are $gpd/mi^2 \times 10^E$

	1968		1969		1970		1971		1972		1973	
		E		E		E		E		E		E
Jan.	0.28	6	0.59	5	0.18	5	0.10	4	0.74	5	0.60	6
Feb.	0.40	6	0.27	6	0.11	5	0.92	3	0.34	5	0.25	6
Mar.	0.58	6	0.57	6	0.36	6	0.90	3	0.20	5	0.86	6
Apr.	0.22	6	0.12	6	0.25	6	0.46	3	0.96	5	0.88	6
May	0.27	6	0.75	6	0.67	5	0.52	3	0.20	6	0.14	6
June	0.43	6	0.62	5	0.50	4	0.90	4	0.11	5	0.15	6
July	0.43	5	0.47	3	0.26	3	0.90	4	0.42	3	0.19	5
Aug.	0.20	4	0.40	4	0.26	3	0.50	4	0.26	3	0.30	4
Sept.	0.10	4	0.22	5	0.21	5	0.56	5	0.25	3	0.33	6
Oct.	0.52	3	0.20	5	0.63	3	0.89	5	0.45	5	0.26	6
Nov.	0.13	5	0.20	5	0.99	3	0.86	5	0.41	6	0.72	5
Dec.	0.73	5	0.19	5	0.10	4	0.29	6	0.17	6	0.14	6
Wtr. Yr.	1.97	5	1.65	5	6.7	4	7.5	3	7.6	4	3.27	5

Annual Recharge Rate $\times 10^E$

		E		E		E		E		E		E
gpd/ft^2	7.07	-3	5.92	-3	2.40	-3	2.68	-4	2.73	-3	1.17	-2
in/yr	4.14		3.47		1.41		1.57		1.60		6.87	

$gpd/ft^2 \times 586 = in/yr$

TABLE XI (Continued)

	Units are gpd/mi^2 x 10^E									
	1974		1975		1976		1977		1978	
		E		E		E		E		E
Jan.	0.67	5	0.20	6	0.20	4	0.10	4	0.26	5
Feb.	0.56	5	0.48	6	0.20	4	0.79	5	0.28	6
Mar.	0.63	6	0.24	6	0.30	4	0.30	5	0.40	6
Apr.	0.12	6	0.20	6	0.54	6	0.62	5	0.51	5
May	0.32	6	0.63	6	0.30	6	0.25	6	0.31	6
June	0.18	5	0.43	6	0.96	5	0.42	5	0.74	6
July	0.26	3	0.14	6	0.18	5	0.20	4	0.12	5
Aug.	0.26	3	0.47	5	0.52	3	0.33	5	0.10	4
Sept	0.30	4	0.60	4	0.97	3	0.48	5	0.10	4
Oct.	0.74	5	0.10	4	0.10	4	0.25	5	0.39	5
Nov.	0.36	6	0.10	4	0.10	4	0.47	5	0.38	5
Dec.	0.11	6	0.10	4	0.84	3	0.27	5	0.39	5
Wtr. Yr.	1.43	5	2.48	5	8.2	4	4.6	4	1.63	5
	Annual Recharge Rate x 10^E									
		E		E		E		E		E
gpd/ft^2	5.13	-3	8.90	-3	2.94	-3	1.65	-3	5.85	-3
in/yr	3.00		5.21		1.72		0.97		3.42	
	gpd/ft^2 x 586 = in/yr									

TABLE XI (Continued)

	Units are gpd/mi^2 x 10^E				
	1979	1980	1981	1982	Avg.
	E	E	E	E	E
Jan.	0.90 5	0.14 5	0.10 4	0.21 5	9.71 4
Feb.	0.91 5	0.56 5	0.95 3	0.22 5	1.35 5
Mar.	0.33 6	0.33 5	0.10 4	0.52 5	2.74 5
Apr.	0.55 6	0.56 5	0.22 6	0.77 5	2.30 5
May	0.26 6	0.22 6	0.48 6	0.17 7	3.95 5
June	0.21 6	0.81 5	0.39 6	0.74 6	2.27 5
July	0.70 4	0.10 4	0.23 5	0.51 5	2.27 4
Aug.	0.56 3	0.10 4	0.40 4	0.10 4	6.86 3
Sept.	0.51 3	0.10 4	0.27 3	0.76 5	3.77 4
Oct.	0.20 4	0.10 4	0.36 6	0.25 5	6.22 4
Nov.	0.20 4	0.10 4	0.40 5	0.32 5	7.54 4
Dec.	0.20 4	0.10 4	0.33 5	0.29 5	6.27 4
Wtr. Yr.	1.63 5	1.41 5	4.0 4	9.4 4	2.72 5
	Annual Recharge Rate x 10^E				
	E	E	E	E	E
gpd/ft^2	5.06 -3	1.43 -3	3.37 -3	9.76 -3	4.95 -3
in/yr	2.96	8.40	1.97	5.71	3.49

gpd/ft^2 x 586 = in/yr

TABLE XII

MONTHLY AND ANNUAL STREAM DISCHARGE, INCHES,
BLUE BEAVER CREEK, 1968-1982 WATER YEARS

	1968	1969	1970	1971	1972	1973	1974	1975	1976	1977	1978	1979	1980	1981	1982	Avg.
Jan.	0.85	0.12	0.03	<.01	0.14	2.49	0.12	0.47	<.01	<.01	0.05	0.22	0.05	0.0	0.04	0.31
Feb.	1.07	0.84	0.02	<.01	0.06	0.51	0.11	1.21	<.01	0.31	0.78	0.18	1.25	0.0	0.04	0.43
Mar.	1.35	1.35	0.86	<.01	0.04	4.19	1.95	0.48	0.01	0.06	0.89	0.97	0.06	<.01	0.10	0.82
Apr.	0.49	0.24	0.68	<.01	0.91	2.44	0.44	0.40	1.97	0.49	0.10	1.75	0.14	0.61	1.49	0.81
May	1.53	2.89	0.15	<.01	0.60	0.27	1.72	3.57	0.86	1.25	5.19	1.34	1.44	1.59	7.68	2.00
June	2.24	0.16	0.01	0.02	0.02	1.45	0.04	1.63	0.27	0.10	2.55	1.08	0.20	1.63	2.01	0.89
July	0.11	<.01	0.0	0.02	<.01	0.04	<.01	0.59	0.04	<.01	0.02	0.02	<.01	0.10	1.13	0.14
Aug.	<.01	<.01	0.0	0.04	0.0	0.01	0.0	0.10	<.01	1.29	0.0	<.01	0.0	0.01	<.01	0.10
Sept.	0.02	0.28	0.04	0.58	0.0	1.38	0.06	0.02	<.01	0.13	0.0	0.0	0.0	0.0	1.10	0.24
Oct.	<.01	0.04	<.01	0.33	0.82	0.65	0.27	<.01	<.01	0.05	0.0	0.0	0.0	1.25	0.05	0.24
Nov.	0.09	0.04	<.01	0.17	1.14	0.15	0.84	<.01	<.01	0.10	0.0	0.0	0.0	0.08	0.06	0.18
Dec.	0.16	0.04	<.01	0.70	0.32	0.28	0.21	<.01	<.01	0.05	0.0	<.01	0.0	0.06	0.06	0.13
Total:																
Cal. Yr.	7.92	6.01	1.80	1.87	4.05	13.86	5.76	8.48	3.17	3.84	9.79	5.58	3.15	5.34	13.76	6.29
Wtr. Yr.	7.89	6.14	1.92	0.67	2.98	15.08	5.53	9.78	3.18	3.65	9.78	5.77	2.04	3.96	12.62	6.07

TABLE XIII

MONTHLY AND ANNUAL BASEFLOWS (FIXED INTERVAL),
BLUE BEAVER CREEK, 1968-1982 WATER YEARS

	1968	1969	1970	1971	1972	1973	1974	1975	1976	1977	1978	1979	1980	1981	1982	Avg.
Jan.	0.50	0.11	0.03	<.01	0.13	1.08	0.12	0.35	0.01	<.01	0.05	0.16	0.03	0.0	0.04	0.17
Feb.	0.72	0.48	0.02	<.01	0.06	0.45	0.10	0.86	<.01	0.14	0.50	0.16	0.10	0.0	0.04	0.24
Mar.	1.04	1.01	0.64	<.01	0.04	1.53	1.13	0.43	<.01	0.05	0.72	0.60	0.06	<.01	0.09	0.49
Apr.	0.40	0.22	0.45	<.01	0.17	1.58	0.21	0.35	0.96	0.11	0.09	0.99	0.10	0.39	0.14	0.41
May	0.48	1.34	0.12	<.01	0.35	0.24	0.57	1.13	0.54	0.44	0.56	0.46	0.40	0.85	3.09	0.70
June	0.77	0.11	0.01	0.02	0.02	0.27	0.03	0.78	0.17	0.08	1.31	0.38	0.14	0.69	1.32	0.41
July	0.08	<.01	0.0	0.02	<.01	0.03	<.01	0.26	0.03	<.01	0.02	0.01	<.01	0.04	0.09	0.04
Aug.	<.01	<.01	0.0	<.01	0.0	<.01	0.0	0.08	<.01	0.06	0.0	<.01	0.0	<.01	<.01	0.01
Sept.	<.01	0.04	0.04	0.10	0.0	0.59	<.01	0.01	<.01	0.09	0.0	0.0	0.0	0.0	0.14	0.07
Oct.	<.01	0.04	<.01	0.16	0.08	0.46	0.13	<.01	<.01	0.04	0.0	0.0	0.0	0.64	0.04	0.11
Nov.	0.02	0.04	<.01	0.15	0.73	0.13	0.64	<.01	<.01	0.09	0.0	0.0	0.0	0.07	0.06	0.13
Dec.	0.13	0.03	<.01	0.52	0.30	0.26	0.20	<.01	<.01	0.05	0.0	<.01	0.0	0.06	0.05	0.11
Total Water Yr.	4.15	3.48	1.42	0.16	1.61	6.89	3.01	5.23	1.74	0.98	3.44	2.97	4.85	1.99	5.72	3.18
% Q	52.6	56.6	73.7	23.3	54.0	45.7	54.4	53.5	54.6	27.0	35.1	51.4	41.6	50.3	45.3	47.9
% Ppt	14.6	10.3	6.4	0.6	8.1	15.0	12.4	14.5	6.4	4.0	11.9	11.6	25.0	6.4	13.6	10.7

DESCRIPTION OF ISOHYETAL METHOD

To determine the average depth of rainfall over the Blue Beaver Creek basin upstream of the gaging station the isohyetal method was applied to the isohyet map (Figure 57; Linsley and others, 1982, p.71). The area of the stream basin within the isohyets was calculated from a gridded map of the basin traced from a topographic map. The total calculated area is 21.0 square miles (54.4 km^2); the reported area upstream of the gaging station is 24.6 mi^2 (63.7 km^2). Normalizing the calculated areas to the reported area had no effect on the final result of the method. The product of the average precipitation between the isohyets and the basin area within the isohyets is the precipitation volume. The ratio of the volume to the basin area is the average rainfall depth over the basin (Table XV).

TABLE XIV

PERIODS OF RECORD FOR WEATHER STATIONS
IN COMANCHE COUNTY AREA

Apache	1945-74	Marlow	1954-83
Baird	1953-78	Snyder	1954-83
Chattanooga	1954-83	Walters	1953-82
Duncan	1954-83	Wichita Mtn. Wildlife Ref.	1954-83
Lawton	1952-81		

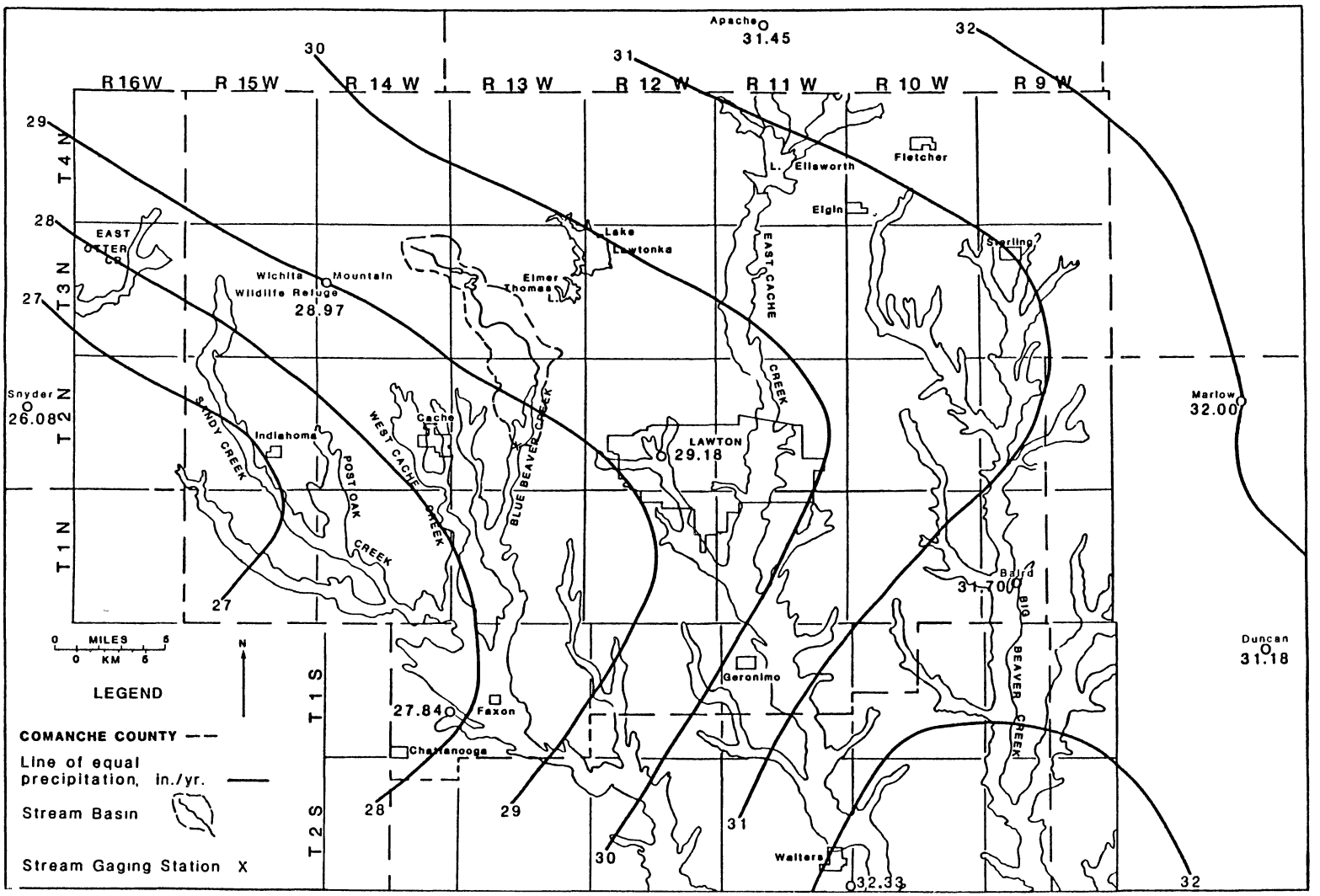

Figure 57. Isohyet Map of Comanche County

TABLE XV

CALCULATION OF AVERAGE RAINFALL DEPTH
OVER BLUE BEAVER CREEK BASIN

(1) Isohyet	(2) Area Enclosed mi^2	(3) Net Area	(4) Average Precip. in.	(5) Precip. Volume (3)x(4) $in\text{-}mi^2$	
28.5-29.0	3.3	3.3	28.75	94.88	
29.0-29.5	21.0	17.7	29.25	517.72	
				612.60	Total

$$\text{Average Depth} = \frac{\text{Total Precipitation Volume}}{\text{Basin Area}}$$

$$= \frac{612.60}{21.0} = 29.17 \text{ inches}$$

TABLE XVI

WATER-TABLE GRADIENTS ALONG CREEKS
IN COMANCHE COUNTY

Sandy Creek	23.4 ft/mi
Post Oak Creek	18.8
West Cache Creek	13.5
Blue Beaver Creek	14
Big Beaver Creek	8.3

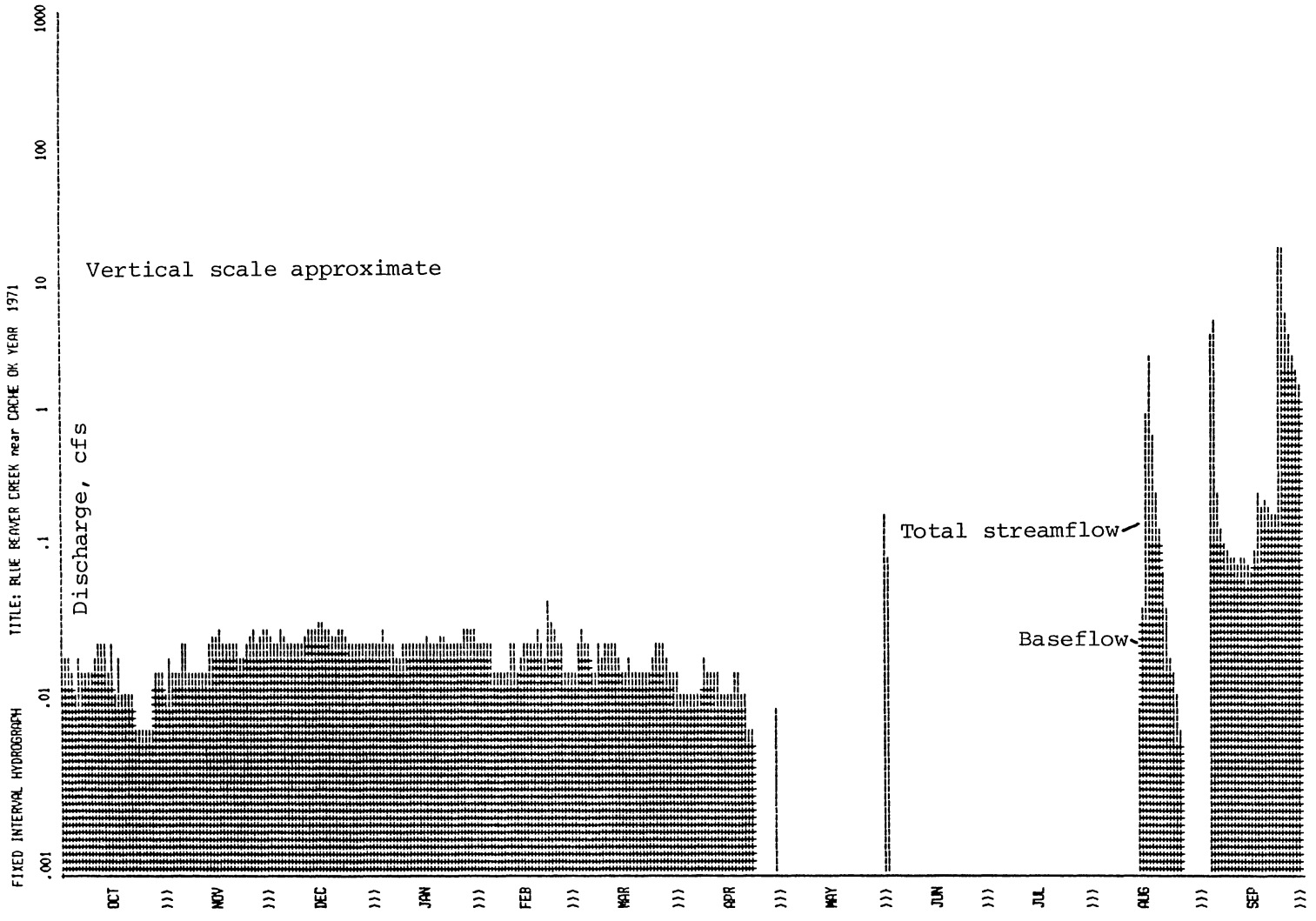

Figure 58. 1971 Stream Hydrograph of Blue Beaver Creek

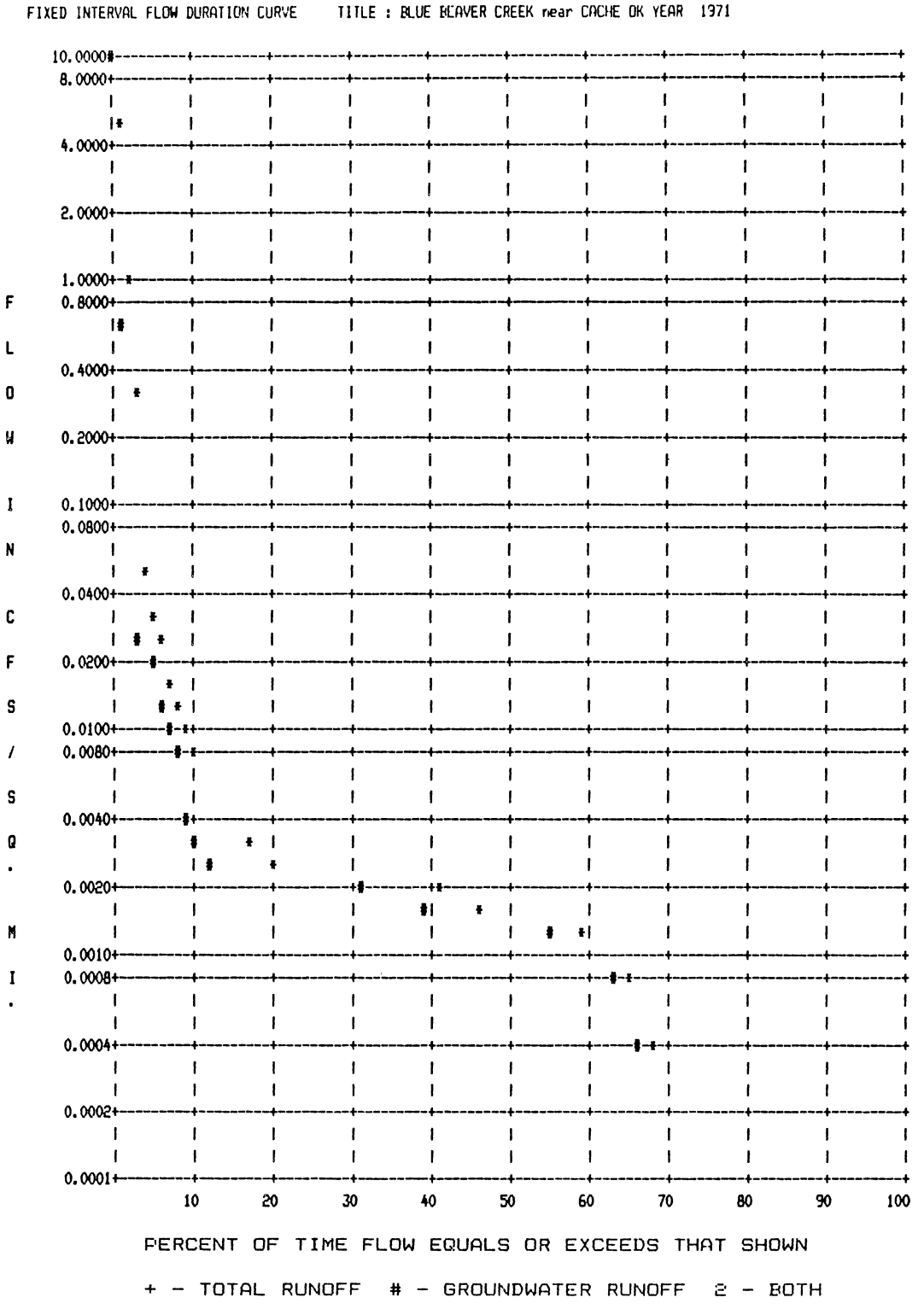

Figure 59. 1971 Flow Duration Curve of Blue Beaver Creek

TABLE XVII

WATER QUALITY DATA FOR BLUE BEAVER CREEK

Date	Streamflow, cfs	Specific Conductance, umhos	pH	Temperature, °C	Hardness, CaCO3	Calcium
	Units are milligrams per liter except as noted					
Dry Water Year						
10/7/70	0.04	228	7.8	--	75	22
10/30/70	0.03	234	7.7	--	76	22
11/19/70	0.04	236	7.8	--	77	19
12/9/70	0.04	229	7.9	--	74	20
12/29/70	0.04	222	7.5	--	70	19
1/20/71	0.04	214	7.5	--	70	18
2/11/71	0.05	218	7.6	--	64	18
3/4/71	0.04	216	7.9	--	66	18
5/7/71	0.02	248	7.9	--	72	--
9/9/71	0.31	237	7.5	--	78	--
9/29/71	9.7	146	--	--	--	--
Wet Water Year						
11/22/72	28	97	6.5	--	70	7.2
12/20/72	4.8	129	6.4	--	89	10
1/4/73	25	106	6.4	--	73	--
1/31/73	30	101	6.8	--	77	9.6
2/22/73	9.5	122	6.9	--	82	--
3/13/73	46	102	6.9	--	80	9.6
4/25/73	63	104	6.9	--	72	--
5/16/73	5.1	182	7.0	--	116	17
6/6/73	17	123	--	--	--	--

TABLE XVII (Continued)

Date	Stream-flow, cfs	Specific Conduc-tance, umhos	pH	Temper-ature, °C	Hardness, CaCO3	Calcium
6/27/73	3.4	182	6.6	--	112	--
7/19/73	0.60	230	7.7	--	129	20
8/10/73	0.19	241	7.5	--	137	22
Wet Water Year						
10/20/81	20	122	7.2	18.5	51	12
2/8/82	0.85	230	7.1	2.5	63	17
5/5/82	3.0	158	6.8	21.0	51	14
Dry Water Year						
11/29/82	1.5	320	7.3	12.0	75	21
3/7/83	6.4	105	6.7	15.0	46	13
5/16/83	6.6	147	7.7	20.5	49	14
1968-1975 Water Years Mean Values	16	161	7.4	--	52	14

Date	Magnesium	Sodium	Potassium	Alka-linity, CaCO3 (or HCO3)	Sulfate
10/7/70	5.1	18	2.9	(106)	17
10/30/70	5.4	18	2.5	(102)	21
11/19/70	7.0	17	2.4	(99)	19
12/9/70	6.1	17	1.7	(93)	19
12/29/70	5.4	17	1.3	(74)	29
1/20/71	5.8	16	1.1	(76)	27
2/11/71	4.9	17	1.2	(76)	29
3/4/71	4.9	17	1.3	(78)	27

TABLE XVII (Continued)

Date	Magnesium	Sodium	Potassium	Alka-linity, CaCO3 (or HCO3)	Sulfate
5/7/71	--	24	--	(88)	31
9/9/71	--	16	--	(100)	20
9/29/71	--	--	--	--	--
11/22/72	3.4	7.0	1.2	(30)	16
12/20/72	3.9	9.3	1.0	(40)	19
1/4/73	--	7.7	--	(36)	15
1/31/73	3.4	7.5	1.1	(38)	14
2/22/73	--	9.4	--	(42)	17
3/13/73	3.4	7.5	1.2	(38)	14
4/25/73	--	7.8	--	(42)	14
5/16/73	3.8	14	1.5	(68)	21
6/6/73	--	--	--	--	--
6/27/73	--	13	--	(76)	18
7/19/73	5.6	18	1.7	(100)	15
8/10/73	6.1	19	1.9	(111)	15
10/20/81	2.8	8.0	1.4	35	8.0
2/8/82	4.9	--	1.5	59	18
5/5/82	3.8	11	1.3	58	12
11/29/82	5.5	17.0	1.6	84	19
3/7/83	3.2	9.8	1.2	51	22
5/16/83	3.5	9.8	1.5	54	14
1968-1975 Water Years Mean Values	4.1	12	2	(66)	17

TABLE XVII (Continued)

Date	Chloride	Fluoride	Dissolved Solids	Nitrite + Nitrate, as N	Iron ug/l
10/7/70	11	0.4	143	--	--
10/30/70	10	0.4	136	--	--
11/19/70	11	0.4	142	--	--
12/9/70	10	0.5	141	--	--
12/29/70	10	0.4	130	--	--
1/20/71	9.5	0.4	126	--	--
2/11/72	9.5	0.3	127	--	--
3/4/71	10	0.3	128	--	--
5/7/71	11	--	137	--	--
9/9/71	8.0	--	147	--	--
9/29/71	--	--	--	--	--
11/22/72	5.0	0.3	70	0.05	--
12/20/72	6.0	0.3	89	0.02	--
1/4/73	5.3	--	73	0.07	--
1/31/73	6.0	0.3	77	0.02	--
2/22/73	6.8	--	82	0.02	--
3/13/73	6.0	0.3	80	0.02	--
4/25/73	3.7	--	72	0.09	--
5/16/73	9.5	0.3	116	0.07	--
6/6/73	--	--	--	--	--
6/27/73	9.3	--	112	0.0	--
7/19/73	13	0.4	129	0.10	--
8/10/73	14	0.4	137	0.13	--

TABLE XVII (Continued)

Date	Chloride	Fluoride	Dissolved Solids	Nitrite + Nitrate, as N	Iron ug/l
10/20/81	5.3	0.30	76*	0.11	--
2/8/82	17	0.40	160*	<0.10	--
5/5/82	6.3	0.50	95*	<0.10	--
11/29/82	16	0.30	150*	<0.10	170
3/7/83	31	0.40	120*	0.11	--
5/16/83	5.3	0.30	94*	0.49	28
1968-1975 Water Years Mean Values	7.4	--	105	0.39**	--

* Sum of constituents
** Nitrate only

Sources: Water Resources Data for Oklahoma, 1971 (U.S. Geological Survey, 1974a), 1973 (U.S. Geological Survey, 1974b), 1982 (Hauth and others, 1984), 1983 (Hauth and others, 1985), and J.K. Kurklin, 1979.

APPENDIX G

LINEAMENT ANALYSIS DATA

DISTRIBUTION OF WELL YIELDS IN THE ARBUCKLE GROUP AND POST OAK AQUIFERS ACCORDING TO LINEAMENT ANALYSIS

As noted previously, well yields from the Arbuckle Group Aquifer vary greatly in Comanche County. To understand better this variation, the distribution of estimated well yields from this aquifer was determined by a lineament analysis of aerial photographs. This approach was applied to the Post Oak Aquifer, also. Ground-water flow in the Arbuckle is through fractures and solutional openings formed during and after the tectonic movements of the Wichita uplift, as described previously. For this analysis, fracture flow was assumed to occur in the Post Oak, also. Areas with more fracturing presumably would have more flow and greater well yield; to locate the fractures aerial photographs were examined by two methods.

For one method it was assumed that lineaments in the Post Oak and Permian rocks above the Arbuckle Group indicate fracture patterns in the underlying Arbuckle Group Aquifer. These lineaments consist of straight segments of stream valleys, segments of several stream valleys that are in alignment, or non-cultivated vegetation in linear patterns. The other method involved extending fracture patterns occurring in the Wichita Mountains into the Arbuckle Group to the south. Fractures in the Wichita Granite Group were studied by Gilbert (1982). A lineament analysis and corresponding geological interpretation of Comanche County is discussed by Donovan and others (1986).

Both methods required the measurement of lengths and orientations of lineaments on a mosaic of aerial photographs at a scale of one to 40,000, or one inch equals approximately one mile (U.S. Department of Agriculture, 1981). A map of the major lineaments in the Wichita Mountains and in the Permian sediments to the south is shown in Figure 60. Fracture lineaments in the Wichita Mountains range in length from 0.2 to 6.2 miles and have three dominant orientations: 60° to 90° west of north, 10° west to 10° east of north, and 80° to 90° east of north (Figure 61). Lineaments of stream valleys and vegetation, most of which are south of the mountains, range in length from 0.3 to 11.4 miles with two dominant orientations: 20° to 30° west of north and zero to 10° east of north (Figure 62). Most of these lineaments are between one and two miles long.

The fracture lineaments can be separated into two sets according to their time of formation (Figures 61 and 62). The east-west trending fracture lineaments formed earlier than the north-south trending set as shown by the lack of an east-west trend in the lineaments of the Post Oak Conglomerate and Permian sediments. Presumably both sets occur in the Arbuckle Group; however, assuming that the north-south set formed after deposition of the Post Oak Conglomerate, only the north-south set propagated upward through the Post Oak. The degree of consolidation of the Permian rocks would enhance the propagation of fractures from the Arbuckle rocks. Determining the absolute time of formation of the fractures was beyond the scope of this study.

Assuming that permeability and well yield are controlled by the density of fractures, the amount of fracturing was studied by two methods. For both methods a grid of cells was used to locate the areas

of fracturing. It was assumed for the first method that a lineament might indicate only part of a fracture and that an area with many intersecting fractures would have a greater permeability; this method was applied to only the Arbuckle Group. The fracture lineaments in the Wichita Mountains were extended across the area on an overlay map using both the east-west and north-south sets of lineaments (Figure 63); it was assumed that both sets occur in the Arbuckle Group. It also was assumed that the fractures in the Wichita Mountains are "throughgoing" into the Arbuckle, that is, that a short fracture on the north side of the mountains extends to the south although its extension is not evident on the surface. This approach maximized the number of extended fractures.

The number of lineament intersections per cell is shown in Figure 64. The bottom row is beyond the area of the overlay map. In order to establish a permeability value for each cell, the average permeability of the Arbuckle Aquifer, 3.5 gpd/ft^2, as determined from the specific capacity data (Chapter VI), was multiplied by the ratio of the number of intersections in a cell to the mean number of intersections per cell (Table XVIII and Figures 65 and 66). Well yield values were calculated for each cell (Table XVIII and Figures 65 and 67) using a formula by Walton (1970, p.315) assuming an average effective aquifer thickness of 500 feet, a well radius of 0.28 feet, a pumping period of 5000 minutes, a drawdown of 350 feet, and a storativity of 0.0001.

It was assumed in the second method that the total length of fractures in an area controls the permeability. Only the lineaments in the Post Oak and Permian rocks were considered because fracture lineaments in the Wichita Mountains are outside the study area, and the lineaments

in the Post Oak indicate fracture patterns in the Arbuckle Group as well as in the Post Oak. Fractures in the Post Oak influence flow separately from the grain-size distribution. Non-channel areas assumed to have lower permeability, transmissivity, and yield because of smaller grain size actually may be more productive because of a higher amount of fracturing.

The sum of lineament lengths per cell is shown in Figure 68. For both aquifers the computation of the permeability for a cell is similar to the procedure used in the first method. The permeability is the product of the average permeability as determined from well data and the ratio of the total lineament length in a cell to the average total length per cell (Table XIX and Figures 69, 70, and 71). Well yield for the Post Oak was determined by Walton's formula (Equation 3-1) assuming a saturated thickness of 20 ft, a well radius of 0.35 ft, a pumping period of 660 min, a drawdown of 11 ft, and a storativity of 0.02 (Table XIX and Figure 72). Well yield for the Arbuckle was calculated according to the assumptions described above (Table XIX and Figure 73). Cells without values are beyond the area of either the aerial photographs or the overlay map.

Figure 74 shows the distribution of well yields by cells in the Post Oak Aquifer according to the grain-size distribution, and Figure 75 shows those areas with greater yield because of both increased fracturing and larger grain-size. Arbuckle well yield values derived from the two methods (Figures 67 and 73) were averaged using an arithmetic mean (Figure 76) and were compared with the average yield (270 gpm) calculated previously according to production well test data (Figure 77). The locations from both maps (Figures 76 and 77) which

correspond to a well yield of more than 270 gpm are shown on the map in Figure 78.

The Indiahoma area of the Arbuckle Group Aquifer (cell B2) is less productive for the amount of fracturing probably because the lithology limited the development of solution openings. Rauch and White (1970) reported that high concentrations of silica and dolomite inhibit cavity development, but small grain size (micrite) enhances carbonate solution. Dreiss (1984) confirmed the effects of small grain size and magnesium carbonate content on solution rate in carbonate aquifers. Within the Arbuckle Group the Cool Creek Formation contains much chert and sand, and the McKenzie Hill Formation has finer-grained layers. Other formations are predominantly dolomite. The areal variability of karst development depends on which of these lithologies subcrops beneath the Permian strata.

Determining the distribution of estimated well yield from the total length of fractures in an area was the more appropriate method of lineament analysis because its assumptions were more valid. The lineaments of stream valleys and vegetation were more apparent on the aerial photographs than the actual intersections of extended fracture lineaments. These methods qualitatively located areas of relatively higher well yields; determining actual aquifer well yields quantitatively for any one location requires actual production well test data for that location.

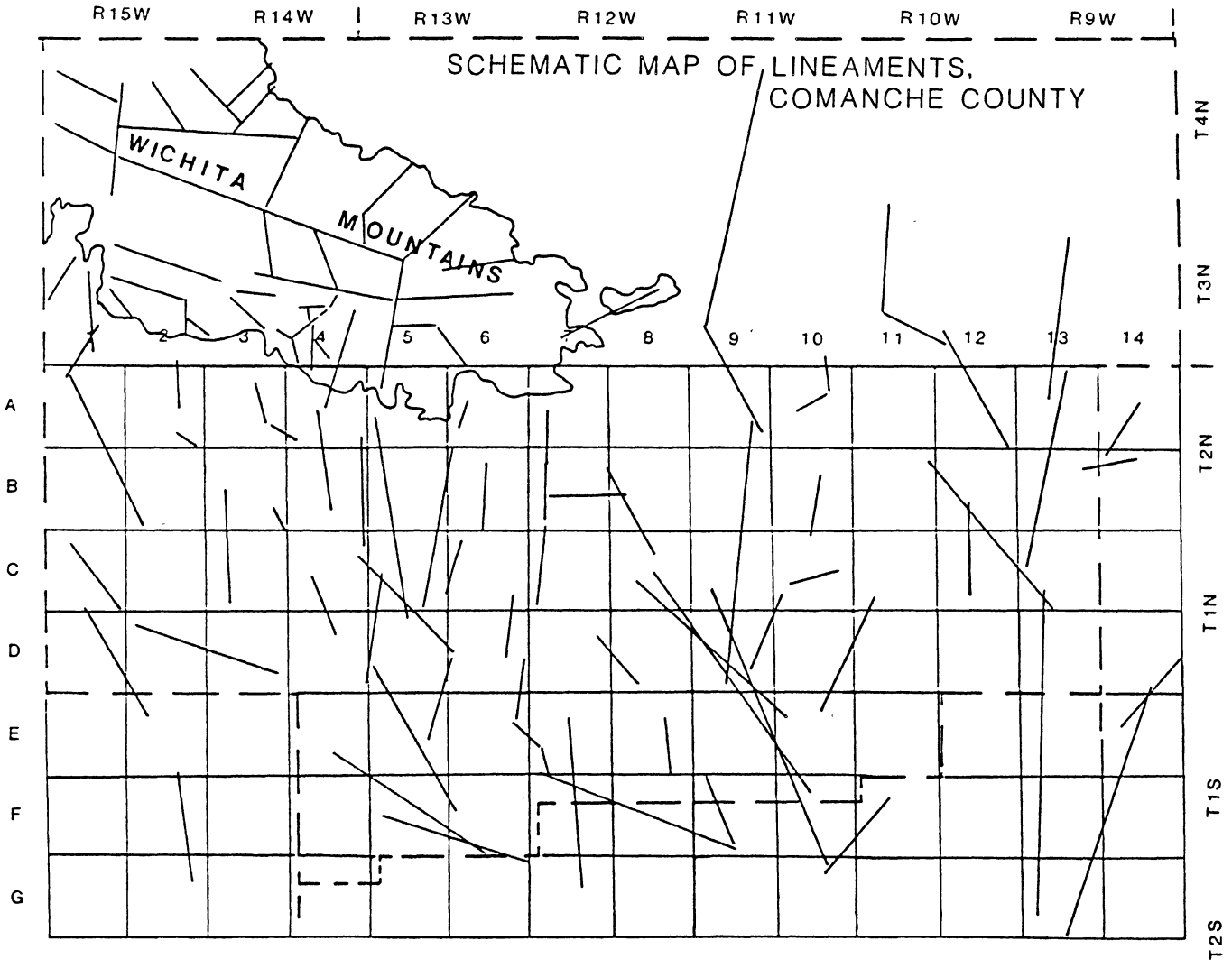

Figure 60. Schematic Map of Lineaments in Comanche County

ORIENTATION FREQUENCY
FRACTURE LINEAMENTS,
WICHITA MTNS., COMANCHE CO.

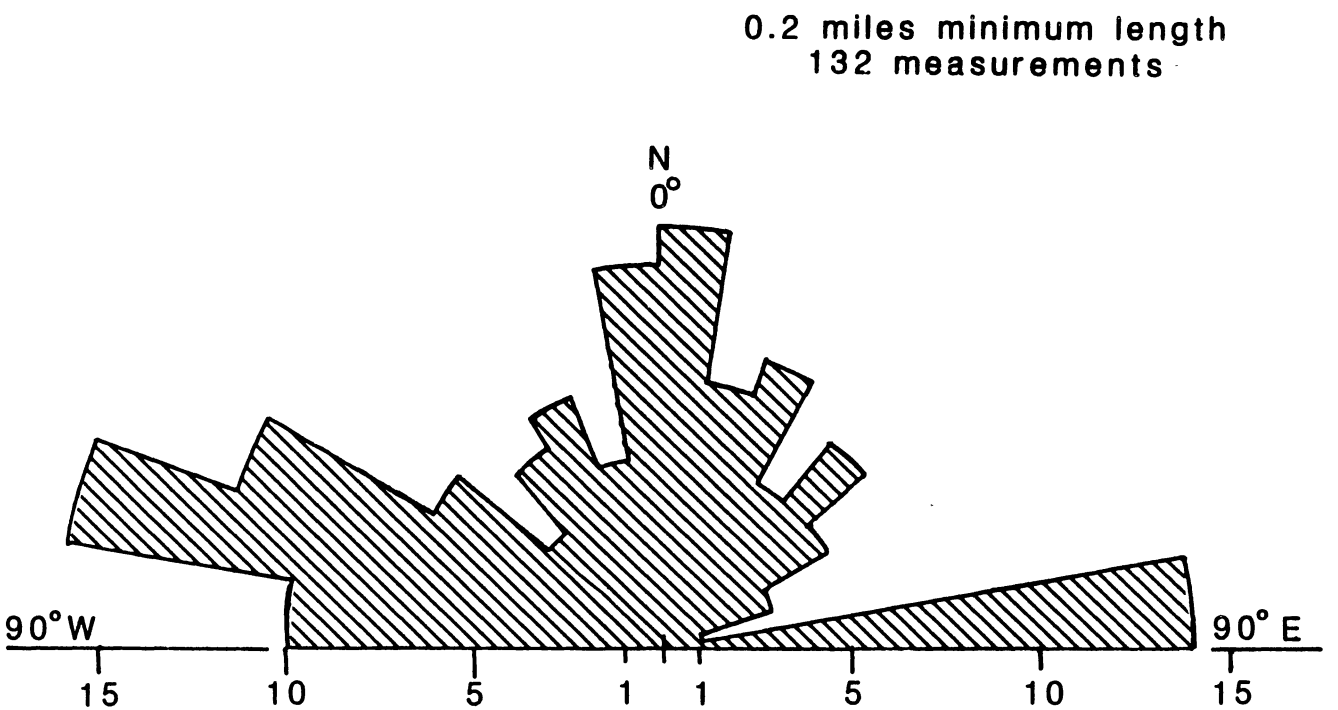

Figure 61. Orientation Frequency of Fracture Lineaments

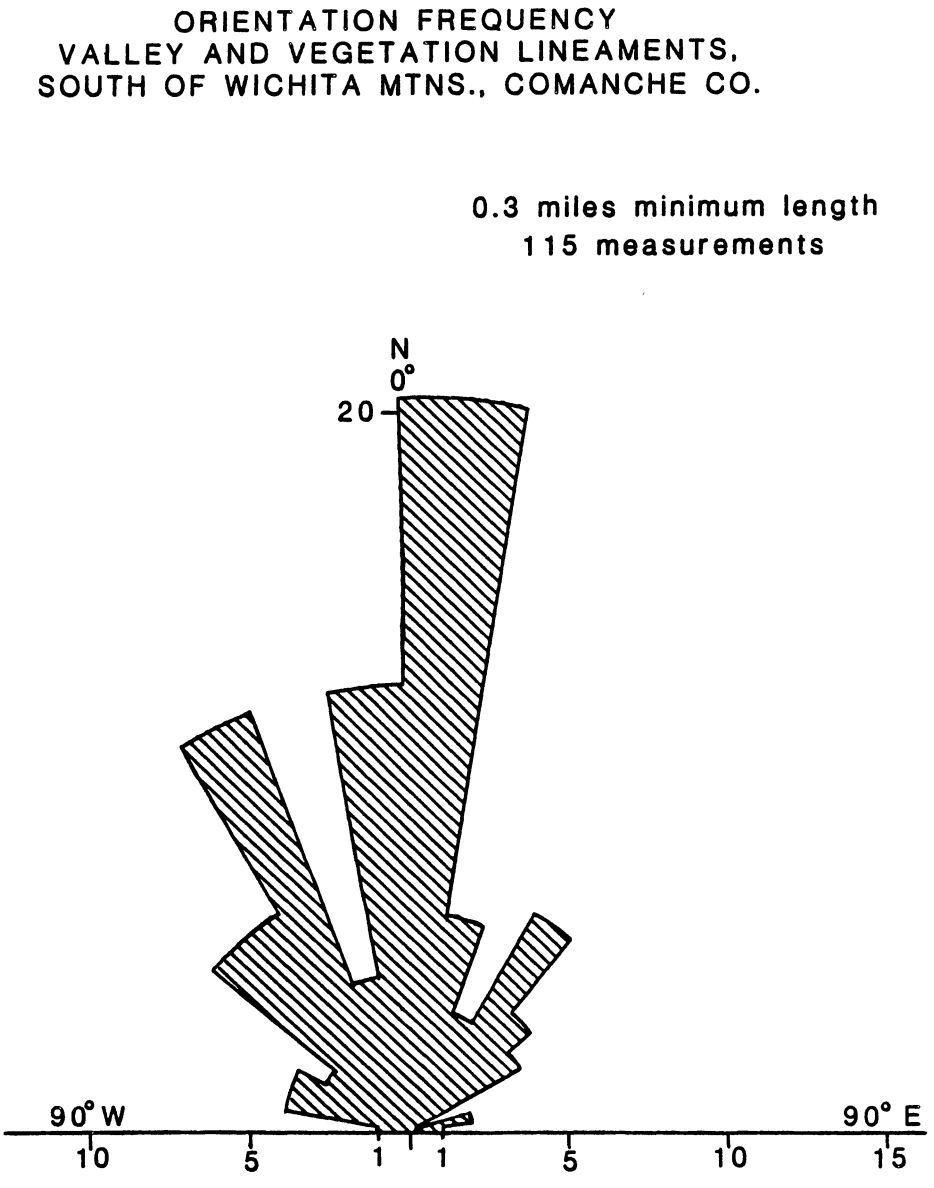

Figure 62. Orientation Frequency of Stream Valley Lineaments

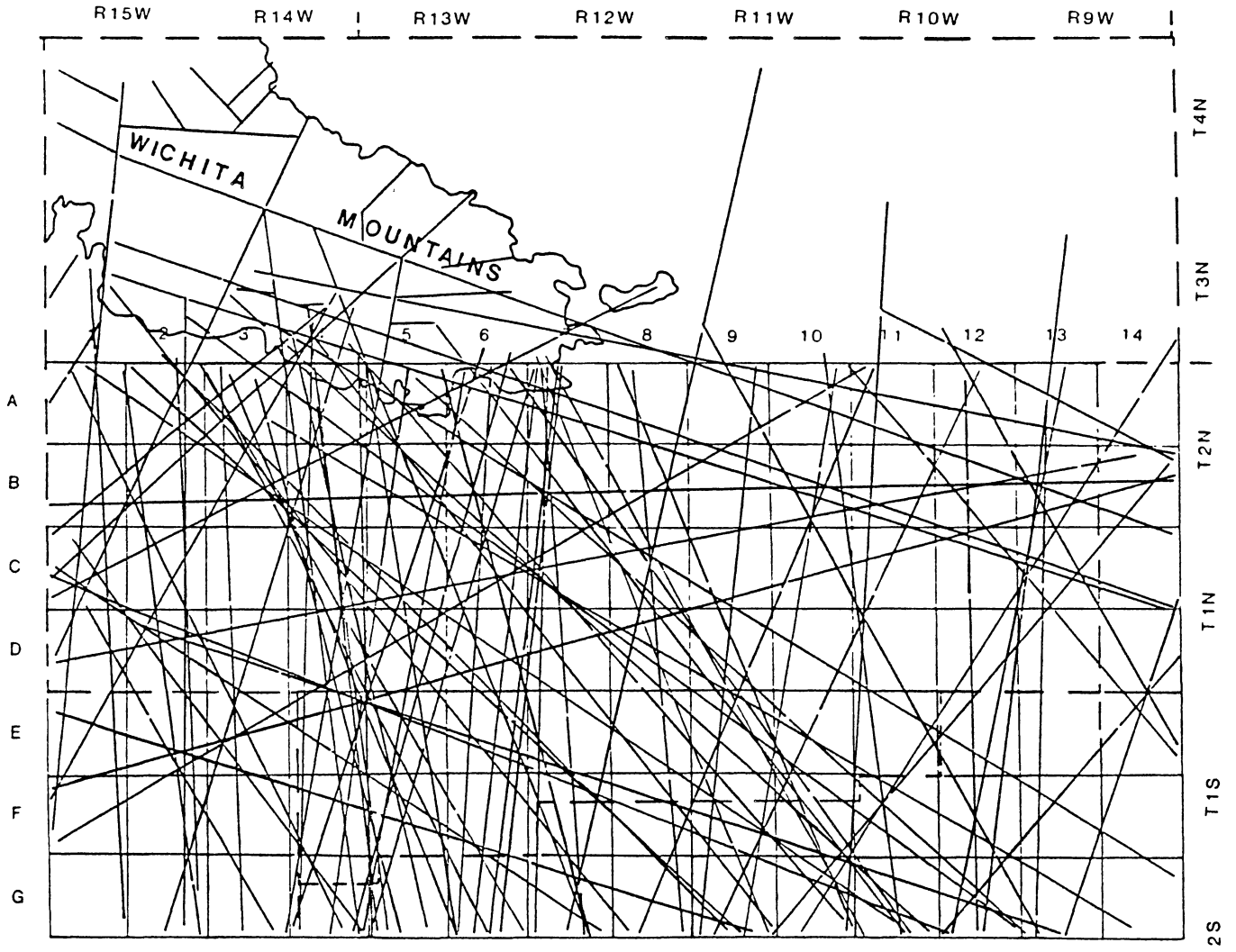

Figure 63. Schematic Map of Extended Fracture Lineaments

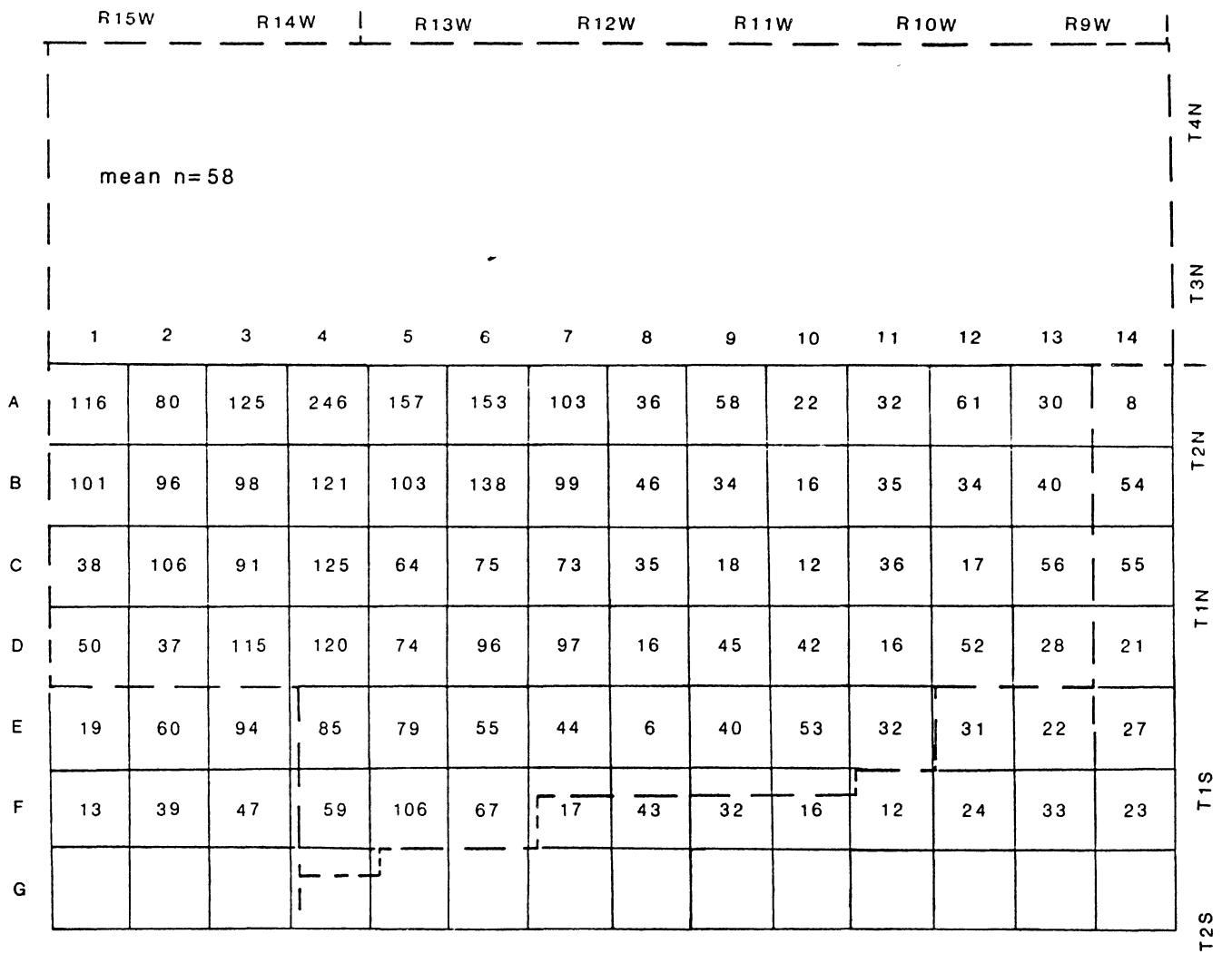

Figure 64. Number of Lineament Intersections per Cell

TABLE XVIII

CALCULATIONS OF PERMEABILITY AND YIELD OF ARBUCKLE GROUP AQUIFER FROM NUMBER OF LINEAMENT INTERSECTIONS FOR CELL B-12

For entire grid, mean number of lineament intersections, $\bar{n}$, = 58
For cell B-12, number of lineament intersections, n, = 34 (Figure 65).
Mean Permeability, $\bar{K}$, = 3.5 gpd/ft^2

Permeability, K, = $\frac{n}{\bar{n}} \times \bar{K}$ = 34 x 3.5 = 2.03 gpd/ft^2 (Significant figures were carried through the calculations.)

Average effective aquifer thickness, b, = 500 ft
Average well radius, r_w, = 0.28 ft
Average pumping period, t, = 5000 min
Average drawdown, s, = 350 ft; storativity, S, = 0.0001

$$\text{Yield, Q, } = \frac{Kbs}{264 \log \left(\frac{Kbt}{2693\, r_w^2\, S} \right) - 65.5}$$

$$= \frac{2.03\ (500)\ (350)}{264 \log \left(\frac{2.03\ (500)\ (5000)}{2693\ (0.28)^2\ (0.0001)} \right) - 65.5} = 165 \text{ gpm}$$

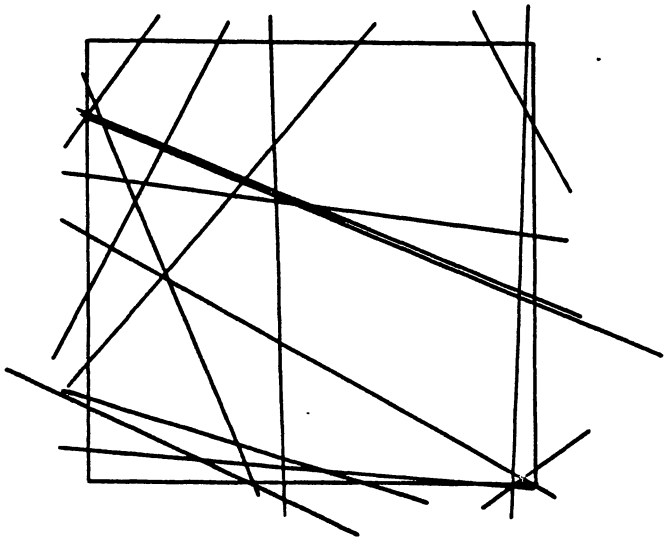

Figure 65. Cell B-12 with Extended Lineaments

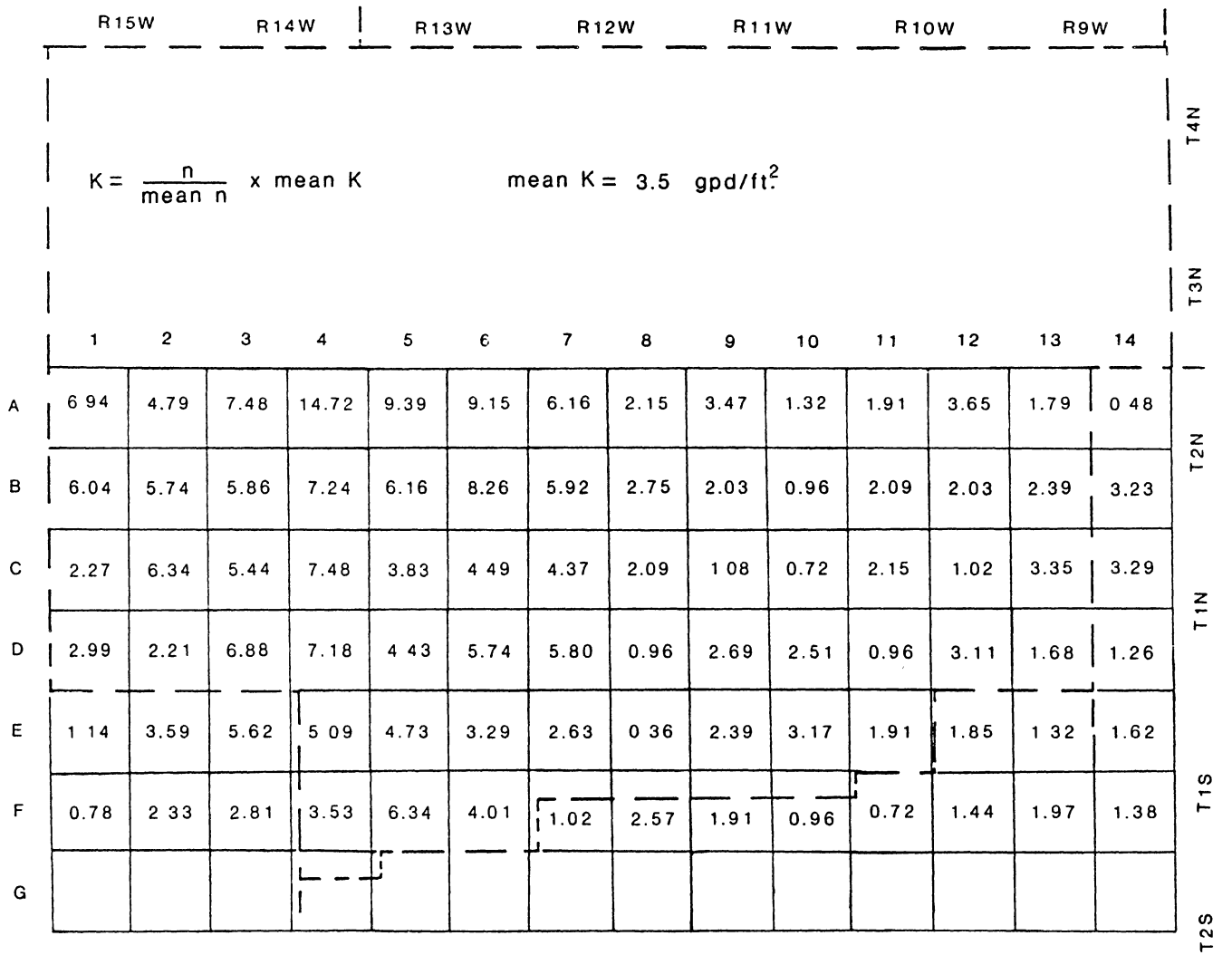

Figure 66. Permeabilities Calculated From Number of Lineament Intersections per Cell

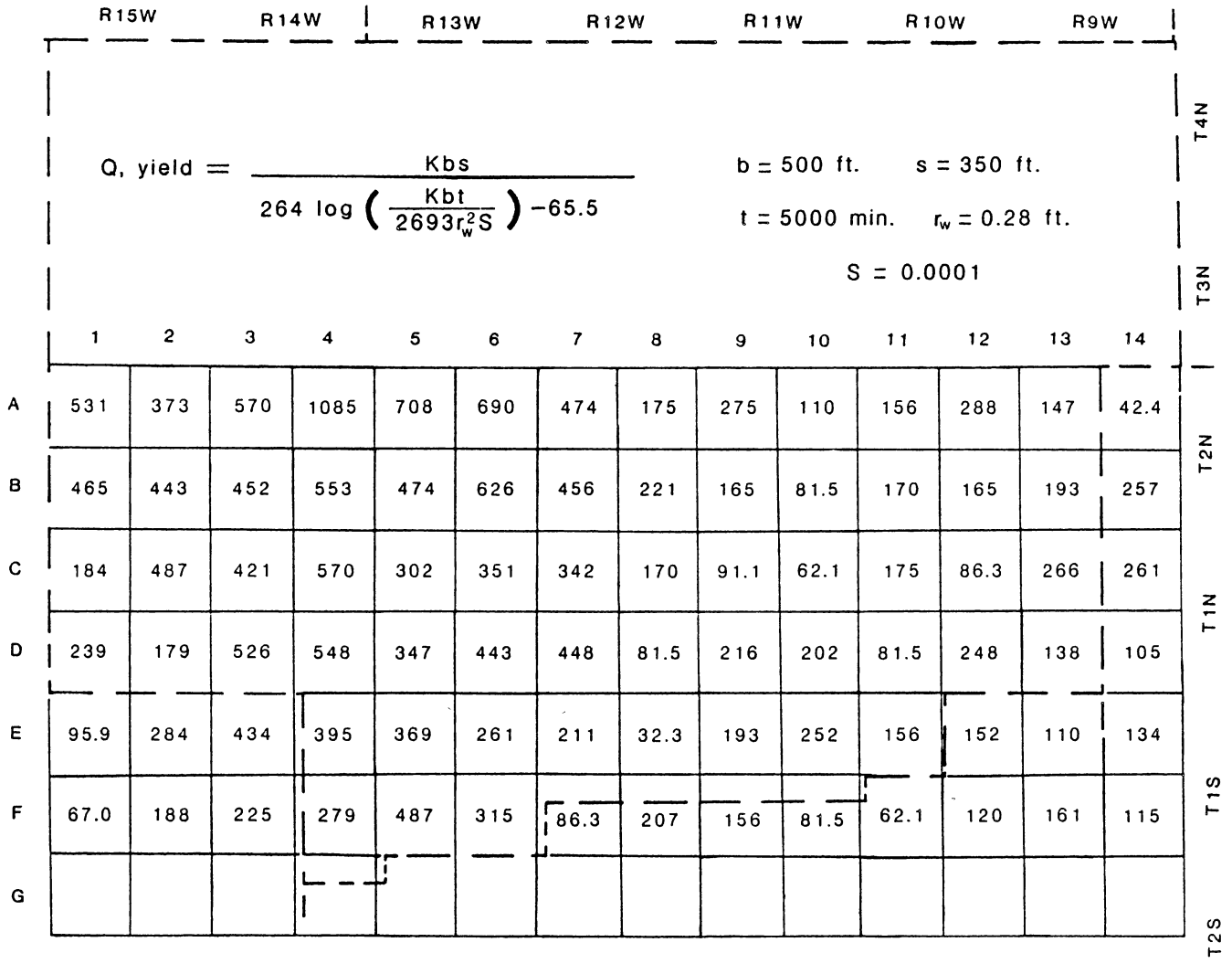

Figure 67. Yield Values Calculated From Number of Lineament Intersections per Cell

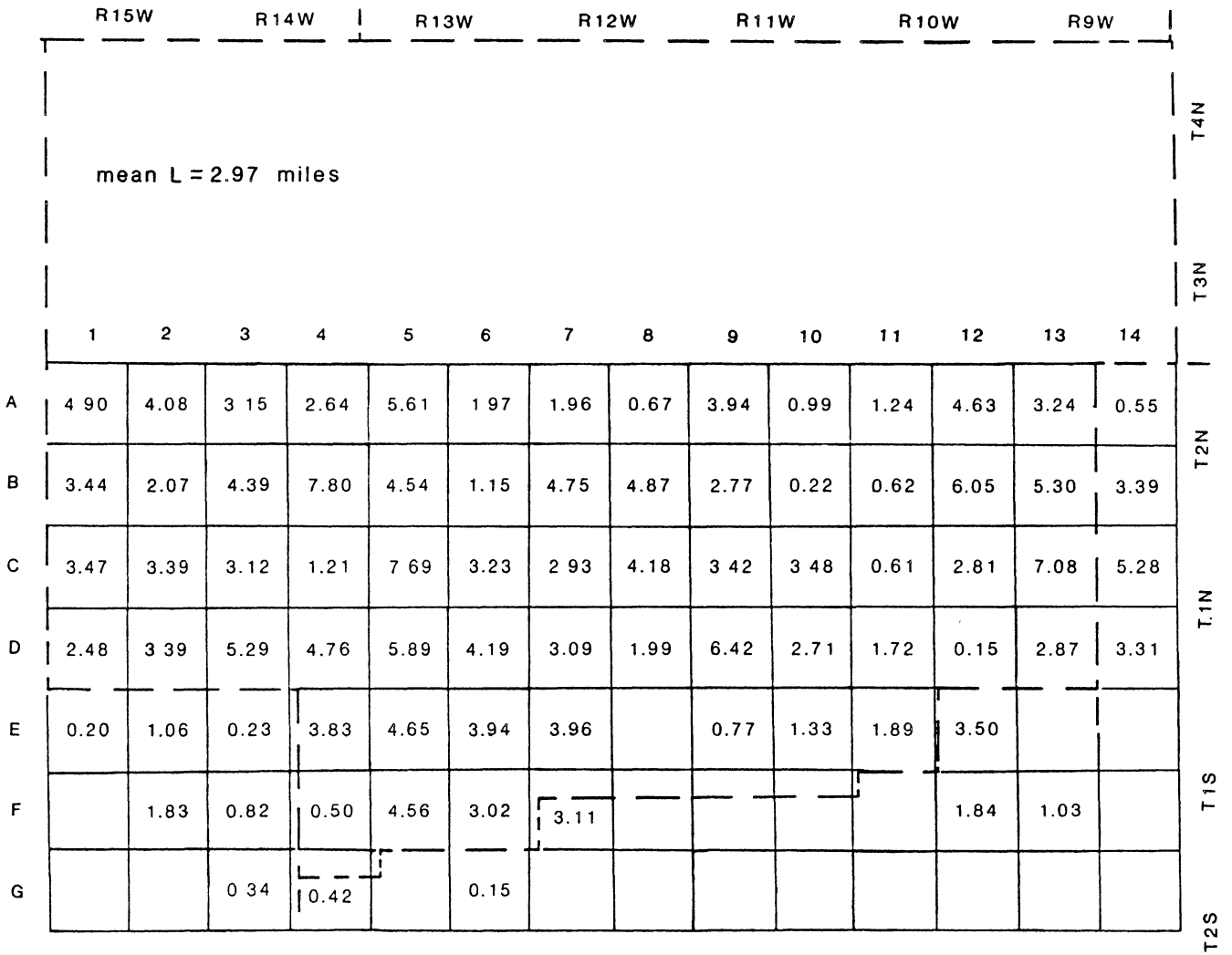

Figure 68. Sum of Lineament Lengths per Cell

TABLE XIX

CALCULATIONS OF PERMEABILITY AND YIELD OF POST OAK AND ARBUCKLE GROUP AQUIFERS FROM SUM OF LINEAMENT LENGTHS FOR CELL B-12

For entire grid, mean sum, $\overline{L}$, = 2.97 miles.
For cell B-12, sum of lineament lengths, L, = 6.05 miles (Figure 69).

Arbuckle Aquifer: Mean permeability, $\overline{K}$, = 3.5 gpd/ft^2

Permeability, $K = \frac{L}{\overline{L}} \times \overline{K} = \frac{6.05}{2.97} \times 3.5 = 7.13$ gpd/ft^2 (Significant figures were carried through the calculations.)

Average effective aquifer thickness, b, = 500 ft
Average well radius, r_w, = 0.28 ft
Average pumping period, t, = 5000 min
Average drawdown, s, = 350 ft
Storativity, S, = 0.0001

$$\text{Yield, } Q, = \frac{Kbs}{264 \log \left(\frac{Kbt}{2693\, r_w^2\, S} \right) - 65.5}$$

$$= \frac{7.13\ (500)\ (350)}{264 \log \left(\frac{7.13(500)\ (5000)}{2693\ (0.28)^2 (0.0001)} \right) - 65.5} = 545 \text{ gpm}$$

Post Oak Aquifer: Mean permeability, $\overline{K}$, = 800 gpd/ft^2

Permeability, $K = \frac{6.05}{2.97} \times 800 = 1630$ gpd/ft^2

Average aquifer (saturated) thickness, b, = 20 ft
Average well radius, r_w, = 0.35 ft
Average pumping period, t, = 660 min
Average drawdown, s, = 11 ft
Specific yield, Sy, = 0.02

$$\text{Yield, } Q, = \frac{1630\ (20)\ (11)}{264 \log \left(\frac{1630\ (20)\ (660)}{2693 (0.35)^2 (0.02)} \right) - 65.5} = 217 \text{ gpm}$$

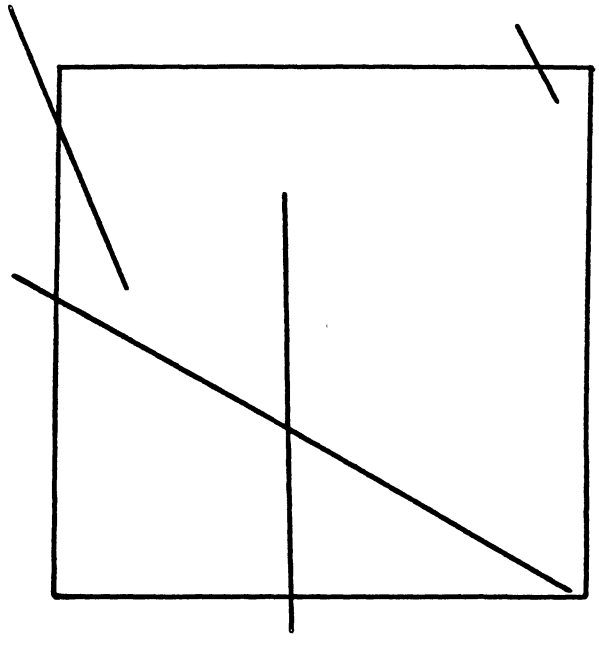

Figure 69. Cell B-12 with Lineaments

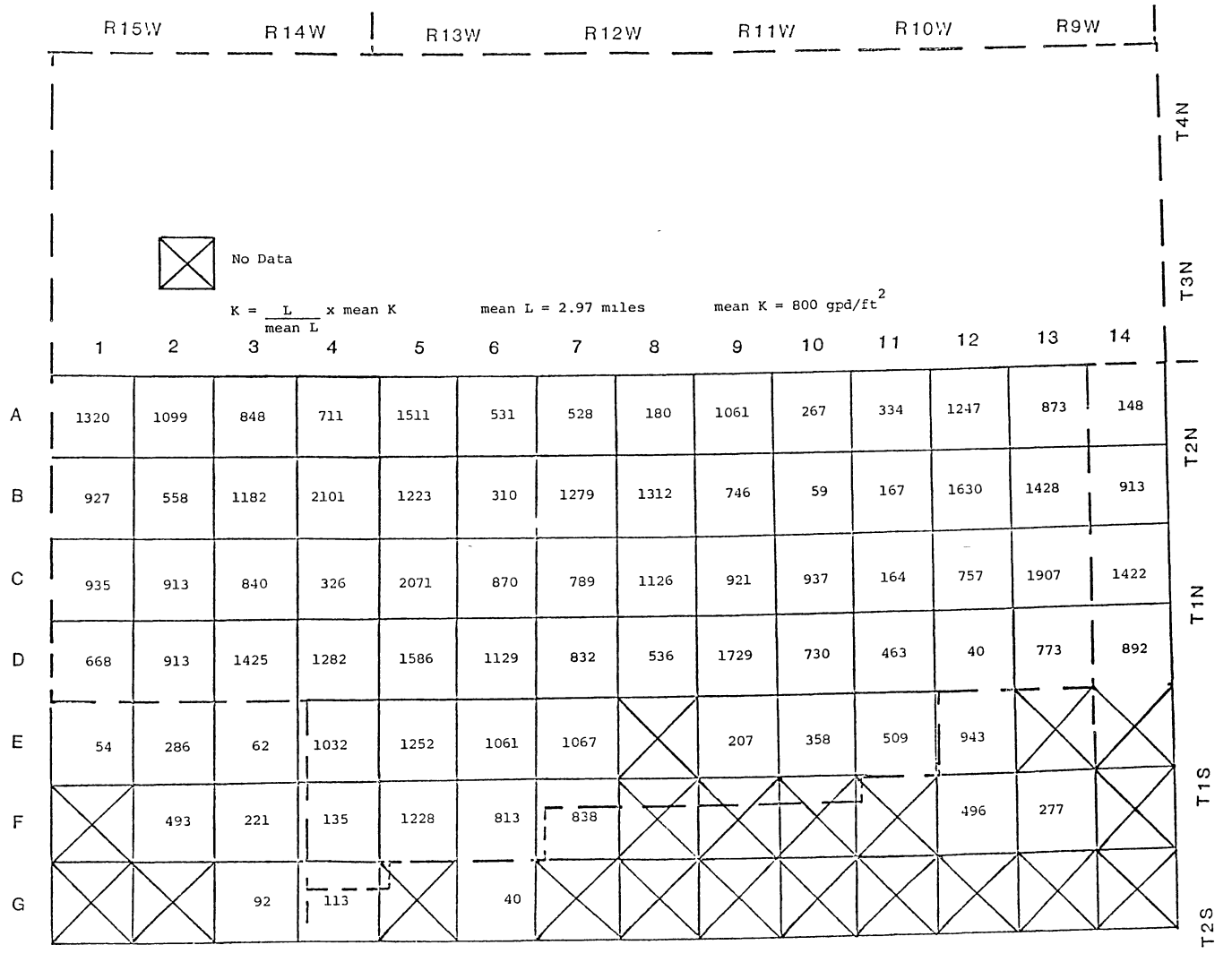

Figure 70. Permeabilities Calculated From Sum of Lineament Lengths per Cell for the Post Oak Aquifer

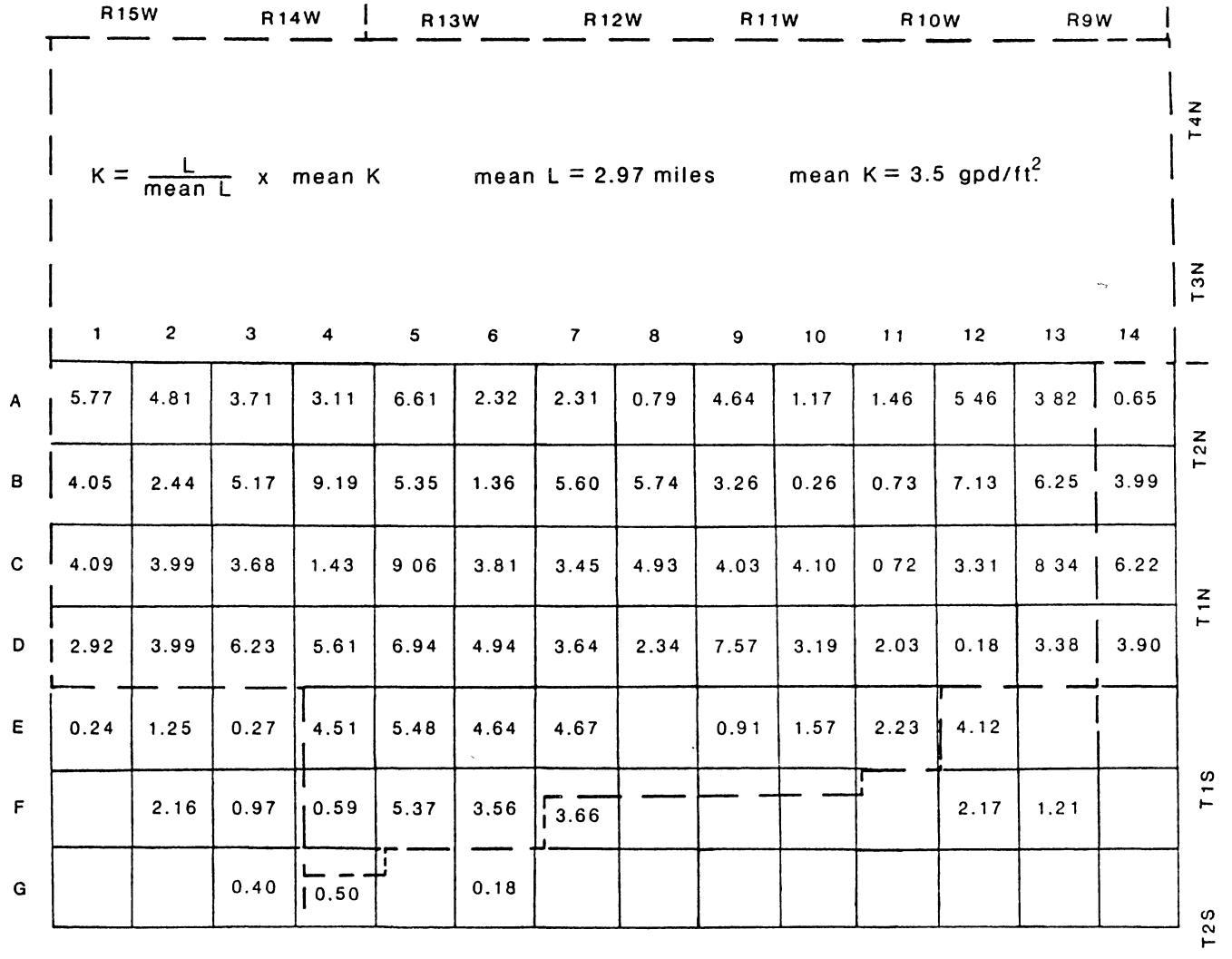

Figure 71. Permeabilities Calculated From Sum of Lineament Lengths per Cell for the Arbuckle Group Aquifer

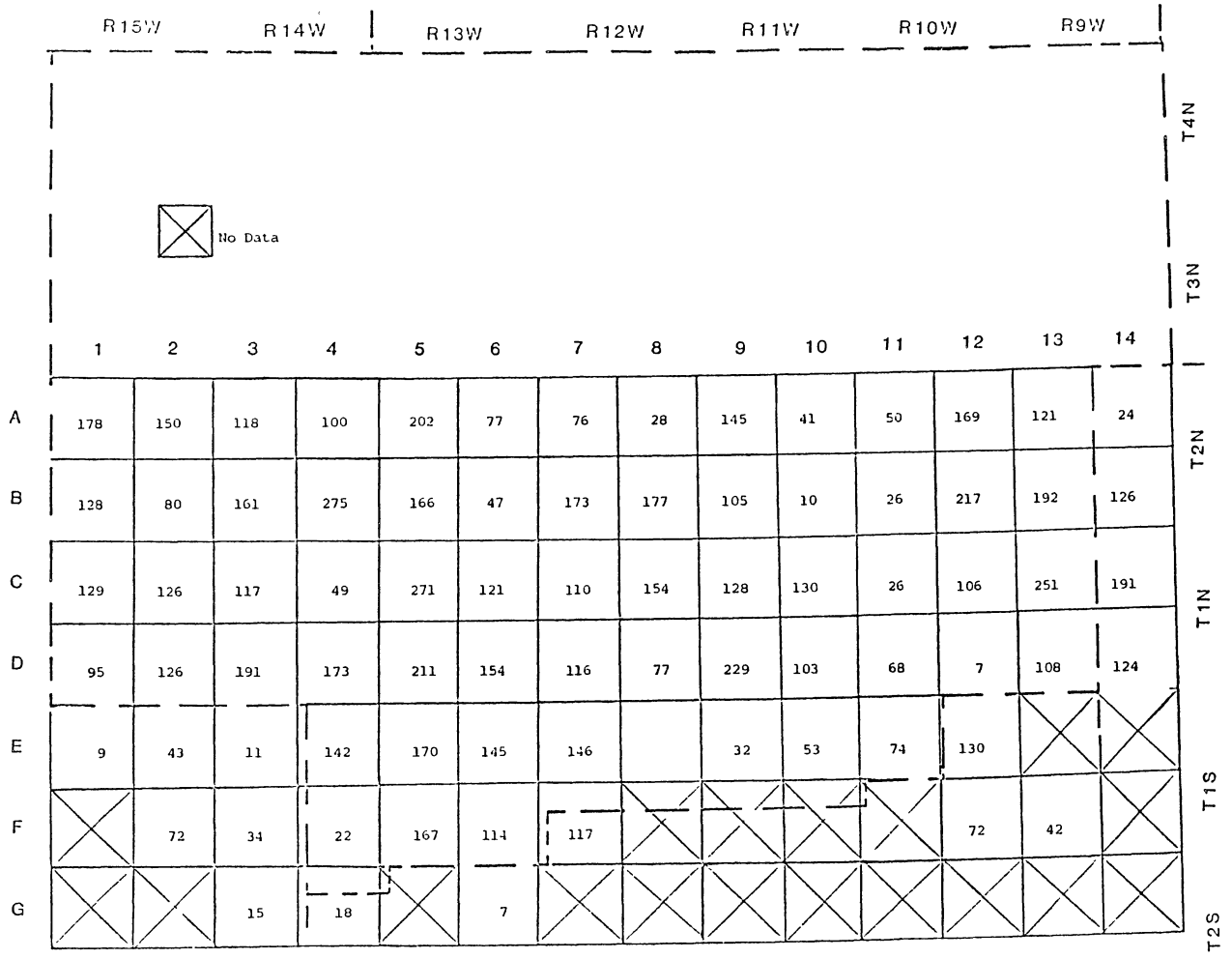

Figure 72. Yield Values Calculated From Sum of Lineament Lengths per Cell for the Post Oak Aquifer

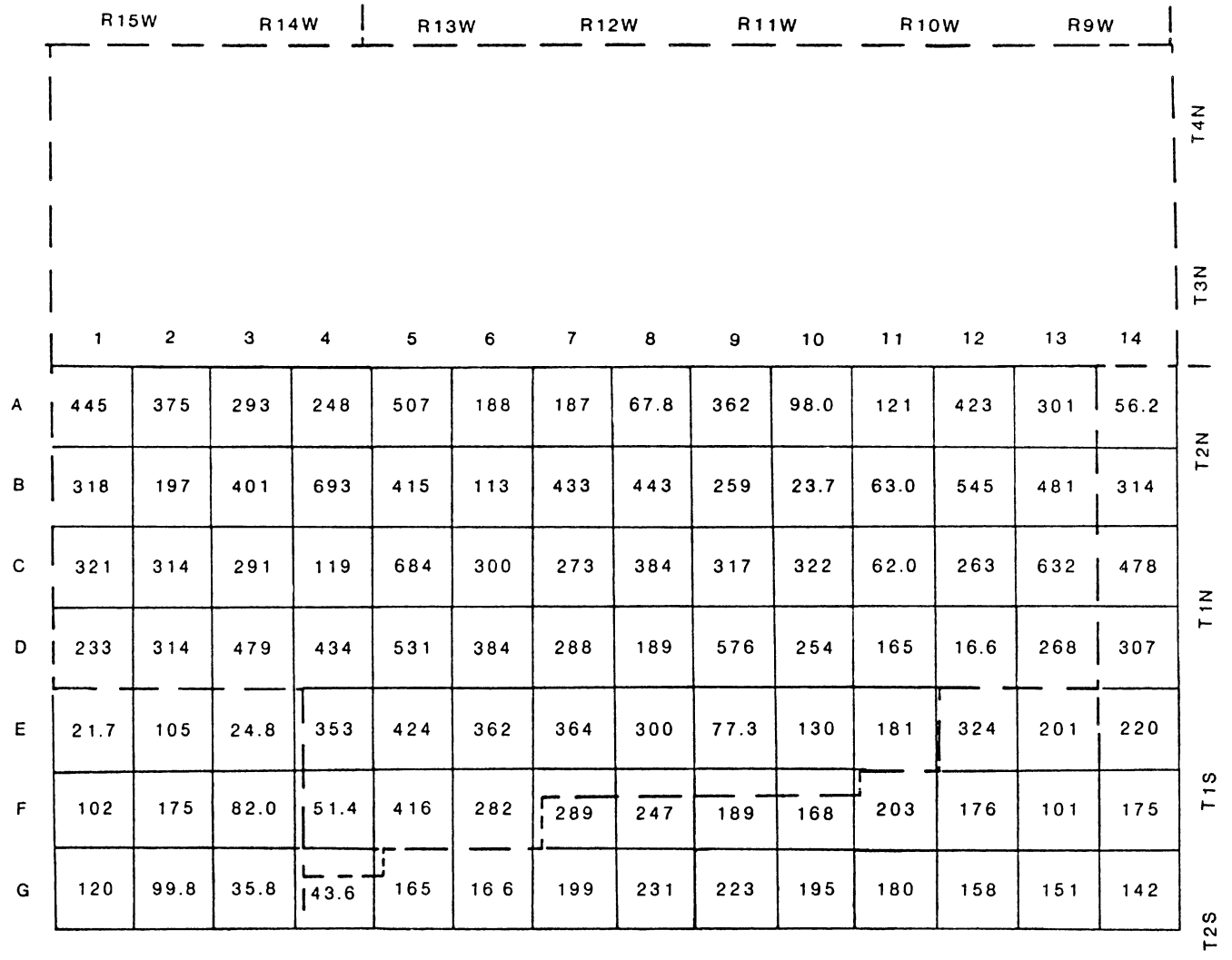

Figure 73. Yield Values Calculated From Sum of Lineament Lengths per Cell for the Arbuckle Group Aquifer

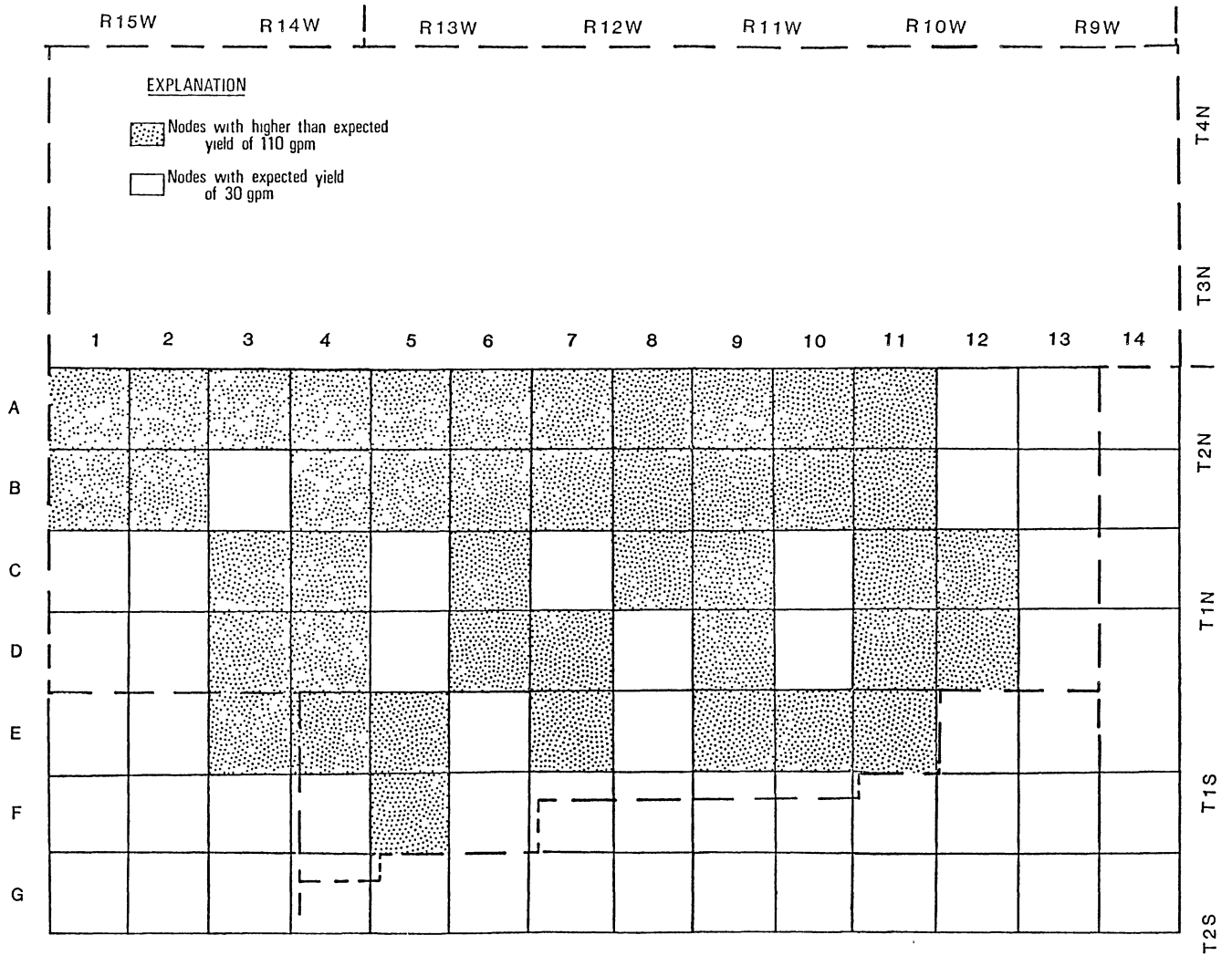

Figure 74. Expected Yield Map of the Post Oak Aquifer (Modified from Figure 30)

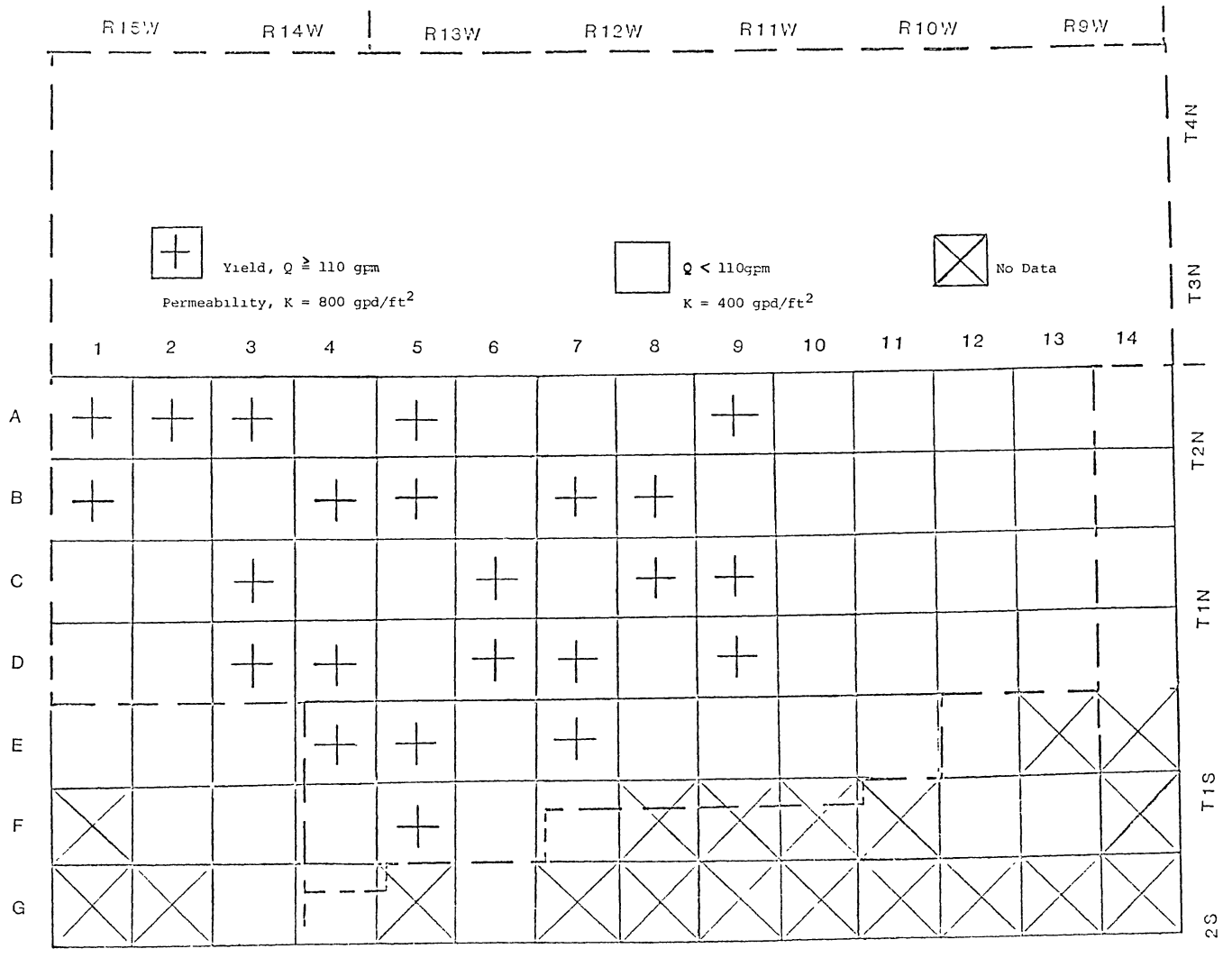

Figure 75. Expected Yield Map of the Post Oak Aquifer According to Grain-Size Distribution and Lineament Analysis

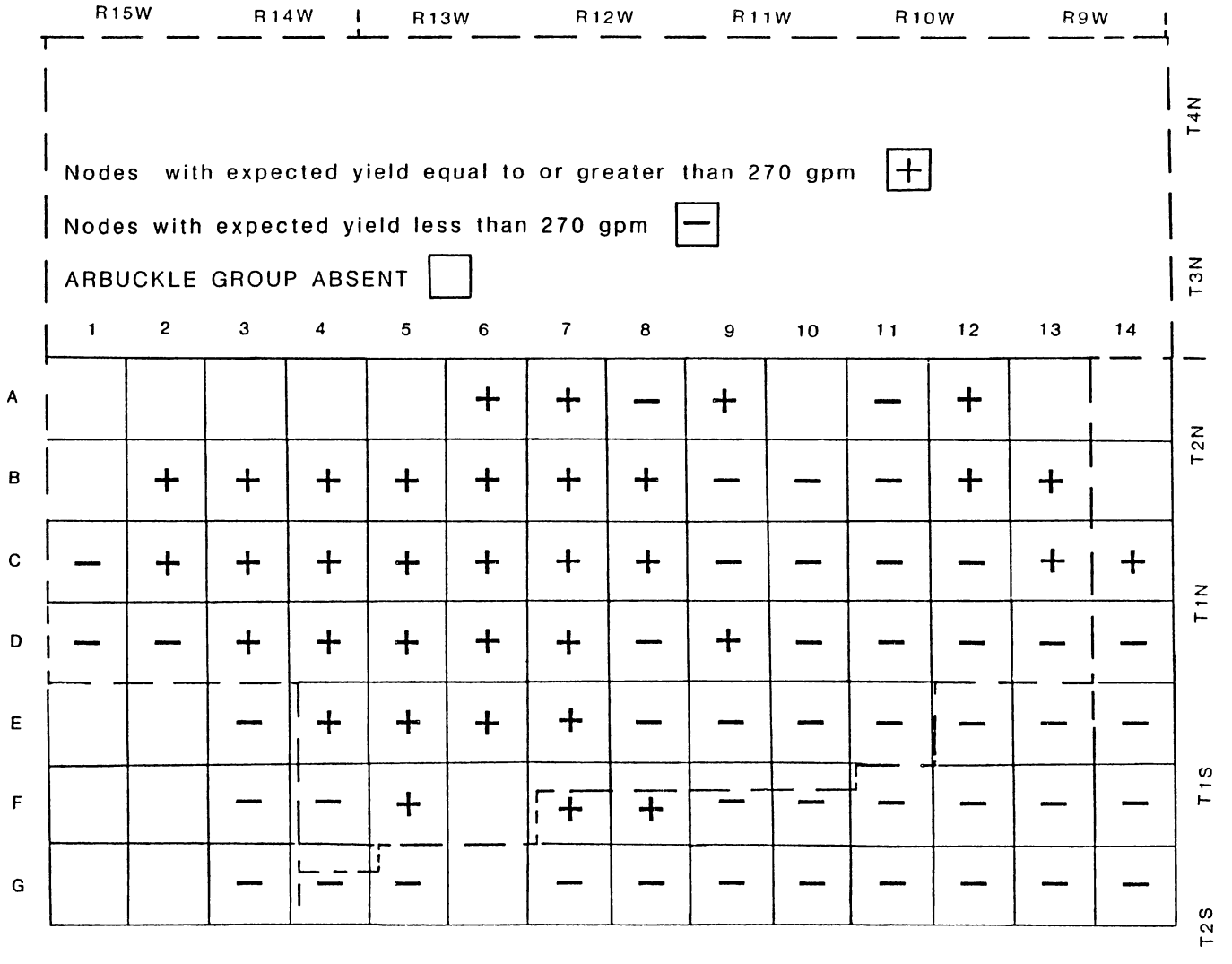

Figure 76. Average Expected Yield of the Arbuckle Group Aquifer Determined by Lineament Analysis

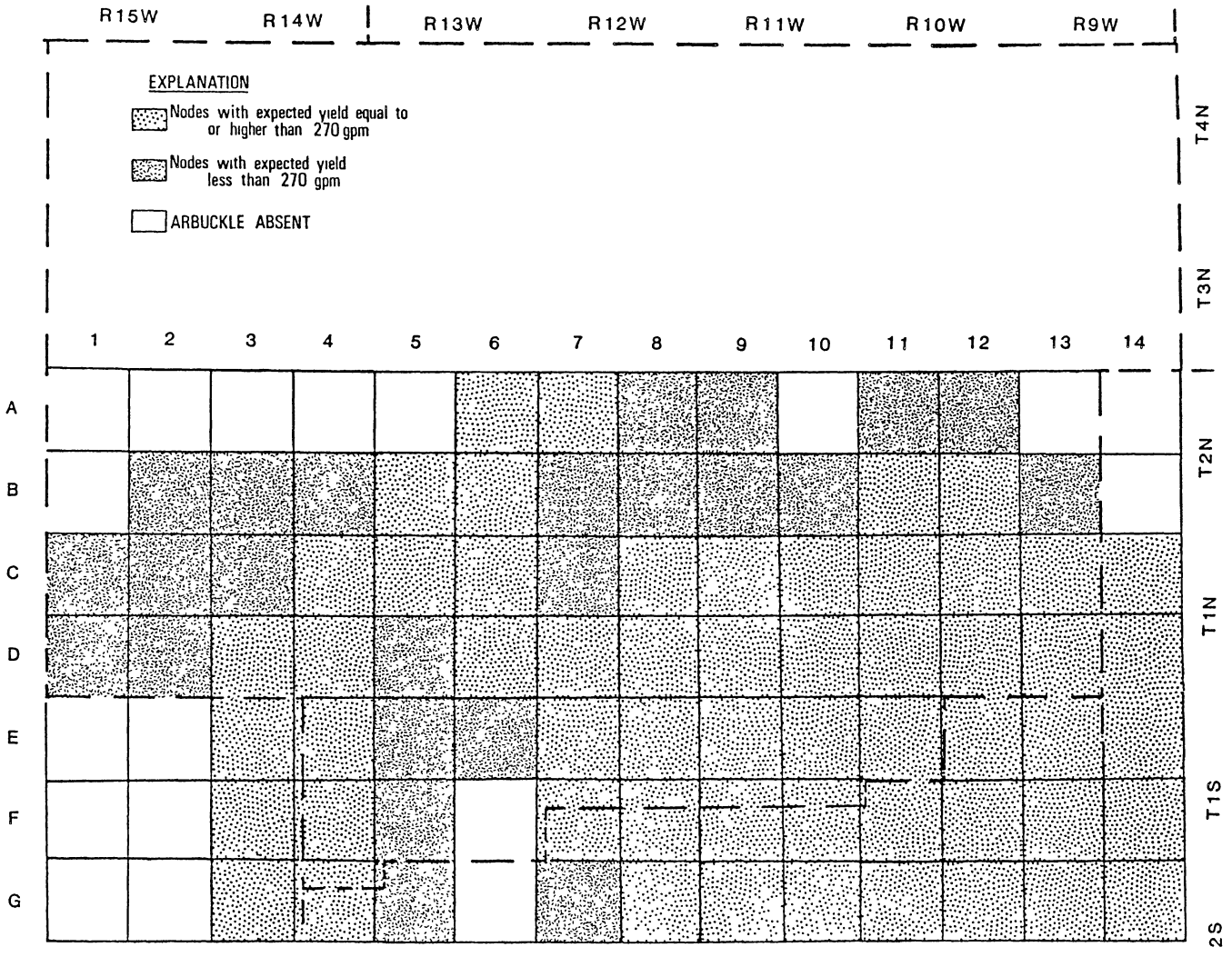

Figure 77. Expected Yield of the Arbuckle Group Aquifer Calculated From Well Data, Modified From Figure 47

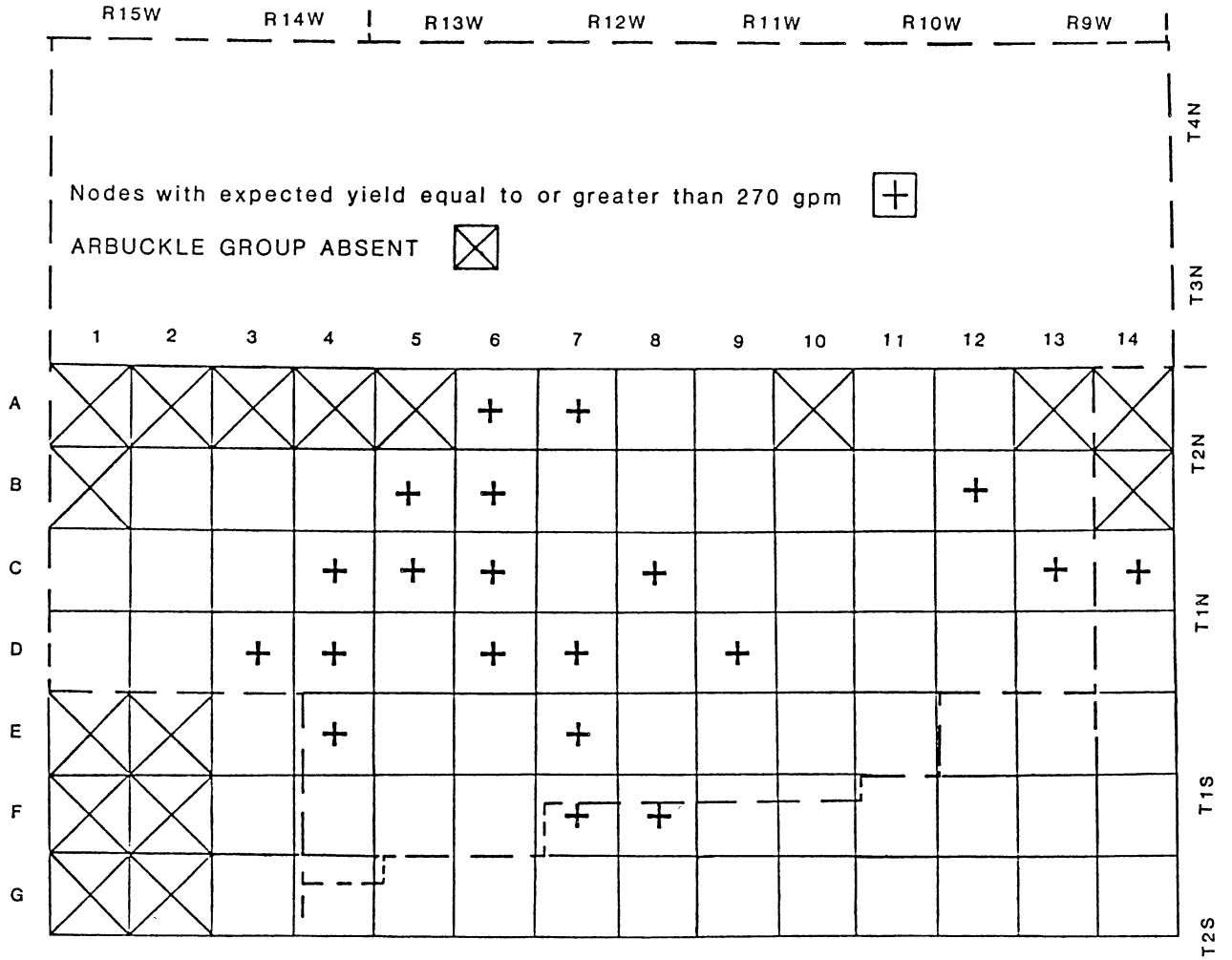

Figure 78. Average Expected Yield of the Arbuckle Group Aquifer According to Well Data and Lineament Analysis

APPENDIX H

KONIKOW MODEL DESCRIPTION

AND COMPUTER DATA

KONIKOW MODEL DESCRIPTION

The model used in this study was developed by Konikow and Bredehoeft (1978); it simulates solute transport in ground water by solving a solute transport equation and a ground-water flow equation. At each node in the model grid an iterative alternating-direction implicit procedure (ADIP) solves numerically an implicit finite-difference equation which approximates ground-water flow.

Tracy (1982) incorporated radioactive decay and equilibrium adsorption of the solute into the Konikow-Bredehoeft model. Kent and others (1986 a, b) made several modifications to the Tracy version. The Kent version includes both the ADIP and the strongly implicit procedure (SIP) to solve the ground-water flow equation and allows separate calibration of the hydraulics and solute transport parts of the model. The SIP requires fewer iterations and less computer time than the ADIP for the calculation of more complex aquifer characteristics (Wang and Anderson, 1982, pp.103, 106, 107, and 111). Kent and others (1986b) also added an interactive (i.e., prompting) preprocessor program to facilitate input of data into the model.

The model required a grid with at most 20 rows and 20 columns of nodes including a frame of outer nodes representing a no-flow boundary; variables at these nodes were assigned values of zero. For this study the model grid contained 17 columns and nine rows of nodes which were located at the centers of three-mile-square cells (Figure 79). The simulation area was 15 columns and seven rows of cells for a total

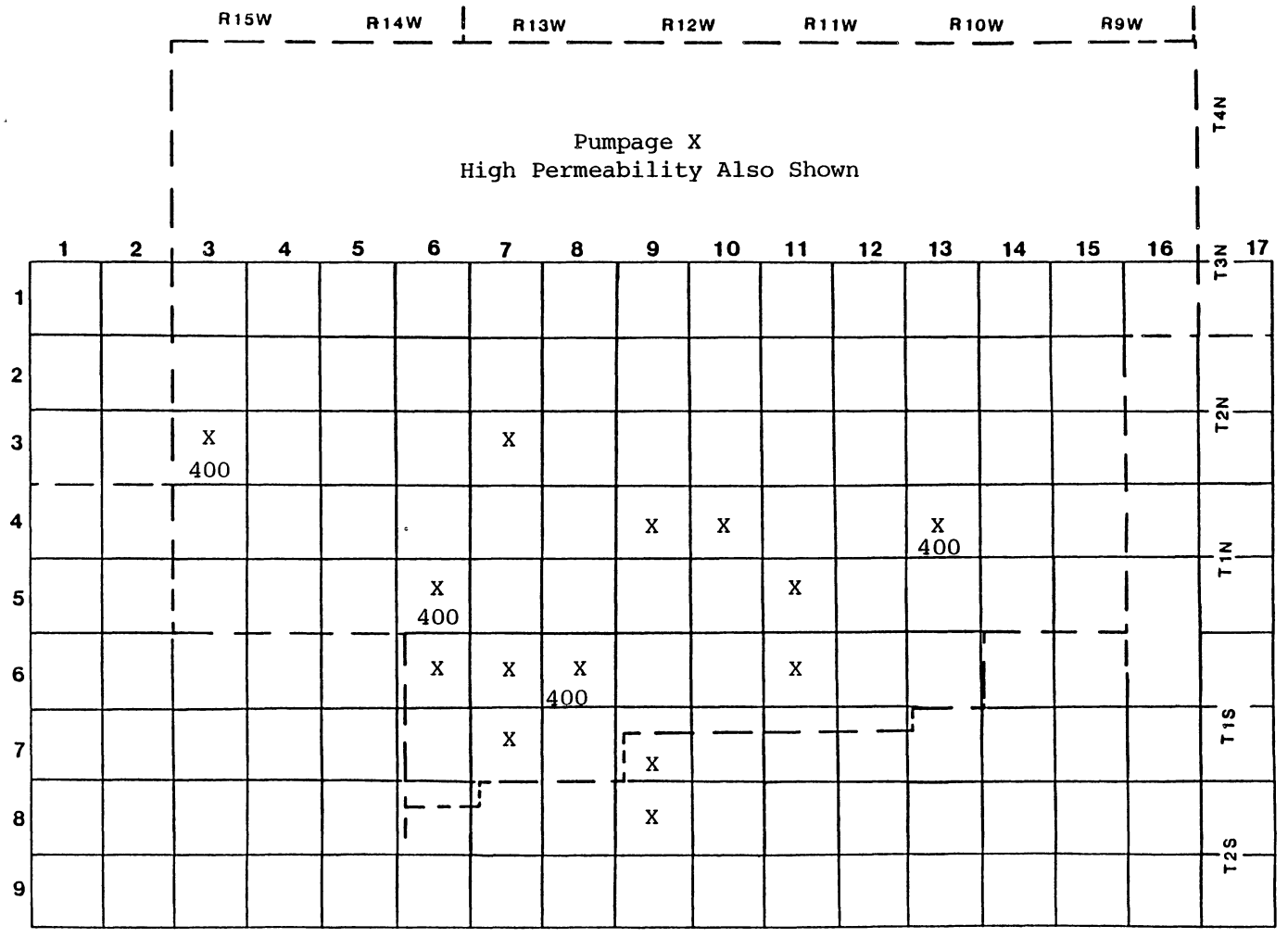

Figure 79. Computer Model Grid, Location of Pumpage, and Location of Pumping Nodes of Greater Permeability

aquifer area of 105 cells, or 945 square miles. The large size of the modelled area and the sparseness of the data required the large cell size.

The grid was entered into the model through the following variables:

NX, number of columns,

NY, number of rows,

XDEL, length of cell in feet, and

YDEL, width of cell in feet.

Thus, for this model

NX = 17,

NY = 9,

XDEL = 15,840 ft, and

YDEL = 15,840 ft.

The total length of the simulation was twenty, one-year pumping periods each containing four time steps. During each time step the model calculates new water-table and transmissivity values in response to recharge, discharge, pumpage, or injection. For these calculations a maximum of 100 iterations was allowed for the model to converge within an error of 0.01 ft. The simulation length was 20 years because the maximum annual yield of a ground-water basin is based on a minimum basin life of 20 years according to the Oklahoma Ground Water Act (Oklahoma Water Resources Board, 1985, p.8).

These data were described by the following variables:

NPMP, number of pumping periods = 20,

NTIM, maximum number of time steps per pumping period = 4,

PINT, length of pumping period = 1 year,

ITMAX, maximum allowable number of iterations = 100,

TINIT, size of initial time step = 7.9×10^6 seconds,

TIMX, time increment multiplier = 1.0,

TOL, convergence criteria for the flow equation = 0.01 ft.

The product of the initial time step length, TINIT, and the multiplier, TIMX, is the length of the next time step. This process ensures that the time steps are of equal length. The model lengthens or shortens the last time step, however, to accommodate the round-off error between the length of the pumping period measured in years and the sum of the time step lengths measured in seconds. The actual number of seconds in a year must be approximated to be entered into the model as an exponential real number.

During the calibration of the model, the simulations were one, five, or ten years long in order to correct errors and to make necessary adjustments to the input. The time step length was one year (3.1×10^7 s), and NTIM was set equal to two time steps per one-year pumping period in order to make the simulations more accurate. Calibration required adjusting the aquifer characteristics until inflow to the model by recharge balanced outflow by aquifer drainage as shown by minimal values of drawdown or mounding in the drawdown matrix. These characteristics included storage coefficient, permeability, potentiometric head, and recharge. Because the modelled aquifer is unconfined, the storage coefficient actually represented specific yield, and the potentiometric head represented water-table elevation. The model was not stressed by pumpage during the calibration.

Changing the specific yield opened or closed the aquifer to flow. This aquifer characteristic was set at 0.3, a high value, for the

entire grid in order to increase the flow through the aquifer and to make the aquifer less sensitive to adjustments in permeability. More realistic values of specific yield were entered when pumpage was established in the model.

Effective porosity was set at 0.25, a high value for the sediments of the Post Oak Aquifer, to reflect the high value of specific yield. Porosity affects the velocity of flow which is important only for a chemical transport simulation, so it was not changed for the later simulations.

Adjustments to permeability also affected the flow through the aquifer, although these changes did not significantly affect the inflow-outflow balance because of the high value of specific yield. Permeability was entered into the preprocessor program in units of gallons per day per square foot (gpd/ft^2); a multiplier converted these values to units of feet per second (ft/s) for the simulation. Integer values of permeability were entered (nnn), but the model required real numbers and inserted a decimal before the last digit (nn.n). Increasing the multiplier by an order of magnitude compensated for the change in format and allowed correct transmissivity calculations.

Permeability values for the Post Oak Aquifer were determined from lithologic well logs (Table VII, Appendix C) and the grain-size-permeability relationship (Figure 54) as described previously (Appendix C). The areal distribution of permeability established in the model followed the grain size dispersal pattern of Stone (1977; Figures 26 and 27). The original permeability values and their distribution were modified to facilitate flow through the model; the values determined previously were 800 gpd/ft^2 for the channel areas and 200 gpd/ft^2

outside the channels. The higher permeability had to be reduced to 400 gpd/ft^2 for the simulation because a low-permeability cell would act as a barrier to flow from a high-permeability cell because of the contrast between the former values.

Since water flows only across the face of a cell and not diagonally, it was difficult to duplicate exactly the geometry of the channels. Thus, it was necessary to straighten the channels in order to drain the aquifer and to prevent mounding against a low-permeability cell (Figure 80).

For the simulation the saturated thickness was a constant value for the entire grid. Twenty feet was the average saturated thickness as determined from well logs (Appendix B). The initial water-table elevation matrix was derived from Figure 36. During the calibration the gradient was smoothed and the matrix was modified to eliminate "holes" where water would accumulate as a mound and "hills" where water would drain and excessive drawdown would occur (Figure 81).

The characteristics of the alluvial aquifer were not included in the simulation because of the sizes of the cells and the modelled area. The creek valleys are narrow compared to the three-mile width of the cells. The calculated transmissivities of the alluvium and the Post Oak Aquifer were equal, however. The alluvium valleys drain the actual Post Oak Aquifer; similarly the high-permeability channels drain the modelled aquifer.

In order to account for greater flow into the aquifer at nodes with higher permeabilities, the node identification (NODEID) matrix replaced the constant recharge input (Figure 82). The boundary conditions were modified to allow recharge in the form of underflow from the

PERMEABILITY MAP FOR MODEL, gpd/ft^2

X	1	2	3	4	5	6	7	8	9	10	11	12	13	14	15	16	17
Y 1	0	0	0	0	0	0	0	0	0	0	0	0	0	0	0	0	0
2	0	400	400	400	400	400	400	400	400	400	400	400	400	200	200	200	0
3	0	200	400	400	400	400	200	400	400	400	200	400	400	200	200	200	0
4	0	200	200	200	400	400	200	400	200	200	200	200	400	200	200	200	0
5	0	200	200	200	400	400	200	400	200	200	200	200	400	200	200	200	0
6	0	200	200	200	400	200	200	400	200	200	200	200	400	200	200	200	0
7	0	200	200	200	400	200	200	400	200	200	200	200	400	200	200	200	0
8	0	200	200	200	400	200	200	400	200	200	200	200	400	200	200	200	0
9	0	0	0	0	0	0	0	0	0	0	0	0	0	0	0	0	0

Figure 80. Permeability Map for Model

WATER-TABLE ELEVATIONS FOR MODEL, ft.

X	1	2	3	4	5	6	7	8	9	10	11	12	13	14	15	16	17
Y 1	0	0	0	0	0	0	0	0	0	0	0	0	0	0	0	0	0
2	0	1350	1325	1314	1273	1237	1202	1170	1121	1110	1125	1135	1145	1150	1160	1170	0
3	0	1313	1307	1283	1253	1221	1193	1168	1119	1095	1120	1130	1140	1145	1155	1160	0
4	0	1261	1257	1245	1211	1192	1183	1165	1118	1080	1088	1110	1116	1125	1130	1135	0
5	0	1220	1209	1200	1187	1173	1170	1150	1116	1067	1060	1066	1067	1060	1050	1040	0
6	0	1190	1185	1181	1172	1151	1133	1125	1109	1060	1046	1035	1028	1027	1009	987	0
7	0	1179	1174	1167	1150	1121	1094	1075	1062	1052	1031	1020	1010	1000	990	980	0
8	0	1170	1160	1155	1136	1103	1075	1053	1036	1020	1010	1005	1000	990	980	975	0
9	0	0	0	0	0	0	0	0	0	0	0	0	0	0	0	0	0

Figure 81. Water-Table Map for Model

northwest where the model area is not immediately adjacent to the Wichita Mountains. Also, it was assumed that direct runoff from the mountains recharged the aquifer along the northern boundary. Underflow is horizontal flow due to the gradient from outside the aquifer area into the aquifer. To prevent mounding at the nodes receiving underflow, water was discharged from those nodes to account for vertical throughflow and leakage to the underlying Arbuckle Aquifer.

X / Y	1	2	3	4	5	6	7	8	9	10	11	12	13	14	15	16	17
1	0	0	0	0	0	0	0	0	0	0	0	0	0	0	0	0	0
2	0	1	1	1	1	1	1	1	1	1	1	1	1	2	2	2	0
3	0	2	6	3	4	3	4	6	3	5	4	3	6	4	4	2	0
4	0	2	4	4	3	3	4	6	4	3	4	4	6	6	6	2	0
5	0	2	4	4	3	3	4	4	4	3	4	4	3	4	3	2	0
6	0	2	4	4	4	4	4	6	6	3	4	4	3	4	4	2	0
7	0	2	4	4	3	4	4	3	4	4	4	4	3	4	4	2	0
8	0	2	2	2	1	2	2	1	2	2	2	2	1	2	2	2	0
9	0	0	0	0	0	0	0	0	0	0	0	0	0	0	0	0	0

Figure 82. Node Identification (NODEID) Matrix

Each node in the NODEID matrix was assigned a code (ICODE(i)) representing values of recharge, discharge, or underflow. Similar to the other matrices in the model, the outer nodes of the NODEID matrix

were assigned values of zero. The nodes within this outer frame were designated as constant-head boundaries through the leakance coefficient, the ratio of permeability to saturated thickness. In the model this coefficient is the variable FCTR1(i). At these boundaries the model maintains a constant head by maintaining a constant flow into or out of the aquifer according to the assigned leakance. The recharge variable is FCTR3(i), a positive value for discharge and a negative value for recharge. The FCTR3 values replace the zero recharge values at nodes designated with the OVERRD(i) variable. A concentration for an ICODE is entered as FCTR2(i), but this variable is used only in a solute-transport simulation. For boundary nodes with a permeability of 400 gpd/ft^2 the NODEID variables were the following:

ICODE(1) = 1,

$$\text{FCTR1(1)} = \frac{400 \text{ gpd/ft}^2}{20 \text{ ft}} = 3.095 \times 10^{-5} \text{ ft}^2/\text{s},$$

FCTR3(1) = 0.125 in/yr = 3.303×10^{-10} ft/s,

OVERRD(1) = 1.

The NODEID variables for the other boundary nodes are in Table XX. For the nodes within the matrix it was necessary to have four additional codes to control discharge from nodes where excessive mounding occurred and recharge where drawdown occurred. ICODE(3) and ICODE(5) remove water, and ICODE(4) and ICODE(6) add water; the locations of these codes (Figure 82) do not necessarily correlate with the distribution of permeability (Figure 80). The recharge and discharge in the NODEID matrix compensate for mounding and drawdown resulting from the water table and permeability matrices.

Pumpage was established in the model following calibration according to data from the Oklahoma Water Use Data System (OWUDS) of the

TABLE XX

CODES AND VARIABLES IN NODE IDENTIFICATION MATRIX

ICODE(i)	FCTR1(i) $ft^2/s \times 10^E$	FCTR3(i) $ft/s \times 10^E$	OVERRD(i)
1	3.0947 E -5	3.3031 E -10	1
2	1.5473 -5	-3.3031 -10	1
3	0.0	3.3031 -10	1
4	0.0	-3.3031 -10	1
5	0.0	1.0570 -9	1
6	0.0	-1.0570 -9	1

$gpd/ft^2 \times 1.54734 \times 10^{-6} = ft/s$

$in/yr \times 2.6425 \times 10^{-9} = ft/s$

$\frac{400}{20}\ ft\ gpd/ft^2 = 3.09467 \times 10^{-5}\ ft^2/s$

$\frac{200}{20}\ ft\ gpd/ft^2 = 1.54734 \times 10^{-5}\ ft^2/s$

$0.125\ in/yr = 3.3031 \times 10^{-10}\ ft/s$

$0.40\ in/yr = 1.0570 \times 10^{-9}\ ft/s$

Oklahoma Water Resources Board (1984). The OWUDS lists water use requiring a permit: irrigation, public supply, industrial use, and mining. Domestic use requires no permit and is not included in the data system. Pumpage from the Post Oak Aquifer for non-domestic use is not extensive; wells in the alluvial aquifer are more common.

For the simulation, wells tapping both aquifers and wells located close to but outside of the grid were placed in the model in order to stress the aquifer. For example, the Brewer well in T 3 N, R 15 W, section 31, was relocated south to node 3,3, and the Comanche Rural Water District #3 wells were moved north from T 2 S, R 12 W, sections 28 and 29, to node 13,4 within that rural water district. The Doye, Geronimo, Kinder, and Jinings wells are in the alluvial aquifer but were added to those in the Post Oak Aquifer.

The discharge assigned to a node was the 1984 water use at a well. Discharge from a node in a cell containing several wells represented the sum of the reported pumpages from each well. To assign discharge to eight wells for which no water use was recorded, the irrigation pumpage from wells not in the Post Oak or alluvial aquifers in Comanche County was divided among the seven cells containing the wells (Table XXI). An equivalent discharge was later assigned to an eighth node, the Hudman well which was relocated from Cotton County, T 2 S, R 12 W, section 6, to node 9,8. The variables pertaining to pumpage from the model are well number, NREC, location, IX and IY, and discharge or injection rate, REC.

This version of the model allowed specific yield to be entered only as a constant for the entire grid. According to the specific yield-permeability relationship (Figure 32), the specific yield corres-

TABLE XXI

1984 WATER USE IN COMANCHE COUNTY

Variable Name	NREC	Location K of Node IX	IY	Owner	Use	Af/yr	10^6 Gal/yr	Ft^3/s REC
	1	3	3*	Brewer	I	3('83)	0.98	0.004144
		400 gpd/ft^2						
	2	6	5	Szatkowski	I	0		0.068551
		400						
	3	6	6	McCollum	I	436	142	0.602237
		200		CKT	S	229	74.6	0.316313
				Total		665	216.7	0.918550
	4	7	3	Funderburg	I	28.7	9.35	0.039643
		200		Rowe	I	0		
	5	7	6	Peters	I	15	4.89	0.020719
		200						
	6	7	7	Kinder	I	0		
		200		Jinings	I	0		
								0.068551
	7	8	6	Carter	I	0		0.068551
		400						
	8	9	4	SW Bell	I	0		0.068551
		200						
	9	9	7	Hensley	I	0		0.068551
		200						
	10	9	8	Hudman	I	0		0.068551
		200						
	11	10	4	Kelsey	I	0		0.068551
		200						
	12	11	5	Doye	I	0		0.068551
		200						
	13	11	6	Geronimo	S		23.9	0.101488
		200						
	14	13	4*	Comanche	S		37.8	0.160468
		400		RWD 3				

I: irrigation S: municipal supply * relocated Af: acre-foot

Non-Post Oak, non-alluvium pumpage = 347.4 af

Number of Post Oak wells with no 1984 pumpage = 7

Assumed pumpage from well = $\frac{347.4 \text{ af}}{7 \text{ wells}}$ = 0.068551 ft^3/s

ponding to a permeability of 400 gpd/ft^2 is 0.279 and that corresponding to 200 gpd/ft^2 permeability is 0.255. To achieve the same effect as a specific yield matrix, with different values corresponding to the different permeabilities, only the more permeable nodes were pumped in simulations with the higher specific yield (Figure 79). With input of the lower specific yield, only the less permeable nodes were pumped.

Various pumpages were established in the calibrated simulations in order to stress the aquifer. These simulations were designated according to the amount of pumpage, Q, and the permeability, K, of the nodes which were pumped (Table XXII). Thus, simulation QA-KL used actual (A) pumpage from the nodes of lower (L) permeability, and simulation QM-KH had maximum (M) pumpage from the nodes of higher (H) permeability.

TABLE XXII

DESIGNATION OF SIMULATIONS

QA:	actual pumpage
QM:	maximum pumpage
QX:	10 x (actual pumpage), Sy = 0.3
QO:	no pumpage
KH:	high permeability nodes are pumped
KL:	low permeability nodes are pumped

Pumpage according to the actual and assumed water use (QA simulations) did not produce significant drawdowns (Figures 83 and 84).

X / Y	1	2	3	4	5	6	7	8	9	10	11	12	13	14	15	16	17
1	0	0	0	0	0	0	0	0	0	0	0	0	0	0	0	0	0
2	0	0	0	0	0	0	0	0	0	0	0	0	0	0	0	0	0
3	0	0	1w	1	2	1	0	1	-1	-1	1	1	0	0	1	0	0
4	0	0	0	1	0	-1	0	1	-1	-1	-1	1	1w	1	1	0	0
5	0	0	-1	-1	0	0w	2	1	0	-1	-1	0	0	-1	0	0	0
6	0	0	0	0	1	0	0	1w	1	0	0	-1	-1	0	-1	0	0
7	0	0	0	0	1	-1	-1	-1	-1	1	0	0	0	-1	0	0	0
8	0	0	0	0	0	0	0	0	0	0	0	0	0	0	0	0	0
9	0	0	0	0	0	0	0	0	0	0	0	0	0	0	0	0	0

(+) drawdown, ft (-) mounding, ft w: well (pumping node)

Figure 83. Drawdown Matrix for QA-KH Simulation (Actual Pumpage from High-Permeability Nodes).

X / Y	1	2	3	4	5	6	7	8	9	10	11	12	13	14	15	16	17
1	0	0	0	0	0	0	0	0	0	0	0	0	0	0	0	0	0
2	0	0	0	0	0	0	0	0	0	0	0	0	0	0	0	0	0
3	0	0	1	1	2	1	0w	1	-1	-2	2	1	0	0	1	0	0
4	0	0	0	1	0	-1	0	1	0w	-1w	-1	1	0	1	1	0	0
5	0	0	-1	-1	0	0	2	1	0	-1	-1w	0	0	-1	0	0	0
6	0	0	-1	0	1	7w	0w	1	1	0	0w	-1	-1	0	-1	0	0
7	0	0	0	0	1	-1	0w	-2	-1w	1	0	0	0	-1	0	0	0
8	0	0	0	0	0	0	0	0	0w	0	0	0	0	0	0	0	0
9	0	0	0	0	0	0	0	0	0	0	0	0	0	0	0	0	0

(+) drawdown, ft (-) mounding, ft w: well (pumping node)

Figure 84. Drawdown Matrix for QA-KL Simulation (Actual Pumpage from Low-Permeability Nodes).

Discharges an order of magnitude greater than the actual pumpage did not produce large drawdowns from the nodes of high permeability (Figure 85), but this pumpage overstressed the lower permeability nodes (Figure 86). Nodes 5,6 and 6,5 drained in order to supply the discharge from node 6,6. The other nodes were not stressed. To determine the maximum allowable pumpages (Table XXIII), the discharges were increased to produce drawdowns of 14 ft, one foot above a five-foot well screen, at the pumping nodes. The non-pumping nodes did not drain significantly. The maximum pumpages ranged from 1.6 to 1.8 ft^3/s (720 to 810 gpm; 45 to 51 1/s) for nodes of both permeabilities. Non-pumping simulations exhibited mounding and slight drainage in the drawdown matrices (Figures 87 and 88).

Hydrographs of the wells in the QA-KL simulation (actual pumpage from low-permeability nodes) showed the steady drawdown that occurred in well #3, node 6,6 (Figure 89). The other wells experienced a constant rate of mounding of less than two feet, similar to that in well #5, over the 20-year simulation. Well #13 remained static. In the QA-KH simulation (actual pumpage from high-permeability nodes) the hydrographs of wells #1, #7, and #14 exhibited similar rates of drawdown (Figure 90), while well #2 experienced mounding of less than a foot. The higher pumpages of the QM simulations (maximum pumpages) produced uniform drawdown rates in all the wells (Figure 91).

Measures of the accuracy of the simulation are the mass balance residual and the percent error calculated after each time step. To achieve a mass balance the net flux, the sum of inflow and outflow, must equal the change in mass stored, or mass accumulation. The flux, Mf, is calculated from the recharge, pumpage, and leakage input; the

X / Y	1	2	3	4	5	6	7	8	9	10	11	12	13	14	15	16	17
1	0	0	0	0	0	0	0	0	0	0	0	0	0	0	0	0	0
2	0	0	0	0	0	0	0	0	0	0	0	0	0	0	0	0	0
3	0	0	1w	1	1	1	0	1	-1	-1	1	1	0	0	1	0	0
4	0	0	0	1	0	0	0	1	-1	-1	0	1	12w	1	1	0	0
5	0	0	-1	0	0	4w	2	1	0	-1	-1	0	1	-1	0	0	0
6	0	0	0	0	1	0	0	6	1	0	0	-1	-1	0	-1	0	0
7	0	0	0	0	1	-1	-1	-1	-1	1	0	0	0	-1	0	0	0
8	0	0	0	0	0	0	0	0	0	0	0	0	0	0	0	0	0
9	0	0	0	0	0	0	0	0	0	0	0	0	0	0	0	0	0

(+) drawdown, ft (-) mounding, ft w: well (pumping node)

Figure 85. Drawdown Matrix for QX-KH Simulation (10 x Actual Pumpage from High-Permeability Nodes; Specific Yield = 0.30).

X / Y	1	2	3	4	5	6	7	8	9	10	11	12	13	14	15	16	17
1	0	0	0	0	0	0	0	0	0	0	0	0	0	0	0	0	0
2	0	0	0	0	0	0	0	0	0	0	0	0	0	0	0	0	0
3	0	0	1	1	1	1	2w	1	-1	-1	1	1	0	0	1	0	0
4	0	0	0	1	0	1	0	1	3w	3w	0	1	0	0	1	0	0
5	0	0	-1	0	4	92	2	1	0	-1	3w	0	0	-1	0	0	0
6	0	0	0	0	120	-157 w	9w	1	1	0	8w	0	-1	0	-1	0	0
7	0	0	0	0	2	1	4w	-1	3w	1	0	0	0	-1	0	0	0
8	0	0	0	0	0	0	0	0	0w	0	0	0	0	0	0	0	0
9	0	0	0	0	0	0	0	0	0	0	0	0	0	0	0	0	0

(+) drawdown, ft (-) mounding, ft w: well (pumping node)

Figure 86. Drawdown Matrix for QX-KL Simulation (10 x Actual Pumpage from Low-Permeability Nodes; Specific Yield = 0.30).

mass accumulation, Δ Ms, is calculated through the storage coefficient or specific yield. The mass balance residual, Rm, is the difference between the net flux and the mass accumulation (Konikow and Bredehoeft, 1978, p.14):

$$Rm = \Delta \text{ Ms} - \text{Mf}.$$

The percent error, E, compares the mass balance residual with the average of the flux and mass accumulation:

$$E = \frac{100 \text{ Mf} - \Delta \text{ Ms})}{0.5 \text{ (Mf} + \Delta \text{ Ms)}} .$$

The mass balance residuals were less than 1.0×10^5 ft^3 compared with masses of 1.0×10^9 ft^3, and the errors were less than 0.01 percent for both calibrated and non-calibrated simulations.

The cumulative mass balance parameters indicate the gross response of the model to the recharge, pumpage, leakage, and storage input. According to these parameters, flow either into the aquifer or into storage is a negative mass balance, and flow out of the aquifer or storage is positive. The sum of recharge and pumpage is the cumulative net pumpage, which is negative if flow is into the aquifer. The water released from storage compensates for the cumulative net pumpage; water is added to storage (negative) if net pumpage adds water to the aquifer. Leakage into the aquifer is a negative mass balance, and leakage out of the aquifer is positive. A positive net recharge indicates flow from the aquifer.

Similar to the cumulative mass balances the recharge rate into the aquifer is negative, and pumpage out of the aquifer is positive. The sum of recharge and pumpage is the net withdrawal rate (TPUM). However, the leakage rate into the aquifer is positive, and the leakage rate out of the aquifer is negative. The net leakage rates (QNET) for

both the QA (actual pumpage) and QM (maximum pumpages) simulations were negative, indicating flow out of the the aquifer.

Differences in the four QA and QM simulations were evident in the cumulative mass balances (Tables XXIV and XXV). The cumulative recharge and cumulative leakage and the recharge and leakage rates were equal for all four simulations. In the KH simulations (pumpage from high-permeability nodes) the cumulative leakages out were greater than those for the KL simulations (pumpage from low-permeability nodes) because the total pumpages were less. To prevent mounding the model removed water by leakage. Thus, the cumulative net leakages were greater also.

In the QA simulations (actual pumpage) the cumulative net pumpages were negative: water was being added to the aquifer. With a negative cumulative net pumpage the release from storage becomes negative: water is added to storage. When pumpage was increased to produce maximum drawdowns in the QM simulations (maximum pumpage), the cumulative net pumpage became positive: water was being removed from the aquifer. When cumulative net pumpage becomes positive, water is released from storage (positive release) to compensate for the loss of water.

The two non-pumping simulations exhibited identical cumulative and rate mass balances except for slight differences in the cumulative net leakages, the leakage rates into the aquifer, and the net leakage rates. Pumpage appeared in the mass balance tables because water was removed by discharge (positive recharge) established by the NODEID matrix. Eliminating ICODE(3), ICODE(4), ICODE(5), and ICODE(6) from the NODEID matrix (Figure 92) and increasing the specific yield to 0.3 removed the pumpage from the mass balances. The drawdown matrix for

this simulation (Figure 93) differed by only one foot from the drawdown matrices of the non-pumping simulations with the lower specific yield values.

TABLE XXIII

MAXIMUM ALLOWABLE PUMPAGES

N	X	Y	Pumping Rate ft^3/s	gpm	Characteristics of Pumping Node Permeability gpd/ft^2	Specific Yield
1	3	3	1.70	760	400	0.279
2	6	5	1.80	810	400	0.279
3	6	6	1.70	760	200	0.255
4	7	3	1.70	760	200	0.255
5	7	6	1.60	720	200	0.255
6	7	7	1.70	760	200	0.255
7	8	6	1.80	810	400	0.279
8	9	4	1.70	760	200	0.255
9	9	7	1.80	810	200	0.255
10	9	8	1.60	720	200	0.255
11	10	4	1.70	760	200	0.255
12	11	5	1.80	810	200	0.255
13	11	6	1.60	720	200	0.255
14	13	4	1.80	810	400	0.279

$ft^3/s \times 450 = gpm$

Maximum pumpage produces drawdown of 14 ft.

X / Y	1	2	3	4	5	6	7	8	9	10	11	12	13	14	15	16	17
1	0	0	0	0	0	0	0	0	0	0	0	0	0	0	0	0	0
2	0	0	0	0	0	0	0	0	0	0	0	0	0	0	0	0	0
3	0	0	1	1	2	1	0	1	-1	-1	1	1	0	0	1	0	0
4	0	0	0	1	0	-1	0	1	-1	-1	-1	1	0	0	1	0	0
5	0	0	-1	-1	0	0	2	1	0	-1	-1	0	0	-1	0	0	0
6	0	0	0	0	1	0	0	1	1	0	0	-1	-1	0	-1	0	0
7	0	0	0	0	1	-1	-1	-1	-1	1	0	0	0	-1	0	0	0
8	0	0	0	0	0	0	0	0	0	0	0	0	0	0	0	0	0
9	0	0	0	0	0	0	0	0	0	0	0	0	0	0	0	0	0

(+) drawdown, ft (-) mounding, ft

Figure 87. Drawdown Matrix for QO-KH Simulation (No Pumpage; Specific Yield = 0.279).

X / Y	1	2	3	4	5	6	7	8	9	10	11	12	13	14	15	16	17
1	0	0	0	0	0	0	0	0	0	0	0	0	0	0	0	0	0
2	0	0	0	0	0	0	0	0	0	0	0	0	0	0	0	0	0
3	0	0	1	1	2	1	0	1	-1	-2	2	1	0	0	1	0	0
4	0	0	0	1	0	-1	0	1	-1	-2	-1	1	0	1	1	0	0
5	0	0	-1	-1	0	0	2	1	0	-1	-1	0	0	-1	0	0	0
6	0	0	-1	0	1	0	0	1	1	0	0	-1	-1	0	-1	0	0
7	0	0	0	0	1	-1	-1	-2	-1	1	0	0	0	-1	0	0	0
8	0	0	0	0	0	0	0	0	0	0	0	0	0	0	0	0	0
9	0	0	0	0	0	0	0	0	0	0	0	0	0	0	0	0	0

(+) drawdown, ft (-) mounding, ft

Figure 88. Drawdown Matrix for QO-KL Simulation (No Pumpage; Specific Yield = 0.255).

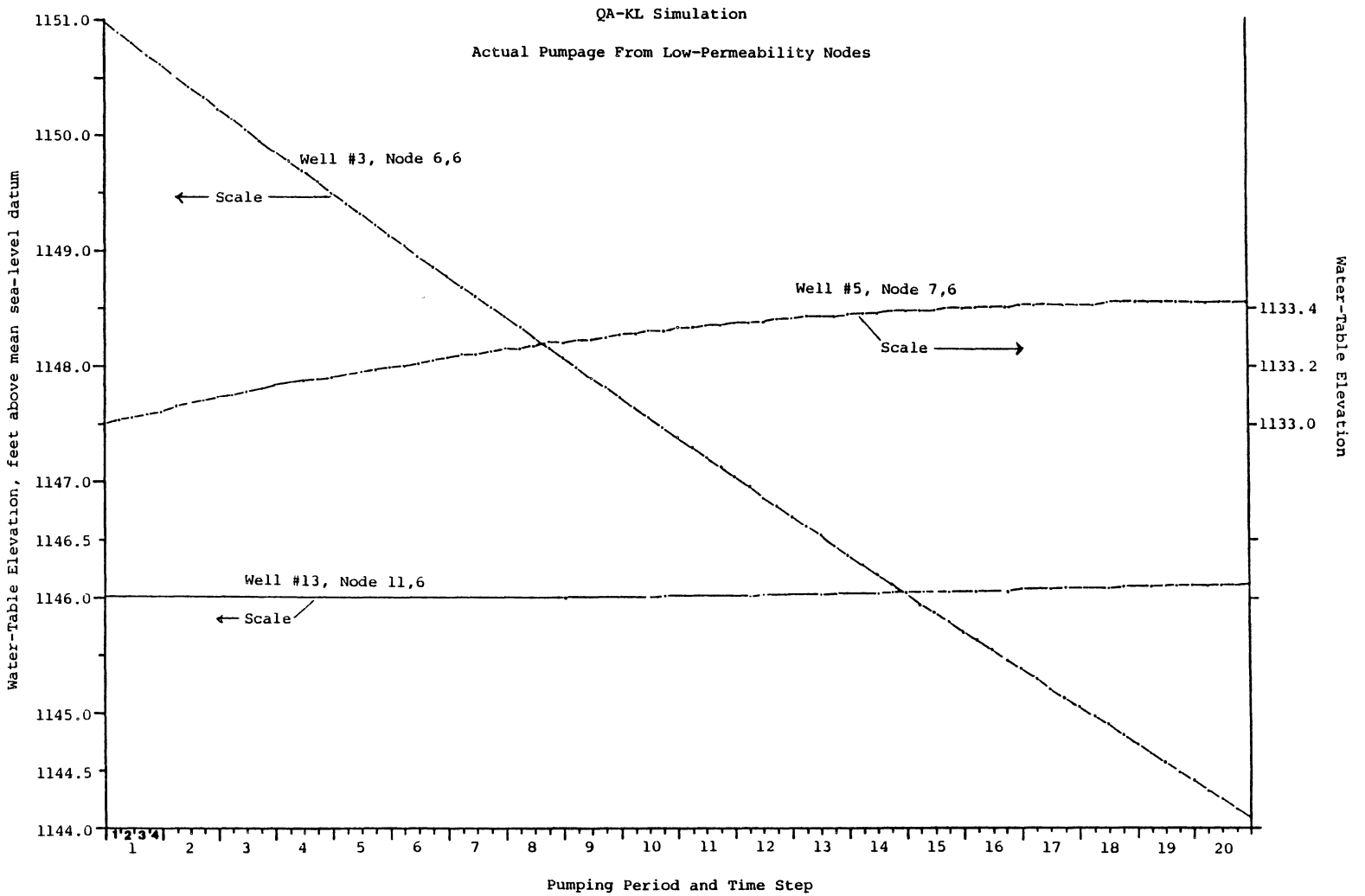

Figure 89. Well Hydrographs for QA-KL Simulation (Actual Pumpage from Low-Permeability Nodes)

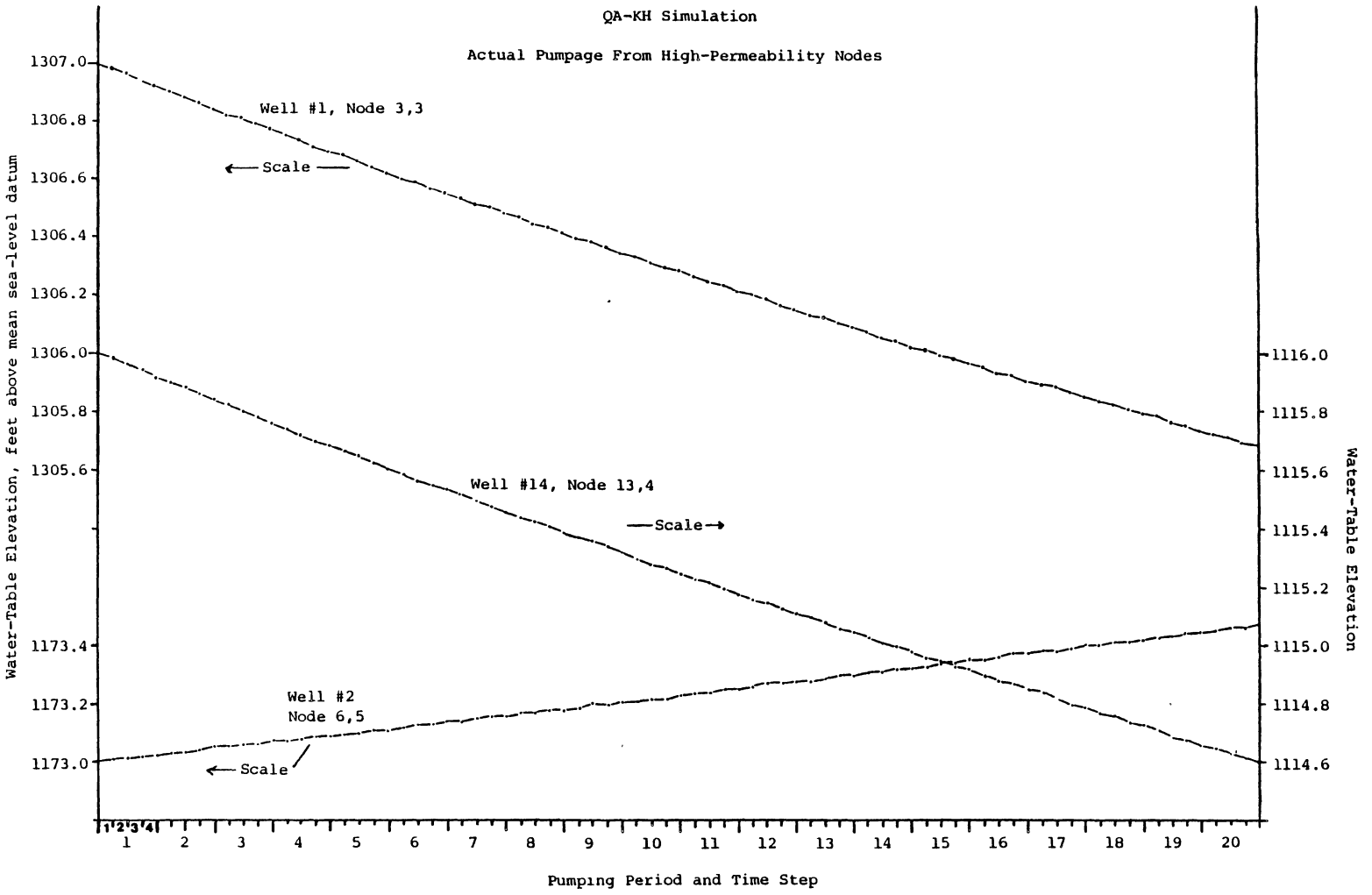

Figure 90. Well Hydrographs for QA-KH Simulation (Actual Pumpage from High-Permeability Nodes)

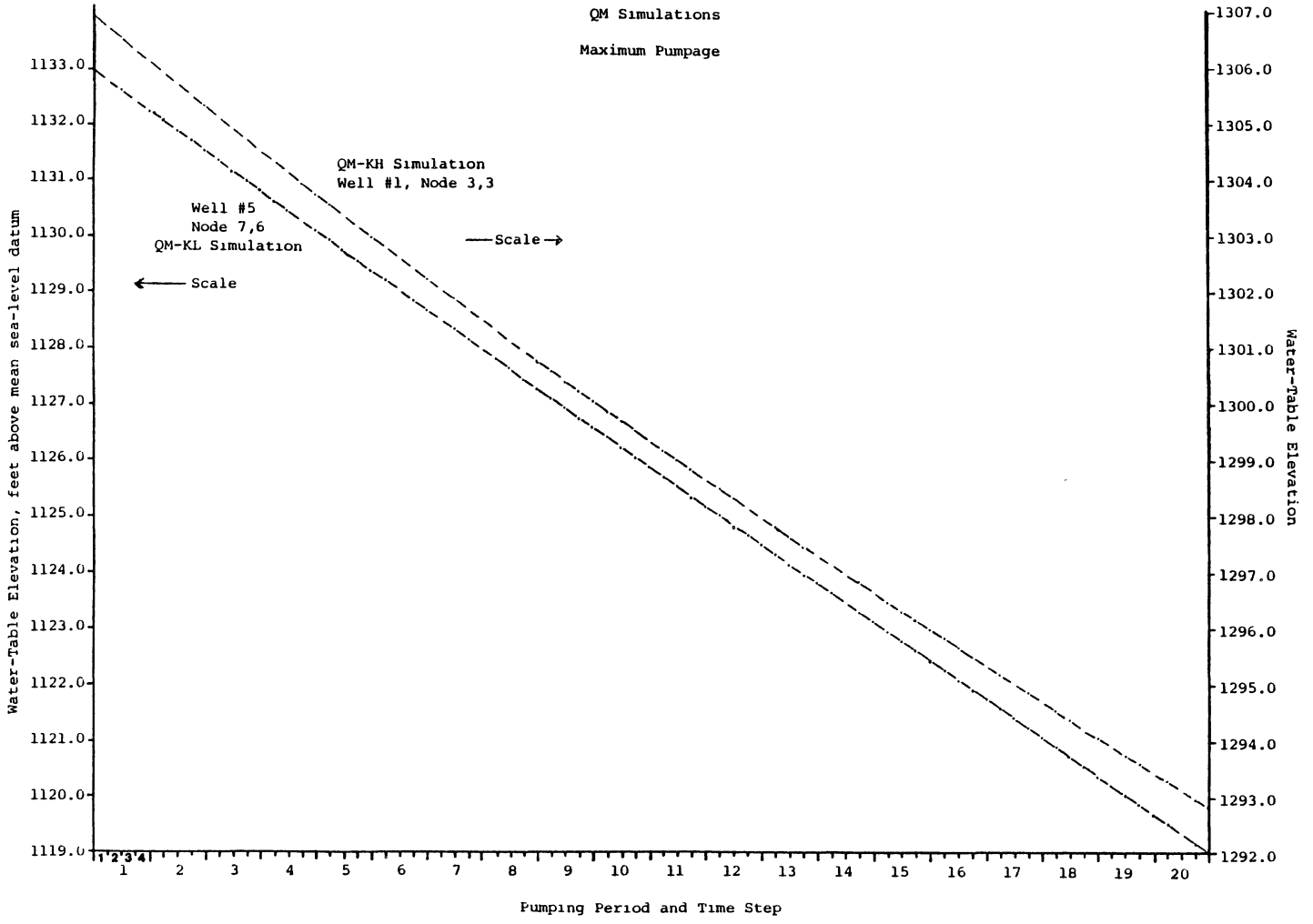

Figure 91. Well Hydrographs for QM Simulation (Maximum Pumpage)

TABLE XXIV

CUMULATIVE MASS BALANCES

Units are 10^{E} ft^{3}

Simulation	Recharge	E	Pumpage	E	Cumulative Net Pumpage	E	Release From Storage	E	Leakage In	E	Leakage Out	E	Cumulative Net Leakage	E	Mass Balance Residual	E	Percent Error	E
QA-KH	-4.80	9	2.03	9	-2.77	9	-2.15	9	-2.35	9	2.97	9	6.18	8	8.19	4	1.64	-3
QA-KL	-4.75	9	2.78	9	-1.97	9	-1.53	9	-2.36	9	2.79	9	4.37	8	7.37	4	1.32	-3
QM-KH	-4.80	9	6.32	9	1.52	9	2.11	9	-2.37	9	2.96	9	5.86	8	9.42	4	1.02	-3
QM-KL	-4.75	9	1.25	10	7.76	9	8.10	9	-2.37	9	2.71	9	3.37	8	1.52	5	9.96	-4
QO-KH	-4.80	9	1.84	9	-2.96	9	-2.34	9	-2.36	9	2.97	9	6.18	8	2.87	4	5.95	-4
QO-KL	-4.80	9	1.84	9	-2.96	9	-2.24	9	-2.36	9	2.98	9	6.23	8	2.46	4	5.10	-4

TABLE XXV

RATE MASS BALANCES

Units are ft^3/s

Simulation	Recharge	Leakage In	Leakage Out	Leakage Net (QNET)	Pumpage	Net Withdrawal (TPUM)
QA-KH	-7.61	3.76	-4.82	-1.06	3.22	-4.39
QA-KL	-7.52	3.77	-4.54	-0.77	4.41	-3.12
QM-KH	-7.61	3.74	-4.78	-1.03	10.0	2.41
QM-KL	-7.52	3.78	-4.32	-0.54	19.8	12.3
QO-KH	-7.61	3.76	-4.83	-1.06	2.92	-4.69
QO-KL	-7.61	3.77	-4.85	-1.08	2.92	-4.69

X / Y	1	2	3	4	5	6	7	8	9	10	11	12	13	14	15	16	17
1	0	0	0	0	0	0	0	0	0	0	0	0	0	0	0	0	0
2	0	1	1	1	1	0	0	0	0	0	0	0	0	0	0	2	0
3	0	2	0	0	0	0	0	0	0	0	0	0	0	0	0	2	0
4	0	2	0	0	0	0	0	0	0	0	0	0	0	0	0	2	0
5	0	2	0	0	0	0	0	0	0	0	0	0	0	0	0	2	0
6	0	2	0	0	0	0	0	0	0	0	0	0	0	0	0	2	0
7	0	2	0	0	0	0	0	0	0	0	0	0	0	0	0	2	0
8	0	2	0	0	0	0	0	0	0	0	0	0	2	2	2	2	0
9	0	0	0	0	0	0	0	0	0	0	0	0	0	0	0	0	0

Leakances: Code 1 = 3.09×10^{-5} ft^2/s Code 2 = 1.55×10^{-5} ft^2/s
No recharge assignments

Figure 92. NODEID Matrix for QO Simulation (No Pumpage; Sy = 0.30)

X / Y	1	2	3	4	5	6	7	8	9	10	11	12	13	14	15	16	17
1	0	0	0	0	0	0	0	0	0	0	0	0	0	0	0	0	0
2	0	0	0	0	0	0	-1	0	-5	-3	-1	-1	-1	-2	-1	0	0
3	0	0	1	-2	-1	-1	-2	0	-4	-6	0	-1	0	-1	0	0	0
4	0	0	-2	-1	-3	-3	-1	0	-2	-5	-2	0	0	0	0	0	0
5	0	0	-3	-3	-1	-3	0	0	0	-5	-3	-2	-2	-3	-4	0	0
6	0	0	-2	-2	0	-2	-2	0	1	-3	-2	-3	-4	-1	-3	0	0
7	0	0	-1	-1	-2	-3	-3	-5	-3	0	-2	-2	-3	-3	-2	0	0
8	0	0	-3	-1	-2	-4	-3	-5	-4	-4	-4	-3	0	0	0	0	0
9	0	0	0	0	0	0	0	0	0	0	0	0	0	0	0	0	0

(+) drawdown, ft (-) mounding, ft

Figure 93. Drawdown Matrix for QO Simulation (No Pumpage) With High Specific Yield = 0.30.

APPENDIX I

WATER-TABLE DATA

TABLE XXVI

POST OAK AQUIFER WATER-LEVEL ELEVATIONS

Mean Sea Level Datum; Measurements in Feet		
Location	Approximate Land Surface Elevation	Static Water Level
3N-10W-4ccd	1250	1242
3N-10W-28bbb	1160	1148
3N-9W-29ccb	1200	1188
2N-15W-22dccc	1320	1311
2N-14W-25ccdb	1220	1217
2N-14W-33dcdd	1240	1226
2N-12W-10 s½ s½	1100	1067
2N-11W-27ddc	1165	1151
2N-10W-16ccc	1200	1184
2N-10W-36 s½	1160	1147
2N-9W-33ddc	1150	1134
1N-15W-22baaa	1250	1231
1N-14W-15ccca	1195	1183
1N-14W-16ccdb	1195	1176
1N-14W-16dc n½	1175	1166
1N-14W-20dadd	1205	1190
1N-14W-20dadd	1205	1168
1N-14W-21ccbb	1220	1160
1N-13W-14ccd	1200	1186
1N-12W-15ddd	1070	1056
1N-11W-13ccc	1120	1106
1N-10W-10cccc	1110	1098

TABLE XXVI (Continued)

Mean Sea Level Datum; Measurements in Feet		
Location	Approximate Land Surface Elevation	Static Water Level
1N-10W-36c e½	1080	1066
1N-9W-20dddd	1050	1037
1S-14W-25 n½ n½	1115	1102
1S-13W-25cccc	1083	1067
1S-12W-4bbbc	1140	1125
1S-11W-21cccc	1059	1047

TABLE XXVII

ARBUCKLE GROUP AQUIFER WATER-LEVEL ELEVATIONS

Mean Sea Level Datum; Measurements in Feet				
Well	Location	Well Depth	Approximate Land Surface Elevation	Static Water Level
Koehler/ Waid	2N-12W-36adba SW corner, S.13th St. and C Ave., Lawton	937r	1110	1074
Cameron University	2N-12W-35bacb	1400r	1150	1069
Indiahoma 1	2N-15W-26bcdb	575r(?)	1360	1142
U.S.G.S. Moore	2N-14W-25adb1	1002	1230	1116 (1972)
Wilson	1N-10W-11bbd	2800r	1070	1070f

r: reported f: flows according to OWRB

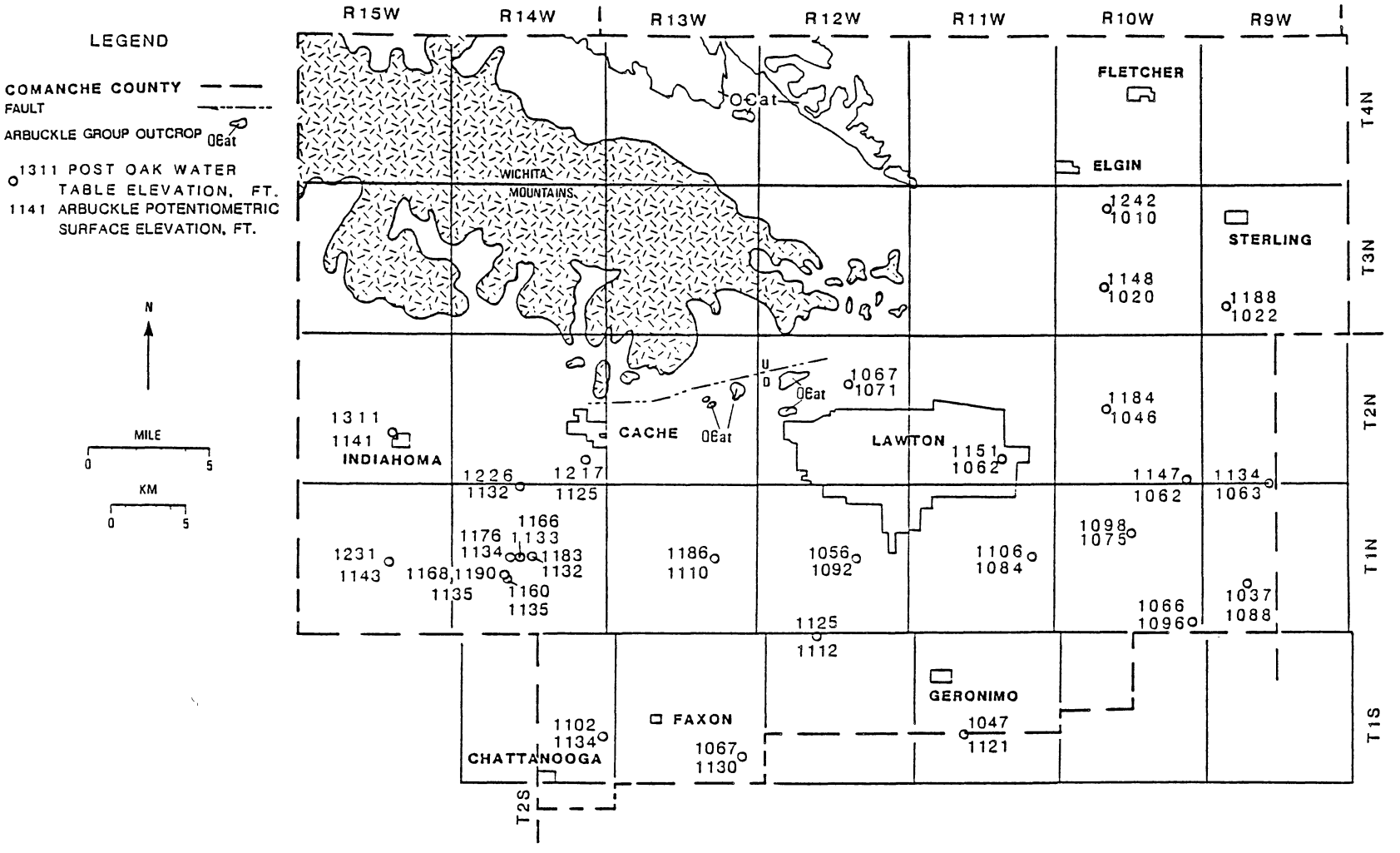

Figure 94. Water-Table Elevations From Post Oak and Arbuckle Group Aquifers

APPENDIX J

POST OAK AQUIFER RECHARGE DATA

CALCULATION OF RECHARGE TO THE POST OAK AQUIFER

Recharge to alluvium was determined from streamflow data as described previously (Appendix F). To calculate recharge to the Post Oak Aquifer, rainfall data was compared with well hydrograph data according to a method described by Lyons (1981, Table II, p.26). The product of the change in water table and the average specific yield is the gross inches of rainfall as recharge. The ratio of the rainfall as recharge to the total rainfall is the percent of precipitation that is recharge.

The total rainfall in October, 1972, was 8.71 inches (221 mm); the corresponding rise in water level in the Post Oak Aquifer was 24 inches (610 mm; Figure 93). The average specific yield of Post Oak type sediments is five percent (Johnson, 1967, pp.D57, D62). The mean annual recharge is thus 14 percent of rainfall, or 4.1 inches (104 mm; Table XXVIII).

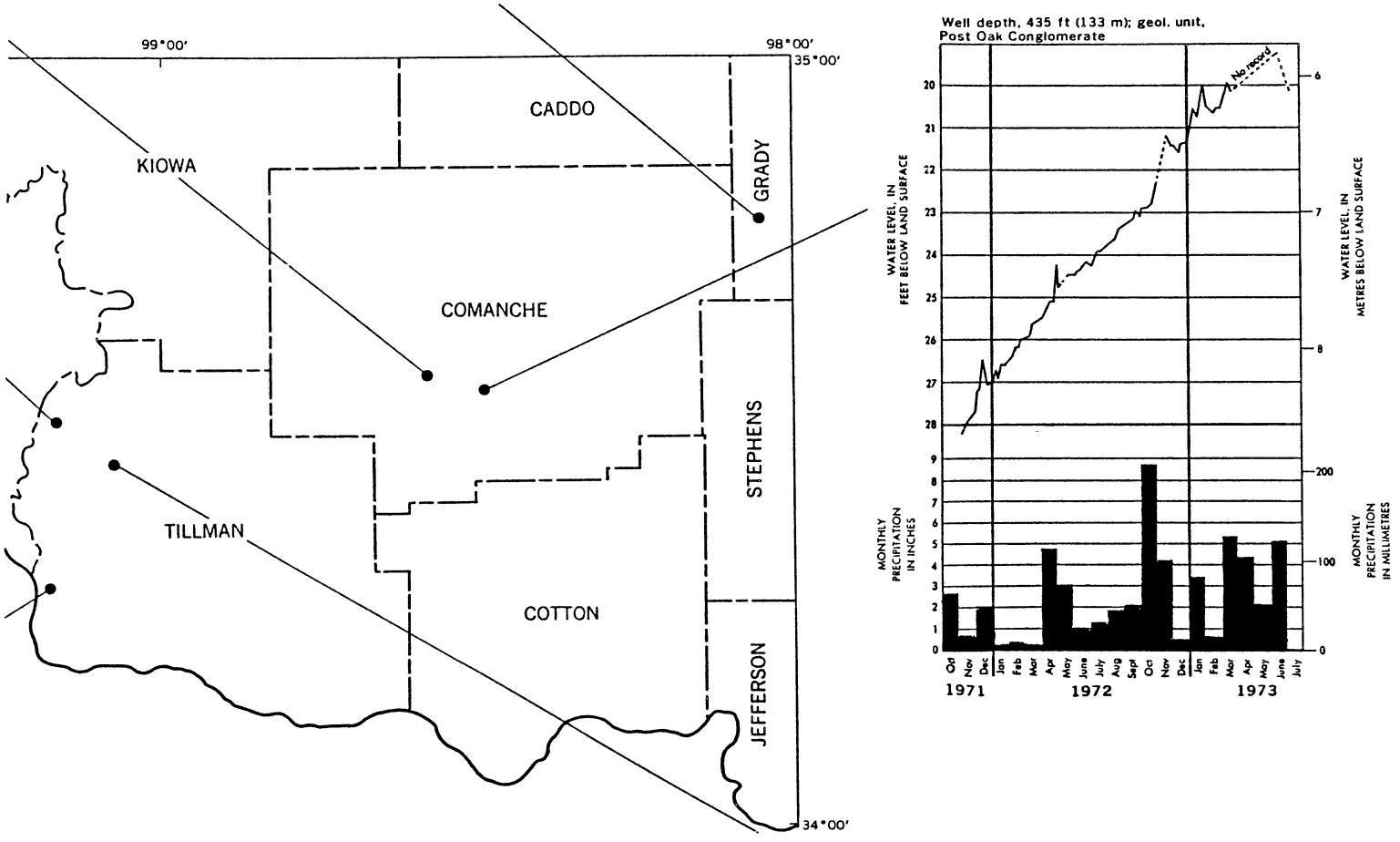

Figure 95. Well Hydrograph From Post Oak Aquifer (Modified from Havens, 1977, Sheet 2, Fig. 6)

TABLE XXVIII

CALCULATION OF MEAN ANNUAL RECHARGE FROM WELL HYDROGRAPH FOR POST OAK AQUIFER

Change in water table (in) x Average Sy = Gross inches of rainfall as recharge

$$\frac{\text{Gross inches of rainfall as recharge}}{\text{Total rainfall}} = \%\text{ of rainfall as recharge}$$

Total Rainfall, October, 1972: 8.71 in. (National Oceanic and Atmospheric Administration, 1973)

Increase in water level in Permian aquifer: 24 in. (Figure 95; Havens, 1977, Sheet 2, Fig.6)

Average Sy of Post Oak type lithologies: 5% (Johnson, 1967, pp.D57, D62)

Δ Water table x Sy = 24 in. x 0.05 = 1.2 in. of rainfall as recharge

$$\frac{1.2 \text{ in}}{8.7 \text{ in total rain}} = 0.138 = 14\% \text{ of rainfall as recharge}$$

14% x 29.18 in. mean annual rainfall, Lawton, = 4.1 in. mean annual recharge

APPENDIX K

WELL DATA FROM U.S. GEOLOGICAL SURVEY

TABLE XXIX

CALCULATIONS OF ARBUCKLE GROUP AQUIFER CHARACTERISTICS
FROM U.S.G.S. AQUIFER TEST DATA

Green Well (Test Well 1)
1N-13W-4baa

Test 1: Drawdown: inconclusive
Recovery: $\Delta s'$ = 20 ft (per log cycle), Q = 22.3 gpm

$$T = \frac{2.3\ Q}{4\ \pi\ \Delta s'} = \frac{2.3(22.3\ \text{gpm})(1440\ \text{min/day})}{4\ \pi\ (20\ \text{ft})} = 294\ \text{gpd/ft}$$

Test 2: Drawdown: Q = 35 gpm, t_o = 0.75 min, r = 0.28 ft, Δs = 91 ft (per log cycle), t = 22 min

$$T = \frac{264\ Q}{\Delta s} = 102\ \text{gpd/ft}$$

$$S = \frac{T\ t_o}{4790\ r^2} = 0.20$$

Test 3: Drawdown: Q = 35 gpm, t_o = 1.45 min, t = 300 min, Δs = 104 ft (per log cycle)
T = 89 gpd/ft S = 0.34

Recovery: $\Delta s'$ = 2 ft (per log cycle)
T = 4612 gpd/ft

Average T from all tests = 1274 gpd/ft

Moore Well (Test Well 2)
2N-14W-25adb

Test 1: Drawdown: inconclusive
Recovery: Q = 27.6 gpm, t/t' = 53, $\Delta s'$ = 27.0 ft (per log cycle)

T = 3637 gpd/ft

Test 2: Drawdown: Q = 27.2 gpm, t_o = 0.27 min, r = 0.28 ft, Δs = 21.2 ft (per log cycle), t = 481 min

T = 339 gpd/ft S = 0.24

Test 2: Recovery: Q = 27.6 gpm, $\Delta s'$ = 24.9 ft (per log cycle)
T = 7274 gpd/ft

Average T from all tests = 3750 gpd/ft

TABLE XXX

AQUIFER TEST DATA FROM U.S.G.S. TEST WELLS
IN ARBUCKLE GROUP AQUIFER

Green Well (Test well 1) 1N-13W-4baa

Test 1: Drawdown

3/28/72
Static water level: 61.24 ft Q = 22.3 gpm
Drawdowns measured with electric tape

Elapsed Time, t, min	Drawdown, s, ft
60	130.01
75	131.64
90	131.56
105	131.36
120	131.61

Test 1: Recovery

3/28/72

Time, t, min	Time Since Pumping Ceased, t', min	Time Ratio t/t'	Residual Drawdown, s', ft
120.17	0.17	706.9	128.76
120.33	0.33	364.6	123.76
120.58	0.58	207.9	118.76
121.08	1.08	112.1	108.76
121.38	1.38	88.0	103.76
121.70	1.70	71.6	98.76
122.0	2.00	61.0	93.76
122.42	2.42	50.6	88.76
122.88	2.88	42.7	83.76
123.43	3.43	36.0	78.76

TABLE XXX (Continued)

Time, t, min	Time Since Pumping Ceased, t', min	Time Ratio t/t'	Residual Drawdown, s', ft
124.08	4.08	30.4	73.76
124.83	4.83	25.8	68.76
125.67	5.67	22.2	63.76
126.67	6.67	19.0	58.76
127.83	7.83	16.3	53.76
129.47	9.47	13.7	48.76
131.50	11.50	11.4	43.76
135.58	15.58	8.7	38.76
151.67	31.67	4.8	33.76
181.00	61.00	3.0	29.04

Test 2: Drawdown

3/29/72

Static Water Level: 74.93 ft Q = 35 gpm ?

Elapsed Time, t, min	Drawdown, s, ft
0.28	15.07
--	25.07
6.00	74.65
7.25	85.07
8.00	90.07
9.33	97.55
10.33	102.02
10.92	104.85
11.67	107.80

TABLE XXX (Continued)

Elapsed Time, t, min	Drawdown, s, ft
12.67	111.25
13.17	113.02
14.17	115.77
15.08	118.41
15.75	120.30
16.58	122.20
17.42	123.89
18.33	125.87
19.00	127.21
20.08	130.00

Test 3: Drawdown

3/29/72

Static Water Level: 91.34 ft Q = 35 gpm

Elapsed Time, t, min	Drawdown, s, ft
0.17	4.16
0.50	8.66
0.88	13.66
1.28	18.66
1.67	23.66
2.17	28.66
2.58	33.66
3.75	38.66
5.17	58.66
5.75	63.66

TABLE XXX (Continued)

Elapsed Time, t, min	Drawdown, s, ft
6.50	68.66
7.25	73.66
8.12	78.66
9.08	83.66
10.17	88.66
11.42	93.66
12.83	98.66
14.72	103.66
17.50	110.02
20.0	113.78
26.0	120.31
30.0	123.27
35.0	125.71
41.0	127.37
50.0	129.19
60.0	130.29
70.0	131.03
80.0	132.14
90.0	132.74
100.0	132.19
120.0	132.87
140.0	136.69
155.0	137.97
170.0	137.76

TABLE XXX (Continued)

Elapsed Time, t, min	Drawdown, s, ft
185.0	136.58
200.0	134.51
215.0	132.75
230.0	131.34
250.0	128.32
265.0	126.98
285.0	130.55
300.0	131.74

Test 3: Recovery

3/29/72

Time, t, min	Time Since Pumping Ceased, t', min	Time Ratio t/t'	Residual Drawdown, s', ft
300.17	0.17	1765.7	128.66
--	--	--	123.66
301.0	1.0	301.0	113.66
303.25	3.25	93.3	73.66
303.58	3.58	84.8	68.66
304.17	4.17	72.9	63.66
304.67	4.67	65.2	58.66
305.33	5.33	57.3	53.66
306.0	6.0	51.0	48.66
306.75	6.75	45.4	43.66
307.58	7.58	40.6	38.66
308.58	8.58	36.0	33.66

TABLE XXX (Continued)

Time, t, min	Time Since Pumping Ceased, t', min	Time Ratio t/t'	Residual Drawdown, s', ft
309.75	9.75	31.8	28.66
311.25	11.25	27.7	23.66
313.17	13.17	23.8	18.66
316.33	16.33	19.4	13.66
324.83	24.83	13.1	8.66
360	60	6.0	4.27
377	77	4.9	3.53
390	90	4.3	2.96
400	100	4.0	2.57

Final water level: 89.43 ft, determined with steel tape, 3/30/72.

Moore Well (Test well 2) 2N-14W-25adb

Test 1: Drawdown

5/16/72

Static water level: 107.09 ft

Elapsed Time, t, min	Drawdown, s, ft	Discharge, Q, gpm
16.0	44.75	28
30.0	43.96	28.5
45.0	43.12	28.5
68.0	41.79	27.6
96.0	40.64	27.6
143.0	40.26	27.6
185.0	39.71	27.6

TABLE XXX (Continued)

Test 1: Recovery

5/16/72

Time, t, min	Time Since Pumping Ceased, t', min	Time Ratio t/t'	Residual Drawdown, s', ft
185.05	0.05	3701	31.05
185.33	0.33	561.6	26.05
185.58	0.58	320.0	21.05
185.92	0.92	202.1	16.05
186.33	1.33	140.1	11.05
188.25	2.25	83.7	6.05
195.0	10.00	19.5	2.74
197.0	12.00	16.4	2.40
202.0	17.00	11.9	2.14
210.0	25.00	8.4	1.93
215.0	30.00	7.2	1.63

Test 2: Drawdown

5/17/72

Static water level: 113.95 ft

Elapsed Time, t, min	Drawdown, s, ft	Discharge, Q, gpm
0.83	11.05	27.2
1.50	16.05	27.2
2.50	21.05	27.2
4.47	26.05	27.2
17.47	31.05	27.2
26.0	--	27.6
34.0	31.96	27.6

TABLE XXX (Continued)

Elapsed Time, t, min	Drawdown, s, ft	Discharge, Q, gpm
56.0	32.56	27.3
75.0	32.15	27.3
98.0	32.03	27.3
129.0	32.17	27.6
163.0	31.82	27.6
219.0	31.98	28
273.0	31.33	27.6
334.0	31.41	28
402.0	31.61	27.3
456.0	31.70	27.6
481.0	31.82	27.6

Test 2: Recovery

5/17/72 Time, t, min	Time Since Pumping Ceased, t', min	Time Ratio t/t'	Residual Drawdown, s', ft
481	0.0	--	31.43
481.27	0.27	1782	26.43
481.50	0.50	963	21.43
481.83	0.83	580	16.43
482.25	1.25	386	11.43
483.0	2.00	241.5	6.43
500.92	19.92	25.1	1.43
511.0	30.0	17.0	1.21
527.0	46.0	11.4	1.04
541.0	60.0	9.0	0.93

TABLE XXX (Continued)

Test 3: Drawdown	
5/18/71	
Static Water Level: 113.57 ft	Q = 28 gpm
Elapsed Time, t, min	Drawdown, s, ft
66.0	30.22

TABLE XXXI

WATER QUALITY DATA FROM U.S.G.S TEST WELLS IN ARBUCKLE GROUP

Location: 1N-13W-4baa (?)				
Depth, ft	--	560	725	970
Specific Conductivity, umhos	1400	3140	3100	3140
Fluoride, mg/1	8.0	14	18	18

Location: 1N-13W-4abc	
Depth unknown	
Specific Conductivity, umhos	2800
Sodium, mg/1	620
Alkalinity, HCO3	504
CO3	10
Sulfate, mg/1	320
Chloride, mg/1	390 (?)
Fluoride, mg/1	28
Hardness, mg/1	20
Total Dissolved Solids, mg/1	1710

APPENDIX L

DATA FOR INDIAHOMA MUNICIPAL WELLS

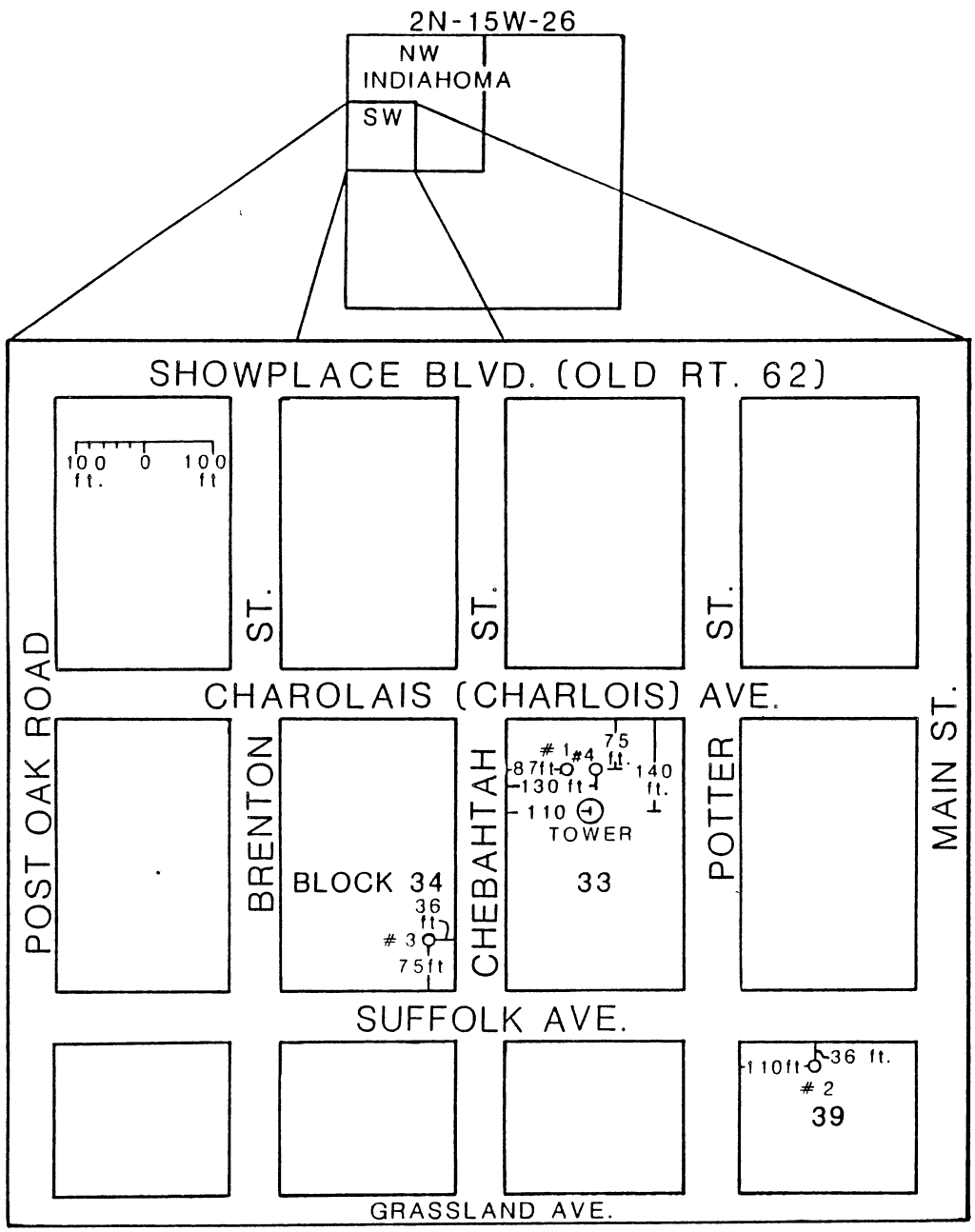

Figure 96. Locations of Indiahoma Municipal Supply Wells

TABLE XXXII

DRILLER'S LOG FOR
INDIAHOMA WELL #1

Formation	Top	Bottom	
Blue shale	5 ft	205	
Red shale	205	250	
Water	250	255	
Blue shale	255	265	
Red shale	265	295	
Blue shale	295	335	
Red shale	335	370	
Gray shale	370	394	
Gray lime	394	434	
Gray shale	434	455	
Red granite wash	455	470	
Arbuckle lime	470	500	
Water	500	542	
Hard lime	542	555	
Hard lime	555	600	
Water	600	605	
Hard lime	605	628	TOTAL DEPTH

Set 396 ft -- 8 1/4 in. -- 28 lbs casing
90 ft -- 6 5/8 in. liner at 476 -- 6 ft in lime (sic)

TABLE XXXIII

DRILLER'S LOG OF
INDIAHOMA WELL #3

Formation	Top	Bottom	
Topsoil	Grass roots	6 ft	
Sand rock	6	10	
Hard red rock	10	21	
Hard red rock	21	100	
Lime stone	100	200	
Hard lime stone	200	250	
Lime rock granite	250	350	
Lime stone, granite wash	350	410	
Porous lime, water bearing	410	450	
Chert	450	500	
Erosion granite	500	575	
Red granite wash	575	600	
Conglomerate	600	620	
Water bearing lime	620	640	
Hard lime gray	640	660	TOTAL DEPTH

Casing: 6 5/8 in. to 500 ft, 5 9/16 in. to 660
Hole size: 7 7/8 in.

AQUIFER TEST CALCULATIONS FOR INDIAHOMA MUNICIPAL WELLS

Walton Specific-Capacity Method

Constant discharge from a fully-penetrating well in a homogeneous, isotropic, nonleaky artesian aquifer infinite in areal extent. Assumptions are that the well penetrates and is uncased through the total saturated thickness of the aquifer; that well development has not affected the effective well radius; and that the effective radius equals the nominal radius.

Average discharge, Q, = 53.3 gpm; total drawdown, s, = 296 ft; specific capacity, Q/s, = 0.180; well radius, r_w, = 0.25 ft; storativity, S, = 0.008 (Fairchild and others, 1983, p.146); time after pumping started, t, = 1440 min

$$T = Q/s \left[264 \log \left(\frac{Tt}{2693\ r_w^2\ S} \right) - 65.5 \right] \quad \text{(Appendix D)}$$

= 246 assuming 100% well efficiency
= 410 assuming 60% well efficiency

Theis Method for Logarithmic Plot of Time-Drawdown Data

Constant discharge from a well in a nonleaky artesian aquifer.

Match point (see Figure 43): 1/u = 1; W(u) = 1; t = 0.63 min; s = 60 ft; r = 0.25 ft; Q = 50.1 gpm

$$T = \frac{Q\ W(u)}{4\ \pi\ s} = \frac{(50.1\ \text{gal/min})(1)(1440\ \text{min/day})}{4\ \pi\ (60\ \text{ft})} = \frac{72144}{754} = 95.7\ \text{gpd/ft}$$

$$S = \frac{4\ T\ t\ u}{r^2} = \frac{4(95.7\ \text{gpd/ft})(0.63\ \text{min})(1)}{(0.25\text{ft})^2(1440\ \text{min/day})\ (7.48\ \text{gal/ft}^3)} = \frac{241}{673} = 0.36$$

Note: Storativity value uncharacteristic of artesian aquifer.

Hantush Method for Logarithmic Plot of Time-Drawdown Data

Constant discharge from a well in a leaky artesian aquifer with storage in leaky confining beds. For description of method and type curves see Reed (1980, p.25 and Fig. 5.2, Plate 1) and Walton (1970, p.220).

Match point: $1/u = 10$; $H(u,B) = 1$; $B = 0.01$; $t = 4.6$ min; $s = 54$ ft; $r = 0.25$ ft; $Q = 50.1$ gpm

$$T = \frac{Q\,H(u,B)}{4\pi s} = \frac{(50.1\text{ gpm})(1)(1440\text{ min/day})}{4\pi(54\text{ ft})} = \frac{72144}{679} = 106\text{ gpd/ft}$$

$$S = \frac{4\,T\,u\,t}{r^2} = \frac{4(106\text{ gpd/ft})(0.1)(4.6\text{ min})}{(0.25\text{ ft}^2)(1440\text{ min/day})(7.48\text{ gal/ft}^3)} = \frac{195}{673} = 0.29$$

Note: Storativity value uncharacteristic of artesian aquifer.

Cooper-Jacob Straight Line Method for Semi-Logarithmic Plot of Time-Drawdown Data

Constant discharge from a well in a nonleaky artesian aquifer.

Calculation of time required for drawdown data to become linear:

distance from pumped well to observation well (well radius), r, = 0.25 ft
storativity, S, = 0.008 (from Fairchild and others, 1983, p.146)
transmissivity, T, = 410 gpd/ft (from specific capacity data)

$$\text{required elapsed time, ts, } = \frac{1.35\,(10^5)\,r^2\,S}{T}$$

$$= \frac{1.35(10^5)(0.25)^2(0.008)}{410} = 0.2\text{ min}$$

From Figure 44: $\Delta s = 247.5 - 134.5 = 113$ ft $t_o = 0.625$ min $Q = 50.1$ gpm $r = 0.25$ ft

$$T = \frac{2.30\,Q}{4\pi\,\Delta s} = \frac{2.30(50.1\text{ gpm})(1440\text{ min/day})}{4\pi(113\text{ ft})} = \frac{165{,}931}{1420} = 117\text{ gpd/ft}$$

$$S = \frac{2.25\,T\,t_o}{r^2} = \frac{2.25(117\text{ gpd/ft})(0.625\text{ min})}{(0.25\text{ft})^2(1440\text{ min/day})(7.48\text{gal/ft}^3)} = \frac{164}{673} = 0.24$$

Note: Storativity value uncharacteristic of artesian aquifer.

Hantush Inflection Point Method for Semi-Logarithmic Plot of Time-Drawdown Data

Constant discharge from a well in a leaky artesian aquifer with no storage in confining beds. For description of method see Fetter (1980, p.282).

From Figure 44: Maximum drawdown, $s_{max} = 296$ ft; drawdown at inflection point, $s_i = 296/2 = 148$ ft; slope at inflection point, $m_i = 226$ ft/log cycle; time at inflection point, $t_i = 13.2$ min; $Q = 50.1$ gpm

$$f(r/B) = e^{x}K_o(x) = \frac{2.3\ s_i}{m_i} = \frac{2.3(148)}{226} = 1.5$$

$K_o(x) = 0.89 \qquad x = 5.2$ (Fetter, 1980, App. 5, p.463)

$r/B = 0.52 \qquad r = 0.25$ ft $\qquad B = 0.48$

$$T = \frac{Q\ K_o(r/B)}{2\ \pi\ s_{max}} = \frac{(50.1\ \text{gpm})(0.89)(0.52)(1440\ \text{min/day})}{2\ \pi\ (296\ \text{ft})}$$

$$= \frac{33{,}388}{1860} = 18\ \text{gpd/ft}$$

$$S = \frac{4\ t_i\ T}{2\ r\ B} = \frac{4(13.2\ \text{min})\ (18\ \text{gpd/ft})}{2(0.25\ \text{ft})(0.48\ \text{ft})(1440\ \text{min/day})(7.48\ \text{gal/ft}^3)}$$

$$= \frac{948}{2590} = 0.37$$

Note: Storativity value uncharacteristic of artesian aquifer.

Theis Method Applied to Logarithmic Plot of Distance-Drawdown Data

Constant discharge from a well in a leaky artesian aquifer with no storage in the confining beds. For description of method and type curves see Walton (1970, p.217) and Fetter (1980, p.275).

Observation Well #1: distance from pumping well, $r = 43$ ft; $r^2 = 1849$

From Figure 97: $u = 1$; $W(u) = 1$; $r^2/t = 200\ \text{ft}^2/\text{min}$; $s = 11.8$ ft; $Q = 50.1$ gpm

$$T = \frac{Q\ W(u)}{4\ \pi\ s} = \frac{(50.1)(1)(1440)}{4\ \pi\ (11.8\ \text{ft})} = \frac{72{,}144}{148} = 487\ \text{gpd/ft}$$

$$S = \frac{4\ T\ t\ u}{r^2} = \frac{4(487\ \text{gpd/ft})(1)}{(200\ \text{ft}^2/\text{min})(1440\ \text{min/day})(7.48\ \text{gal/ft}^3)}$$

$$= \frac{1948}{2{,}154{,}240} = 0.0009$$

Observation Well #2: $r = 540$ ft; $r^2 = 291{,}600$

From Figure 97: $u = 1$; $W(u) = 1$; $r^2/t = 21{,}200\ \text{ft}^2/\text{min}$; $s = 1.98$ ft; $Q = 50.1$ gpm

$$T = \frac{72144}{24.9} = 2897\ \text{gpd/ft} \qquad S = \frac{11588}{247{,}737{,}600} = 5.1 \times 10^{-5}$$

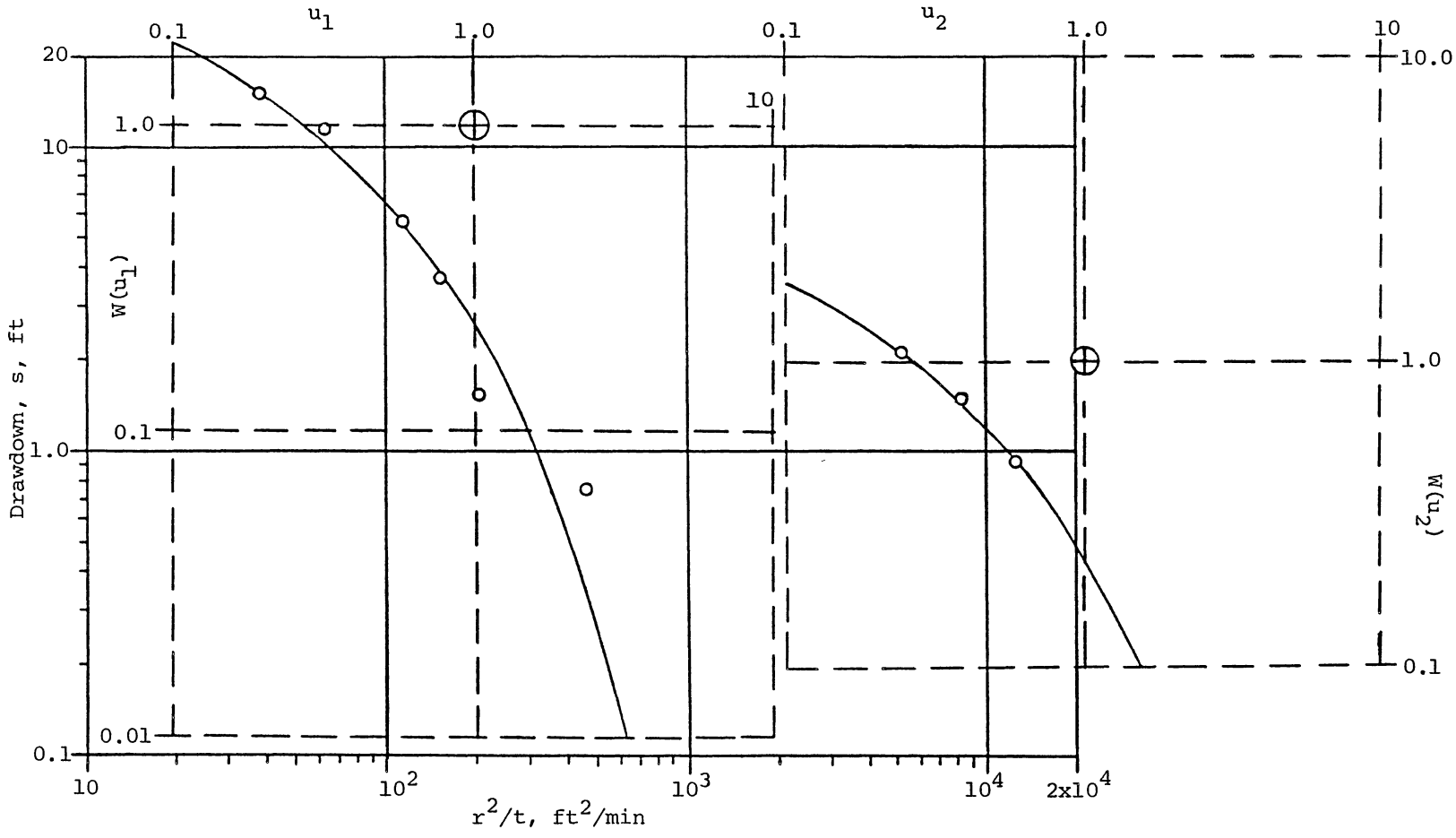

Figure 97. Theis Nonequilibrium Distance-Drawdown Analysis for Indiahoma Wells #1 and #2

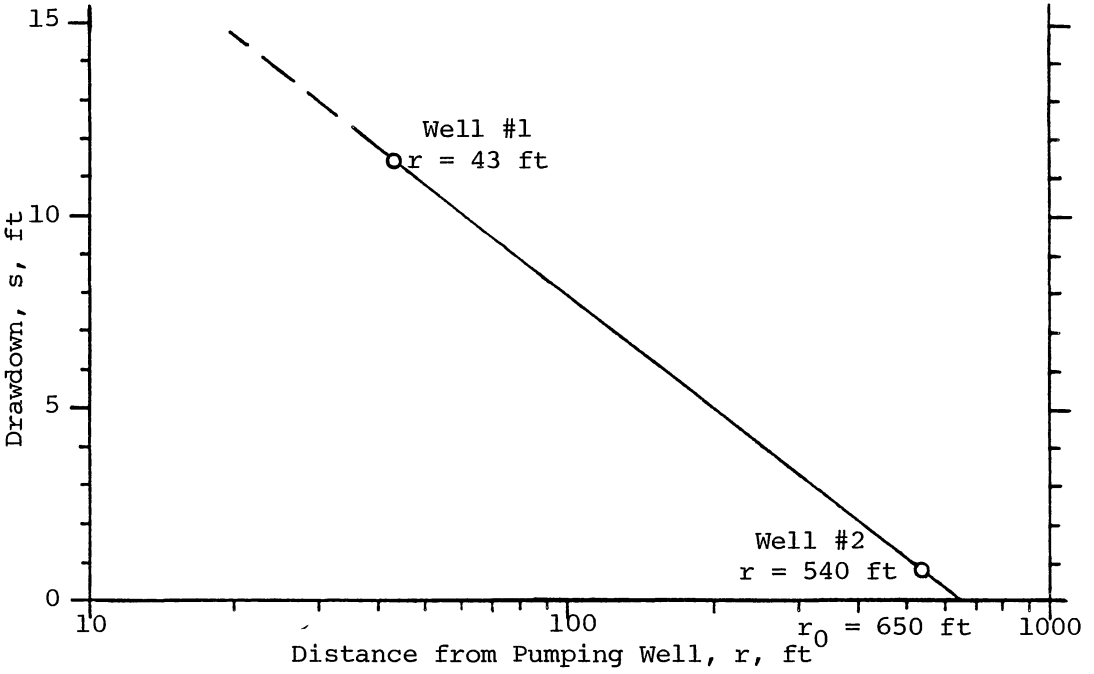

Figure 98. Jacob Distance-Drawdown Analysis for Indiahoma Wells #1 and #2

Jacob Method Applied to Semi-Logarithmic Plot of Distance-Drawdown Data

Constant discharge from a well in a nonleaky artesian aquifer (Fetter, 1980, p.269). See Figure 98.

Well #1: distance from pumping well, r = 43 ft
s = 11.5 ft
t = 29 min

Well #2: distance from pumping well, r = 540 ft
s = 0.92 ft
t = 23 min

Q = 50.1 gpm r_o = 650 ft

Δs = 14.64 - 5.00 = 9.64 ft/log cycle

Calculation of time required for drawdown data to become linear:

r = distance from pumped well to observation well (well radius), ft,
storativity, S, = 0.0012 (a low value from Fairchild and others, 1983, p.146)
transmissivity, T, = 1800 gpd/ft (a high value from Walton's distance-drawdown method; see below.)

Well #1: required elapsed time, ts, = $\frac{1.35\ (10^5)\ r^2\ S}{T}$

$$ts = \frac{1.35(10^5)(43)^2(0.0012)}{1800} = 166 \text{ min}$$

Well #2: $$ts = \frac{1.35(10^5)(540)^2(0.0012)}{1800} = 26{,}244 \text{ min}$$

$$T = \frac{2.3\ Q}{2\ \pi\ \Delta s} = \frac{2.3\ (50.1 \text{ gpm})\ (1440 \text{ min/day})}{2\ \pi\ (9.64 \text{ ft})} = \frac{165931}{60.6} = 2740 \text{ gpd/ft}$$

$$S = \frac{2.25\ T\ t_1}{r_o^2} = \frac{2.25\ (2740 \text{ gpd/ft})\ (29 \text{ min})}{(650 \text{ ft})^2(1440 \text{ min/day})(7.48 \text{ gal/ft}^3)}$$

$$= \frac{178{,}785}{4{,}550{,}832{,}000} = 3.9 \times 10^{-5}$$

Walton Method for Logarithmic Plot of Distance-Drawdown Data

Constant discharge from a well in a leaky artesian aquifer without water released from storage in confining beds (Walton, 1970, p.145 and 217). See Figure 45.

Well #1: Distance from pumping well, r = 43 ft
s = 5.75 ft
t = 16 min

Well #2: Distance from pumping well, r = 540 ft
s = 0.92 ft
t = 23 min

u = 0.1 W(u,r/B) = 1 r/B = 1
s = 3.2 ft r = 298 ft Q = 50.1 gpm

$$T = \frac{114.6\ Q\ W(u,r/B)}{s} = \frac{114.6\ (50.1\ gpm)(1)}{3.2\ ft} = \frac{5741}{3.2} = 1800\ gpd/ft$$

$$S = \frac{T\ u\ t}{1.87\ r^2} = \frac{1800\ gpd/ft\ (0.1)(16\ min)}{1.87\ (298\ ft)^2\ 1440\ min/day} = \frac{2880}{239{,}131{,}411} = 1.2 \times 10\text{-}5$$

Assumed aquitard thickness, m' = 400 ft
Vertical permeability of aquitard, $P' = \frac{T\ m'\ (r/B)^2}{r^2}$

$$P' = \frac{(1800\ gpd/ft)(400\ ft)(1)^2}{(43)^2} = \frac{720000}{1849} = 390\ gpd/ft^2$$

Linear (Nonradial) Flow Analysis for Arithmetic Plot of Time-Drawdown Data from Observation Wells

Constant discharge from a well in an artesian aquifer with a long, finite, fully penetrating, vertical fracture having infinitesimal width and no storage capacity; observation wells are on the same side of the fracture (Jenkins and Prentice, 1982). See Figures 47 and 99.

Well #1:
$(t_{o1})^{\frac{1}{2}} = 2.6$
$t_{o1} = 6.76$ min
distance from pumping well, $r_1 = 43$ ft

Well #2:
$(t_{o2})^{\frac{1}{2}} = 2.5$
$t_{o2} = 6.25$ min
distance from pumping well, $r_2 = 540$ ft

$\Delta\theta = 126.5°$

$$\theta_1 = \tan^{-1}\left[\frac{r_2\,(t_{o1})^{\frac{1}{2}}(\sin\Delta\theta)}{r_1(t_{o2})^{\frac{1}{2}} - r_2(t_{o1})^{\frac{1}{2}}(\cos\Delta\theta)}\right]$$

$$= \tan^{-1}\left[\frac{540(2.6)(\sin 126.5°)}{43(2.5) - 540(2.6)(\cos 126.5°)}\right] = \tan^{-1}\left(\frac{1129}{943}\right)$$

$$= \tan^{-1} 1.1973 = 50.13°$$

$\theta_2 = \theta_1 + \Delta\theta = 50.13° + 126.5° = 176.6°$

Orientation of fracture: 90° - 50.1° = 40° W of N (Figure 99)

$x_1 = r_1 \sin\theta_1 = 43 \sin 50.1° = 43(0.767) = 33.0$ ft

$x_2 = r_2 \sin\theta_2 = 540 \sin 176.6° = 540(0.0588) = 31.8$ ft

$$\frac{T_1}{S_1} = \frac{\pi\ x_1^2}{4(t_{o1})} = \frac{\pi\ (33.0\ ft)^2(1440\ min/day)}{4\ (6.76\ min)} = \frac{4{,}926{,}520}{27.0} = 182{,}000\ ft^2/day$$

$$\frac{T_2}{S_2} = \frac{\pi\ x_2^2}{4(t_{o2})} = \frac{\pi\ (31.7\ ft)^2(1440\ min/day)}{4\ (6.25\ min)} = \frac{4{,}546{,}015}{25.0} = 182{,}000\ ft^2/day$$

Assuming S = 0.001, $T = (182{,}000\ ft^2/day)(0.001)(7.48\ gal/ft^3)$
$T = 1400$ gpd/ft

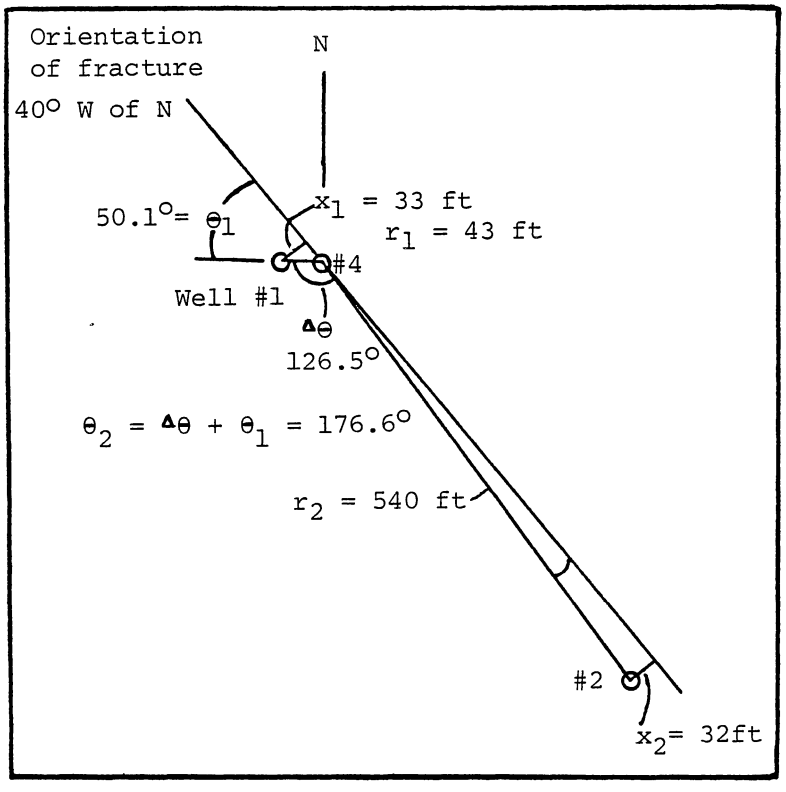

Figure 99. Diagram of Linear (Nonradial) Flow Analysis for Indiahoma Wells

Recovery Method for Semi-Logarithmic Plot of Time-Drawdown Data

Recovery of water level following constant discharge from a well in an artesian aquifer (Todd, 1980, p.131). See Figure 46.

Avg. Q = 53.3 gpm $\quad \Delta s' = 80 - 40 = 40$ ft per log cycle

$$T = \frac{2.3\,Q}{4\,\pi\,\Delta s'} = \frac{2.3\,(53.3\text{ gpm})(1440\text{ min/day})}{4\,\pi\,(40\text{ ft})} = \frac{176{,}530}{503} = 350\text{ gpd/ft}$$

TABLE XXXIV

AQUIFER TEST DATA FROM INDIAHOMA WELL #4

Well radius = 0.25 ft
Static Water Level = 235 ft below top of casing

Elapsed Time, t min	Drawdown, ft	$t^{\frac{1}{2}}$	Pumping Rate, Q gpm
5	100	2.24	50.1
7	117	2.65	50.1
9	133	3.00	50.1
11	143	3.32	50.1
15	154	3.87	50.1
20	159	4.47	50.1
25	177	5.00	50.1
30	188	5.48	50.1
35	197	5.92	50.1
40	200	6.32	50.1
45	210	6.63	50.1
50	210	7.07	47.8
60	220	7.75	47.8
70	222	8.37	57.5

TABLE XXXIV (Continued)

Elapsed Time, t min	Drawdown, ft	$t^{\frac{1}{2}}$	Pumping Rate, Q gpm
80	228	8.94	53.4
90	226	9.49	52.3
100	223	10.00	51.2
120	222	10.95	50.1
150	220	12.25	50.1
180	216	13.42	50.1
210	226	14.49	50.1
240	210	15.49	50.1
270	207	16.43	51.2
300	213	17.32	51.2
330	212	18.17	51.2
360	217	18.97	51.2
390	226	19.75	50.1
420	231	20.49	50.1
450	223	21.21	51.2
480	224	21.91	51.2
510	288	22.58	64.1
540	280	23.24	57.5
570	265	23.88	56.5
600	252	24.50	55.5
660	247	25.69	54.4
720	245	26.83	53.4
780	242	27.93	52.3
840	245	28.98	53.4

TABLE XXXIV (Continued)

Elapsed Time, min	Drawdown, ft	$t^{\frac{1}{2}}$	Pumping Rate, Q gpm
900	238	30.00	52.3
960	290	30.98	60.4
1020	275	31.94	56.5
1080	285	32.86	59.5
1140	290	33.76	60.4
1200	280	34.64	58.5
1260	281	35.50	60.4
1320	296	36.33	60.4
1380	296	37.15	61.3
1440	296	37.95	62.3

Measurement method: pneumatic guage and air line with a precision of ±1 ft.

TABLE XXXV

AQUIFER TEST RECOVERY DATA FROM INDIAHOMA WELL #4

Elapsed Time, t min	Time Since Pumping Ceased, t' min	Time Ratio t/t'	Residual Drawdown, s' ft
1441	1	1441	230
1455	15	97.0	228
1460	20	73.0	147
1465	25	58.6	140
1470	30	49.0	105

TABLE XXXV (Continued)

Elapsed Time, t min	Time Since Pumping Ceased, t' min	Time Ratio t/t'	Residual Drawdown, s' ft
1475	35	42.1	65
1480	40	37.0	62
1490	50	29.8	60

Measurement method: pneumatic guage and air line with a precision of ±1 ft.

TABLE XXXVI

AQUIFER TEST DATA FROM INDIAHOMA OBSERVATION WELLS

Well #1 Distance, r, from pumped well = 43 ft		Well #2 Distance, r, from pumped well = 540 ft	
Elapsed time, t, min	Drawdown, s, ft	Elapsed time, t, min	Drawdown, s, ft
4	0.75	--	--
9	1.54	--	--
12	3.71	--	--
16	5.75	--	--
--	--	23	0.92
29	11.46	--	--
--	--	35	1.5
48	15.17	--	--
--	--	56	2.12

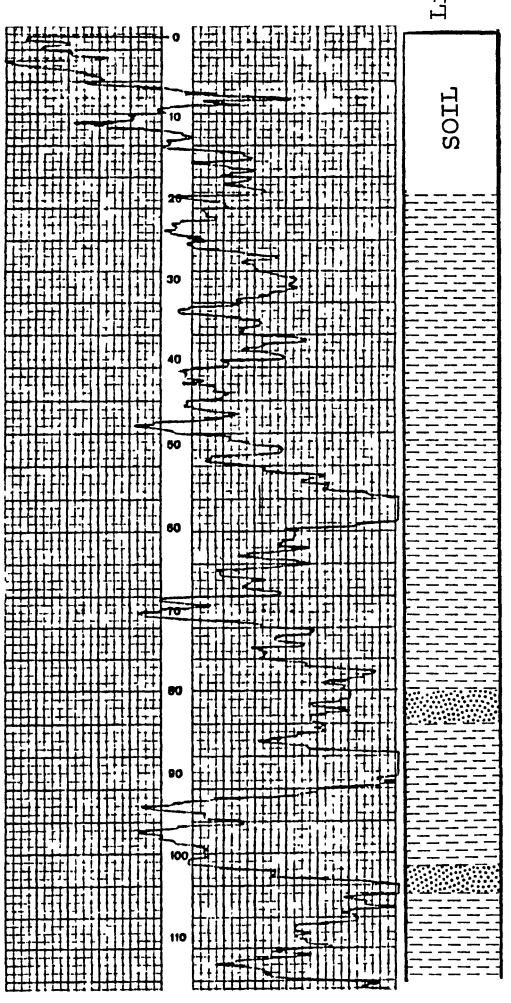

Note: Lithologic log is not necessarily representative of gamma-(ray) log.

Driller's Log of Indiahoma Test Well

0	Soil: light brown, greenish, calcareous; quartz and feldspar grains, silt-sized on clay bits about 1\2 to 1 cm-sized
5	Soil: finer-grained, calcareous, with smaller clay balls
10	Soil: coarser, calcareous, with pink calcareous claystone pieces
15	Soil: light brown, reddish, fine-grained, calcareous; very-fine-silt-sized feldspar (predominant) and quartz grains on clay bits (1\2 cm.
20	Clay: olive-green, calcareous, with very fine silt-sized quartz and feldspar grains
50	Siltstone: dark gray, very-fine-grained with silt-sized quartz and feldspar grains; indurated, easily disaggregated; becomes darker with depth; some very-fine-silt-sized glauconite grains.
55	Claystone: dark red, brown, sandy silty with quartz and feldspar; harder
65	Claystone: gray, silty, quartz and feldspar grains, some carbonate, slightly glauconitic
68	Claystone: lighter bluish gray with coarse sand of quartz and feldspar, reddish
72	Claystone: dark to light gray, very-fine to medium-grained silty, with reddish, sandy silt, quartz and feldspar grains
75	Claystone: reddish, silty with very-fine-grained quartz and feldspar; becomes gray-brown and darker.
80	Sandstone: brownish with light gray; claystone: blue-gray, very-fine-silty; some carbonate.
	Siltstone: gray, fine-grained, sandy, clay matrix; larger quartz grains; arkosic
88	Siltstone: brownish gray, sandy, arkosic, calcareous, slightly glauconitic
92	Siltstone: reddish gray, arkosic, calcareous
93	Shale: light gray, silty, arkosic, quartz, less carbonate
95	Shale: brown, fine-grained, silty, with some carbonate
102	Sandstone: light gray, arkosic, calcareous
105	Shale: dark brown, silty, some carbonate.
106	Shale: as above, sandier, less carbonate.

Figure 100. Gamma-Log, Driller's Log, and Lithologic Log of Well #4

Gamma-(ray) Log

Approximate Scale

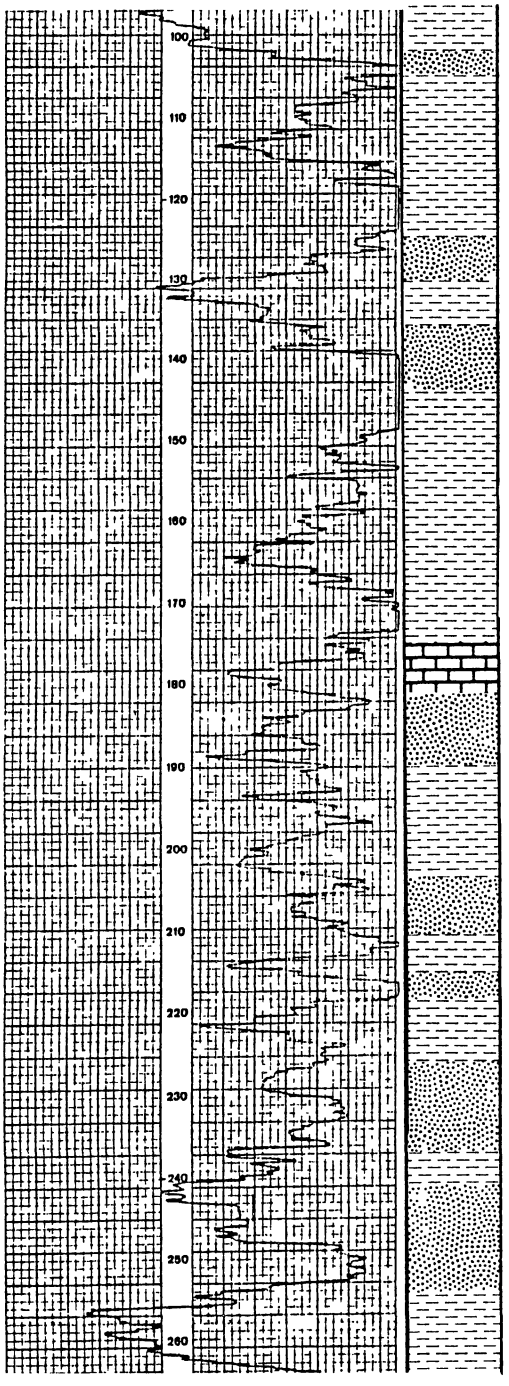

Note: Lithologic log is not necessarily representative of gamma-(ray) log.

111	Siltstone: light gray, limey, sandy, arkosic
117	Shale: dark brown, very fine silty, some carbonate
123	Shale: gray, very fine silty, some carbonate
126	Sandstone: gray, fine- to coarse-grained, arkosic
131	Shale: brown, sandy, silty
137	Sandstone: gray, medium- to coarse-grained, arkosic, slightly calcareous
141	Sandstone: brown, arkosic, silty
145	Shale: brown, silty
147	Siltstone: brown, quartz sandy
155	Shale: dark gray, silty
156	Shale: brown, fine-grained, silty
169	Shale: brown, calcareous, silty
176	Limestone: gray, silty, sandy with quartz and feldspar
182	Sandstone: pink and gray, arkosic, slightly calcareous
184	Sandstone: as above, finer grained, redder.
186	Sandstone: gray and pink, coarser
188	Sandstone: brown, silty, clayey, arkosic, slightly calcareous
191	Shale: brown, silty, slightly calcareous
198	Siltstone: gray, fine-grained, arkosic, non-calcareous
201	Siltstone: as above, becomes red-brown.
205	Sandstone: pink and gray, fine- to coarse-grained, arkosic, calcareous
211	Siltstone: brown, very-fine-grained, some sand, some carbonate
216	Sandstone: brown-gray, fine- to coarse-grained, arkosic, slightly calcareous
219	Siltstone: brown-gray, sandy, arkosic, non-calcareous
227	Sandstone: light gray, fine- to coarse-grained, arkosic, calcareous
238	Siltstone: gray, fine-grained, slightly calcareous
242	Sandstone: gray, fine- to coarse-grained, arkosic, calcareous
250	Sandstone: as above, lighter gray.
256	Siltstone: brown, sandy, varying sand content.

Figure 100. Gamma-Log, Driller's Log, and Lithologic Log of Well #4

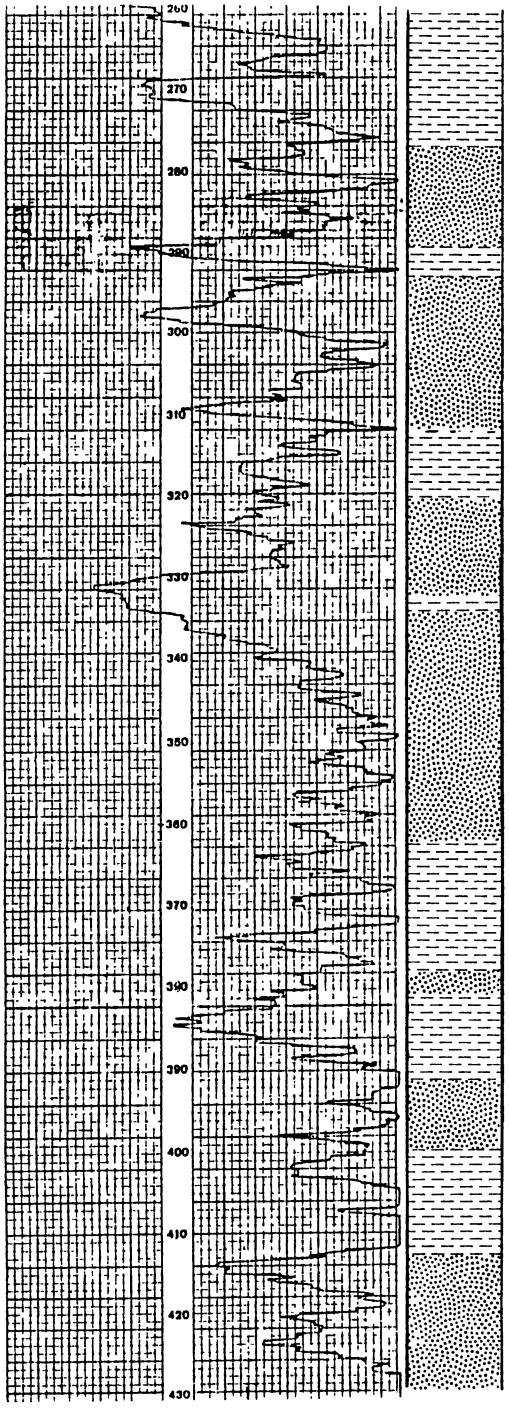

276	Siltstone: gray
278	Sandstone: pinkish gray, arkosic
280	Sandstone: brown, medium- to coarse-grained, arkosic, calcareous
282	Sandstone: as above, light gray, more calcareous
290	Siltstone: dark gray and brown, sandy
294	Sandstone: light gray, arkosic
301	Sandstone: brown, arkosic
305	Sandstone: gray, limey, arkosic
312	Siltstone: brown, sandy, calcareous
321	Sandstone: dark gray and brown, arkosic
326	Sandstone: gray, fine- to medium-grained
333	Siltstone: gray and brown, sandy
335	Sandstone: dark gray, sandy, arkosic
340	Sandstone: lighter gray, medium- to coarse-grained, arkosic, calcareous
345	Sandstone: as above, coarser
360	Sandstone: gray-pink, coarse, arkosic, granite rock bits
363	Siltstone: dark gray, sandy
370	Siltstone: gray, sandy, non-calcareous
373	Siltstone: as above, darker, less sandy.
374	Siltstone: brown, clayey, sandy, non-calcareous
379	Sandstone: gray, fine to coarse, arkosic, slightly calcareous
380	Sandstone: brown-gray, fine- to medium-silty, non-calcareous
382	Siltstone: gray, clayey
384	Siltstone: dark gray
385	Siltstone: gray
388	Siltstone: gray-brown, some quartz sand
390	Siltstone: gray, some quartz sand
392	Sandstone: light brown, gray, fine- to medium-grained, arkosic, non-calcareous.
400	Shale: brown, fine-grained, silty
406	Siltstone: gray, sandy
413	Sandstone: gray, fine- to medium-grained, arkosic, silty, non-calcareous
419	Sandstone: gray, fine- to medium-grained, arkosic, silty, slightly calcareous
422	Sandstone: as above, coarser, more feldspar
424	Sandstone: as above, non-calcareous.

Figure 100. Gamma-Log, Driller's Log, and Lithologic Log of Well #4

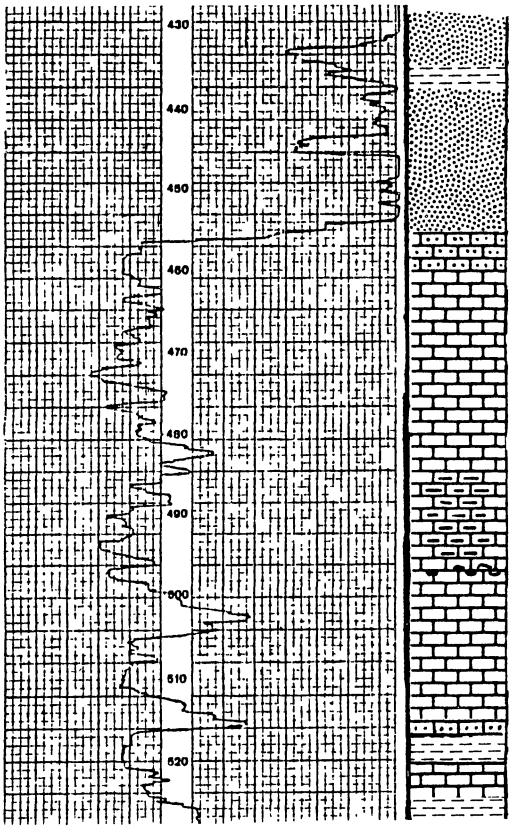

Note: Lithologic log is not necessarily representative of gamma-(ray) log.

431 Sandstone: gray, fine- to medium-grained, arkosic, silty, non-calcareous, becomes redder.

436 Siltstone: gray-brown, medium-grained, calcareous

438 Sandstone: gray, fine- to coarse-grained, arkosic, non-calcareous

443 Sandstone: as above, siltier, slightly calcareous

450 Sandstone: as above, brownish, non-calcareous

455 Sandstone: as above, light gray, non-calcareous.

456 Limestone: very light gray, fine- to coarse-grained, siliceous, sandy; oolites, chert, some feldspar.

460 Limestone: light gray, fine-grained, siliceous, oolites absent, some quartz; siltstone: dark gray, calcareous

465 Limestone: white, fine-grained, sucrosic, siliceous, pyrite clusters

470 Limestone: white, buff, and light gray, some quartz

475 Limestone: white and buff, siliceous, very-fine-grained pyrite clusters

480 Limestone: as above; some quartz sand, very-fine-silt-sized hematite.

485 Limestone; shale pieces: dark gray-green, glauconitic; more quartz.

490 Limestone with shale pieces, some quartz, pyrite.

495 Limestone: white, fine-grained; chert: buff, ~25% of sample;
Shales: gray-green glauconitic and dark brown.

497 Chert: buff, crystalline, ~75-80%; Limestone: white, fine-grained, siliceous; some shale: brown, fine-silty.

498 Limestone: white, fine-grained, siliceous, less chert, ~10%; quartz, some feldspar; some shale: brown, fine-silty.

500 Limestone: white, siliceous; more chert, ~40%, more shale, ~10%;

505 Limestone: as above, less chert and shale, <10%.

515 Quartz, clear to dark orange; shale: gray-green, glauconitic; limestone: white, fine-grained, siliceous; brown siltstone.

517 Limestone: white, 40%; brown shale, 40%; shale: dark gray-green, silty, glauconitic, 10%; quartz, 10%.

520 Limestone: white, fine-grained, siliceous, 70%; limestone: light gray-green, very-fine-grained, 20%; dark brown shale, 10%.

522 Limestone: as above with less gray-green and brown shale and siltstone.

Figure 100. Gamma-Log, Driller's Log, and Lithologic Log of Well #4

525 Limestone, 50%; brown siltstone, 40%; chert, 10%.

530 Limestone, 70%; brown siltstone, 20%; siltstone: gray-green, non-calcareous, 10%; some quartz.

535 Limestone: as above, less siltstone, 20%; more quartz, 10%.

537 Limestone; siltstone: red and green, quartz: clear and orange

540 Limestone; siltstone: gray-green, glauconitic; chert; quartz: white and clear, pyrite.

545 Limestone, 80%, chert, 20%, pyrite, siltstone, quartz

550 Limestone: white, fine-grained, siliceous, 70%; siltstone: green, fine to coarse, glauconitic, 10%; chert: dark orange-yellow, 10%; sandstone: fine glauconitic.

555 Limestone, 40%; siltstone: dark brown, fine, 40%; siltstone: green, fine-grained, glauconitic; sandstone: fine-grained, glauconitic; quartz.

560 Limestone, 40%, glauconitic siltstone, 40%, chert, quartz, sandstone, much less brown siltstone.

564 Limestone: white and buff, siliceous; some glauconitic siltstone and sandstone; light brown sample.

565 Limestone, 90%, glauconitic siltstone, 10%; light blue-gray sample.

570 Limestone, brown siltstone, glauconitic siltstone and sandstone, quartz, minor greenish-yellow altered glauconite; brown sample.

575 Limestone, siltstone, sandstone, and quartz as above, altered glauconite absent; lighter brown.

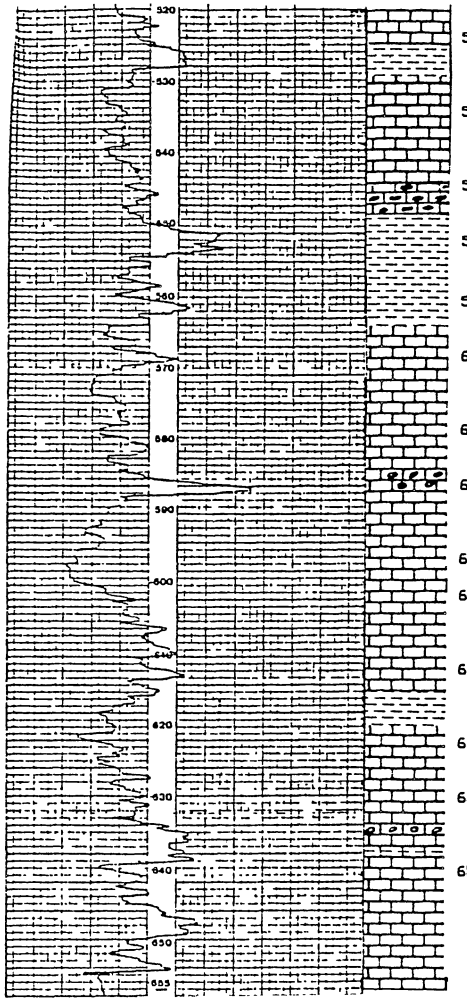

585 Limestone, 70%; chert: orange, oolitic, 20%; glauconitic siltstone and sandstone, 10%; gray.

587 Limestone, siltstone, and sandstone as above, less chert, minor pyritized limestone; browner.

590 Limestone, 90%; glauconitic siltstone, chert; lighter brown.

595 Limestone; siltstones: brown and glauconitic; chert, minor pyrite and altered glauconite; brown.

599 Limestone, siltstone, and chert as above, more altered glauconite; darker brown.

612 Limestone, minor chert, glauconitic siltstone; lighter brown.

615 Limestone; siltstones: brown and glauconitic; minor chert; brown.

620 Limestone, minor siltstone, quartz, and chert; gray.

630 Limestone: white and buff

634 Limestone: white and buff, 60%; chert: light yellow, granular and crystalline, 40%; gray sample.

635 Limestone, 60%; brown siltstone, 20%; siltstone: green, glauconitic, 15%; chert, 5%; dark brown.

638 Shale: green-gray, glauconitic; limestone, brown siltstone.

639 Limestone, glauconitic siltstone and sandstone, quartz, some brown siltstone

655 Limestone, siltstone, sandstone, and quartz as above with more chert.
TOTAL DEPTH

Figure 100. Gamma-Log, Driller's Log, and Lithologic Log of Well #4

APPENDIX M

DRILLING OF INDIAHOMA TEST WELL AND CHEMICAL ANALYSES OF WATER SAMPLES

DRILLING OF INDIAHOMA TEST WELL AND CHEMICAL ANALYSES OF WATER SAMPLES

In December, 1985, a test well (well #4) was drilled in Indiahoma as part of a municipal water supply project. The plan was to drill into the Arbuckle Group Aquifer, adequately sample the ground water for fluoride analyses, and design the production well to avoid the zones with high levels of fluoride. Because of the high fluoride content, the ground water would be blended with the current supply for Indiahoma from the CKT Rural Water System.

Figure 101 shows the location of the test well and other former supply wells. Table XXXVII lists the status of these other wells. The drilling contractor was the Layne-Western Company, and Glenn Briggs and Associates designed the well and pump house, blending station, and distribution facilities.

Drilling Procedure

The test well was drilled with a dual-wall, reverse circulation rotary method (Figure 102). In this method the drilling fluid, either air or water, is pumped down the outer annulus to the drill bit. The fluid carries the cuttings back up the center of the pipe. The cuttings and fluid are then discharged. Advantages of this method over conventional rotary drilling techniques are that rock samples are uncontaminated by drilling mud and caving of the bore hole, water samples can be obtained from aquifer zones because the outer pipe acts

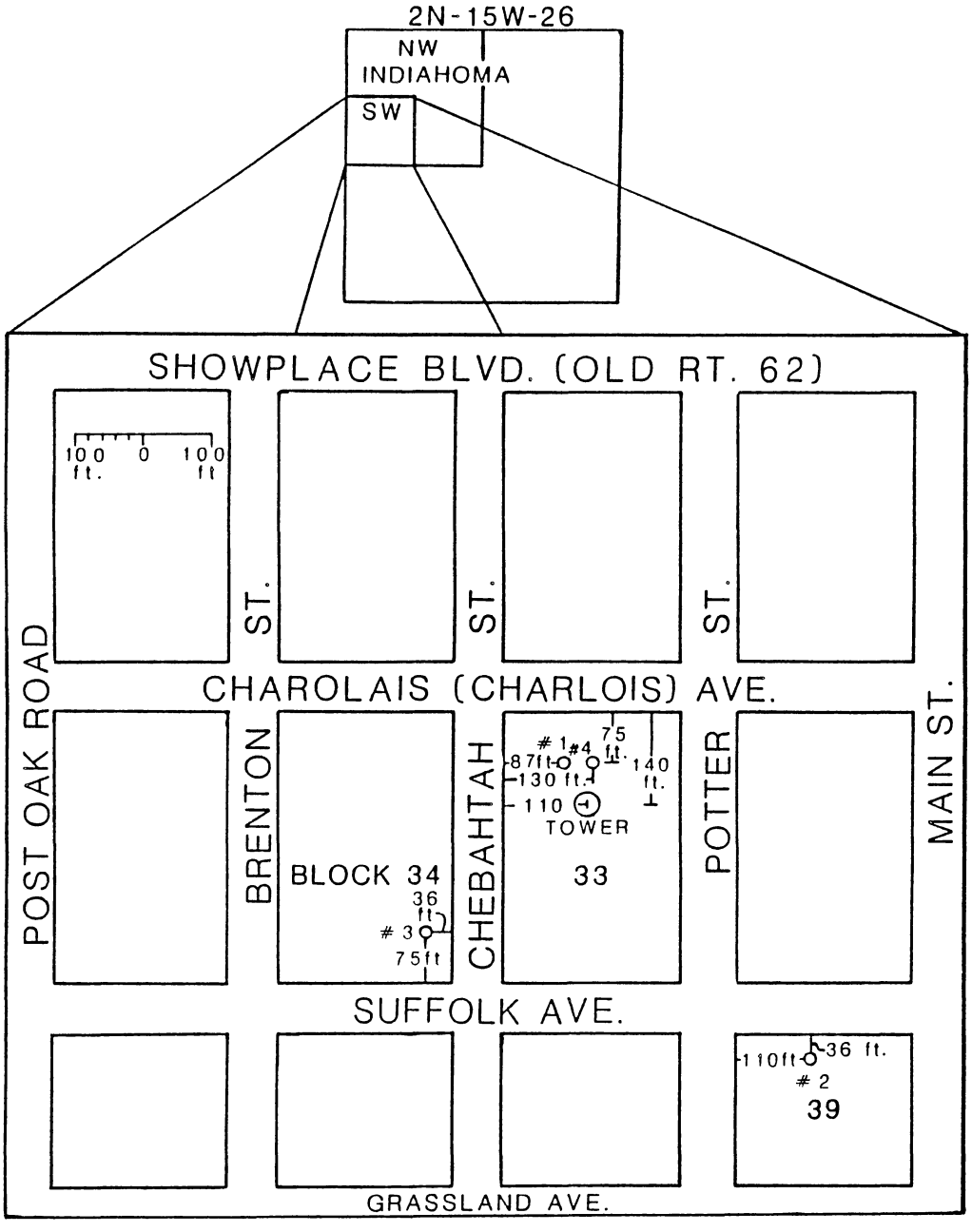

Figure 101. Locations of Indiahoma Municipal Supply Wells

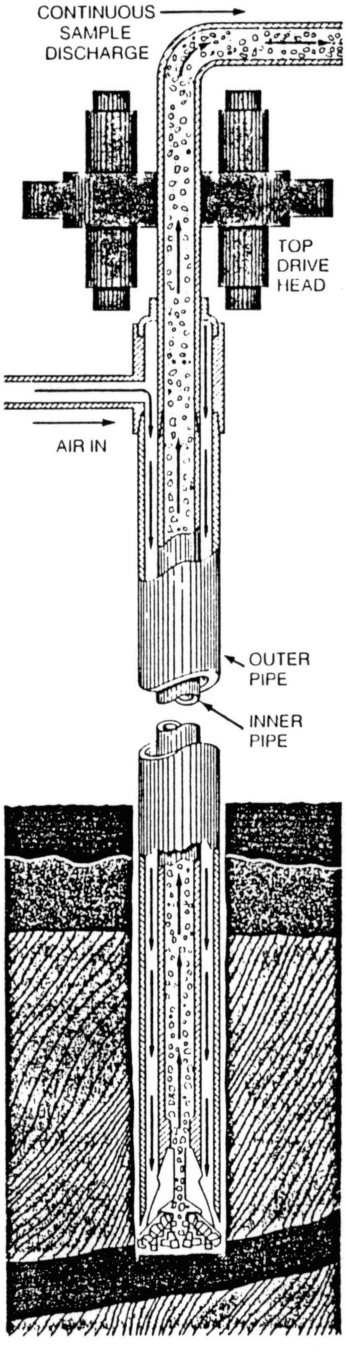

Figure 102. Dual-Wall, Reverse-Circulation Rotary Drilling Method (from Layne-Western Company, 1983)

as a casing, and a gamma radiation logging sonde can be lowered through the drill pipe. Both a rotary cone drill bit and a pneumatic hammer drill were used for the Indiahoma well because of the hard rock encountered.

A lithologic log, a gamma-log, and a driller's log are shown in Figure 100, Appendix L. The gamma-log records the natural radioactivity of the formation: shales containing clays with certain radioactive isotopes of potassium and thorium have a greater radioactivity than a clean sandstone or carbonate. The Permian sediments are highly radioactive and exhibit positive gamma-log responses because of their granitic material. The clean siliceous limestone at the top of the Arbuckle Group has a low radioactivity and, therefore, exhibits a sharp, negative gamma-log response at a depth of 456 ft (139 m). Table XXXII is a driller's log of well #1, and a driller's log for well #3 is in Table XXXIII.

The depths at which water samples were collected are shown in Table XXXVIII. The 420-foot sample represented an interval from 420 to 440 feet, and the 455-foot sample represented a five-foot interval to 460 feet. The other samples were considered representative of their respective depths.

Water Analyses

The types of analyses performed and the treatment of the samples are listed in Table XXXVIII. Because of the duration of the drilling, these were not identical for all the samples. Temperature, pH, and specific conductance were determined at the site with an Orion Research model 211 digital pH meter equipped with a 91-06 combination electrode

and an Amber Science model 1061 specific conductance meter with temperature compensation.

Dissolved metals, anions, nitrate, and nitrite were determined by the Oklahoma Department of Health Environmental Laboratory. Sampling bottles for these analyses were rinsed with a 50 percent solution of nitric or sulfuric acid, a 50 percent solution of hydrochloric acid, and deionized water. The samples analyzed for total dissolved metals were acidified with nitric acid to a pH of two. The acid dissolved suspended metals, especially in the 420- and 455-foot samples which were very turbid. The samples analyzed for nitrate and nitrite required acidification with sulfuric acid to a pH of two. The other samples were not acidified. All water samples were chilled to about four degrees celsius. The treatment of the samples is summarized in Table XXXVIII.

Additional analyses in the office for fluoride and nitrate used colorimeter and spectrophotometer methods. These involve reacting the water sample with a reagent. The resulting color, or light wavelength, depends on the concentration of the substance being determined. The colors of the sample and a filter are compared, and the concentration is shown directly on a calibrated scale (Hach, 1972). The instruments used for these analyses were the Hach DR-100 colorimeter and the Hach DR-3 spectrophotometer.

For fluoride analysis the required reagent is sodium 2-(parasulfophenylazo)-1,8-dihydroxy-3,6-naphthalene disulfonate (SPADNS). The analysis method and theory are described in Hach (1972) and American Public Health Association (1981, p.337). The two instruments required various dilutions of the sample (Table XXXIX) because of the high

concentrations of fluoride in these water samples. The colorimeter method was considered more accurate because less dilution was required.

The analysis for nitrate used the cadmium reduction method (Hach, 1972; APHA, 1981, p.370) in which NitraVer IV cadmium granules (Hach Chemical Company trademark) are the reagent.

Analyses by all methods are listed in Tables XXXIX and XL. The specific conductance and pH values are rounded arithmetic means of the values shown in Table XLI.

Public Health Implications

For public water supplies the U.S. Environmental Protection Agency has established toxic limits for the chemical parameters in these analyses based on health, aesthetic, or economic criteria (U.S.E.P.A., 1976a, and 1976b). The state of Oklahoma uses those limits to regulate only fluoride, nitrate, and barium (OWRB, 1982).

The maximum contaminant level of fluoride depends on the annual average maximum daily air temperature of the locality (U.S.E.P.A., 1976a). For this temperature in the Lawton area, 75.5°F (Havens, 1983), the corresponding toxic limit is 1.6 milligrams per liter (mg/l). This is equivalent to the limit measured at 90°F as established by the state (OWRB, 1982). The fluoride levels in the test well water samples greatly exceeded the allowable limit, ranging from 4.2 mg/l to 16.0 mg/l. These results were consistent with ground water quality analyses for the area listed in Havens (1983) and Back (1985).

Excessive consumption of fluoride during childhood can lead to dental fluorosis, or mottled teeth, a condition of imperfect calcification of tooth enamel which appears as white chalky patches on the

teeth. Skeletal fluorosis is calcification of tissue around the joints which develops after many years of low but persistent fluoride consumption (Waldbott, 1973, pp.155-156).

The E.P.A. criteria for nitrogen compounds is based on the increased risk of infant methemoglobinemia from water with nitrogen concentrations above 10 mg/l (U.S.E.P.A., 1976b, p.108). Therefore, the maximum contaminant level of nitrate-as-nitrogen (NO_3-N) is 10 mg/l, that for nitrite-as-nitrogen (NO_2-N) is 1.0 mg/l, and that for the nitrate ion is 45 mg/l. The ratio of the molecular weight of nitrate to that of nitrogen is 4.5; therefore, the limits were established at the same ratio.

Methemoglobinemia is a condition in which nitrate is converted to nitrite in an infant's stomach. The nitrite changes oxygen-bearing hemoglobin to methemoglobin, which does not transport oxygen in the blood. The result is oxygen deprivation. In adults the effect of nitrates is diarrhea (U.S.E.P.A., 1976a, p.81; Waldbott, 1973, p.259).

In Comanche County nitrate levels in shallow (less than 150 feet deep) ground water can range up to 40 mg/l (Havens, 1983; Back, 1985). Deeper waters generally have levels less than five milligrams per liter; an analysis of water from the Arbuckle Group Aquifer at a depth of 550 ft (168 m) reported to contain 85 mg/l (Havens, 1983, Table 1) probably represents contamination from the surface. In the Indiahoma test well nitrate levels were much below the detection limit of the laboratory analysis. The 460-foot sample had a level of 2.8 mg/l nitrate as determined by colorimeter.

The only other chemical parameter in these samples for which there is a toxic limit established by the state is barium. The 1.0 mg/l

limit avoids toxic effects on the heart, blood vessels, and nerves (U.S.E.P.A., 1976a, p.58). The 460-foot sample contained 5500 ug/1 (5.5 mg/1) barium; the concentrations in the other samples were less than the detection limit (Table XL).

To minimize staining and taste effects the limit for iron is 0.3 mg/1 for domestic water supplies (U.S.E.P.A., 1976b, p.78). Because of the acidification of the samples analyzed for total iron, the concentrations greatly exceeded this limit. These high iron levels interfered with the colorimetric determinations of total hardness by the laboratory. A titration method was considered more accurate.

The E.P.A. criteria for chloride and sulfate are based on taste and health effects (U.S.E.P.A., 1976b, p.205). The limit for both of these parameters is 250 mg/1. This limit protects against laxative effects by sulfate and minimizes any salty taste due to chloride. The 460-foot sample contained excessive sulfate, and the chloride concentration approached the 250 mg/1 limit. The chloride levels in the other samples were below the limit.

A limit for sodium of 270 mg/1 is recommended for moderately restricted sodium diets (U.S.E.P.A., 1976b, p.205). This level is also a recommended aesthetic limit. The sodium-adsorption ratio (SAR) is a more significant measure of the hazard in irrigation water quality of high sodium concentrations because a clayey soil structure is damaged by the exchange of sodium for adsorbed calcium and magnesium (Hem, 1970, p.228). The 490-foot samples had high SAR values, greater than 18. The values for the other samples (Table XLII) were in the medium range, 10 to 18 (Johnson, 1966, p.79).

The E.P.A. criterion for alkalinity has been established as a minimum of 20 mg/l because water treatment requires the pH buffering capacity of alkalinity. Also, the carbonate and bicarbonate components of alkalinity can reduce the toxicity of certain heavy metals (U.S.E.P.A., 1976b, p.7). Excessive alkalinity is undesirable for some industrial processes, and in irrigation water high levels may indirectly increase the sodium in soil water (U.S.E.P.A., 1976b, p.8). The range of maximum alkalinity for these reasons is 85 to 600 mg/l. Four of the test well water samples exhibited high alkalinities, about 300 mg/l. The 460-foot sample contained about 75 mg/l. Because of the high pH values, 8.7 to 9.0, the bicarbonate ion accounted for close to 100 percent of the alkalinity (Hem, 1970, Fig. 19). A more accurate study of the carbonate equilibria of the ground water would require field determinations of alkalinity.

The E.P.A. criteria for dissolved solids are based on taste and economics, that is, the costs of damage to water distribution systems from hard water (U.S.E.P.A., 1976b, p.206). The recommended maximum is 500 mg/l although higher levels (1000 mg/l) are allowed if another supply is unavailable. The total dissolved solids content can be computed from the specific conductance measurements (Hem, 1970, p.99). The conversion factor ranges from 0.55 to 0.75 depending on sulfate concentration, but the mean value of 0.65 was used in this study. The TDS values for the test well samples ranged from 845 to 1170 mg/l (Table XL). These would be significant to irrigation water quality as sensitive crops would be affected by these high concentrations.

None of these chemical parameters indicated saline water; however, according to a study by Hart (1966), the base of fresh ground water is

about 200 feet deep as determined from electric logs. There is a lack of well control for the map in the western part of Comanche County. Unless there are perched saline zones, the fresh ground water probably extends deep into the Arbuckle Aquifer as indicated by Hart (1966) for the Lawton area.

TABLE XXXVII

STATUS OF INDIAHOMA MUNICIPAL SUPPLY WELLS

Well	Depth	Status	Drilling Date	Information	Source of Information
#1	475, 575(?)	Collapsed; new casing to 375 ft, 25 ft open hole	1947(?)	D (Table XXXII)	C.C.
2	250	Collapsed	?	--	USGS
3	660	Not in use	Apr.-June, 1974	D (Table XXXIII)	I
4	655	Test well and new production well	Dec. 1985 Feb. 1986	D,G (Fig. 100)	L-W

D: driller's log
G: gamma log

C.C.: Oklahoma Corporation Commission, Oil and Gas Conservation Dept.
I: Town of Indiahoma files and officials
L-W: Layne-Western Co., Wichita, KS
USGS: U.S. Geological Survey open files, Oklahoma City

TABLE XXXVIII

DISPOSITION OF WATER SAMPLES FROM INDIAHOMA TEST WELL

Analysis Location	Laboratory	Laboratory	Laboratory	At Site	Office	Office
Analyses	F, Cl, SO_4, pH alkalinity, total dissolved solids, specific conductance	Fe, Mg, Ca, Na, K, Ba, total hardness	NO_3-N, NO_2-N NO_3+NO_2	pH temperature, specific conductance	NO_3, within 24 hours	F
Sample Preparation	Chilled, bottles rinsed with HNO_3, HCl, deionized H_2O	Acidified with HNO_3, chilled; bottles rinsed with HNO_3, HCl, deionized H_2O	Acidified with H_2SO_4, chilled; bottles rinsed with HCl, H_2SO_4, deionized H_2O	Bottles rinsed with sample	Chilled	Chilled
Samples						
420-440, 455, 460, 480	X	X	X	X	X	--
490a, b	X	X	X	X	X	--
490c	--	--	X	--	--	--
420, 455, 480-650 (every 10ft), 655	--	--	--	--	--	*
420-620	--	--	--	--	--	**
610-655	--	--	--	--	--	†

* Colorimeter method, 2 ml sample diluted to 8 ml
** Spectrophotometer method, 5 ml sample diluted to 25 ml
† Spectrophotometer method, 2.5 ml sample diluted to 25 ml

TABLE XXXIX

FLUORIDE ANALYSES OF GROUND WATER
FROM INDIAHOMA TEST WELL,
JANUARY, 1986

Units are milligrams per liter

Depth	Fluoride			
Method:	Lab	Colorimeter 2 ml to 8 ml dilution	Spectrophotometer- 5 ml to 25 ml dilution	2.5 ml to 25 ml dilution
420-440	8.60	7.16	4.20	--
455-460	7.80	7.00	6.50	--
480	8.90	6.40	5.60	--
490a	9.90	7.52	5.65	--
490b	10.80	--	--	--
490c	--	--	--	--
500	--	7.24	5.70	--
510	--	7.48	6.90	--
520	--	5.50	4.75	--
530	--	8.40	5.75	--
540	--	7.44	7.00	--
550	--	7.48	4.65	--
560	--	7.20	6.00	--
570	--	6.40	7.05	--
580	--	7.12	5.80	--
590	--	7.40	6.50	--
600	--	7.20	6.10	--
610	--	7.20	6.70	7.80
620	--	4.80	5.80	6.80

TABLE XXXIX (Continued)

Units are milligrams per liter

Depth	Method:	Lab	Fluoride Colorimeter 2 ml to 8 ml dilution	Fluoride Spectrophotometer 5 ml to 25 ml dilution	Fluoride Spectrophotometer 2.5 ml to 25 ml dilution
630		--	▵10 Off scale	--	16.00
640		--	▵10 Off scale	--	13.80
650		--	8.3	--	11.20
655		--	8.2	--	11.20

TABLE XL

CHEMICAL ANALYSES OF GROUND WATER
FROM INDIAHOMA TEST WELL
JANUARY, 1986

Laboratory analyses except as noted
Units are milligrams per liter except as noted
* Less than detection limit

Depth	Nitrogen, Nitrate as N Lab	Nitrogen, Nitrate as N Colori-meter	Nitrogen, Nitrite as N	Nitrite-Nitrate as N	Calcium, Total
420-440	*0.50	--	*0.500	*0.5	9
455-460	*0.50	2.8	*0.500	*0.5	180
480	*0.50	0.2	*0.500	*0.5	21
490a	*0.50	0.0	*0.500	*0.5	15
490b	*0.50	<0.1	*0.500	*0.5	11
490c	*0.50	0.0	*0.500	*0.5	--

Depth	Magnesium, Total	Hardness, Total	Chloride, Total	Sodium, Total	Potassium, Total
420-440	46	*10	108	390	9.8
455-460	910	*100	241	1390	151.4
480	21	20	185	390	2.3
490a	14	27	225	440	2.3
490b	15	26	226	460	2.5
490c	--	--	---	---	---

TABLE XL (Continued)

Units are mg/l except as noted
* Less than detection limit

Depth	Total Alkalinity,	Sulfate, Total	Iron, Total	Barium, Total ug/l
420-440	309.0	179	244	*400
455-460	75.0	359	7100	5500
480	294.0	204	39.0	*200
490a	319.0	241	18.7	*200
490b	322.0	242	32.0	*200
490c	---	---	--	---

	pH		Conductance umhos/cm		Temperature °C	(°F)	Total Dissolved Solids Calculated
	Lab	Field T °C	Lab	Field T °C	Lab	Field	Lab Cond. x 0.65
420-440	9.0	9.0 7	1800 5.0	1800 5	5.0 (41.0)	--	1170
455-460	9.0	9.1 6	1300 7.0	1300 7	7.0 (44.6)	--	845
480	8.8	8.9 5	1500 18.0	1450 5	18.0 (64.4)	--	975
490a	8.7	8.7 7	1750 18.0	1700 7	18.0 (64.4)	18.3 (65)	1138
490b	8.7	8.8 7	1700 7.0	1700 7	7.0 (44.6)	--	1105
490c	8.7	8.8 6	1650 7.0	1600 6	7.0 (44.6)	--	1072

ug: micrograms umhos: micromhos

TABLE XLI

SPECIFIC CONDUCTANCE AND PH VALUES OF GROUND WATER FROM INDIAHOMA TEST WELL, DECEMBER, 1985

Depth	Values were measured at well site: Specific Conductance umhos/cm^2	Temp. °C	Average, rounded to nearest 50 umhos		pH	Temp. °C	Average	
420-	1750	7			9.0	7		
440	1800	5	1800	5°C	9.1	6	9.0	7°C
455-	1300	7			8.9	7		
460	1300	7	1300	7°C	9.1	6	9.1	6°C
	1300	5			9.2	4		
480	1500	5			8.8	5		
	1450	5	1450	5°C	8.9	5	8.9	5°C
	1350	5			8.9	5		
490a	1750	7			8.8	7		
	1750	7	1700	7°C	8.7	7	8.8	7°C
	1650	8			8.8	8		
490b	1750	7			8.8	7		
	1650	9	1700	7°C	8.7	9	8.8	7°C
	1650	7			8.8	7		
490c	1600	6			8.8	6		

TABLE XLII

SODIUM-ADSORPTION RATIOS OF GROUND WATER FROM INDIAHOMA TEST WELL, JANUARY, 1986

Depth	Sodium		Chloride		Calcium		Magnesium		SAR
	mg/l	meq/l	mg/l	meq/l	mg/l	meq/l	mg/l	meq/l	
420-440	390	16.96	108	3.05	9	0.449	46	3.784	11.66
455-460	1390	60.46	241	6.80	180	8.982	910	74.86	9.34
480	390	16.96	185	5.22	21	1.048	21	1.727	14.40
490a	440	19.14	225	6.35	15	0.748	14	1.152	19.64
490b	460	20.01	226	6.38	11	0.549	15	1.234	21.19

Conversion Factors, mg/l to meq/l

0.04350 0.02821 0.04990 0.08226

$$SAR = \frac{Na}{[0.5\ (Ca + Mg)]^{\frac{1}{2}}}$$

VITA

Benjamin Betke Greeley

Candidate for the Degree of

Master of Science

Thesis: GROUND-WATER RESOURCES OF SOUTHERN COMANCHE COUNTY, SOUTHWESTERN OKLAHOMA

Major Field: Geology

Biographical:

Personal Data: Born in Oak Ridge, Tennessee, January 19, 1959, the son of Richard S. and Loretta B. Greeley.

Education: Graduated from St. Albans School, Washington, D.C., in June, 1977; received Bachelor of Arts Degree in Geology from the University of Pennsylvania in May, 1981; attended the University of Illinois; completed requirements for the Master of Science degree at Oklahoma State University in December, 1986.

Professional Experience: Research Assistant, School of Geology, Oklahoma State University, June to September, 1983, January, 1984, to July, 1985; member Association of Ground Water Scientists and Engineers, National Water Well Association, and the Geological Society of America.